

**A STUDY OF GAMMA, RADON, THORON AND THEIR  
PROGENY LEVELS IN MOKOKCHUNG, DIMAPUR  
AND KOHIMA DISTRICTS OF NAGALAND**

*by*

**SUPONGTOSHI JAMIR**



*Submitted to*

**NAGALAND UNIVERSITY**

*In Partial Fulfillment of the Requirements for Award of the Degree*

*of*

**DOCTOR OF PHILOSOPHY IN CHEMISTRY**

**DEPARTMENT OF CHEMISTRY**

**NAGALAND UNIVERSITY**

**LUMAMI-798627**

**NAGALAND, INDIA**

**2023**

**DEDICATED**

***To***

***My Family***



# नागालैण्ड विश्वविद्यालय NAGALAND UNIVERSITY

(केंद्रीय विश्वविद्यालय) / (A Central University)

मुख्यालय : लुमामी, जिला : जुन्हेबोटो (नागालैण्ड) – 798 627

Hqrs: Lumami, Dist: Zunheboto, Nagaland – 798 627

Prof. Dipak Sinha

Department of Chemistry

[dipaksinha@nagalanduniversity.ac.in](mailto:dipaksinha@nagalanduniversity.ac.in)

e-mail: [dipaksinha@gmail.com](mailto:dipaksinha@gmail.com)

## CERTIFICATE

This is to certify that **Mr. Supongtoshi Jamir**, a registered Research Scholar for Ph.D. degree in Chemistry under Nagaland University has carried out his research work under my guidance. His thesis entitled “**A STUDY OF GAMMA, RADON, THORON AND THEIR PROGENY LEVELS IN MOKOKCHUNG, DIMAPUR AND KOHIMA DISTRICTS OF NAGALAND**” embodies the original research work and has fulfilled all the requirements according to the rules of this University regarding investigations.

Further, to the best of my knowledge, the research work has not been submitted to any university for the award of any degree or diploma to any other University/Institution.

(Prof. Dipak Sinha)  
Supervisor




Dr. Rosaline Mishra (SO/F)  
E&BDS, RP&AD  
Tel : 91-22-25597823  
Email: [rosaline@barc.gov.in](mailto:rosaline@barc.gov.in)  
[rosaline.mishra@gmail.com](mailto:rosaline.mishra@gmail.com)

Government of India  
Bhabha Atomic Research Centre  
Radiological Physics & Advisory Division  
Mumbai- 400 094

## CERTIFICATE

This is to certify that **Mr. Supongtoshi Jamir**, a registered Research Scholar for Ph.D. degree in Chemistry under Nagaland University has carried out his research work under my co-supervision. His thesis entitled “**A STUDY OF GAMMA, RADON, THORON AND THEIR PROGENY LEVELS IN MOKOKCHUNG, DIMAPUR AND KOHIMA DISTRICTS OF NAGALAND**” is being forwarded for submission for the Ph.D. degree of Nagaland University.

Further, to the best of my knowledge, the research work has not been submitted to any university for the award of any degree or diploma.

  
(Dr. Rosaline Mishra)  
Co-supervisor



# नागालैण्ड विश्वविद्यालय NAGALAND UNIVERSITY

(केंद्रीय विश्वविद्यालय) / (A Central University)

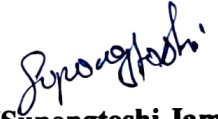
मुख्यालय : लुमामी, जिला : जुन्हेबोटो (नागालैण्ड) – 798 627  
Hqrs: Lumami, Dist: Zunheboto, Nagaland – 798 627

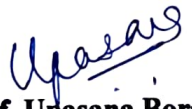
Department of Chemistry.


## DECLARATION

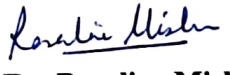
I, Mr. Supongtoshi Jamir, bearing registration No. PhD/CHE/00002 hereby declare that the content of the thesis entitled “**A STUDY OF GAMMA, RADON, THORON AND THEIR PROGENY LEVELS IN MOKOKCHUNG, DIMAPUR AND KOHIMA DISTRICTS OF NAGALAND**” is the result of my own research on the subject. I also declare that the contents of this thesis did not form the basis of the award of any previous degree to me or to the best of my knowledge to anybody else and that the thesis has not been submitted by me for any research degree in any other University/Institute.

This is being submitted to Nagaland University for the degree of Doctor of Philosophy in Chemistry.

  
(Supongtoshi Jamir)  
Research Scholar

  
(Prof. Upasana Bora Sinha)  
Head  
Department of Chemistry  
Nagaland University, Lumami

  
(Prof. Dipak Sinha)  
Supervisor

  
(Dr. Rosaline Mishra)  
Co-supervisor  
RP & AD  
BARC, Mumbai

# NAGALAND UNIVERSITY



HEAD QUARTERS : LUMAMI

## Ph. D COURSE WORK EXAMINATION

This is to certify that **Mr/Ms.....** **Supongtoshi Janir**.....  
of Nagaland University bearing Roll No..... **12/16**..... is qualified in the Ph.D Course Work Examination  
in the Department of..... **Chemistry**..... Nagaland University held in the Year 20..... 17

  
Head of Department

Department of Chemistry  
Nagaland University



Dean  
School of Sciences  
Nagaland University  
Hqs. Lumami Nagaland

## Acknowledgments

Firstly, I would like to thank Almighty God for blessing me with wisdom, good health, and guidance throughout my research journey.

I take this moment to extend my appreciation and gratitude to every individual for their help and support through the course of my Ph.D. journey. THANK YOU.

I extend my heartfelt and profound gratitude to **Prof. Dipak Sinha**, my research supervisor, for allowing me to work under him. His constant and patient guidance, enthusiastic motivation, and encouragement have always been the fuel to move one step further. His valuable and constructive critiques have always been the pillar, without which the completion of this work would not have been possible. The years spent under his guidance have been a worthy experience that has molded me into the person I am today.

I would also like to thank my co-supervisor **Dr. Rosaline Mishra**, Department of Radiological Physics and Advisory Division, Bhabha Atomic Research Centre (BARC), Mumbai for her thoughtful advice and brilliant ideas. Her ever-ready attitude and excellent caliber to proofread my manuscripts whenever I approach her, despite her busy schedule has contributed significantly to the success of my research work.

I extend my sincere gratitude to **Dr. B.K. Sahoo**, Department of Radiological Physics and Advisory Division, Bhabha Atomic Research Centre (BARC), Mumbai for extended help during my research.

I also would acknowledge a deep sense of gratitude to all the teaching faculties of the Chemistry department, Nagaland University: **Prof. Upasana Bora Sinha** (Head of Department), **Prof. M. Indira Devi**, **Dr. I. Tovishe Phucho**, **Dr. M. Prabhakar**, **Dr. Nurul Alam Choudhury**, and **Dr. Seram Dushila Devi**, for their useful suggestions and assistance that helped me to keep my progress on track.

My sincere gratitude to **Nagaland University**, for providing the basic facilities to conduct my research. I am also grateful to the Board of Research in Nuclear Sciences (BRNS) [project no. 36(4)/47/2015-BRNS/ 360/5] and the University Grant Commission (UGC) (NU/RDC/NNF-125/2021) for providing financial assistance.

My gratitude and thanks to the non-teaching staff: **Mr. S. Bendangtemsu**, **Ms. Sunepjungla**, **Ms. Temsuienla Amer**, **Mr. Johnny Yanthan**, and **Mr. Phyobemo Patton** for their immense support throughout my research period.

My great indebtedness goes to my labmates **Dr. Chubaakum Pongener**, **Dr. Parimal Chandra Bhomick**, **Dr. Aola Supong**, **Dr. Mridushmita Baruah**, **Mr. Soremo L**

**Ezung, Mr. Suraj Kumar, Mr. Shisak Sharma, Mr. Raplang Steven Umdor and Miss Imotila Longchar** for their unwavering support and encouragements.

Special thanks to my research scholar friends from other laboratories and departments for their wonderful friendship and encouragement.

On a personal note, I would like to acknowledge my family members and friends whose love, support, guidance, and prayers have encouraged and pushed me to achieve where I have reached now.

Last but not the least, I want to acknowledge everyone who has directly or indirectly influenced and contributed in furnishing to completing this research work.

**Supongtoshi Jamir**



## Lists of Figures

| <b>Figure number</b> | <b>Figure caption</b>   | <b>Page number</b> |
|----------------------|---|--------------------|
| <b>Chapter-1</b>     |   |                    |
| <b>Fig. 1.1</b>      | Schematic diagram of radon emanation process into the environment.  | 2                  |
| <b>Chapter-2</b>     |   |                    |
| <b>Fig. 2.1</b>      | LR-115 detector schematic diagram.  | 26                 |
| <b>Fig. 2.2</b>      | Schematic diagram of Chain scission in polymers.  | 27                 |
| <b>Fig. 2.3</b>      | Temperature-controlled water bath.  | 28                 |
| <b>Fig. 2.4</b>      | (a) Spark counter photo (b) Mylar placed over R-115.  | 29                 |
| <b>Fig. 2.5</b>      | Applied voltage vs Count showing the plateau region.  | 30                 |
| <b>Fig. 2.6</b>      | Twin cup pinhole dosimeter schematic diagram.   | 31                 |
| <b>Fig. 2.7</b>      | DTPS/DRPS schematic diagram.  | 32                 |
| <b>Fig. 2.8</b>      | Photograph of the Smart Rn Duo.   | 33                 |
| <b>Fig. 2.9</b>      | Experimental setup for $^{222}\text{Rn}$ mass exhalation rate measurement from the soil.                                    | 40                 |
| <b>Fig. 2.10</b>     | Set up for $^{220}\text{Rn}$ surface exhalation measurement from the soil.  | 41                 |
| <b>Fig. 2.11</b>     | Schematic diagram of water sample collection.   | 43                 |
| <b>Fig. 2.12</b>     | Set up for measurement of $^{222}\text{Rn}$ in water.   | 43                 |
| <b>Chapter-3</b>     |   |                    |
| <b>Fig. 3.1</b>      | The different geographical locations of the study area under Mokokchung district, Nagaland, India.                          | 51                 |
| <b>Fig. 3.2</b>      | Types of houses (a) brick (b) wooden (c) bamboo in Mokokchung district, Nagaland, India.                                    | 52                 |
| <b>Fig. 3.3</b>      | Deployment of DTPS/DRPS and Pin hole dosimeter in different types of houses a) Brick house b) Wooden house c) Bamboo house. | 53                 |
| <b>Fig. 3.4</b>      | Seasonal variation of average indoor $^{222}\text{Rn}$ and $^{220}\text{Rn}$ concentration.                                 | 61                 |

|                  |  |     |
|------------------|--|-----|
| <b>Fig. 3.5</b>  | Variation of indoor $^{222}\text{Rn}$ and $^{220}\text{Rn}$ concentration in different types of houses.  | 63  |
| <b>Fig. 3.6</b>  | Box and whisker plot of radon and thoron equilibrium factor in different house types.  | 65  |
| <b>Fig. 3.7</b>  | Annual average inhalation dose due to $^{222}\text{Rn}$ and its progeny.   | 66  |
| <b>Fig. 3.8</b>  | Annual average inhalation dose due to $^{220}\text{Rn}$ and its progeny.   | 67  |
| <b>Chapter-4</b> |  |     |
| <b>Fig. 4.1</b>  | Map of the area under study in Dimapur district, Nagaland, India. Dimapur is a district in Nagaland that is bordered on the south and east by Kohima district, on the west by Assam's Karbi Anglong district, and on the north by a stretch of Assam's district. | 76  |
| <b>Fig. 4.2</b>  | Types of houses (a) concrete (b) semi-wood/bamboo (c) bamboo   | 77  |
| <b>Fig. 4.3</b>  | Deployment of DTPS/DRPS and Pin hole dosimeter in different types of houses a) concrete house b) semi-wood/bamboo house c) bamboo house.   | 78  |
| <b>Fig. 4.4</b>  | (a) $^{222}\text{Rn}$ and $^{220}\text{Rn}$ in different seasons (b) EERC and EETC in different seasons.   | 88  |
| <b>Fig. 4.5</b>  | (a) Box plot of $^{222}\text{Rn}$ and EERC in different seasons (b) Box plot of $^{220}\text{Rn}$ and EETC in different seasons.   | 90  |
| <b>Fig. 4.6</b>  | (a) $^{222}\text{Rn}$ and $^{220}\text{Rn}$ in different types of houses (b) EERC and EETC in different types of houses.   | 91  |
| <b>Fig. 4.7</b>  | Equilibrium factor in different types of houses.   | 92  |
| <b>Fig. 4.8</b>  | Total inhalation dosage frequency distribution.  | 93  |
| <b>Chapter-5</b> |  |     |
| <b>Fig. 5.1</b>  | Map of the area under study in Kohima district.  | 103 |
| <b>Fig. 5.2</b>  | Types of houses (a) concrete (b) semi-wood/bamboo (c) bamboo.  | 104 |
| <b>Fig. 5.3</b>  | Deployment of DTPS/DRPS and Pin hole dosimeter in different types of houses (a) concrete house (b) semi-wood/bamboo house (c) bamboo house.  | 105 |

|                  |  |     |
|------------------|--|-----|
| <b>Fig. 5.4</b>  | (a) $^{222}\text{Rn}$ and its progeny correlation plot (b) $^{220}\text{Rn}$ and its progeny correlation plot. | 116 |
| <b>Fig. 5.5</b>  | $^{222}\text{Rn}$ and $^{220}\text{Rn}$ in different house types.  | 117 |
| <b>Fig. 5.6</b>  | EEC in different house types.  | 117 |
| <b>Fig. 5.7</b>  | Dose distribution frequency in 50 dwellings.   | 118 |
| <b>Chapter-6</b> |  |     |
| <b>Fig. 6.1</b>  | $^{222}\text{Rn}$ mass exhalation rate set-up.   | 127 |
| <b>Fig. 6.2</b>  | $^{220}\text{Rn}$ surface exhalation rate set up.  | 128 |
| <b>Fig. 6.3</b>  | Schematic diagram of water sample collection.  | 129 |
| <b>Fig. 6.4</b>  | $^{222}\text{Rn}$ in the water measurement setup   | 130 |
| <b>Fig. 6.5</b>  | Various sites of the study area in Mokokchung district, Nagaland, India.                                       | 132 |
| <b>Fig. 6.6</b>  | Mass exhalation rate of $^{222}\text{Rn}$ in various villages of Mokokchung district, Nagaland, India.         | 134 |
| <b>Fig. 6.7</b>  | Surface exhalation rate of $^{220}\text{Rn}$ in various villages of Mokokchung district, Nagaland, India.      | 135 |
| <b>Fig. 6.8</b>  | Radon concentration in water in various villages of Mokokchung district, Nagaland, India.                      | 138 |
| <b>Fig. 6.9</b>  | Various sites of the study area in Dimapur district, Nagaland, India.  | 140 |
| <b>Fig. 6.10</b> | $^{222}\text{Rn}$ mass exhalation rate.  | 142 |
| <b>Fig. 6.11</b> | $^{220}\text{Rn}$ surface exhalation rate.   | 143 |
| <b>Fig. 6.12</b> | $^{222}\text{Rn}$ in water in different sites.   | 144 |
| <b>Fig. 6.13</b> | Various sites of the study area in Kohima district, Nagaland, India.   | 147 |
| <b>Fig. 6.14</b> | Mass exhalation rate of $^{222}\text{Rn}$ in various sites of Kohima district, Nagaland, India.                | 149 |
| <b>Fig. 6.15</b> | Surface exhalation rate of $^{220}\text{Rn}$ in various sites of Kohima district, Nagaland, India.             | 149 |
| <b>Fig. 6.16</b> | $^{222}\text{Rn}$ in water in different sites.   | 151 |

## Lists of Tables

| <b>Table number</b> | <b>Table caption</b>   | <b>Page number</b> |
|---------------------|--|--------------------|
| <b>Chapter-1</b>    |  |                    |
| <b>Table 1.1</b>    | Energy and decay parameters of radon and thoron.   | 6                  |
| <b>Table 1.2</b>    | Physical properties of Radon.  | 8                  |
| <b>Table 1.3</b>    | Physical properties of Thoron.   | 9                  |
| <b>Table 1.4</b>    | National and International recommendations for Indoor Radon level.   | 16                 |
| <b>Chapter-2</b>    |  |                    |
| <b>Table 2.1</b>    | Smart RnDuo specifications.  | 33                 |
| <b>Table 2.2</b>    | Average global level of $^{222}\text{Rn}$ , $^{220}\text{Rn}$ , and their offspring in the atmosphere, along with their associated annual effective doses. | 38                 |
| <b>Chapter-3</b>    |  |                    |
| <b>Table 3.1</b>    | Gamma level in different houses of the study in Mokokchung district, Nagaland.   | 54                 |
| <b>Table 3.2</b>    | Zone-wise house distribution of Mokokchung district, Nagaland, India where DTPS/DRPS and Pinhole twin cup dosimeters were installed.                       | 57                 |
| <b>Table 3.3</b>    | Distribution of detectors in each village of Mokokchung district, Nagaland.  | 58                 |
| <b>Table 3.4</b>    | Annual average radon, thoron, EERC, and EETC in Mokokchung district, Nagaland.   | 60                 |
| <b>Table 3.5</b>    | Seasonal concentration of indoor $^{222}\text{Rn}$ and $^{220}\text{Rn}$ in Mokokchung district, Nagaland.   | 62                 |
| <b>Table 3.6</b>    | Annual average E.F observed in Mokokchung district, Nagaland.  | 64                 |
| <b>Table 3.7</b>    | Annual average dose in Mokokchung district, Nagaland.  | 65                 |
| <b>Chapter-4</b>    |  |                    |
| <b>Table 4.1</b>    | Gamma level in different houses of the study in Dimapur district, Nagaland, India.   | 79                 |

|                  |  |     |
|------------------|--|-----|
| <b>Table 4.2</b> | Zone-wise house distribution of Dimapur district, Nagaland, India where DTPS/DRPS and Pinhole twin cup dosimeters were installed.          | 81  |
| <b>Table 4.3</b> | Distribution of detectors in each site of Dimapur district, Nagaland.  | 82  |
| <b>Table 4.4</b> | Annual average radon, thoron, and their progeny concentration in Dimapur district, Nagaland.   | 84  |
| <b>Table 4.5</b> | $^{222}\text{Rn}$ (and its progeny) and $^{220}\text{Rn}$ (and its progeny) parameters in different seasons in Dimapur district, Nagaland. | 87  |
| <b>Chapter-5</b> |  |     |
| <b>Table 5.1</b> | Gamma level in different houses of the study in Kohima district, Nagaland, India.  | 106 |
| <b>Table 5.2</b> | Zone wise house distribution of Kohima district, Nagaland, India where DTPS/DRPS and Pinhole twin cup dosimeters were installed.           | 107 |
| <b>Table 5.3</b> | Distribution of detectors in each site of Dimapur district, Nagaland.  | 108 |
| <b>Table 5.4</b> | Annual average $^{222}\text{Rn}$ , $^{220}\text{Rn}$ , EEC, and inhalation dose.   | 111 |
| <b>Table 5.5</b> | Indoor radon and thoron parameters in three seasons.   | 114 |
| <b>Table 5.6</b> | Radon and thoron E.F in different seasons.   | 115 |
| <b>Chapter-6</b> |  |     |
| <b>Table 6.1</b> | Exhalation rates of $^{222}\text{Rn}$ , $^{220}\text{Rn}$ .  | 133 |
| <b>Table 6.2</b> | Comparing the current data on $^{222}\text{Rn}/^{220}\text{Rn}$ exhalation rates with those obtained from other parts of the nation.       | 136 |
| <b>Table 6.3</b> | $^{222}\text{Rn}$ content and its effective dose in the water samples of Mokokchung district of Nagaland.                                  | 137 |
| <b>Table 6.4</b> | Exhalation rates of $^{222}\text{Rn}$ and $^{220}\text{Rn}$ obtained from Dimapur district, Nagaland.                                      | 141 |
| <b>Table 6.5</b> | Inter-comparison of the current data of $^{222}\text{Rn}/^{220}\text{Rn}$ exhalation rates with worldwide values.                          | 144 |
| <b>Table 6.6</b> | $^{222}\text{Rn}$ and its dose detected in drinking water of Dimapur district, Nagaland.   | 145 |

|                  |  |     |
|------------------|--|-----|
| <b>Table 6.7</b> | Exhalation rates of $^{222}\text{Rn}$ , $^{220}\text{Rn}$ .  | 148 |
| <b>Table 6.8</b> | Comparing the current data on $^{222}\text{Rn}/^{220}\text{Rn}$ exhalation rates with those obtained from other parts of the nation. | 150 |
| <b>Table 6.9</b> | $^{222}\text{Rn}$ content and its effective dose in the water samples of Kohima district of Nagaland.                                | 151 |

# CONTENTS

*List of figures*

*(viii)-(x)*

*List of Tables*

*(xi)-(xiii)*

|                  |   |              |
|------------------|---|--------------|
| <b>Chapter-1</b> | <b>Introduction</b>   | <b>1-23</b>  |
| 1.1              | Radon: An Overview  | 1-2          |
| 1.2              | Production and transport of radon                           | 2-5          |
| 1.3              | $^{222}\text{Rn}$ , $^{220}\text{Rn}$ , and their Progenies | 5-9          |
| 1.4              | Indoor radon/thoron   | 9-11         |
| 1.5              | Indoor radon/thoron progeny                                 | 11           |
| 1.6              | Time dependence of Indoor radon Concentration               | 12           |
| 1.7              | Radon in soil   | 12           |
| 1.8              | Radon in water  | 12-13        |
| 1.9              | Radon and its health effects                                | 13-14        |
| 1.10             | Global recommended value of radon                           | 14-16        |
| 1.11             | Importance of radon study in Nagaland                       | 17           |
| 1.12             | Aims and objectives of the study                            | 17           |
|                  | References  | 18-23        |
| <b>Chapter-2</b> | <b>Methodology</b>  | <b>24-47</b> |
| 2.1              | Introduction  | 24           |
| 2.2              | Radon Measurement Techniques                                | 24-25        |
| 2.2.1            | Passive technique   | 25           |
| 2.2.1.1          | Solid-State Nuclear Track Detectors (SSNTD)                 | 25-26        |
| 2.2.1.2          | Charged particle tracks in polymers                         | 26-27        |
| 2.2.1.3          | Etching   | 27-28        |
| 2.2.1.4          | Constant water bath   | 28           |
| 2.2.1.5          | Spark Counter   | 29-30        |
| 2.2.1.6          | Pinhole twin cup dosimeter                                  | 30-31        |
| 2.2.1.7          | Direct radon/thoron progeny sensors (DRPS/DTPS)             | 31-32        |
| 2.2.2            | Active technique  | 32           |
| 2.2.2.1          | Portable Smart Rn Duo (Radon monitor)                       | 32-34        |
| 2.3              | Present Study   | 34           |
| 2.4              | Indoor radon measurement                                    | 34           |

|                  |  |              |
|------------------|--|--------------|
| 2.4.1            | Selection of dwellings   | 34-35        |
| 2.4.2            | Deployment of Dosimeters   | 35           |
| 2.4.3            | Retrieval of dosimeter and etching   | 35-36        |
| 2.4.4            | Calculation of indoor radon and thoron concentration.  | 36           |
| 2.4.5            | Calculation of progeny concentration.  | 36-37        |
| 2.4.6            | Equilibrium factor (E.F)   | 37           |
| 2.4.7            | Inhalation dose  | 37-38        |
| 2.5              | $^{222}\text{Rn}$ and $^{220}\text{Rn}$ exhalation rates from the soil                                     | 38-39        |
| 2.5.1            | Collection of soil samples   | 39           |
| 2.5.2            | $^{222}\text{Rn}$ mass exhalation rate measurement   | 39-40        |
| 2.5.3            | $^{220}\text{Rn}$ surface exhalation rate measurement  | 41           |
| 2.6              | $^{222}\text{Rn}$ measurement in water   | 42           |
| 2.6.1            | Protocols for water sampling and measurement   | 42-43        |
| 2.6.2            | Calculation of $^{222}\text{Rn}$ in water  | 43-44        |
| 2.6.3            | Dose calculations  | 44           |
|                  | References   | 45-47        |
| <b>Chapter-3</b> | <b>A study on indoor radon, thoron, and their progeny levels in Mokokchung district of Nagaland, India</b> | <b>48-72</b> |
| 3.1              | Introduction   | 48-49        |
| 3.2              | Methodology  | 49           |
| 3.2.1            | Study area   | 49-50        |
| 3.2.2            | $^{222}\text{Rn}/^{220}\text{Rn}$ and progeny measurement  | 50           |
| 3.2.3            | Deployment strategy  | 50-53        |
| 3.2.3.1          | Gamma survey for site selection  | 54-57        |
| 3.2.3.2          | Deployment of detectors  | 57-58        |
| 3.2.4            | Post-processing of dosimeters  | 58-59        |
| 3.2.5            | Calculation of $^{222}\text{Rn}$ , $^{220}\text{Rn}$ , and Progeny Concentration                           | 59-60        |
| 3.3              | Results and discussions  | 60           |
| 3.3.1            | Annual average $^{222}\text{Rn}$ , $^{220}\text{Rn}$ , EERC/EETC   | 60           |
| 3.3.2            | Seasonal variation of radon, and thoron concentration  | 61-63        |
| 3.3.3            | Variation of $^{222}\text{Rn}$ , and $^{220}\text{Rn}$ concentrations in different types of house          | 63           |



|                  |  |                |
|------------------|--|----------------|
| 3.3.4            | Equilibrium Factor (EF)  | 64-65          |
| 3.3.5            | Inhalation dose  | 65-67          |
| 3.4              | Conclusion   | 67-68          |
|                  | References   | 69-72          |
| <b>Chapter-4</b> | <b>A comprehensive study on indoor radon, thoron, and their progeny level in Dimapur district of Nagaland, India</b>                 | <b>73-79</b>   |
| 4.1              | Introduction   | 73-74          |
| 4.2              | Methodology  | 74             |
| 4.2.1            | Study area   | 74-75          |
| 4.2.2            | $^{222}\text{Rn}/^{220}\text{Rn}$ and progeny measurement  | 75             |
| 4.2.3            | Deployment strategy  | 75-78          |
| 4.2.3.1          | Gamma survey for site selection  | 79-81          |
| 4.2.3.2          | Deployment of detectors  | 81-82          |
| 4.2.4            | Post-processing of dosimeters  | 82-83          |
| 4.2.5            | Calculation of $^{222}\text{Rn}$ , $^{220}\text{Rn}$ , and Progeny   | 83-84          |
| 4.3              | Results and discussions  | 84             |
| 4.3.1            | Annual average $^{222}\text{Rn}$ , $^{220}\text{Rn}$ , EERC/EETC   | 84-87          |
| 4.3.2            | Seasonal variations of radon, thoron, and their corresponding EEC  | 87-90          |
| 4.3.3            | $^{222}\text{Rn}$ , $^{220}\text{Rn}$ , EERC, EETC in various types of houses  | 90-91          |
| 4.3.4            | Equilibrium factor (E.F) in various types of houses  | 92             |
| 4.3.5            | Inhalation dose  | 92-93          |
| 4.4              | Conclusion   | 93-94          |
|                  | References   | 95-99          |
| <b>Chapter-5</b> | <b>A case study on seasonal and annual average indoor radon, thoron, and their progeny level in Kohima district, Nagaland, India</b> | <b>100-123</b> |
| 5.1              | Introduction   | 100-101        |
| 5.2              | Methodology  | 101            |
| 5.2.1            | Study area   | 101-102        |
| 5.2.2            | $^{222}\text{Rn}/^{220}\text{Rn}$ and progeny measurement  | 102            |
| 5.2.3            | Deployment strategy  | 102-105        |
| 5.2.3.1          | Gamma survey for site selection  | 106-107        |

|                  |   |                |
|------------------|---|----------------|
| 5.2.3.2          | Deployment of detectors   | 108-109        |
| 5.2.3.3          | Post-processing of dosimeters   | 109            |
| 5.2.4            | Calculation of $^{222}\text{Rn}$ , $^{220}\text{Rn}$ , EEC, E.F, and inhalation dose  | 109            |
| 5.2.4.1          | $^{222}\text{Rn}$ and $^{220}\text{Rn}$ gas measurement   | 109            |
| 5.2.4.2          | Progeny measurement   | 110            |
| 5.2.4.3          | Measurement of the equilibrium factor (EF) and inhalation dosage  | 110            |
| 5.3              | Results and discussions   | 110            |
| 5.3.1            | Annual average $^{222}\text{Rn}$ , $^{220}\text{Rn}$ concentration values and also their EEC, E.F, and inhalation dose.   | 110-113        |
| 5.3.2            | Seasonal changes in $^{222}\text{Rn}$ and $^{220}\text{Rn}$ , as well as their corresponding EECs   | 113-114        |
| 5.3.3            | Equilibrium factor (E.F)  | 114-115        |
| 5.3.4            | Correlation of $^{222}\text{Rn}$ (and its EERC) and $^{220}\text{Rn}$ (and its EETC)  | 115            |
| 5.3.5            | $^{222}\text{Rn}$ , $^{220}\text{Rn}$ , EERC, EETC in various types of houses   | 115-117        |
| 5.3.6            | Inhalation dose   | 118            |
| 5.4              | Conclusion  | 119            |
|                  | References  | 120-123        |
| <b>Chapter-6</b> | <b>Estimation of radon in groundwater and analysis of radon and thoron exhalation rates of the soil in Mokokchung, Dimapur, and Kohima districts of Nagaland, India</b> | <b>124-157</b> |
| 6.1              | Introduction  | 124-125        |
| 6.2              | Materials and method  | 125-126        |
| 6.2.1            | $^{222}\text{Rn}$ mass exhalation rate measurement  | 126-128        |
| 6.2.2            | $^{220}\text{Rn}$ surface exhalation rate measurement   | 128-129        |
| 6.2.3            | $^{222}\text{Rn}$ concentration in water  | 129-131        |
| 6.2.4            | Dose calculations due to $^{222}\text{Rn}$ in water   | 131            |
| 6.3              | Study Area-1  | 131-132        |
| 6.3.1            | Results and discussions of study area-1   | 133-134        |
| 6.3.1.1          | $^{222}\text{Rn}/^{220}\text{Rn}$ exhalation rates  | 134-136        |

|                   |  |                |
|-------------------|--|----------------|
| 6.3.1.2           | $^{222}\text{Rn}$ in water                         | 136-139        |
| 6.4               | Study Area-2                                       | 139-140        |
| 6.4.1             | Results and discussions of study area-2            | 141            |
| 6.4.1.1           | $^{222}\text{Rn}/^{220}\text{Rn}$ exhalation rates | 142-144        |
| 6.4.1.2           | $^{222}\text{Rn}$ in water                         | 144-146        |
| 6.5               | Study Area-3                                       | 146-147        |
| 6.5.1             | Results and discussions of study area-3            | 148            |
| 6.5.1.1           | $^{222}\text{Rn}/^{220}\text{Rn}$ exhalation rates | 148-150        |
| 6.5.1.2           | $^{222}\text{Rn}$ in water                         | 150-152        |
| 6.6               | Conclusion   | 152            |
|                   | References   | 153-157        |
| <b>Appendix-1</b> | <b>Plagiarism report</b>                           | <b>158-159</b> |
| <b>Appendix-2</b> | <b>Workshops and seminars attended</b>             | <b>160</b>     |
| <b>Appendix-3</b> | <b>Lists of publications</b>                       | <b>161-162</b> |

## **CHAPTER- 1**

### **INTRODUCTION**

---

*In this chapter, information on the discovery, production, transport, properties, and time dependence of radon is provided. The health effects, global recommended value, and importance of radon are also discussed in detail. Furthermore, the aims and objectives of the study are highlighted in this chapter.*

---

## 1.1 Radon: An Overview

Radiation is ubiquitous and inevitable. Studies on natural environment radiation and natural radioactivity are of great significance in radiation physics, health physics, and other allied branches of natural science. Humans are continuously exposed to radiation either from natural or man-made radiation sources. Radiation can be defined as the type of energy traveling across space as particles or waves that have been divided into ionizing and non-ionizing categories based on how they interact with matter.

There are several different types of radiation, and among them, ionizing radiation refers to those energies which have enough energy to produce ionization and subsequently cause biological damage. Non-ionizing radiations, on the other hand, have less energy than what is required to ionize matter and are only capable of changing the rotation, vibration, or electron valence configuration of an atom. There are two categories of ionizing radiation: naturally occurring radiation and man-made radiation or other artificial sources.

The natural sources are cosmic rays emitting from primordial radionuclides that have been present in the earth's crust since the origin of the earth while the man-made include nuclear explosions, radionuclides used in industry, agriculture, and various kinds of electronic devices. Of the two types of radiation, naturally occurring radiations account for the majority of the radiation in the environment [1]

To date, there are only around 60 radionuclides that have been discovered in nature. It has been well established that ~82% of the total radiation dosage received by people comes from natural sources, of which 52% is attributable to indoor exposure to radon, thoron, and their progeny [1]. In this regard, there are several studies conducted by researchers worldwide to carry out extensive studies and establish a potential link between radon exposure and the occurrence of diseases in humans such as lung cancer, prostate, leukemia, etc [2-4]. Such diseases caused by radon have been a matter of concern and there is substantial evidence that has been reported in different parts of the world [5-7]. In this regard, there has been an upsurge amount of interest

prompted in the research community worldwide to investigate the radon study in more detail.

## 1.2 Production and transport of radon

The disintegration of radium isotopes ( $^{226}\text{Ra}$  and  $^{224}\text{Ra}$ ), which are essentially produced from uranium ( $^{238}\text{U}$ ) and thoron ( $^{232}\text{Th}$ ), the fundamental elements of the earth's crust, respectively, results in the generation of radon and thoron [8]. As the common contributors of radon/thoron in the interior environment, soil, rock, water, and construction materials typically contain trace amounts of radium. These sources are termed Naturally Occurring Radioactive Materials (NORMs). Additionally, radon may be produced by human activity, including waste from uranium mining and processing facilities, coal industries, etc. These sources are known as Technologically Enhanced Naturally Occurring Radioactive Materials (TENORMs) [8, 9].

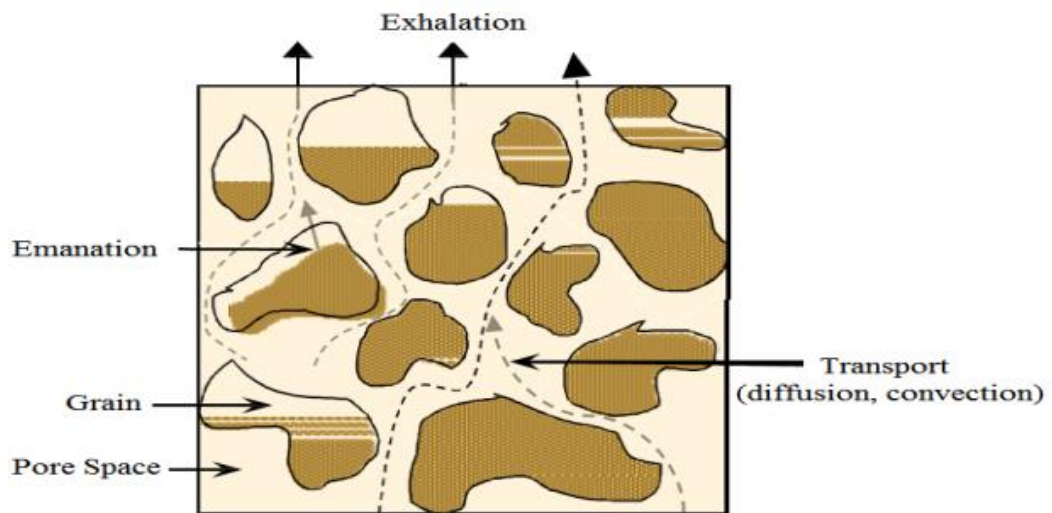


**Fig. 1.1:** Schematic diagram of radon emanation process into the environment [7].

They can, however, migrate to the surface when the grains are interstitial/pore spaces between them. Thus, the following mechanisms lead to the escape of radon to the environment from a matrix containing radium (figure 1.1) [7].

1. **Emanation** – Here, as radium decays, radon atoms are produced. These atoms migrate from the grains and enter the interstitial space between the grains, primarily as a result of recoil.

2. Transport – Here, the released radon atoms migrate through the soil matrix's pore space and up to the earth's surface due to advective flow and diffusion.
3. Exhalation – It involves the movement of air-filled pores releasing  $^{222}\text{Rn}$  gas into the atmosphere.

After being produced by their respective parent radionuclides inside the soil grain, radon and thoron either stay entrenched in that grain and become immobile, traverse a pore space as well as disperse into the pore space or become stuck in a nearby grain. Just a tiny fraction of radon/thoron atoms produced due to the decomposition process inside soil/rock grains gets transported into a porous medium and becomes mobilized. This tiny fraction is called the emanation coefficient. The shape of the soil grains is what largely determines this coefficient, the amount and dispersion of  $^{226}\text{Ra}$ , the porosity, the soil temperature, the ambient temperature, and the moisture content [10].

Given that radon diffuses through solid materials at a rate of  $10\text{-}20\text{ cm}^2\text{s}^{-1}$  and that soil grains have a half-life of  $^{222}\text{Rn}$ , any  $^{222}\text{Rn}$  generated is likely to dissolve after the  $^{226}\text{Ra}$  transition. This indicates that  $^{222}\text{Rn}$  comes only from a range of 30 to 50 nm on the surface of a soil particle [11]. Although the precise mechanisms causing radon to emit from grains are not well known, it is thought that the recoil processes play a major role in the emanation [12, 13]. The emanation of radon is greatly influenced by the soil's moisture level, while temperature dependency is little [14, 15]. The radon emission coefficient is influenced by moisture in small portions, but over time, the emanation coefficient decreases as moisture levels rise further. The nature of the soil, grain size, and porosity all influence how much moisture is needed to achieve the highest level of emanation [16, 17]. Higher moisture content is associated with a decrease in the emission coefficient due to a decrease in radon contained in the water's diffusion. Furthermore, grain size has an inverse relationship with the radon emission coefficient and yet is directly related to porosity [18]. Following emission from the soil matrix, radon can be transported in porous media by two different processes. Variations in the spatial distribution of radon concentration allow for the diffusional  $^{222}\text{Rn}/^{220}\text{Rn}$  movement. Diffusive transport is regarded as being among the primary methods for  $^{222}\text{Rn}/^{220}\text{Rn}$  exhalation from soils, construction materials, and other permeable media. Fick's Law can be used to numerically explain the diffusion

process. The intensity of diffusion is determined by a parameter known as the pore space diffusion coefficient, which takes into consideration the paths that diffusing species must travel across a porous media. The tortuosity correction diffusion coefficient for radon in dry soils is roughly  $2 \times 10^{-6} \text{ m}^2 \text{ s}^{-1}$ , which in comparison with the molecular diffusion coefficient is 4 to 5 times lower.

Radioactive materials' half-lives set a limit on how far radon atoms can move via diffusion. This can be identified by a mean diffusion length, which is commonly known as diffusion length. This distance, for normal soils, is approximately 1 m and 2 cm for radon and thoron respectively [19]. As a result, radium that is present in the soil approximately one meter deep effectively leads to surface exhalation through the diffusion mechanism. The amount of radium activity which is situated at more than one meter below the surface of the earth would have little impact on the flux at the surface. This fact allows for the ability to utilize soil covers to reduce radon emissions.

A process called advective transport, which is quantitatively characterized by Darcy's Law, could also carry radon or thorium across long distances. Advection is not limited to the air that travels between open areas owing to pressure variations in the pore air, it can however also be found in porous materials. In addition to the size of the pressure difference, the hydraulic conductivity of soils relies upon soil permeability and affects the advection velocity in soils. The typical soil permeability is  $1.5 \times 10^{-11} \text{ ms}^{-1}$ , and the hydraulic conductivity in terms of permeability and air viscosity is  $10^{-6} \text{ m}^3 \text{ s kg}^{-1}$ . Variable pressure differences can be created in soils subjected to an open environment by atmospheric pressure changes. The diffusion coefficient of the produced pressure pulse in the soil is around  $0.1 \text{ m}^2 \text{ s}^{-1}$ , which is much larger than the radon's molecular diffusion coefficient ( $10^{-5} \text{ m}^2 \text{ s}^{-1}$ ). Because of this, the produced difference in pressure diffuses rapidly in a short while and cancels all long-lasting atmospheric and soil pressure differences. Therefore, for those experiments which are conducted in open atmospheres for the exhalation of radon, diffusive transport is typically preferred over Darcian flow-induced advective transport. In places with cold temperatures and wet soil, the most significant method is 'advective transport' for  $^{222}\text{Rn}/^{220}\text{Rn}$  present in buildings [20]. The primary component influencing radon



transport and exhalation, along with radon emanation, is soil moisture. A modest moisture content enhances  $^{222}\text{Rn}$  exhalation while also increasing the moisture content decreases the  $^{222}\text{Rn}$  level. Peak  $^{222}\text{Rn}$  exhalation rates were discovered to correlate with the same saturation level that causes peak  $^{222}\text{Rn}$  emanation [21]. The diffusivity, and hence the exhalation rate, can be influenced by a wide range of environmental factors. The exhalation rate is decreased by rain, snow, freezing, and an increase in air pressure, but it can be increased by a rise in wind speed and temperature.

### 1.3 $^{222}\text{Rn}$ , $^{220}\text{Rn}$ , and their Progenies

Friedrich Ernst Dorn, a German physicist, made the discovery of radon in 1898, while in 1900, E. Rutherford and R.B. Owens made the discovery of thoron. In 1900, radon was known as radium emission; however, Robert Whylaw Gray and William Ramsay changed its name to niton (Nt) in 1908, which comes from the Latin word nitens, which means brilliant or having the ability to radiate light. The present term Radon was decided in 1923 by the International Union of Pure and Applied Chemistry (IUPAC).

Noble gas radon ( $^{222}\text{Rn}$ ), which has an atomic number of 86, is colorless, odorless tasteless, and radioactive. It is widely distributed in the environment plus it is readily soluble in water. It can be found predominantly in the soil as well as in seawater. At standard temperature and pressure, radon is colorless but when cooled below its freezing point of 202 K ( $-71^{\circ}\text{C}$ ), it glows brilliantly by changing its color from yellow to orange-red as the temperature dips under 93 K. ( $-180.1^{\circ}\text{C}$ ). It has a very high density as compared to most other gases, making it one of the heaviest gases presently known. Radon naturally exists in three isotopic forms:  $^{222}\text{Rn}$  (radon),  $^{220}\text{Rn}$  (thoron), and  $^{219}\text{Rn}$  (actinon) which are formed from the spontaneous alpha decay of radium isotopes as part of the decay series of  $^{238}\text{U}$  (uranium),  $^{232}\text{Th}$  (thorium), and  $^{235}\text{U}$  (actinium) respectively. Their respective half-lives are 3.82 days, 55.6 seconds, and 3.96 seconds. Therefore, in many instances, actinon is neglected as it does not possess a radiological risk to humans due to its much shorter half-life and low relative natural abundance as compared to radon and thoron [8]. Due to this, radon and thoron are often given much importance in epidemiological studies. The decay properties of radon, thoron, and their progeny are shown in table 1.1 [9].

**Table 1.1:** Energy and decay parameters of radon and thoron.

| Radionuclide      | Half-life         | Radiation               | $E_\alpha$ (MeV) | $E_\beta$ (MeV) |
|-------------------|-------------------|-------------------------|------------------|-----------------|
| $^{226}\text{Ra}$ | 1600 y            | $\alpha$                | 4.78 (94.3%)     | 0.186 (3.3%)    |
| $^{222}\text{Rn}$ | 3.824 d           | $\alpha$                | 5.49 (100%)      |                 |
| $^{218}\text{Po}$ | 3.05 m            | $\alpha$                | 6.00 (100%)      |                 |
| $^{214}\text{Pb}$ | 26.8 m            | $\beta, \gamma$         |                  | 0.295 (19%)     |
|                   |                   |                         |                  | 0.352 (36%)     |
| $^{214}\text{Bi}$ | 19.7 m            | $\beta$                 |                  | 0.609 (47%)     |
|                   |                   |                         |                  | 1.12 (15%)      |
|                   |                   |                         |                  | 1.76 (16%)      |
| $^{214}\text{Po}$ | 164 $\mu\text{s}$ | $\alpha$                | 7.69 (100%)      |                 |
| $^{224}\text{Ra}$ | 3.66 d            | $\alpha$                | 5.45 (6%)        | 0.241 (3.9%)    |
|                   |                   |                         | 5.68 (94%)       |                 |
| $^{220}\text{Rn}$ | 55.6 s            | $\alpha$                | 6.29 (100%)      |                 |
| $^{216}\text{Po}$ | 0.15 s            | $\alpha$                | 6.78 (100%)      |                 |
| $^{212}\text{Pb}$ | 10.64 h           | $\beta, \gamma$         |                  | 0.239(47%)      |
|                   |                   |                         |                  | 0.3 (3.2%)      |
| $^{212}\text{Bi}$ | 1.01 h            | $\alpha, \beta, \gamma$ | 6.05 (25%)       | 0.727 (11.8%)   |
|                   |                   |                         | 6.09 (10%)       | 1.62 (2.8%)     |
| $^{212}\text{Po}$ | 298 ns            | $\alpha$                | 8.78 (100%)      |                 |
| $^{208}\text{Tl}$ | 3.05 m            | $\beta, \gamma$         |                  | 0.511 (23%)     |
|                   |                   |                         |                  | 0.583 (86%)     |
|                   |                   |                         |                  | 0.86 (12%)      |
|                   |                   |                         |                  | 2.614 (100%)    |

It has been discovered that all people are exposed to indoor air pollutants in dwellings, such as  $^{222}\text{Rn}/^{220}\text{Rn}$  and their offspring, which raises concerns for the public's health. The main factor contributing to the total inhalation dose each year is exposure to radon, thoron, and their offspring. Therefore, it is essential to do a quantitative measurement or investigation of their concentrations in homes. In this regard, a considerable amount of focus has been directed toward long-term and large-scale measurements of radon, thoron, and their progeny concentrations in India [22].

There are 35 isotopes of radon, but only two ( $^{222}\text{Rn}$  and  $^{220}\text{Rn}$ ) are significant for the environment [23]. The most abundant natural radionuclides found in nature are  $^{219}\text{Rn}$ ,  $^{220}\text{Rn}$ , and  $^{222}\text{Rn}$ . Except for  $^{222}\text{Rn}$  (3.825 days),  $^{211}\text{Rn}$  (14.7 hours), and  $^{210}\text{Rn}$  (2.5 hours), all other isotopes exhibit half-lives of less than 1 hour. As radon decays spontaneously, the polonium isotopes emit alpha radiation, namely  $^{218}\text{Po}$ ,  $^{214}\text{Pb}$ ,  $^{214}\text{Bi}$ , and  $^{214}\text{Po}$ . Over half of the overall radiation exposure to humans due to natural sources is caused by radon, thoron, and their offspring when they are inhaled [24]. Radon, except when it is confined in a small area like a room or cave, is not toxic as it quickly escapes into the surrounding air. However, radon can be dangerous when there is less air movement because of its progeny which creates the alpha particle [25]. During respiration, the majority of the radon gas absorbed into the lungs is breathed out, however, a certain fraction of the radon progeny gets attached to the lung tissue and has the potential to harm DNA in the lung's delicate tissues and can cause lung cancer [26]. Of the noble gases, radon is the heaviest. It is heavier than air by 7.5 times and hydrogen by 100 times and has the highest melting, boiling, critical temperature, and critical pressure of all the noble gases. In cold water, it is soluble, and as the temperature rises, so does its solubility. Because of this property, radon can be expelled during washing, bathing, and cleaning with water in the home. It has a high toluene solubility. It is undoubtedly the most prevalent harmful radionuclide.

The most stable isotope of thorium ( $^{232}\text{Th}$ ) produces thoron as a natural byproduct of disintegration. Since  $^{222}\text{Rn}$  along with its offspring is a significant source of atmospheric ions close to the earth's surface, much attention has been given to thoron studies in recent years. Numerous atmospheric phenomena, including the development of thunderstorms, are caused by these atmospheric ions [27]. Additionally, the investigation of atmospheric transport processes like eddy diffusion has made use of thoron and its offspring as tracers.

There is less data on thoron than there is on radon. This is because of the shorter half-life (~55.6 sec) of thoron and that its role in inhalation dosage is normally neglected in comparison to other major natural radiation. Table 1.2 depicts some properties of radon.

**Table 1.2:** Physical properties of Radon [28, 29]

| SI. No. | Properties               | Values                                 |
|---------|--------------------------|--|
| 1       | Atomic Radius            | 1.34 Å                                 |
| 2       | Atomic Volume            | 50.5 cm <sup>3</sup> mol <sup>-1</sup> |
| 3       | Molar Volume             | 50.5 cm <sup>3</sup> mol <sup>-1</sup> |
| 4       | Mean Excitation Energy   | 794.0 eV                               |
| 5       | Melting Point            | -71°C                                  |
| 6       | Boiling Point            | -61.85°C                               |
| 7       | Critical Point           | 377 K at 6.28 MPa                      |
| 8       | Critical Temperature     | 104°C                                  |
| 9       | Critical Pressure        | 62 atm.                                |
| 10      | Heat of Vaporization     | 16.4 – 18.1 kJmol <sup>-1</sup>        |
| 11      | Heat of Fusion           | 2.89 – 3.247 kJmol <sup>-1</sup>       |
| 12      | Specific Heat Capacity   | 94 J/kg.K                              |
| 13      | Enthalpy of Fusion       | 2.7 kJmol <sup>-1</sup>                |
| 14      | Enthalpy of Vaporization | 18.1 kJmol <sup>-1</sup>               |
| 15      | Thermal Entropy          | 176.1 kJ/mol.K at 298.15               |
| 16      | Thermal Conductivity     | 3.61 mW/m.K at 300 K                   |
| 17      | Electrical Conductivity  | 0.1 mOhm-cm                            |
| 18      | Polarizability           | 5.3 Å <sup>3</sup>                     |
| 19      | Ionization Energy        | 10.745 eV                              |
| 20      | Density                  | 0.00973 gcm <sup>-3</sup> at 293K      |

Recent investigations that were conducted as a result of the finding of high <sup>220</sup>Rn concentrations in a variety of countries' living situations suggest that this may not be the case. For a comprehensive view of the inhalation dose, it is becoming ever more regarded that knowledge of <sup>220</sup>Rn levels in the environment may be required. In comparison to short-lived radon offspring, the estimated radiation exposure by breathing in thoron progeny is in the range of 20 ± 10% [1]. Although <sup>222</sup>Rn decay products are the primary radiation source, it is important to consider the dose resulting from <sup>220</sup>Rn decay products since, in some circumstances, its progeny <sup>212</sup>Pb (half-life= 10.6 hours) can build up to considerable quantities in the air [30].

According to certain research, the dose caused by  $^{220}\text{Rn}$  and its offspring can sometimes be on a level with or even higher than that caused by  $^{222}\text{Rn}$  and its offspring in certain places [31]. As a result, thorium might not always be insignificant, particularly in areas with thorium-bearing sediments, often known as High Background Radiation Areas (HBRAs) (like monazite-bearing sand in Kerala, India). The characteristics of the thoron are shown in table 1.3.

**Table 1.3:** Physical properties of Thoron [28, 29]

| Sl.No. | Properties                             | Values                              |
|--------|--|-------------------------------------|
| 1      | Boiling Point                          | -61.8°C                             |
| 2      | Melting Point                          | -71°C                               |
| 3      | Diffusion Coefficient in air at STP    | $0.1 \text{ cm}^2\text{s}^{-1}$     |
| 4      | Diffusion Coefficient in water at 18°C | $10^{-5} \text{ cm}^2\text{s}^{-1}$ |
| 5      | Solubility in water at 0°C             | 0.51                                |
|        | Solubility in water at 20°C            | 0.25                                |
|        | Solubility in water at 50°C            | 0.14                                |

The radioactive elements  $^{222}\text{Rn}$  and  $^{220}\text{Rn}$  are free to migrate through rock cracks and soil pores before escaping into the atmosphere. They can travel into houses and gather in large numbers indoors to pose a threat to people's health. Radon and thoron behavior are unaltered by chemical processes, and their levels are highly influenced by atmospheric, geological, and geophysical factors.

#### 1.4 Indoor radon/thoron

In the environment, radon/thoron is mostly produced by uranium/thorium decay products and the deposition of uranium/thorium in soil. To a depth of six inches, the surface soil in each square mile contains roughly one gram of radium, which moderately emits radon into the environment [32]. The following are the primary causes of indoor radon/thoron levels:

**Soil and Rock** - The surrounding soil is the primary source of radon/thoron in the interior environment. This gas is created by the radioactive disintegration of the trace element radium ( $^{226}\text{Ra}/^{224}\text{Ra}$ ), which is present in trace amounts. Variable element concentrations in the  $^{238}\text{U}$  and  $^{232}\text{Th}$  decay series can be found in soil and rock. Each uranium and thorium series has an average soil concentration of  $25 \text{ Bqkg}^{-1}$  [33]. The chemically inert radon gas is then carried into residences through gaps in the structure. When there is inadequate ventilation for optimal air circulation, radon gas may accumulate indoors. There are two ways that radon can enter a home. Firstly, it involves the  $^{222}\text{Rn}$  transportation through the soil's air pore system via molecular diffusion, where the soil is presumptively largely stationary while the pressure-driven flow, which is caused by factors that allow air to enter buildings, is the second significant entry. Building foundations can have cracks and holes as tiny as 0.5 mm, which is sufficient to allow gas transmission and convective migration.

**Building materials**- The building materials might have a higher impact on the indoor radon concentration in larger and taller constructions, but their overall impact is typically negligible. Ingersoll [34] has assessed the radon emission rates of several building materials. The findings indicate that wood is the lowest radon emitter and that concrete is the highest. Sand emits the most energy when measured as an emanator from concrete components, whereas cement emits the least. The rate of radon emission within a particular type of construction material varied greatly between samples. Materials may have almost the same uranium concentration, yet their radon emission rates may differ significantly. It was shown that the physical characteristics of the different material types contribute to the significant variation in escape-to-production ratios. As a result, studies of the radon exhalation rates for different materials are essential. Thus, the type of structure and the materials utilized will have a significant impact on the radon/thoron concentration indoors.

**Water**- Radon can enter a home by water transportation, which is a significant method. Radon levels in water have been observed to range widely. Drilled wells have been shown to have the largest concentrations of water, particularly in granite regions, while dug wells and surface water have the lowest concentrations. Although radon that has been dissolved in water is a potential source of indoor airborne radon,

the transfer factor for the resulting concentration in water is only about  $10^{-4}$  Bqm<sup>-3</sup> [35]. Radium levels in the soil or rock nearby and radon's emissivity into the water both affect the amount of radon in a body of water. The amount of radon emitted into the water is significantly influenced by the physical state of the rock matrix. Typically radon concentrations in homes are not high when it escapes from groundwater. This is due to the fact that levels in the soil are typically higher than those found in groundwater and that soil directly above the water table has such a high water content that soil-based diffusion is hindered. When <sup>222</sup>Rn levels in groundwater are much higher than <sup>222</sup>Rn present in soil and there is a movement of groundwater, then there is a possibility that enough <sup>222</sup>Rn would be discharged to alter the amount of radon in the building.

### 1.5 Indoor radon/thoron progeny

The three elements that affect the level of <sup>222</sup>Rn/<sup>220</sup>Rn and their offspring indoors are the rate of ventilation, the entry or production of these gases from different sources, as well as how quickly they are changing or being removed chemically or physically. Since they are chemically inert, radon and thoron behave like stable pollutants, with the indoor concentration only influenced by the rate of entry and rate of ventilation. The behavior of their offspring, however, is significantly more complicated and depends on the amount of radon/thoron present, the ventilation rate, as well as how radioactive decay, chemical reactivity, and particle concentration interact. Furthermore, it depends on the type of layer that separates the interior atmosphere from the outside surface. The number of offspring in the atmosphere is typically expressed as a collective concentration, or equilibrium-equivalent concentration, which, instead of being expressed as an individual decay-product concentration, is normalized to the quantity of energy produced by the alpha decay which will eventually be produced from the combination of the progenies present. The amount of progenies, as determined by the EEC (equilibrium equivalent concentrations), is primarily dependent on the concentrations of the first three decay products (<sup>218</sup>Po, <sup>214</sup>Pb, and <sup>214</sup>Bi for the <sup>222</sup>Rn series, and <sup>212</sup>Pb and <sup>212</sup>Bi for the <sup>220</sup>Rn series), as well as on how much polonium-alpha energy each will produce throughout radioactive breakdown.

## 1.6 Time dependence of Indoor radon Concentration

Numerous long-term studies of  $^{222}\text{Rn}/^{220}\text{Rn}$  in residences have shown how the level of  $^{222}\text{Rn}$ ,  $^{220}\text{Rn}$  along with their offspring changes over time. This variance depends on the season, the weather, and the period of the day. According to a study from the United Kingdom, radon levels are at their highest at night [36] and Gesell's presentation of the diurnal/daily variations studied by numerous researchers in four nations (the United States, Hungary, Germany, and Russia) highlighted the requirement for measurements to be taken continuously or multiple samples taken over a minimum of 24 hours to acquire the average radon concentration in homes in representative values [37]. The importance of long-term integrated monitoring is highlighted by a study that examined the seasonal variation of radon concentration in homes [38]. This study revealed large seasonal variations in the quantities of radon and its daughter gases. Their research demonstrates that the winter months have the maximum indoor radon levels, while the summer months have the least.

## 1.7 Radon in soil

Due to the prolonged half-life disintegration of uranium and radium, as well as their prevalence on the earth's surface, radon is continuously generated in soil and released into the atmosphere. There are numerous aspects that affect the concentration of radon in the soil such as the moisture of the soil, the particle size of the soil, radium concentration, and the rate at which soil-entrapped air pockets exchange with the air. Several factors including soil porosity, radon concentration in the pore spaces, and meteorological factors, such as precipitation and atmospheric pressure, determine the efficiency with which radon is eventually released into ambient air, termed exhalation. Once radon is discharged into the surrounding air, its dispersion is mainly influenced by temperature gradients, wind direction, turbulence, and vertical temperature gradients.

## 1.8 Radon in water

Radon will be absorbed by groundwater that comes into contact with rocks that contains radium. The main factors influencing radon transfer in groundwater are diffusion patterns and the mechanical movement of the water. Due to its short



radioactive half-life and low solubility in water, most of the  $^{222}\text{Rn}$  in groundwater will disintegrate before it could be released. Regardless of whether brought to the surface by natural or artificial means, the  $^{222}\text{Rn}$  contained in groundwater will undoubtedly be released into the air once it comes up to the surface. Groundwater is considered the second most significant source of environmental radon despite the fact that most of the radon will disintegrate before it reaches the surface. The annual atmospheric contribution of groundwater is thought to be around  $5 \times 10^8$  Ci  $^{222}\text{Rn}$ . The amount of  $^{222}\text{Rn}$  contamination in rural residential wells could be very significant.  $^{222}\text{Rn}$  concentrations in deep aquifers are extremely varied and are influenced by the uranium concentration of the rock, where the aquifer is located in relation to the rock, and the patterns of groundwater movement.

## 1.9 Radon and its health effects

Numerous health problems can develop as a result of radon exposure and its offspring. Radon exposure has been linked to various cancers, including kidney and prostate cancer, leukemia, and melanoma, and is known to increase the risk of developing lung cancer. Radon and its offspring were once thought to be radiation health risks that could only be found at uranium ore processing and mining sites. After smoking, radon is the second-leading cause of lung cancer [39]. Taking these reports into account, epidemiological findings provide strong evidence that radon has an influence on the development of lung cancer. In this regard, there have been initiatives to monitor radon in buildings, non-uranium mines, and locations presumed to have high atmospheric radon levels. UNSCEAR has reported that environmental radon is responsible for half of a person's radiation exposure resulting from natural sources [40].

Due to its ease of dispersion into the atmosphere, radon levels in the outdoor air are generally low. However, when radon enters a home, it can accumulate to levels that represent a serious health danger to those residing inside. When radon decays radioactively, particles like  $^{218}\text{Po}$ ,  $^{214}\text{Pb}$ ,  $^{214}\text{Bi}$ , and  $^{218}\text{Po}$  are produced. The "radon daughters" are the byproducts of radon decomposition and they are solid particles, unlike their parent gas. Radon daughters adhere to minute dust or aerosol particles in the indoor air. Although the majority of the radon gas that is inhaled is expelled, the

radon progeny that results from radon's disintegration adheres to the respiratory tract and deposits radon progeny in the tracheobronchial system of the body. Radon progeny release alpha particles into the lung, where they are received by surrounding lung tissues. The buildup of this radon progeny in the lung and its subsequent passage via the lymphatic system and blood arteries may cause other types of cancer to develop throughout the body in addition to lung cancer.

According to Henshaw et al, exposure to radon indoors raises the risk of developing leukemia and a few various cancers, including melanoma, kidney, and prostate cancers. These claims were supported by international correlation research, where rates of cancer incidence and the average indoor radon activity of different countries are compared. Numerous investigations on the connection between indoor radon levels and the occurrence of lung cancer have been conducted during the past two decades. Although some research is equivocal, some show a favorable association between radon levels and lung cancer [41-48]. According to the International Commission for Radiological Protection (ICRP), radon remedial actions are always required in residential areas. In this regard, the commission further suggests that action levels should be placed between 3 and 10 mSvy<sup>-1</sup>.

### **1.10 Global recommended value of radon**

The threat of indoor radon is not just a national but also a global concern. The following international organizations are engaged in radon research- The “World Health Organization (WHO)”, “The International Agency for Research on Cancer (IARC)”, the “United Nations Scientific Committee on the Effects of Atomic Radiation (UNSCEAR)”, and “The International Commission on Radiological Protection (ICRP)”.

Numerous nations, especially developed nations, have implemented national radon monitoring programs. Initially, radon investigations in the environment were mostly focused on outdoor air. Since the 1970s, indoor air has also been included in such type of investigation.

The Swedish Radon Commission was established in 1979, marking the beginning of the Swedish program [49]. In 1996, it had tested about 340,000 homes out of the 4.04 million total nationwide, and it was estimated that about 25,000 of them have already been mitigated. There is a limit of radon gas in Sweden that should not exceed 400 Bqm<sup>-3</sup> and corrective action is advised if they do. The recommended guideline for homes and workplaces is 200 Bqm<sup>-3</sup>.

The National Radiological Protection Board (NRPB) was established in the United Kingdom by the Radiation Protection Act of 1970 as a body to offer guidance, carry out research, and offer technical assistance in the area of radiation protection. A total of 2100 households were surveyed in detail and the results were made public. The subsequent surveys were more extensive and covered wider areas [50].

One of the key incidents that triggered extensive radon research in the United States was the incident concerning a worker at the Limerick Nuclear Power Plant in eastern Pennsylvania [51]. Stanely Watras, an employee, was discovered to activate a radiation alarm each day as he traveled to work. Later, radon gas in Watras House was identified as the source of this radiation. Watra's home had radon levels that were measured to be in the range of 105 Bqm<sup>-3</sup>. Since then, many programs have been launched by the US Environmental Protection Agency (EPA) to measure the radon levels in homes and workplaces and to begin corrective measures.

In India, sources of radon and thoron have been extensively studied, resulting in a reliable database on the country's overall exposure to radiation from the outside. Areas with high background radiation levels and soil with a high uranium content were given special consideration. The short-lived decay products make measuring <sup>222</sup>Rn, <sup>220</sup>Rn, and their offspring rather more challenging. In this regard, better methods for detecting radon inside that were developed by Mayya's team in 1998 were found to exhibit great effectiveness in reducing <sup>220</sup>Rn from <sup>222</sup>Rn and their offspring [52]. By employing this method, the Department of Atomic Energy (DAE), India, supported a statewide radon mapping program that included multiple universities and research institutions [53]. The results of this investigation demonstrate that the quantities of <sup>222</sup>Rn gas at various regions ranged from 4.6 to

147.3 Bqm<sup>-3</sup>, with a geometric mean of 23 Bqm<sup>-3</sup>. While <sup>220</sup>Rn gas levels ranged from 3.5 to 42.8 Bqm<sup>-3</sup>, with a geometric concentration range of 12.2 Bqm<sup>-3</sup>, which is lower than radon gas levels at some of these regions. Among the inhalation dosage rates resulting from <sup>222</sup>Rn, <sup>220</sup>Rn, and their progeny Kalpakkam showed the lowest doses of 0.27 mSvy<sup>-1</sup> and Digboi showed the highest (geometric mean= 0.97 mSvy<sup>-1</sup>).

In general, indoor thoron along with its offspring is about half as concentrated as radon and its offspring and produces about half the dose. Direct progeny sensors (DPS), developed by Mishra and Mayya, are a new technology for monitoring exclusively the offspring of these gases (DPS) [54]. This method makes it easier to determine the EEC of radon and thoron in an indoor setting.

The 'ICRP 60' guideline in 1993 was adopted into India's regulatory framework by the Atomic Energy Regulatory Board (AERB). The Bhabha Atomic Research Center (BARC) and several universities around the nation that are part of the IARP (Radon Measurement Groups) have reported indoor <sup>222</sup>Rn varying from 1.5 to 2000 Bqm<sup>-3</sup>, while the usual level is between 10 and 60 Bqm<sup>-3</sup> [55]. There is a significant range in radon levels, according to numerous indoor radon surveys conducted in India and other countries. Table 1.4 includes the radon concentrations in indoor air recommendations from several national and international organizations.

**Table 1.4:** National and International recommendations for Indoor Radon level.

| Recommended Radon level (Bqm <sup>-3</sup> ) | Reference   |
|--|-------------|
| 150  | USEPA, 1986 |
| 400 (for existing houses)                    | ICRP, 1984  |
| 200 (for future)                             | ICRP, 1988  |
| 250  | FRG, 1988   |
| 200  | NRPB, 1990  |
| 200 – 600 (for dwellings)                    | ICRP, 1993  |
| 500 – 1500 (for the workplace)               | ICRP, 1993  |

### 1.11 Importance of radon study in Nagaland

The present study areas were originally chosen due to their geological characteristics. The state of Nagaland in India is an area containing metamorphic, igneous, and sedimentary rocks—predominantly shale (Disang category), sandstone (Barail category), volcanic sediments, limestone, and pelagic [56]. These types of rocks and stones are known to contain naturally-occurring radioactive elements like radium, uranium, and thorium. These naturally occurring elements can break down or decay into radioactive radon gas. Depending on the amount of these materials present, they may also cause small increases in radiation levels. In this regard, the assessment of radon was carried out in the air, soil, and water in the present study region.

### 1.12 Aims and objectives of the study

The present study's objective is to investigate the levels of  $^{222}\text{Rn}$ ,  $^{220}\text{Rn}$ , and their progeny in the three districts of Nagaland viz., Mokokchung, Kohima, and Dimapur districts as it will enhance the mapping of these gases' concentrations in these locations. The three districts are so chosen because they are known to contain some of the potential radioactivity-emitting materials [57, 58]. The present study is expected to help locate the areas with noticeably higher radon and thoron levels and to gather baseline information for radon/thoron concentrations that will serve as areas of particular interest for future investigations. With these facts in mind, the objectives of the present study area have been framed accordingly:

1. To carry out gamma radiation levels in an indoor environment.
2. To study the variation of indoor levels of radon, thoron, and their progeny in various types of homes.
3. To study the variation of indoor radon, thoron, and their progeny in different seasons.
4. To estimate the radon and thoron equilibrium factors.
5. To estimate the Inhalation dose due to indoor radon, thoron, and their progeny
6. To measure the radon and thoron exhalation rates in the soil.
7. To measure the radon present in the water.

## References

1. UNSCEAR (1998) United Nations Scientific Committee on the Effects of Atomic Radiation Sources, effects and risks of ionizing radiation, New York.
2. Cohen BI (1986) A national survey of radon in US homes and correlation factors. *Health Phys* 51: 175-183. <https://doi.org/10.1097/00004032-198608000-00002>
3. Hughes JS, Shaw KB & O'Riordan MC (1989) Radiation exposure of the UK population-1988 review (No. NRPB-R--227). National Radiological Protection Board.
4. Lubin JH (1994) Radon and lung cancer risk: a joint analysis of 11 underground miners studies (No. 94). US Department of Health and Human Services, Public Health Service, National Institutes of Health.
5. BEIR VI (1999) Report of the Committee on the biological effects of ionizing radiation: health effects of exposure to radon. Natl. Res. Council. Natl. Acad. Press, Washington. <https://doi.org/10.17226/5499>
6. Smith H (1987) Lung cancer risk from indoor exposures to radon daughters. *Radiat Prot Dosim* 20: 195–196. <https://doi.org/10.1093/oxfordjournals.rpd.a080031>
7. Nazaroff WW & Nero AV (1988) Radon and its Decay Products in Indoor Air. John Wiley & Sons, New York. ISBN: 0-471-62810-7.
8. Durrani SA & Ilic R (Eds.) (1997) Radon Measurements By Etched Track Detectors-Applications In Radiation Protection, Earth Sciences. World Scientific.
9. Sabol J and Weng PS (1995) Introduction to radiation protection dosimetry, World Scientific.
10. Kigoshi K (1971) Alpha-recoil thorium-234: dissolution into water and the uranium-234/uranium-238 disequilibrium in nature. *Science* (New York, N.Y.), 173(3991): 47–48. <https://doi.org/10.1126/science.173.3991.47>
11. Tanner AB (1980) Radon migration in the ground: A supplementary review. *The Natural Radiation Environment*. 3: 161-190. Springfield, VA, National Technical Information Service.

12. Sasaki T, Gunji Y, Okuda T (2004) Radon emanation dependence on grain configuration, J Nucl Sci Technol 41(10): 993-1002. <https://doi.org/10.1080/18811248.2004.9726322>
13. Semkow TM and Parekh PP (1990) The role of radium distribution and porosity in radon emanation from solids, Geophys Res Lett 17(6): 837-840. <https://doi.org/10.1029/GL017i006p00837>
14. Thamer BJ, Nielson KK & Felthausen K (1981) Effects of moisture on radon emanation including the effects on diffusion. Open file report oct 79-Nov 81 (No. PB-83-136358). Ford, Bacon and Davis Utah, Inc., Salt Lake City (USA).
15. Sakoda A, Ishimori Y, Yamaoka K (2011) A comprehensive review of radon emanation measurements for mineral, rock, soil, mill tailing and fly ash, Appl Radiat Isot 69(10): 1422–1435. <https://doi.org/10.1016/j.apradiso.2011.06.009>
16. Schumann RR and Gundersen LC (1996) Geological and climatic controls on the radon emanation coefficient. Environment International 22: 439 – 446. [https://doi.org/10.1016/S0160-4120\(96\)00144-4](https://doi.org/10.1016/S0160-4120(96)00144-4)
17. Fleischer RL (1987) Moisture and <sup>222</sup>Rn emanation. Health Phys 52(6): 797-799. <http://pascal-francis.inist.fr/vibad/index.php?action=getRecordDetail&idt=7630000>
18. Maraziotis EA (1996) Effects of intraparticle porosity on the radon emanation coefficient. Environ Sci Technol 30(8): 2441-2448. <https://doi.org/10.1021/es950386r>
19. Tanner AB (1980) Radon migration in the ground: a supplementary review. The Natural Radiation Environment 3 161-190. Springfield, VA, National Technical Information Service.
20. Sahoo BK (2014) Modeling and Measurement of Radon and Thoron Emission from Naturally Occurring Radioactive Materials. A thesis submitted to Homi Bhabha National Institute for the Degree of Doctor of Philosophy (Physics).
21. Stranden E, Kolstad A and Lind B (1984) Radon exhalation: moisture and temperature dependence. Health Phys 47(3): 480-484.
22. Mayya, YS., Eappen, KP. and Nambi, KSV (1998) Methodology for mixed field inhalation dosimetry in Monazite areas using a twin-cup dosimeter with

- three track detectors. Rad Prot Dosim 77: 177-184. <https://doi.org/10.1093/oxfordjournals.rpd.a032308>
23. Wiegand J (2001) A guideline for the evaluation of the soil radon potential based on geogenic and anthropogenic parameters. Environ Geo 40(8): 949–963. <https://doi.org/10.1007/s002540100287>
24. UNSCEAR (1994) United Nations Scientific Committee on the effects of atomic radiation, ionizing radiation: Sources and biological effects. United Nations, New York.
25. Majumdar D (2000) Radon: not so noble. Resonance 5(7): 44–55. <https://doi.org/10.1007/BF02867246>
26. Edling C, Wingreen G & Axelson O (1986) Quantification of the lung cancer risk from radon daughter exposure in dwellings- an epidemiological approach. Environment International 12(1 – 4): 55 – 60. [https://doi.org/10.1016/0160-4120\(86\)90013-9](https://doi.org/10.1016/0160-4120(86)90013-9)
27. Ramachandran TV (2010) Environmental thoron ( $^{220}\text{Rn}$ ): A review. Iran J Radiat Res 8(3): 129-147.
28. UNSCEAR (1982) United Nations Scientific Committee on the effect of atomic radiations, ionizing radiation: Sources and biological effects, United Nations Press, New York.
29. Nussbaum E (1957) AEC Research and Development Report, UR-503, University of Rochester, Rochester, New York.
30. Kochowska E, Kozak K, Kozłowska B, Mazur J and Dorda J (2009) Test measurements of thoron concentration using two ionization chambers Alpha GUARD vs. radon monitor RAD7. Nukleonika, 54: 189-192.
31. Deka PC, Sarma H, Sarkar S, Goswami TD and Sarma BK (2009) Study of indoor radon and thoron progeny levels in surrounding areas of Nalbari, Assam, India. Indian J Phys 83(7): 1025-1030. <https://doi.org/10.1007/s12648-009-0063-6>
32. EPA (1990). Toxological profile for radon. Agency for Toxic Substances and Disease Registry, U.S. Public Health Service, In collaboration with U.S. Environmental Protection Agency.



33. UNSCEAR (1986) Sources and effects of ionizing radiation. United Nations Scientific Committee on the Effect of Atomic Radiation, United Nations, New York.
34. Ingersoll JG (1983) A survey of radionuclide content and radon emanation rates in building materials used in the U. S. A. Health Phys 45(2): 363-368. <https://doi.org/10.1097/00004032-198308000-00008>
35. Nazaroff WW, Doyle SM, Nero AV and Sextro RG (1985) Potable water as a source of airborne radon-222 in U.S. dwellings: A Review and Assessment, Lawrence Berkeley Laboratory Report (LBL-18514). Berkeley, CA. <https://doi.org/10.1097/00004032-198703000-00002>
36. Davies BL and Forward J (1970) Measurement of atmospheric radon in and out of doors. Health Phys 19, 136.
37. Gesell TF (1983) Background atmospherics <sup>222</sup>Rn concentrations outdoor and indoors: A review, Health Phys 45(2): 289-302. <https://doi.org/10.1097/00004032-198308000-00002>
38. Ramachandran TV, Muraleedharan TS, Shaikh AN, Subba Ramu MC (1990) Seasonal variation of indoor radon and its progeny concentration in a dwelling. Atmos Environ 24(3): 639-643. [https://doi.org/10.1016/0960-1686\(90\)90019-J](https://doi.org/10.1016/0960-1686(90)90019-J)
39. Sevc J, Kunz E, Placek V (1976) Lung cancer in uranium miners and long-term exposure to radon daughter products. Health Phys 30(6): 433-437. <https://doi.org/10.1097/00004032-197606000-00001>
40. UNSCEAR (2000). Annexure B. Exposures from natural radiation, Report to the General Assembly with Scientific Annexes, United Nations. 97-105.
41. Henshaw DL, Eatough JP and Richardson RB (1990) Radon as a causative factor in induction of myeloid leukaemia and other cancers. Lancet 355(8696): 1008-1012. [https://doi.org/10.1016/01swed6736\(90\)91071-h](https://doi.org/10.1016/01swed6736(90)91071-h)
42. Archer V E, Wagoner JK & Lundin FE (1973) Lung cancer among uranium miners in the United States. Health Phys 25(4): 351-371. <https://doi.org/10.1097/00004032-197310000-00001>
43. Waxweiler RJ, Roscoe RJ, Archer VE, Thun MJ, Wagoner JK & Lundin Jr FE (1981) Mortality follow-up through 1977 of the white underground

uranium miners cohort examined by the United States Public Health Service. In Radiation hazards in mining: control, measurement, and medical aspects.

44. Sevc J, Kunz E, Tomasec L, Placek V and Horacek J (1998) Cancer in man after exposure to Rn daughters. Health Phys 54: 27-46. <http://dx.doi.org/10.1097/00004032-198801000-00001>
45. Pershagen G, Liang ZH, Hrubec Z, Svenson C and Boice Jr JD (1993) Residential radon exposure and lung cancer in Swedish women. Health Phys 63(2): 179-186. <https://doi.org/10.1097/00004032-199208000-00004>
46. Bochicchio F, Forastiere F, Abeni D and Rapiti E (1998) Epidemiologic Studies on Lung Cancer and Residential Exposure to radon in Italy and Other Countries. Radiat. Prot Dosim 78(1): 33-38. <https://doi.org/10.1093/oxfordjournals.rpd.a032329>
47. Fisher EL, Field RW, Smith BJ, Lynch CF, Steck DJ & Neuberger JS (1998) Spatial variation of residential radon concentrations: the Iowa Radon Lung Cancer Study. Health Phys 75(5): 506-513. <https://doi.org/10.1097/00004032-199811000-00007>
48. Field RW, Steck DJ, Smith BJ, Brus CP, Fisher EL, Neuberger JS, Charles EP, Robinson RA, Woolson RF, Lynch CF (2000) Residential Radon Gas Exposure and Lung Cancer: The Iowa Radon Lung Cancer Study, Am J Epidemiol 151(11): 1091–1102. <https://doi.org/10.1093/oxfordjournals.aje.a010153>
49. Swedjemarm, GA (1996) Swedish radon program. Environ. Radon Newsletter, 6, 4.
50. Wrixon AD, Green BMR, Lomas PR, Miles JCH, Cliff KD, Francis EA, Driscoll CMH, James AC, O’Riordan MC (1988) Natural radiation exposure in UK dwellings, A report to National Radiological Protection Board, Report No NRPB-R - 190, ISBN: 0-85951-260-6.
51. Joyce C, Kenward M, & Pearce F (1986) SCIENCE ACROSS THE UNITED-STATES-PERILS IN THE ALL-AMERICAN HOME. New Scientist, 110(1511), 22.
52. Mayya YS, Eappen KP, Nambi KSV (1998) Methodology for mixed field inhalation dosimetry in monazite areas using a twin-cup dosimeter with three track detectors. Radiat Prot Dosim 77: 177–184. <https://doi.org/10.1093/oxfordjournals.rpd.a032308>

53. Ramachandran TV, Eappen KP, Nair RN, Mayya YS, & Sadasivan S (2003) Radon-thoron levels and inhalation dose distribution patterns in India dwellings (No. BARC--2003/E/026). Bhabha Atomic Research Centre.
54. Mishra R & Mayya YS (2008) Study of a deposition-based direct thoron progeny sensor (DTPS) technique for estimating equilibrium equivalent thoron concentration (EETC) in indoor environment. Radiat Meas 43(8): 1408-1416. <https://doi.org/10.1016/j.radmeas.2008.03.002>
55. IARP (1994) Indian Association for Radiation Protection, Ubiquitous Radon, Special Issue, IARP, Bombay, Vol. 17, No. 3 & 4, July-December, 100 pages.
56. Ao A, Bhowmik SK (2014) Cold subduction of the Neotethys: the metamorphic record from finely banded lawsonite and epidote blueschists and associated metabasalts of the Nagaland Ophiolite Complex, India. J Metamorph Geol 32: 829–860. <https://doi.org/10.1111/jmg.12096>
57. Sinha D, Sinha UB, Kibami D, Pongener C, Mishra R, Prajith R, Mayya YS (2013) Measurement of Radon and Thoron progeny concentration in some dwellings of Nagaland state- an initial report. J Appl Chem 2: 825–831.
58. Singh AK, Khan AJ, Prasad R (1997) Distribution of  $^{222}\text{Rn}$  levels in Indian dwellings. Radiat Prot Dosim 74: 189–192. <https://doi.org/10.1093/oxfordjournals.rpd.a032196>

## **CHAPTER- 2**

### **METHODOLOGY**

---

*In this chapter, the formulas utilized and the protocols used for the measurement of radon present in the soil, air, and water is provided. Furthermore, a thorough discussion of the detectors, techniques, and theory behind the calibration of the techniques utilized in the current study is also included.*

---

## 2.1 Introduction

This chapter includes a detailed description of detectors, instrumentations, and the methodology used for this present study. The detectors used in the present study are pinhole twin cup dosimeter and direct thoron/radon Progeny Sensors (DTPS/DRPS) in determining the progeny concentrations. Equilibrium factors and inhalation doses are calculated from the obtained experimental data using the related equation. A portable scintillation-based Radon/Thoron monitor known as Smart RnDuo is used for radon mass exhalation rate and thoron surface exhalation rate from the study area. The necessary methodology and the different related equations involved in calculating the radon, thoron, and their progeny, the radioactivity content of soil samples with the calculations of equilibrium factor and inhalation doses are discussed and explained thoroughly in this chapter.

## 2.2 Radon Measurement Techniques

To measure and monitor the concentrations of  $^{222}\text{Rn}$ ,  $^{220}\text{Rn}$ , and their progeny in the air, soil, and water, a variety of tools and methods are available. Each has particular advantages and disadvantages when it comes to measurement accuracy, etc. These devices can be widely classified into active or passive. The terms active and passive reflect their operating modes, with active devices requiring a power source and passive devices requiring no power to operate.

Most of these devices have a common operating concept, which is the detection of alpha particles generated during the decay process of radon, thoron, and their offspring, although some are designed to detect beta and gamma rays as well. Active techniques are often used for short-term measurement, whereas passive techniques are usually employed for long-term measurement. The detector employed in this study is LR-115 Type-II film. The devices used are single-entry pin-hole dosimeters, direct radon and thoron progeny sensors for indoor investigations, and Smart RnDuO, which is typically used for in-situ measurement and occasionally for continuous measurement in an indoor environment. Additionally, devices such as a constant water bath and spark counter are used for processing the detectors after retrieval. In general, measuring techniques are categorized into two types.

1) Passive or Time integrated long-term radon measurement techniques

## 2) Active or Instantaneous radon measurement technique

The following section discusses passive techniques involved in radon measurements.

### 2.2.1 Passive technique

Time-integrated methods include radon buildup over a longer period of time, ranging from a few days to a week or more. Radon is measured in these approaches either directly by detecting the alpha emission or by detecting the radioactive decay products of radon.

#### 2.2.1.1 Solid-State Nuclear Track Detectors (SSNTD)

The detector used in the passive technique is a Solid-State Nuclear Track Detectors which has a wide range of applications in radon monitoring techniques ranging from soil gas to indoor environments. As per the current research scenario, LR-115 and CR-39 plastic detectors are commonly used. These detectors are particularly designed to detect alpha particles released by radioactive materials such as uranium and thorium during the decay process. The released alpha radiation damages the detector, causing tracks to develop, and the recorded tracks are then converted to activity concentrations of radionuclides, primarily radon and thoron.

Thus, in our present work, LR-115 was used which is manufactured by Kodak Pathe, France under the trade name LR-115. It is made up of a thin layer of deep red cellulose nitrate film coated on a polyester-based substrate 100  $\mu\text{m}$  thick. The chemical composition of cellulose nitrate film is  $\text{C}_6\text{H}_8\text{O}_6\text{N}_{12}$  and its specific gravity is 1.4. Based on the thickness of the cellulose nitrate layer, LR-115 detectors are divided into two types. The type-I films have 6  $\mu\text{m}$  thick cellulose nitrate coating, while type-II has 12  $\mu\text{m}$  cellulose nitrate coating. The cellulose nitrate film is sensitive to alpha particles in the energy range of 1.9 – 4.2 MeV [1, 2]. While, the LR-115 type II plastic detector due to its special design does not record the background tracks and is not altered by electrons or by radiations in the electromagnetic spectrum such as gamma rays, X-rays, or infrared radiations and visible light (figure 2.1). It starts to record the tracks only when its sensitive surface is exposed to the atmosphere or only when it is in contact with alpha particles having energy within the energy range [3].

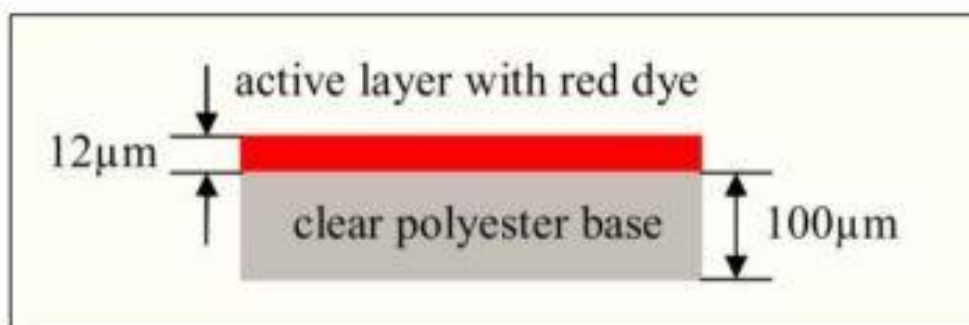


**Fig. 2.1:** LR-115 detector schematic diagram.

#### 2.2.1.2 Charged particle tracks in polymers

Charged particle tracks in polymers excluding fields like geology and high-temperature environments such as nuclear reactors and polymeric plastic detectors are being used universally. They are broadly used in radon-related studies, neutron monitoring, space research, etc. Some of their notable properties include good geometry and their ability to integrate responses over large-scale measurements. Amongst the known nuclear track detectors, plastics are the most sensitive due to their ability to record very low-charge projectiles up to the level of the proton, but they are insensitive to  $\beta$ -particles.

In organic polymers, the passage of heavily charged particles results in scissions polymer chains as shown in figure 2.2. A thermal spike along the trajectory of the charged particles causes localized melting, and this, along with excitation leads to chain breaking and the production of new chain ends. According to Durrani and Bull [4], in plastics, ionized and excited molecules and electrons are produced by ionizing radiations.

Excited energy can be transferred from one molecule to another. Perhaps the electrons that are trapped at different sites combine with molecules/positive ions to form negative ions/excited molecules respectively. Both the ions and excited molecules may obtain a significant amount of vibrational energy and undergo bond rupture to form a complex array of stable molecules, free radicals, and ionized molecules. As a result, the net effect on the plastic will be the production of many broken molecular chains

and the production of a damaged region known as a latent track thereby reducing the average molecular weight of the polymers.

On treating the plastic with a proper etchant such as an aqueous NaOH solution, the scission part is dissolved, and the hole formed is broadened by factors of  $10^2$  -  $10^3$ . The damaged trails stay permanently as ‘tracks’, unaffected by heat to avoid annealing. The size of the etched track depends essentially on the rate of energy transfer of the charged particle over its trajectory.

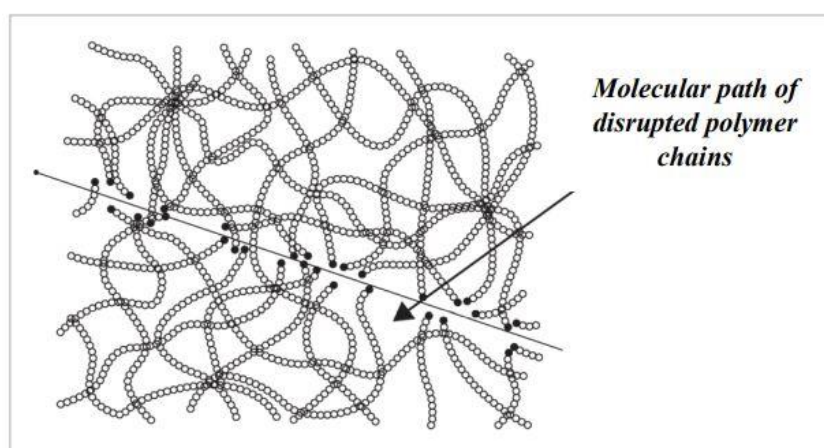


**Fig. 2.2:** Schematic diagram of Chain scission in polymers.

### 2.2.1.3 Etching

Chemical etching is the process of using an appropriate chemical agent to enlarge the latent radiation damage pathways. One of the methods for measuring  $^{222}\text{Rn}$ ,  $^{220}\text{Rn}$ , and progeny that is most frequently employed is the track-etch method [5, 6]. In this method, a solid-state nuclear track detector (SSNTD) serves as the monitoring instrument.

Normally, chemical etching is performed in a temperature-controlled water bath, operated at a temperature range of  $40^\circ\text{C}$  to  $70^\circ\text{C}$ . However, in some exceptional cases, a temperature of  $90^\circ\text{C}$  can also be used. Etchant in the form of aqueous solution such as NaOH or KOH is used usually at 2.5 N (normality). The duration for etching may vary from 1.5 to 6 hours, depending on the bulk etch rate calibration of the detectors.



In order to enhance the sensitivity in the track registration of some detectors, ethyl alcohol can also be added [4, 7].

Depending on the average exposure rate and exposure period, the detector's amount of tracks per unit area increases. While many other types of detector materials have been created, the two most often utilized track detectors for integrated radon studies are undoubtedly LR-115 and CR-39. In the track-etching technique, there are several advantages such as convenience as it does not require electric power, is inexpensive, and is efficient in conducting large-scale radon surveys.

#### 2.2.1.4 Constant water bath

In the present study, an etching bath using 2.5N NaOH solution at 60°C for 90 minutes is used to etch the exposed films (LR-115) from DTPS/DRPS and dosimeter. It can accommodate around  $24 \times 3$  films for etching at once (figure 2.3). It is built with two walls and features an electrical temperature controller. Track density counting was performed after the detector had been chemically etched and cleaned in running water and the cellulose nitrate layer pilled off from a polyester-based substrate.

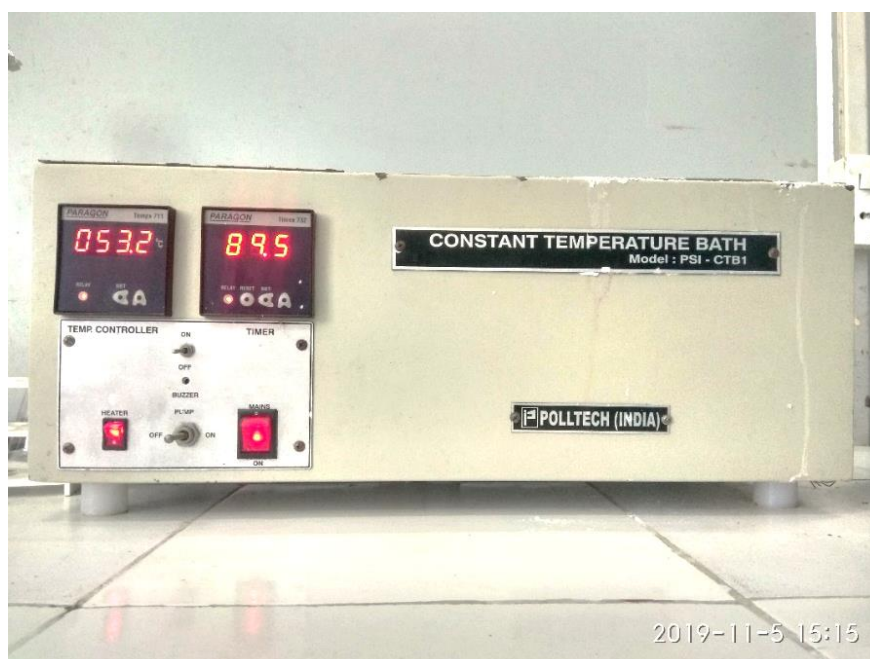


**Fig. 2.3:** Temperature-controlled water bath

### 2.2.1.5 Spark Counter

The Spark counting technique was first invented by Cross and Tommasino in 1970 (Cross and Tommasino, 1970) [8]. This is the most widely used non-optical technique for alpha particle track counting and is especially useful for the counting of low track densities in the order of  $\leq 10^3 \text{ cm}^{-2}$ . The Spark Counter Model used in the present work is PSI-SC1 (figure 2.4a).

The process of counting is carried out by placing the aluminized mylar film over the etched detector (figure 2.4b), thus creating a conducting path between the electrodes. The presence of an electric current helps the spark to percolate the aluminum foil just above the hole to avoid the spark going through the same hole.



**Fig. 2.4a:** Spark counter photo.



**Fig. 2.4b:** Mylar placed over LR-115.

The operating voltage of a Spark counter is the specific voltage by which the counting of tracks should be done. Normally, when the instrument purchased is used for the first time, it is necessary to set an operating voltage which is usually done by plotting a graph between applied voltage and counts, and as a result, a plateau region/curve is produced as shown in figure 2.5. Prior to actual track counting, it is always necessary to apply a higher voltage to the track detector to punch out those tracks which have not been completely etched through. In practice, pre-sparking at 700 to 900 V is carried out before the actual track counting. The graph plotted between applied voltage and the tracks obtained per unit area (counts) is shown in figure 2.5.

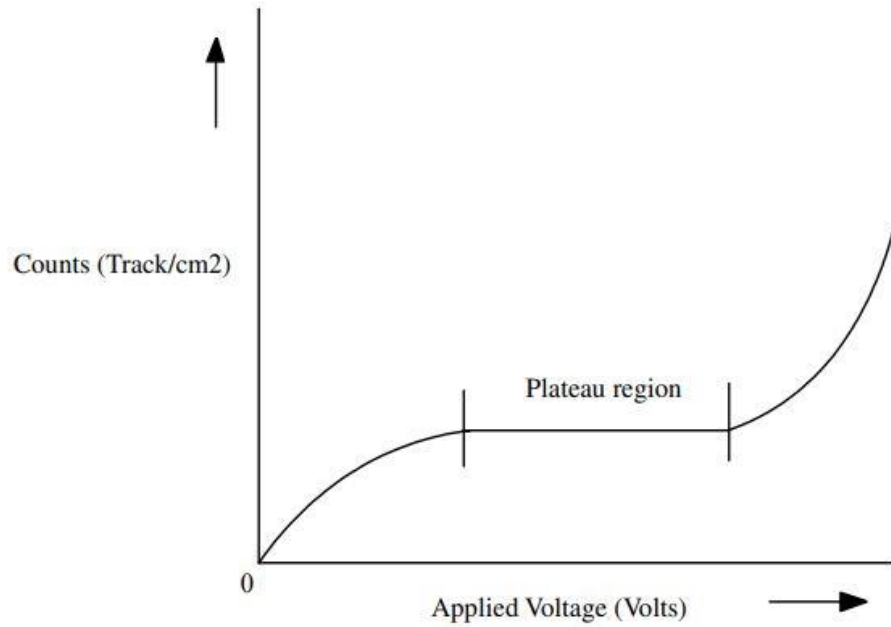


**Fig. 2.5:** Applied voltage vs Count showing the plateau region.

#### 2.2.1.6 Pinhole twin cup dosimeter

In the present study, time-integrated parent  $^{222}\text{Rn}$  and  $^{220}\text{Rn}$  concentrations were measured using the single-entry twin-cup pinhole dosimeter (figure 2.6) [9].

The main motive for the use of this pinhole twin-cup dosimeter was to remove the interference from decay products in  $^{222}\text{Rn}$  and  $^{220}\text{Rn}$  gas and to obtain the  $^{222}\text{Rn}$  and  $^{220}\text{Rn}$  gas concentrations only [10].

The dosimeter consists of two chambers and a central pinhole disc separates them. Each chamber is cylindrical in shape having a length of 4.1 cm and a radius of 3.1 cm. The dosimeter has a single face entry through which the gas enters into the first chamber known as the ' $^{222}\text{Rn} + ^{220}\text{Rn}$ ' chamber via a glass filter paper ( $0.56\mu\text{m}$ ) and the gas further ascends to the second chamber known as the ' $^{222}\text{Rn}$ ' chamber. The detectors in the first chamber register the tracks produced due to both  $^{222}\text{Rn}$  and  $^{220}\text{Rn}$  while the detectors in the second chamber detect the tracks produced due to  $^{222}\text{Rn}$  only. It is pertinent to mention that  $^{222}\text{Rn}$  transmission through pinhole plates is 98% and  $^{220}\text{Rn}$  transmission is less than 2% [9].

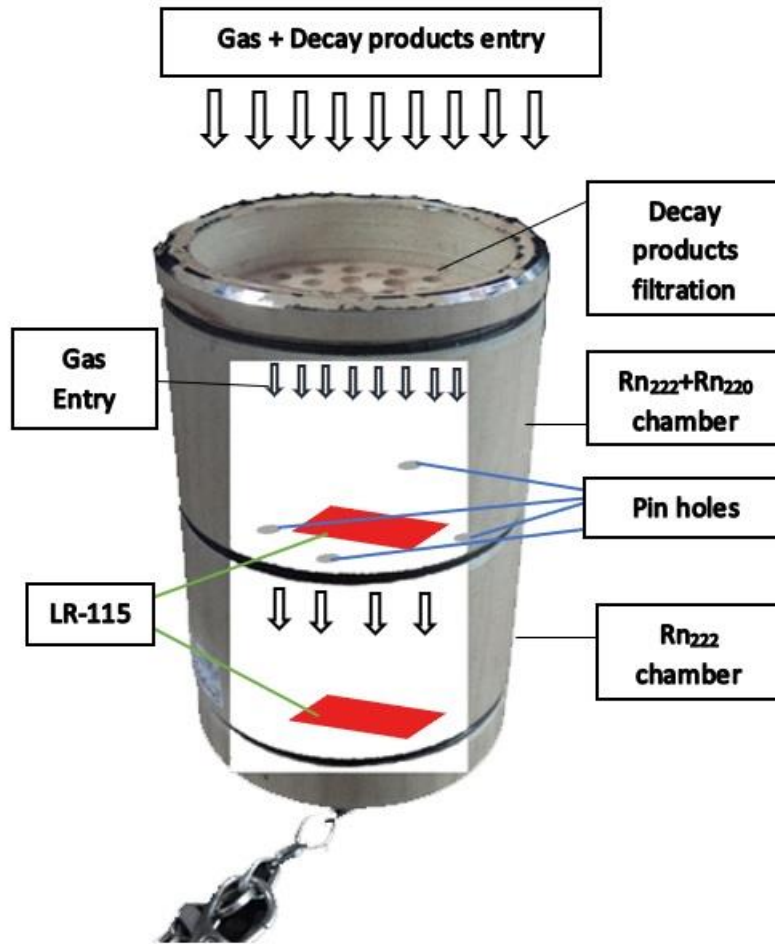


**Fig. 2.6:** Twin cup pinhole dosimeter schematic diagram.

#### 2.2.1.7 Direct radon/thoron progeny sensors (DRPS/DTPS)

Time-integrated radon and thoron progeny were measured using deposition-based direct progeny sensors (figure 2.7). The main advantage of this technique is that there is no interference from gas and thus it gives a direct estimation of the airborne concentration of the alpha-emitter progeny. DTPS/DRPS consists of a passive nuclear track detector (LR-115) with an aluminized mylar mounted over it which acts as an absorber. For  $^{220}\text{Rn}$  progeny (DTPS), the absorber is 50 microns in thickness and detects only 8.78 MeV emitted from thoron progeny ( $^{212}\text{Po}$ ). In the case of DRPS, the absorber for  $^{222}\text{Rn}$  progeny is a 25micron aluminized mylar mounted over 12micron LR-115 (Cellulose Nitrate) i.e., a total thickness of 37microns which selectively detects the required 7.69 MeV alpha particles emitted from radon progeny ( $^{214}\text{Po}$ ) [11]. The calibration factor of DTPS and DRPS for indoor environments is 0.94

$\text{Trcm}^{-2}\text{d}^{-1}/\text{EETC}$  ( $\text{Bqm}^{-3}$ ) and  $0.09 \text{ Trcm}^{-2}\text{d}^{-1}/\text{EETC}$  ( $\text{Bqm}^{-3}$ ) respectively. The DTPS has no interference from Radon progeny because the thickness of the absorber foil is so calibrated that it does not register even the highest alpha particle energy from Radon progeny i.e., 7.69 MeV. The thoron progeny alpha has interference in DRPS which is taken care of while estimating the EERC. DRPS and DTPS are calibrated for the aerosol concentration between 15,000 and 40,000  $\text{pcm}^{-3}$  (average  $\sim 20 \text{ Kpcm}^{-3}$ ) and a ventilation rate between 0.5 and  $1.5 \text{ h}^{-1}$ . These conditions were established for Indian dwellings in general. So, the calibration factors remain constant in these environmental parameter ranges [11, 12].

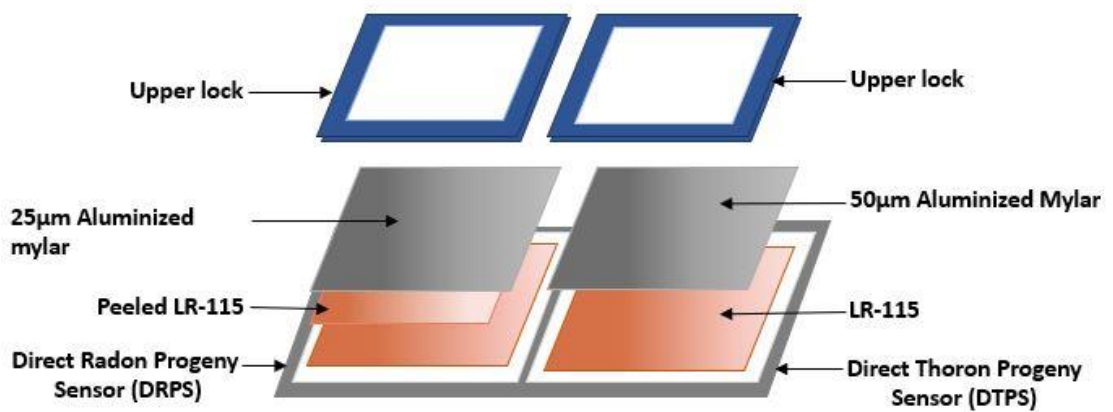


Fig. 2.7: DTPS/DRPS schematic diagram.

### 2.2.2 Active technique

Active methods involve estimating radon buildup over a short period of time. The instrument used in this technique is a portable Smart RnDuo. Radon is measured in these approaches directly by detecting the alpha emitted from radon, thoron, and their progeny. In the present case, the active technique has been used for the determination of radon in soil and water. The following section discusses the instrument used for this present study.

#### 2.2.2.1 Portable Smart Rn Duo (Radon monitor)

Smart RnDuo is a portable and continuous monitor, designed at Bhabha Atomic Research Centre, BARC, Mumbai, and manufactured by Aqtek Systems Pvt. Ltd, Mumbai for multiple applications in radon and thoron studies (figure 2.8) [13]. It

works on the principle of scintillation (ZnS:Ag) by detecting alpha particles emitted from radon, thoron, and their progeny. The alpha counts are converted to radon/thoron activity concentration with the help of an algorithm that is built based on radioactive decay and growth laws incorporated in the microcontroller.



**Fig. 2.8:** Photograph of the Smart Rn Duo.

The algorithm is based on the theoretical decay and growth of decay products of radon during the ongoing measurement cycle and from the preceding radon concentration. Some of the important features of Smart RnDuo (table 2.1) [14].

**Table 2.1:** Smart RnDuo specifications.

|                           |   |
|---------------------------|---|
| Scintillation cell volume | 153 cm <sup>3</sup>   |
| Sensitivity               | 1.2 CPH/(Bqm <sup>-3</sup> )  |
| Sampling type             | Diffusion/Flow  |
| Sampling flow rate        | 0.5 to 2 L/min  |
| Memory                    | Approximately 32000 readings can be stored                              |
| Response time             | 15 minutes for <sup>222</sup> Rn/ <sup>220</sup> Rn levels to reach 95% |
| Detection range           | 8 Bqm <sup>-3</sup> to 50 MBqm <sup>-3</sup>                            |



The alpha counts obtained are processed by a microprocessor unit as per the developed algorithm to display the concentration of radon. Thus, this device is not affected by humidity since it is based on direct scintillation with silver-activated zinc sulphide. Furthermore, this instrument has appreciably high sensitivity and relatively low detector volume making it more suitable for sample analysis.

## **2.3 Present Study**

In the present study, indoor radon measurements have been carried out by using a passive technique that involves the estimation of radon/thoron gas, equivalent equilibrium concentration (EEC), determination, Equilibrium factor (E.F), and total inhalation dose. While the active technique has been used for the determination of radon mass exhalation rate/thoron surface exhalation rate of the soil as well as for the determination of radon present in water.

## **2.4 Indoor radon measurement**

The indoor radon study has been measured in Mokokchung, Dimapur, and Kohima districts. The details of the study will be given in each chapter.

### **2.4.1 Selection of dwellings**

The selection of dwellings was based on a preliminary gamma survey and statistics of different types of houses in the study region. Initially, before the deployment of the detectors, gamma dose rate measurements were carried out in the different types of selected houses using a portable gamma survey meter (Polimaster/PM-1405, Republic of Belarus). The survey meter has a response to gamma energies varying from 0.04 to 3 MeV and has a detection range varying from  $0.01 \mu\text{Svh}^{-1}$  to  $130 \text{ mSvh}^{-1}$ . During the gamma survey in the study region, the readings were taken at 1 m height from the ground to get a converged value of the gamma dose rate. The gamma dose rate served as an index for the radioactivity content variation in the study region. Based on the gamma dose rate readings obtained from the survey, the villages in the study region were categorized into 3 different gamma zones in each study region. Subsequently, the data on the different types of houses in the study region were collected from the database of the housing census of India. Houses of the study region were categorized

based on the type of building materials used for construction viz., Type 1 (houses with brick walls and brick roof, and cemented floor), Type 2 (houses with wooden walls and wooden roof, and cement floor), Type 3 (houses with bamboo walls and bamboo roof and cement floor), Type 4 (the floor is cemented, walls and roof is made of concrete), Type 5 (the floor is cemented, the roof is either made of wooden or bamboo, walls are made of half cement and half wooden/bamboo). A gamma zone-wise house statistic table was made and then multivariate regression analysis was carried out to estimate the optimum number of the dosimeter to be deployed in each type of house in the respective gamma zone.

#### **2.4.2 Deployment of Dosimeters**

After the selection of dwellings according to the above protocol, dosimeters were deployed in the study region. As per the regression analysis, dosimeters were deployed in the selected houses, and a set of detectors (Pinhole based radon-thoron discriminating dosimeter, Direct Radon and Thoron Progeny Sensors) were deployed in each of these houses by suspending 90 cm away from the wall (care was taken to expose these dosimeters in the living room). The assessment was done for three different seasons to understand the seasonal variation pattern of  $^{222}\text{Rn}$ ,  $^{220}\text{Rn}$ , and their progeny levels in the study area. The annual year was divided into summer, rainy, and winter seasons each comprising nearly 120 days (4 months) where LR-115 film is being replaced on a quarterly basis to assess seasonal variation of different indoor parameters. In winter, doors, and windows are normally kept closed and heating devices are used, while during the rainy season, mostly doors and windows are kept closed, but heating devices are not used. However, unlike during the winter and rainy seasons, doors and windows are kept open during summer.

#### **2.4.3 Retrieval of dosimeter and etching**

Following the exposure period, the exposed detectors were removed, and a new detector is deployed for another period of exposure at the same house where the detectors were kept. The retrieved detectors were taken to the laboratory and then subjected to chemical etching in 2.5N NaOH solutions at a constant temperature of 60°C for about 90 minutes. These films were then washed in running tap water and kept in a tissue roll for drying. The alpha tracks formed on the films are counted by



using the standard spark counter at an operating voltage of 500 V prior to a pre-sparking voltage of 900V [9].

#### 2.4.4 Calculation of indoor radon and thoron concentration.

The track density formed by the parent radon/thoron gas on LR-115 inside the pinhole twin cup dosimeter can be used directly in calculating radon/thoron concentration. Thus, the  $^{222}\text{Rn}$  concentration,  $C_r$  ( $\text{Bqm}^{-3}$ ), and  $^{220}\text{Rn}$  concentration,  $C_t$  ( $\text{Bqm}^{-3}$ ) were calculated using the formulas given below [9].

$$C_r = \frac{T_1}{d.K_r} \quad (1)$$

$$C_t = \frac{T_2 - T_1}{d.K_t} \quad (2)$$

where  $T_1$ ,  $T_2$  are the tracks registered in ' $^{222}\text{Rn}$ ' and ' $^{222}\text{Rn} + ^{220}\text{Rn}$ ' compartments respectively,  $d$  corresponds to exposure time in days.  $K_r = 0.017 \pm 0.002 \text{ tr.cm}^{-2}\text{d}^{-1} \text{ Bqm}^{-3}$  and  $K_t = 0.010 \pm 0.001 \text{ tr.cm}^{-2}\text{d}^{-1} \text{ Bqm}^{-3}$  are the calibration factors of  $^{222}\text{Rn}$  and  $^{220}\text{Rn}$  in the pinholes twin cup dosimeters [9].

#### 2.4.5 Calculation of progeny concentration.

The activity concentration of  $^{222}\text{Rn}/^{220}\text{Rn}$ , which would have been in equilibrium with a non-equilibrium mixture of short-lived  $^{222}\text{Rn}/^{220}\text{Rn}$  offspring in the air is called equilibrium equivalent concentration (EEC) [15]. The progeny of  $^{220}\text{Rn}/^{220}\text{Rn}$  was measured using passive detectors based on depositions such as DTPS and DRPS in bare modes [11].

To determine the track densities found on the LR-115 detectors, a spark counter was utilized in accordance with standard track etching techniques. EETC and EERC can be calculated using the track density that results from DTPS and DRPS, respectively. However, the  $\alpha$ -energy of thoron progeny ( $^{212}\text{Po}$ ) is much higher than that of radon progeny ( $^{214}\text{Po}$ ), and there is a high chance of its interference in the registered tracks on the DRPS element. Therefore, the contribution of thoron progeny tracks in DRPS was subtracted for estimating the tracks due to radon progeny alone in DRPS. Thus, the Equilibrium Equivalent Concentrations of Radon (EERC) and Thoron (EETC) are determined using equations (3) and (4) [11, 12].

$$\text{EERC} = T_c (\text{Tracks.cm}^{-2}.\text{d}^{-1} / S_R (\text{Tracks.cm}^{-2}.\text{d}^{-1} / \text{EEC (Bqm}^{-3}) \quad (3)$$

$$\text{EETC} = T_c (\text{Tracks.cm}^{-2}.\text{d}^{-1} / S_T (\text{Tracks.cm}^{-2}.\text{d}^{-1} / \text{EEC (Bqm}^{-3}) \quad (4)$$

where  $S_R = 0.09$  corresponds to the sensitivity factor for Radon progeny in DRPS and  $S_T = 0.94$  is the sensitivity factor for Thoron progeny in DTPS, and  $d$  corresponds to the exposure period in days [16].

#### 2.4.6 Equilibrium factor (E.F)

E.F is determined by dividing  $\alpha$ -energy for actual daughter concentrations by the total potential  $\alpha$ -energy of the daughter in equilibrium with the  $^{222}\text{Rn}/^{220}\text{Rn}$  concentration. According to the literature based on inhalation dosimetry,  $\text{E.F}_T$  is traditionally expressed as the track density estimated for exposure to one day in an environment containing 1  $\text{Bqm}^{-3}$  of EETC. In a similar manner, after deducting the track density estimated from 1  $\text{Bqm}^{-3}$  of EETC, the track density for a 1-day exposure to an environment containing 1  $\text{Bqm}^{-3}$  of EERC is represented by  $\text{E.F}_R$ . Thus, the E.F for the radon/thoron is of the utmost interest in passive dosimetry applications. The formulas used to obtain the equilibrium factor of radon and thoron are calculated by using equations (5) and (6) respectively [11].

$$\text{E.F}_R = \text{EERC (Bqm}^{-3}) / C_r (\text{Bqm}^{-3}) \quad (5)$$

$$\text{E.F}_T = \text{EETC (Bqm}^{-3}) / C_t (\text{Bqm}^{-3}) \quad (6)$$

#### 2.4.7 Inhalation dose

Annual inhalation dose is the amount of radon and/or thoron inhaled per year ( $\text{mSvyr}^{-1}$ ) by the individuals inside the dwellings. Utilizing the measured concentrations of the parent and progeny nuclei, the inhalation dose can be determined. For a minimum of 3 months, the dosimeters along with DTPS/DRPS were deployed in different types of selected dwellings.

The annual effective dose due to exposure to  $^{222}\text{Rn}$ ,  $^{220}\text{Rn}$ , and their progeny is estimated using the standard UNSCEAR equations given below, where an indoor occupancy of 7000 hr per year is considered [16, 17].

$$\text{TID}_r (\text{mSvy}^{-1}) = [(C_r \times 0.17) + (\text{EERC} \times 9)] \times 8760 \times 0.8 \times 10^{-6} \quad (7)$$

$$\text{TID}_t (\text{mSvy}^{-1}) = [(C_t \times 0.11) + (\text{EERC} \times 40)] \times 8760 \times 0.8 \times 10^{-6} \quad (8)$$

where the values, 0.17, and 0.11 nSvBq<sup>-1</sup> h<sup>-1</sup>m<sup>3</sup> are the dose conversion factor of radon and thoron concentrations respectively and values 9, and 40 nSvBq<sup>-1</sup> h<sup>-1</sup>m<sup>3</sup> are the dose conversion factors of radon and thoron progeny concentrations respectively. 0.8 is the standard occupancy factor for a period of one-year exposure [16, 17]. The estimated inhalation dose based on the level of radon and thoron as averaged around the globe is shown in table 2.2.

**Table 2.2:** Average global level of <sup>222</sup>Rn, <sup>220</sup>Rn, and their offspring in the atmosphere, along with their associated annual effective doses [18].

| Radionuclide   | Location | Concentration (Bqm <sup>-3</sup> ) |                  | Effective dose equivalent (nSv/Bqhm <sup>-3</sup> ) |                  | Annual effective dose (μSv) |                  |
|--|----------|------------------------------------|------------------|---|------------------|-----------------------------|------------------|
|  |          | Gas                                | EEC <sup>+</sup> | Gas   | EEC <sup>+</sup> | Gas                         | EEC <sup>+</sup> |
| Radon  | Outdoor  | 10                                 | 6                | 0.17  | 9                | 3                           | 95               |
|  | Indoor   | 40                                 | 16               | 0.17  | 9                | 48                          | 1009             |
| Total (Numerical)  |          |                                    |                  |   |                  |                             | 1155             |
| Thoron   | Outdoor  | 10                                 | 0.1              | 0.11  | 40               | 2.0                         | 7.0              |
|  | Indoor   | 10                                 | 0.3              | 0.11  | 40               | 8.0                         | 84               |
| Total (Numerical)  |          |                                    |                  |   |                  |                             | 101              |
| Total annual effective dose equivalent due to radon and thoron (μSv) |          |                                    |                  |   |                  |                             | 1256             |

+ is the EEC of <sup>222</sup>Rn and <sup>220</sup>Rn and is determined by multiplying gas concentration with the E.F. For radon, the E.F. was determined to be 0.6 for outdoor exposure and 0.4 for indoor exposure. While for thoron, E.F. is calculated as 0.01 for outdoor and 0.03 for indoors.

\* When calculating the annual effective dose, occupancy factors of 0.2 for outdoor exposure and 0.8 for indoor exposure are used [18].

## 2.5 <sup>222</sup>Rn and <sup>220</sup>Rn exhalation rates from the soil

In addition to the indoor radon measurement, another very important study is to find out the measurement of radon present in the soil. Among all radiation sources, soil

infiltration is considered the primary source of indoor radon. Radon is released from the soil into the environment via exhalation and emanation processes. In this regard, radon measurements namely radon mass exhalation rate and thoron surface exhalation rate in the soil were also carried out using the Smart RnDuo monitor.

In the present study, radon measurement in the soil was performed in Mokokchung, Dimapur, and Kohima districts and the details of the study will be discussed in chapter 6. Given below are some of the steps involved in the study of radon/thoron exhalation rates from the soil.

### **2.5.1 Collection of soil samples**

In the present study, soil samples were collected from the region where the detectors are being exposed. The soil samples were dug at a minimum depth of 30 cm and this depth may further be increased depending on the availability of the base layer soil. A grub hoe is used for digging the soil and the collected samples are packed in an air-tight plastic bag and then finally brought to the laboratory for sample analysis.

### **2.5.2 $^{222}\text{Rn}$ mass exhalation rate measurement**

For the  $^{222}\text{Rn}$  mass exhalation rate ( $J_m$ ) measurement, an accumulation chamber of proper dimension is used. Before the measurement is carried out, firstly the weight of the soil sample is weighed using a weighing balance after which the samples are filled up to the neck of the exhalation chamber. The chamber is then attached to the main processing device-Smart RnDuo (figure 2.9) using a suitable connecting cable. When the arrangement is complete, the device is switched 'ON', and the configuration of a few parameters needs to be performed which includes selecting the Radon mode and a few more settings. The measurement time is usually maintained over a duration of 11 to 12 hours. The model equation may be used to fit the radon data after the measurements are finished, and the build-up data of radon will be available with elapsed time.

At the end of the measurements, build-up data of radon with elapsed time can be retrieved and the least square fitting may be carried out using the model equation [19].

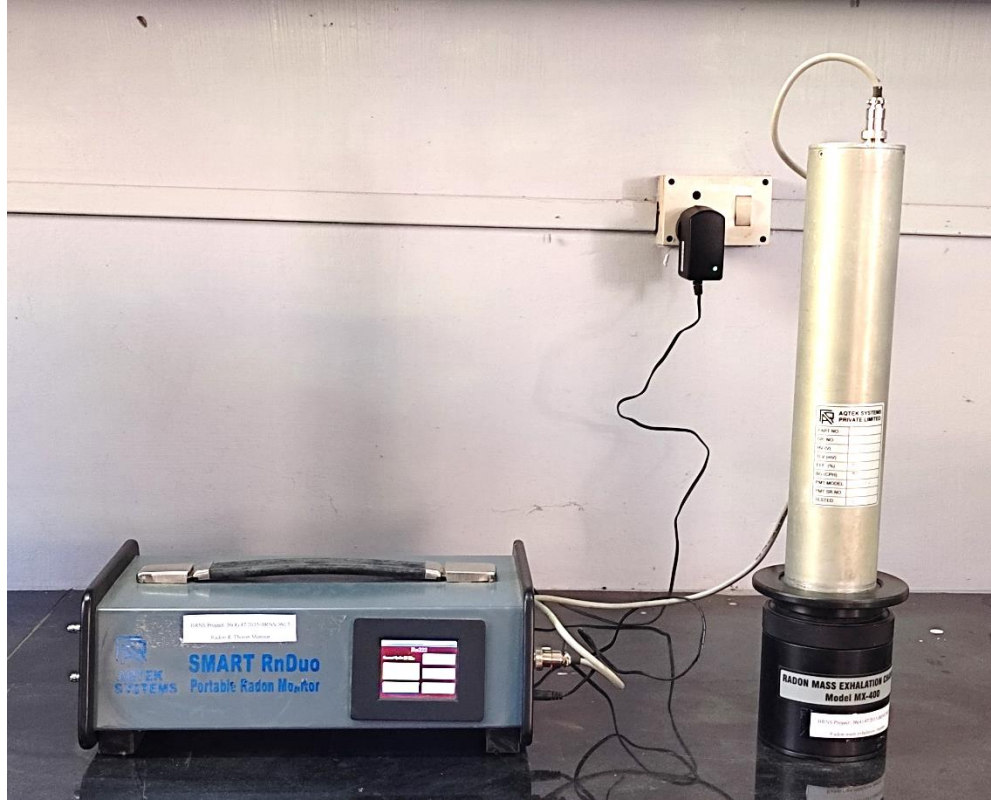


**Fig. 2.9:** Experimental setup for  $^{222}\text{Rn}$  mass exhalation rate measurement from the soil.

$$C(t) = (J_m M/V)t + C_0 \quad (9)$$

where  $C(t)$  is the radon concentration ( $\text{Bqm}^{-3}$ ) at time  $t$ ,  $C_0$  is the radon concentration ( $\text{Bqm}^{-3}$ ) present in the chamber at time  $t = 0$ ,  $M$  is the total mass (kg) of the sample,  $V$  is the effective volume (volume of the detector + porous volume of the sample + residual air volume of the mass exhalation chamber). The porous volume ( $V_p$ ) of the sample can be estimated by the equation below.

$$V_p = V_s - \frac{M}{\rho_s} \quad (10)$$

where  $V_s$  is the sample volume in the mass exhalation chamber,  $\rho_s$  is the specific gravity of the sample which can be taken as  $2.7 \text{ gcm}^{-3}$  for a typical clay soil sample [19]. Substituting the values of mass sample  $M$ , detector effective volume  $V$ ,  $J_m$  may be finally derived from the fitted slope.

### 2.5.3 $^{220}\text{Rn}$ surface exhalation rate measurement

For the measurement of thoron surface exhalation rate, the soil sample is filled up to a certain height of the accumulation chamber which is then connected to the scintillation detector using flexible tubing. The tubing length is kept as short as possible (preferably below 2m) due to the shorter half-life of the  $^{220}\text{Rn}$  as shown in the figure below (figure 2.10). Before performing the measurement, the used scintillation cell is replaced with another background-free scintillation cell to avoid possible errors. The device is then switched 'ON' with Thoron mode being selected on the display screen.

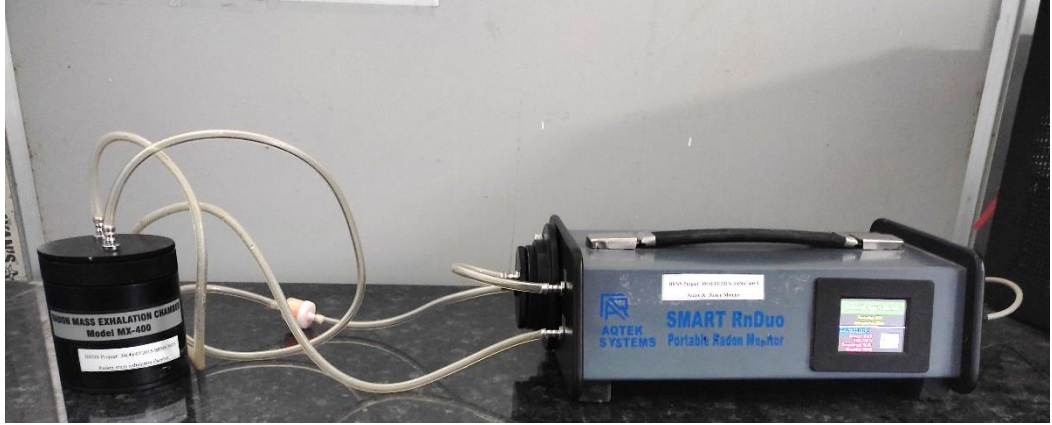


**Fig. 2.10:** Set up for  $^{220}\text{Rn}$  surface exhalation measurement from the soil.

The measurement time given for each sample will be 60 minutes. Here, the configuration of a few parameters needs to be performed which includes selecting the Thoron mode, keeping the cycle for 15 minutes, etc., The counting starts after 5 minutes of connecting the setup, and only the average of the first two readings as equilibrium thoron concentration,  $C_{eq}$  ( $\text{Bqm}^{-3}$ ).

The thoron surface exhalation rate can be estimated by using the following equation

$$J_S = \frac{C_{eq}V\lambda}{A} \quad (11)$$

where  $C_{eq}$  is the equilibrium thoron concentration ( $\text{Bqm}^{-3}$ ),  $\lambda$  is the thoron decay constant ( $0.0126 \text{ s}^{-1}$ ),  $V$  is the sum of residual volume of mass exhalation chamber, the internal volume of RnDuo detector and tubing volumes ( $\text{m}^3$ ), and  $A$  is the surface area ( $\text{m}^2$ ) of the sample emitting thoron [20].

## 2.6 $^{222}\text{Rn}$ measurement in water

If the  $^{222}\text{Rn}$  concentrations in the soil near a house are high, then there is a probability of high radon concentrations in nearby water wells [21]. Thus, it is desired that in addition to the study of radon in air and soil, equal emphasis may also be given to the study of radon in water.

In the present study, radon measurement in the water was performed in Mokokchung, Dimapur, and Kohima districts which will be discussed in chapter 6.

Given below are some of the steps involved in the study of radon present in water.

The measurement of radon in the water study was also conducted by using the Smart RnDuo monitor. Water samples are collected from different sources such as springs, bore well, dug wells, and rivers from the three districts. For investigations such as adsorption and partition coefficient determination and ingestion dosimetry,  $^{222}\text{Rn}$  testing in liquid samples like groundwater, drinking water, different oils, etc., is important. These measurements can be performed using suitable experimental methods like the bubbling technique and appropriate radon monitor, especially one which is free from humidity interference. In this respect, RnDuo is a coherent method for the measurement of radon in liquid samples.

### 2.6.1 Protocols for water sampling and measurement

The Smart RnDuo system includes a leak-proof sampling vial that is used to gather the water samples. Caution was taken to prevent the creation of bubbles or disturbances in the water when sampling into the bottle. Using a sampling tube that had one end inside a tap or open end of flowing water and the other end inside a bottle, the sample was transferred by placing one end inside the tap or open end of the flowing water (figure 2.11). The bottles were entirely filled, leaving no room for air, and then tightly capped to prevent leaks.



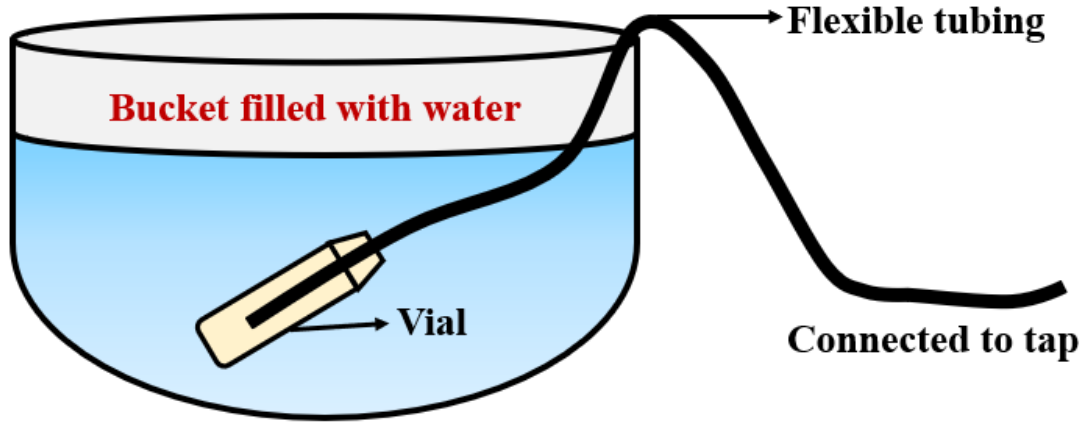


**Fig. 2.11:** Schematic diagram of water sample collection.

The sampling time was recorded, and dissolved  $^{222}\text{Rn}$  measurements were taken 4-5 hours after the sampling. When the setup is complete, the monitor is switched 'ON' and a few configurations were done in the device which include selecting the radon mode, keeping the pump ON, and a few more settings. Following the pump's shut-off, a 5-minute delay is specified. The measurement's initial reading is ignored, while only the average of the subsequent readings ( $C_{\text{air}}$ ) was taken into account (figure 2.12).



**Fig. 2.12:** Set up for measurement of  $^{222}\text{Rn}$  in water.

### 2.6.2 Calculation of $^{222}\text{Rn}$ in water

The relation to estimating the  $^{222}\text{Rn}$  concentration in liquid ( $C_{\text{liq}}$ ) ( $\text{Bqm}^{-3}$ ) from the concentration measured in air ( $C_{\text{air}}$ ) is given as [22]:



$$C_{liq} = C_{air} \left( K + \frac{V_{air}}{V_{liq}} \right) \quad (12)$$

Where  $K = {}^{222}\text{Rn}$ 's liquid-to-air partitioning coefficient (= 0.25 for water),  $V_{air}$  = Amount of air contained within the closed-loop system ( $\text{m}^3$ ) (Bubbler volume + tubings volume + detector volume) and  $V_{liq}$  = Sample bottle's liquid volume ( $\text{m}^3$ ).

### 2.6.3 Dose calculations

The following formula can be used to determine the effective ingestion dose ( $D_{ing}$ ) [18]

$$D_{ing} (\mu\text{Svy}^{-1}) = C_{water} (\text{Bql}^{-1}) \times 365 \text{ ly}^{-1} \times A_{DWI}^{-3} \times \text{DF} \quad (13)$$

$D_{ing}$  is the annual ingested dosage ( $\mu\text{Svy}^{-1}$ ),  $C_{water}$  is the water's radon content, and  $A_{DWI}$  is the age-wise daily water intake, for newborns (0-2 years) (0.8 L), children (8-12 years) (2.5 L), and adults (above 17 years) (3 L) [23]. DF stands for dose conversion factor. Radon doses for adults are  $3.5 \text{ nSvBq}^{-1}$ , children are  $5.9 \text{ nSvBq}^{-1}$ , and newborns are  $23 \text{ nSvBq}^{-1}$  [18]

The following formula can be used to determine the effective inhalation dose ( $D_{inh}$ ) [18]

$$D_{inh} (\mu\text{Svy}^{-1}) = C_{water} (\text{Bql}^{-1}) \times \frac{R_a}{w} \times F \times I \times \text{DF} \quad (14)$$

where  $C_{water}$  represents  ${}^{222}\text{Rn}$  content in water,  $\frac{R_a}{w}$  is the ratio of radon in the air to radon in water ( $=10^{-4}$ ), and  $F$  is the ratio at which radon and its daughter products are in equilibrium ( $F = 0.4$ ). For newborns/infants, children, and adults, the conversion factors for radon inhalation are  $33 \text{ nSv}/(\text{Bqh}/\text{m}^{-3})^{-1}$ ,  $31.4 \text{ nSv}/(\text{Bqh}/\text{m}^{-3})^{-1}$ , and  $28.3 \text{ nSv}/(\text{Bqh}/\text{m}^{-3})^{-1}$ , respectively.  $I$  is the average amount of time spent indoors per person ( $=7000 \text{ hy}^{-1}$ ) [24].

## References

1. Somogyi G (1986) Track detection methods of radium measurements. Atomki Reprints E/25, 1.
2. Abu-Jarad F, Fremlin JH, & Bull R (1980) A study of radon emitted from building materials using plastic  $\alpha$ -track detectors. *Phys Med Biol* 25(4): 683. <https://doi.org/10.1088/0031-9155/25/4/007>
3. Mayya YS, Eappen KP, Nambi KSV (1998) Methodology for mixed field inhalation dosimetry in monazite areas using a twin-cup dosimeter with three track detectors. *Radiat Prot Dosim* 77: 177–184. <https://doi.org/10.1093/oxfordjournals.rpd.a032308>
4. Durrani SA and Bull RK (1987) *Solid State Nuclear Track Detection: Principles, Methods and Applications*. Pergamon Press, Oxford.
5. Bhagwat AM (1993) *Solid state nuclear track detection: Theory and applications* (No. ISRP-K-TD--2). Indian Society for Radiation Physics.
6. Kumar R, Sengupta D, & Prasad R (2003) Natural radioactivity and radon exhalation studies of rock samples from Surda Copper deposits in Singhbhum shear zone. *Radiat Meas* 36(1-6): 551-553. [https://doi.org/10.1016/S1350-4487\(03\)00201-4](https://doi.org/10.1016/S1350-4487(03)00201-4)
7. Durrani SA & Ilic R (Eds.) (1997) *Radon Measurements By Etched Track Detectors-Applications In Radiation Protection, Earth Sciences*. World Scientific.
8. Cross WG and Tommasino L (1970) A rapid technique for nuclear particle damage tracks in thin foils. *Radiation Effects* 5(1): 85-89. <https://doi.org/10.1080/00337577008235000>
9. Sahoo BK, Sapra BK, Kanse SD, Gaware JJ, Mayya YS (2013) A new pin-hole discriminated  $^{222}\text{Rn}/^{220}\text{Rn}$  passive measurement device with single entry face. *Radiat Meas* 58: 52–60. <https://doi.org/10.1016/j.radmeas.2013.08.003>
10. Eappen KP, Mayya YS (2004) Calibration factors for LR-115 (type-II) based radon thoron discriminating dosimeter. *Radiat Meas* 38:5–17. <https://doi.org/10.1016/j.radmeas.2003.09.003>

11. Mishra R, Mayya YS, Kushwaha HS (2009) Measurement of  $^{220}\text{Rn}/^{222}\text{Rn}$  progeny deposition velocities on surfaces and their comparison with theoretical models. *J Aerosol Sci* 40: 1–15. <https://doi.org/10.1016/j.jaerosci.2008.08.001>
12. Mishra R, Mayya YS (2008) Study of a deposition-based direct thoron progeny sensor (DTPS) technique for estimating equilibrium equivalent thoron concentration (EETC) in indoor environment. *Radiat Meas* 43: 1408–1416. <https://doi.org/10.1016/j.radmeas.2008.03.002>
13. Gaware JJ, Sahoo BK, Sapra BK and Mayya YS (2011) Development of online radon and thoron monitoring systems for occupation and general environments., *BARC News Letters*, 318, 45-51.
14. Operational Manual of SMART RnDuo, March (2015)
15. Ramachandran TV, Mayya YS, Sadashivan S, Nair RN, and Eappen KP (2003) Radon-Thoron Levels and Inhalation Dose Distribution Patterns in Indian Dwellings, *BARC Report.*, *BARC/2003/E/026*. Bhabha Atomic Research Center, Mumbai, Government of India, 1– 43.
16. Mayya YS, Eappen KP, Nambi KSV (1998) Methodology for mixed field inhalation dosimetry in monazite areas using a twincup dosimeter with three track detectors. *Radiat Prot Dosim* 77: 177–184. <https://doi.org/10.1093/oxfordjournals.rpd.a032308>.
17. UNSCEAR (2008) Report: Sources and effects of ionizing radiation, Volume II, United Nations, New York, 2011 (e-ISBN-13: 978–92–1–054482–5).
18. UNSCEAR (2000) Annexure B. Exposures from natural radiation, Report to the General Assembly with Scientific Annexes, United Nations. 97-105.
19. Sahoo BK, Mayya YS, Sapra BK, Gaware JJ, Banerjee KS and Kushwaha HS (2010) Radon exhalation studies in an indian uranium tailings pile. *Radiat Meas* 45: 237–241.
20. Sahoo BK, Agarwal TK, Gaware JJ and Sapra BK (2014) Thoron interference in radon exhalation rate measured by solid state nuclear track detector based can technique. *J Radioanal Nucl Chem* 302(3): 1417–1420. <https://doi.org/10.1007/s10967-014-3580-5>
21. Moldovan M, Benea V, Niță DC, Papp B, Burghiele BD, Bican-Brișan N, Cosma C (2014) Radon and radium concentration in water from North-West

- of Romania and the estimated doses. *Radiat Prot Dosim* 162(1-2): 96–100.  
<https://doi.org/10.1093/rpd/ncu230>
22. Sapra BK, Sahoo BK, Mishra R, Kanse SD, Rout RP, Aggarwal TK, Prajith R, Gaware JJ, Jalaluddin S and Kumbhar DS (2010) Handbook BARC, Vol. 51 (BARC Newsletter, Mumbai).
23. WHO (2004) Guidelines for drinking-water quality. Recommendations.
24. Brudecki K, LiWB, Meisenberg O, Tschiersch J, Hoeschen C, & Oech U (2014) Age dependent inhalation dose to members of the public from indoor short-lived radon progeny. *Radiat Environ Biophys*. 53(3): 535–549.  
<https://doi.org/10.1007/s00411-014-0543-8>

## CHAPTER- 3

### A study on indoor radon, thoron, and their progeny levels in Mokokchung district of Nagaland, India

---

*This chapter deals with the assessment of indoor radon, thoron, and their progeny concentrations in the Mokokchung district of Nagaland, India over three different seasons by using Direct Radon and Thoron Progeny Sensors and Pinhole type radon-thoron discriminating dosimeters. The indoor radon and thoron concentrations were found to vary between  $44 \pm 6$  to  $75 \pm 16$  Bqm<sup>-3</sup> and  $25 \pm 2$  to  $62 \pm 49$  Bqm<sup>-3</sup> while their corresponding progeny concentrations varied between  $3.2 \pm 2.1$  to  $17.3 \pm 8.7$  Bqm<sup>-3</sup> and  $0.21 \pm 0.06$  to  $1.49 \pm 0.86$  Bqm<sup>-3</sup> respectively. Based on the study, it was found that the total inhalation dose varied between 0.35 and 1.64 mSvy<sup>-1</sup> and is within the recommended values as suggested by ICRP, 2018. The equilibrium factor (E.F) varied from 0.06 to 0.29 for indoor radon and from 0.01 to 0.02 for indoor thoron.*

---

---

The text of this chapter has been published as:

**Jamir S, Sahoo BK, Mishra R, Bhomick PC and Sinha D (2021) A study on indoor radon, thoron and their progeny level in Mokokchung district of Nagaland, India.** Radioanal. Nucl. Chem. 331, 21–30. <https://doi.org/10.1007/s10967-021-08096-x>.

### 3.1 Introduction

Radon, thoron, and their progeny contribute about one-half of the total background radiation dose received from all-natural sources. Prolonged exposure to radon ( $^{222}\text{Rn}$ ), thoron ( $^{220}\text{Rn}$ ), and their progeny in indoor air is considered the second most cause of lung cancer [1-5]. Radon ( $^{222}\text{Rn}$ ) is a decay product of uranium ( $^{238}\text{U}$ ) and has a half-life of 3.82 days [6] while thoron ( $^{220}\text{Rn}$ ), which is an isotope of  $^{222}\text{Rn}$  has a half-life of 55.6 seconds and originates from the  $^{232}\text{Th}$  decay series. Radon and thoron gases that are generated inside the rock and soil grains migrate to the environment by either emanation processes or exhalation processes [7, 8, 9]. The primary contributors of  $^{222}\text{Rn}$  are exhalation from bases soil (~ 41 %) and building materials (~ 21%), infiltration of outdoor air (~ 20%), de-emanation from the water supply, (~ 2%), and consumption of natural gas (~ 1%) [8, 10, 11, 12].

$^{222}\text{Rn}$ ,  $^{222}\text{Rn}$ , and their progeny concentrations in the indoor air of a dwelling primarily depend on the local geology, type of building materials used, air exchange rate, shape, and size of dwellings [8]. In closed environments such as homes, closed buildings, caves, mines, etc., radon accumulates at a higher level due to poor ventilation, which may be harmful to human health [13, 14, 15]. It is important to note that the inhalation dose to a respiratory tract is mainly attributed to their progeny rather than radon/ thoron gases themselves. In order to have a reliable estimate of inhalation dose, direct progeny concentration measurement is very important in addition to the measurement of radon/thoron gases. Traditional practice is to measure radon/thoron gas concentration and estimate progeny concentration based on an assumed/default equilibrium factor. However, this practice may become unreliable and involves a lot of uncertainty in the estimation of progeny concentration. Thus, in order to provide a realistic assessment of indoor progeny in a closed environment, it is necessary to conduct direct measurements of radon and thoron progeny and there are reports on the use of DTPS (Direct Thoron Progeny Sensor) and DRPS (Direct Radon Progeny Sensor) for this purpose [16-18]. The risks associated with indoor radon and thoron exposure have been a matter of concern and in this regard, different studies have been conducted worldwide [19-23].

The state of Nagaland in India is an area containing metamorphic, igneous, and sedimentary rocks—predominantly shale (Disang category), sandstone (Barail

category), volcanic sediments, limestone, and pelagic [24, 25]. Thus, a thorough study of the radon levels is significant for the state of Nagaland as it will give an idea about the presence of environmental radon in this region. To date only two reports are available [26, 27], and according to one of the reports, measurements showed the concentration of mean radon progeny lied between  $1.85 \text{ Bqm}^{-3}$  to  $10.68 \text{ Bqm}^{-3}$ , and thoron varied from  $0.06 \text{ Bqm}^{-3}$  to  $2.67 \text{ Bqm}^{-3}$  in some parts of Nagaland, viz., Wokha, Kohima and Dimapur districts [26]. In another report [27], the potential alpha energy concentration (PAEC) was measured in the Kohima district in the year 1997 using LR-115 film in bare mode and the geometrical mean was found to be  $88 \text{ Bqm}^{-3}$ . But so far no study has been done in the Mokokchung district of Nagaland. Thus the present study aims to carry out a comprehensive measurement of  $^{222}\text{Rn}$ ,  $^{220}\text{Rn}$ , and their progeny concentration in the Mokokchung district of Nagaland. A time-integrated  $^{222}\text{Rn}$ ,  $^{220}\text{Rn}$ , and progeny assessment were made using a newly developed single-entry pinhole-based radon/thoron discriminating dosimeter while their progenies were measured by deploying deposition-based direct radon/thoron progeny sensors (DRPS/DTPS) covering 11 villages of Mokokchung district, Nagaland over three different seasons.

## 3.2 Methodology

### 3.2.1 Study area

Mokokchung district is one of the 12 districts of Nagaland and it shares its boundaries with Assam on the North, Tuensang district on the East, Wokha and Zunheboto districts on the south. It is situated at  $25^{\circ}56'\text{N}$  to  $27^{\circ}40'\text{N}$  latitude and  $93^{\circ}53'\text{E}$  to  $94^{\circ}53'\text{E}$  longitude (figure 3.1) and covers an area of  $1615 \text{ km}^2$  (1325 meters above sea level). The two most popular rocks found in the district are the Disang series (Eocene), and the Barial series (Oligocene). Younger rocks of the Tipam series are also seen that border the plains of Assam. The oldest category of rocks belonging to the Disang group is a combination of splintery shales [28].

People of the selected study region dwell in various types of houses (figure 3.2) and for our present study, we have divided the houses into 3 main categories as follows:

(i) Type A: These are the brick type of houses and about 30 percent of the houses in the study region fall into this group.

(ii) Type B: These are the wooden type of houses and about 35 percent of the houses in the study region fall into this group.

(iii) Type C: These are the bamboo type of houses and about 35 percent of the houses in the study region fall into this group.

The study was carried out during a one-year period (1<sup>st</sup> April, 2017 to 5<sup>th</sup> May, 2018) which was divided into summer, rainy and winter seasons each comprising nearly 120 days (4 months).

### 3.2.2 $^{222}\text{Rn}/^{220}\text{Rn}$ and progeny measurement

For this study, two methods; pin-hole twin cup dosimeter, and DTPS/DRPS were deployed for the measurement of  $^{222}\text{Rn}$ ,  $^{220}\text{Rn}$ , and progeny concentration indoors [29-32]. The details of the methods of measurement have already been described in chapter 2.

### 3.2.3 Deployment strategy

Pin-hole dosimeter, DTPS/DRPS were deployed to calculate the indoor  $^{222}\text{Rn}$ ,  $^{220}\text{Rn}$ , and their progeny. A total of 121 households from eleven different villages of Mokokchung district, Nagaland were selected for the study from 1st April 2017 to 5th May, 2018. Three different types of houses— brick (42), bamboo (41), and wooden (38) houses—were selected for the present study, and the detectors were deployed in each of these houses by suspending 90 cm away from the wall (care was taken to expose these dosimeters in the living room, figure 3.3). The assessment was done for three different seasons to understand the seasonal variation pattern of  $^{222}\text{Rn}$ , and  $^{220}\text{Rn}$  and their progeny levels in the study area. Around 6 to 18 houses were chosen from each village as per the house distribution and their building material (bamboo, wooden, and brick type). The annual year was divided into summer, rainy, and winter seasons each comprising nearly 120 days (4 months). In winter, doors, and windows are normally kept closed and heating devices are used, while during the rainy season, mostly doors and windows are kept closed, but heating devices are not used. However, unlike during the winter and rainy seasons, doors and windows are kept open during summer.



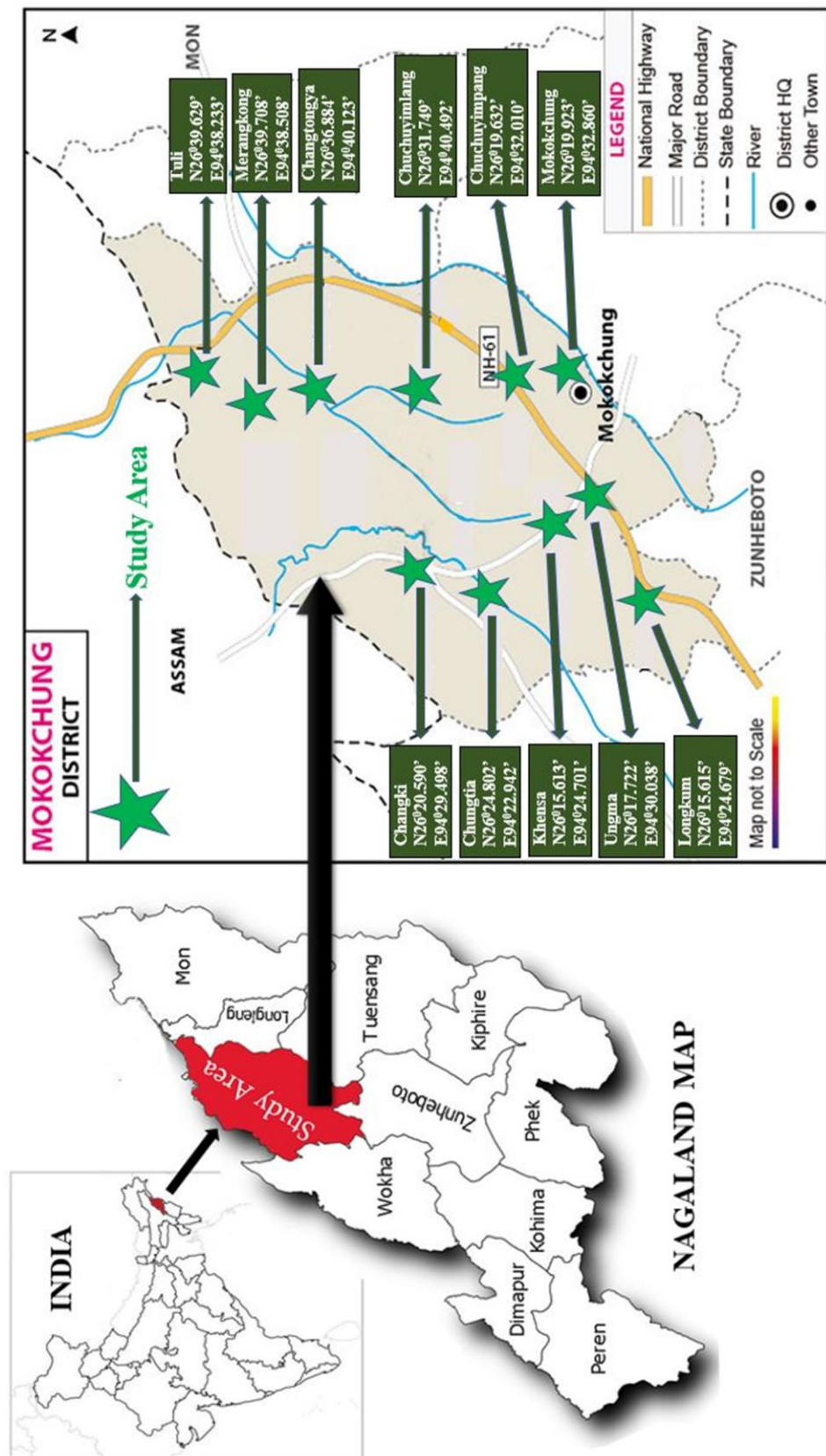


Fig. 3.1: The different geographical locations of the study area under Mokokchung district, Nagaland, India.

(a)



(b)



(c)



**Fig. 3.2:** Types of houses (a) brick (b) wooden (c) bamboo in Mokokchung district, Nagaland, India.



(a)



(b)



(c)

**Fig. 3.3:** Deployment of DTPS/DRPS and Pin hole dosimeter in different types of houses a) Brick house b) Wooden house c) Bamboo house.

### 3.2.3.1 Gamma survey for site selection

The selection of sites of the dwellings was based on a preliminary gamma survey carried out to assess the gamma level falling into different zones. Initially, before the installation of the detectors, gamma dose rate measurements were carried out in the different types of selected houses using the gamma survey meter. Table 3.1 shows the gamma levels that were measured in some of the residences where the detectors were kept.

**Table 3.1:** Gamma level in different houses of the study in Mokokchung district, Nagaland.

| SI. No. of houses | Gamma level (nSvhr <sup>-1</sup> ) | SI. No. of houses | Gamma level (nSvhr <sup>-1</sup> ) |
|-------------------|------------------------------------|-------------------|------------------------------------|
| 1.                | 144                                | 16.               | 134                                |
| 2.                | 144                                | 17.               | 127                                |
| 3.                | 150                                | 18.               | 105                                |
| 4.                | 126                                | 19.               | 132                                |
| 5.                | 120                                | 20.               | 132                                |
| 6.                | 153                                | 21.               | 175                                |
| 7.                | 160                                | 22.               | 136                                |
| 8.                | 158                                | 23.               | 151                                |
| 9.                | 162                                | 24.               | 145                                |
| 10.               | 182                                | 25.               | 150                                |
| 11.               | 142                                | 26.               | 147                                |
| 12.               | 143                                | 27.               | 139                                |
| 13.               | 154                                | 28.               | 125                                |
| 14.               | 114                                | 29.               | 123                                |
| 15.               | 139                                | 30.               | 148                                |



|     |     |     |     |
|-----|-----|-----|-----|
| 31. | 135 | 55. | 120 |
| 32. | 132 | 56. | 136 |
| 33. | 143 | 57. | 140 |
| 34. | 150 | 58. | 135 |
| 35. | 141 | 59. | 165 |
| 36. | 130 | 60. | 136 |
| 37. | 118 | 61. | 150 |
| 38. | 161 | 62. | 125 |
| 39. | 152 | 63. | 115 |
| 40. | 131 | 64. | 120 |
| 41. | 156 | 65. | 163 |
| 42. | 180 | 66. | 105 |
| 43. | 163 | 67. | 120 |
| 44. | 166 | 68. | 126 |
| 45. | 190 | 69. | 125 |
| 46. | 136 | 70. | 110 |
| 47. | 122 | 71. | 150 |
| 48. | 130 | 72. | 140 |
| 49. | 132 | 73. | 135 |
| 50. | 154 | 74. | 145 |
| 51. | 150 | 75. | 175 |
| 52. | 135 | 76. | 170 |
| 53. | 135 | 77. | 133 |
| 54. | 130 | 78. | 128 |

|      |     |      |     |
|------|-----|------|-----|
| 79.  | 140 | 101. | 110 |
| 80.  | 135 | 102. | 115 |
| 81.  | 148 | 103. | 125 |
| 82.  | 148 | 104. | 130 |
| 83.  | 133 | 105. | 135 |
| 84.  | 125 | 106. | 135 |
| 85.  | 115 | 107. | 128 |
| 86.  | 135 | 108. | 131 |
| 87.  | 110 | 109. | 134 |
| 88.  | 143 | 110. | 92  |
| 89.  | 145 | 111. | 114 |
| 90.  | 168 | 112. | 108 |
| 91.  | 149 | 113. | 102 |
| 92.  | 179 | 114. | 123 |
| 93.  | 174 | 115. | 148 |
| 94.  | 140 | 116. | 112 |
| 95.  | 119 | 117. | 132 |
| 96.  | 130 | 118. | 102 |
| 97.  | 111 | 119. | 125 |
| 98.  | 129 | 120. | 110 |
| 99.  | 120 | 121. | 95  |
| 100. | 115 |      |     |

Based on the multivariate regression analysis, the gamma level was divided into three zones in each type of house (Brick, wooden, bamboo) in the study area as shown in table 3.2. The gamma levels were found to be in the range of 112-190nSv/hr in brick houses, 102-182 nSv/hr in wooden houses, and 92-150 nSv/hr in bamboo houses.

**Table 3.2:** Zone-wise house distribution of Mokokchung district, Nagaland, India where DTSP/DRPS and Pinhole twin cup dosimeters were installed.

| Total no. of dosimeters to be deployed= 121 |                                       |        |        |        |
|---|---------------------------------------|--------|--------|--------|
| Fitting parameter, K= 1.00E + 00            |                                       |        |        |        |
| Zone  | Gamma level<br>(nSvhr <sup>-1</sup> ) | Type A | Type B | Type C |
| 1   | 0 - 90                                | 12     | 19     | 14     |
| 2   | 90 – 180                              | 14     | 11     | 15     |
| 3   | 180 – 270                             | 16     | 11     | 9      |

### 3.2.3.2 Deployment of detectors

Deployment of detectors was calculated using the regression formula, where the number of detectors to be installed was calculated by dividing the zone of gamma radiation level as well as the types of houses. Based on statistical distribution, the selection of various categories of houses in different villages was done as shown in table 3.3.

The villages falling into different gamma zones were categorized based on the range of gamma radiation levels recorded during the preliminary survey, an index for the radioactivity content in the location. Once the gamma data is acquired, zone wise house statistic table was made by using a multivariate regression analysis for estimating the number of dosimeters to be deployed in each type of dwelling in the respective zone. Subsequently, after the selection of dwellings according to the above protocol, dosimeters were deployed in the study region. Around six to eighteen dwellings of each

village were selected for the radon and thoron assessment and the GPS coordinates of the location where the detectors were deployed were also recorded. Accordingly, deployment was done in 121 households in the study area as given in table 3.3.

**Table 3.3:** Distribution of detectors in each village of Mokokchung district, Nagaland.

| Sl.no | Name of village | No. of DTPS/DRPS and Pinhole dosimeters deployed in different types of houses | Total No. of DTPS/DRPS and Pinhole dosimeters deployed in different types of houses |
|-------|-----------------|---|---|
| 1     | Chuchuyimpang   | (brick=4, wooden=4, bamboo=4)   | 12  |
| 2     | Mokokchung      | (brick=4, wooden=4, bamboo=4)   | 12  |
| 3     | Ungma           | (brick=6, wooden=6, bamboo=5)   | 17  |
| 4     | Longkum         | (brick=6, wooden=6, bamboo=4)   | 16  |
| 5     | Khensa          | (brick=3, wooden=3, bamboo=2)   | 8   |
| 6     | Changki         | (brick=2, wooden=2, bamboo=2)   | 6   |
| 7     | Chungtia        | (brick=3, wooden=3, bamboo=3)   | 9   |
| 8     | Tuli            | (brick=4, wooden=3, bamboo=3)   | 10  |
| 9     | Merangkong      | (brick=3, wooden=3, bamboo=3)   | 9   |
| 10    | Changtongya     | (brick=3, wooden=3, bamboo=4)   | 10  |
| 11    | Chuchuyimlang   | (brick=4, wooden=4, bamboo=4)   | 12  |
|       | <b>Total</b>    | <b>121</b>  | <b>121</b>  |

### 3.2.4 Post-processing of dosimeters

After exposure to different periods, the dosimeters/progeny sensors were retrieved from the dwellings of the study area. A solution of 2.5N NaOH was then used to etch the exposed LR-115 films at a constant temperature of 60°C for 90 minutes in a temperature-controlled water bath (model PSI-CTB1). After the etching process was



over, the etched films were rinsed thoroughly with tap water and kept overnight in a tissue roll for drying. The alpha tracks formed in the LR- 115 were pre-sparked at 900 V and counted at an operating voltage of 500 V using a spark counter (model PSI-SC1).

### 3.2.5 Calculation of $^{222}\text{Rn}$ , $^{220}\text{Rn}$ , and Progeny Concentration

Following are the formulas used for the calculations of different parameters of  $^{222}\text{Rn}$ ,  $^{220}\text{Rn}$ , and their Progeny concentrations. The details of the calculation have been discussed in chapter 2.

The  $^{222}\text{Rn}$  concentration,  $C_r$  ( $\text{Bqm}^{-3}$ ), and  $^{220}\text{Rn}$  concentration,  $C_t$  ( $\text{Bqm}^{-3}$ ) were calculated using the formulae given below [29]

$$C_r = \frac{T_1}{d.K_r} \quad (1)$$

$$C_t = \frac{T_2 - T_1}{d.K_t} \quad (2)$$

Where  $T_1$ ,  $T_2$  are the tracks registered in ' $^{222}\text{Rn}$ ' and ' $^{222}\text{Rn} + ^{220}\text{Rn}$ ' compartments respectively,  $d$  is the exposure time in days. The calibration factors for  $^{222}\text{Rn}$  and  $^{220}\text{Rn}$  in the dosimeter are  $K_r = 0.017 \pm 0.002 \text{ tr.cm}^{-2}\text{d}^{-1}\text{Bqm}^{-3}$  and  $K_t = 0.010 \pm 0.001 \text{ tr.cm}^{-2}\text{d}^{-1}\text{Bqm}^{-3}$ , respectively [29].

The equilibrium equivalent progeny concentration (EEC) of radon (EERC) and thoron (EETC) was calculated using Equation (3) and Equation (4) respectively [32, 33].

$$EERC = T_c(\text{Tracks.cm}^{-2}.D^{-1}/S_R(\text{Tracks.cm}^{-2}.D^{-1}/EEC(\text{Bq.m}^{-3})) \quad (3)$$

$$EETC = T_c(\text{Tracks.cm}^{-2}.D^{-1}/S_T(\text{Tracks.cm}^{-2}.D^{-1}/EEC(\text{Bq.m}^{-3})) \quad (4)$$

Where  $S_R = 0.09 \text{ trcm}^{-2}\text{d}^{-1}\text{Bqm}^{-3}$  corresponds to the sensitivity factor for Radon progeny in DRPS, while  $S_T = 0.94 \text{ trcm}^{-2}\text{d}^{-1}\text{Bqm}^{-3}$  corresponds to the sensitivity factor for Thoron progeny in DTPS [32, 33]. When assessing the tracks owing to radon progeny alone in DRPS, the contribution of thoron progeny tracks were excluded.

The values of EETC/EERC are used to calculate the equilibrium factor (E.F)—the ratio of EETC/EERC to their respective  $^{222}\text{Rn}$  and  $^{220}\text{Rn}$  concentration. The world average value of E.F for indoor radon is 0.4 and 0.02 for indoor thoron [2].

Inhalation doses of radon and thoron were calculated using equations (5) and (6) [33, 34]

$$\text{TID}_r (\text{mSvy}^{-1}) = [(C_r \times 0.17) + (\text{EERC} \times 9)] \times 8760 \times 0.8 \times 10^{-6} \quad (5)$$

$$\text{TID}_t (\text{mSvy}^{-1}) = [(C_t \times 0.11) + (\text{EETC} \times 40)] \times 8760 \times 0.8 \times 10^{-6} \quad (6)$$

Where the dosage conversion factors for  $^{222}\text{Rn}$  and  $^{220}\text{Rn}$  concentrations are 0.17 and 0.11  $\text{nSvBq}^{-1}\text{h}^{-1}\text{m}^3$ , respectively, while the dose conversion factors for  $^{222}\text{Rn}$  and  $^{220}\text{Rn}$  progeny concentrations are 9, and 40  $\text{nSvBq}^{-1}\text{h}^{-1}\text{m}^3$ , respectively. The standard occupancy factor for a one-year exposure period is 0.8 [33, 34].

### 3.3 Results and discussions

#### 3.3.1 Annual average $^{222}\text{Rn}$ , $^{220}\text{Rn}$ , EERC/EETC

Table 3.4 gives the details about the annual average of  $^{222}\text{Rn}$ ,  $^{220}\text{Rn}$ , EERC, and EETC during the study period of each village.

**Table 3.4:** Annual average radon, thoron, EERC, and EETC in Mokokchung district, Nagaland.

| Name of the Village | Radon ( $\text{Bq/m}^3$ ) | Thoron ( $\text{Bq/m}^3$ ) | EERC ( $\text{Bq/m}^3$ ) | EETC ( $\text{Bq/m}^3$ ) |
|---------------------|---------------------------|----------------------------|--------------------------|--------------------------|
| Changki             | 59.81±10.68               | 43.41±21.51                | 13.13±5.40               | 0.75±0.29                |
| Changtongya         | 44.68±6.40                | 25.29±2.74                 | 3.48±0.79                | 0.37±0.09                |
| Chuchuyimlang       | 50.36±10.57               | 34.91±11.14                | 3.25±2.15                | 0.21±0.06                |
| Chuchuyimpang       | 65.29±17.48               | 34.51±6.77                 | 6.83±4.12                | 0.68±0.39                |
| Chungtia            | 51.56±40.96               | 35.01±17.91                | 7.28±6.18                | 0.73±0.69                |
| Khensa              | 75.32±16.88               | 45.23±10.67                | 6.85±3.98                | 0.71±0.47                |
| Longkum             | 47.74±17.83               | 33.07±12                   | 7.88±3.45                | 0.55±0.20                |
| Merangkong          | 59.27±29.46               | 62.15±49.37                | 17.38±8.77               | 1.49±0.86                |
| Mokokchung          | 65.93±23.38               | 40.83±6.55                 | 8.02±5.97                | 0.83±0.62                |
| Tuli                | 56.84±33.32               | 45.85±32.37                | 5.25±4.48                | 0.53±0.34                |
| Ungma               | 61.32±26.23               | 38.40±7.37                 | 7.49±3.43                | 0.53±0.09                |

It was found that the annual average concentration of indoor  $^{222}\text{Rn}$  concentration ranges between  $44.68 \pm 6.40 \text{ Bqm}^{-3}$  to  $75.32 \pm 16.88 \text{ Bqm}^{-3}$  while the average  $^{220}\text{Rn}$  concentration varies from  $25.29 \pm 2.74 \text{ Bqm}^{-3}$  to  $62.15 \pm 49.37 \text{ Bqm}^{-3}$  respectively. The annual average  $^{222}\text{Rn}$  concentration was observed to be more than the  $^{220}\text{Rn}$  concentration but falls within the reference value of  $300 \text{ Bqm}^{-3}$  as prescribed by ICRP, 2018 [1]. The concentration of indoor radon and thoron progeny ranges from  $3.25 \pm 2.15$  to  $17.38 \pm 8.77 \text{ Bqm}^{-3}$  and from  $0.21 \pm 0.06$  to  $1.49 \pm 0.86 \text{ Bqm}^{-3}$  respectively and lied within the reference value (for radon progeny=  $2\text{-}50 \text{ Bqm}^{-3}$  and thoron progeny=  $0.04\text{-}2 \text{ Bqm}^{-3}$ ) as prescribed by ICRP, 2014 [35].

### 3.3.2 Seasonal variation of radon, and thoron concentration

It was observed that the levels of  $^{222}\text{Rn}$  and  $^{220}\text{Rn}$  concentration were highest during the winter season as compared to the rainy and summer seasons (figure 3.4).

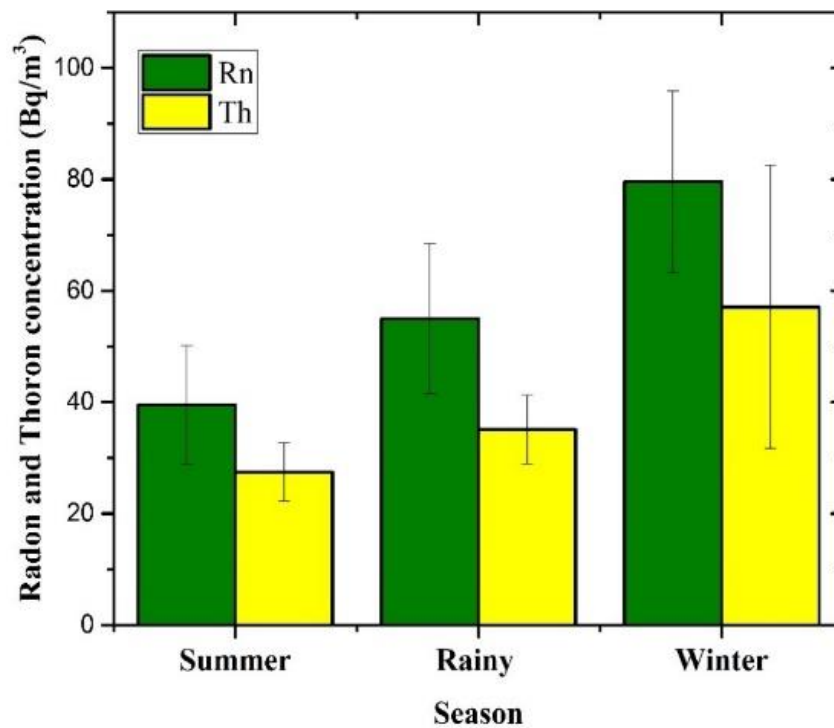


**Fig. 3.4:** Seasonal variation of average indoor  $^{222}\text{Rn}$  and  $^{220}\text{Rn}$  concentration.

The reason for this could be attributed to the reduced ventilation during winter, which enhances the building up of radon and thoron gases inside the dwellings as compared to the summer or rainy season [36]. Figure 3.4 also reflects the higher concentration of

radon as compared to the thoron concentration in the dwellings for all three seasons. This is because of the shorter half-life of  $^{220}\text{Rn}$  (55.6 seconds) as compared to  $^{222}\text{Rn}$  (half-life is 3.8 days) and thus cannot be accumulated in closed rooms as compared to  $^{222}\text{Rn}$ .

Table 3.5 presents the variation in radon and thoron parameters for the Mokokchung district for different seasons. From the table, it is clear that during the summer season,  $^{222}\text{Rn}$  concentration varied from  $5.61 \text{ Bqm}^{-3}$  to  $170.54 \text{ Bqm}^{-3}$  with an average of  $39.49 \pm 10.66 \text{ Bqm}^{-3}$ , which is below the recommended safe level of  $300 \text{ Bqm}^{-3}$  [1]. On the other hand, the average  $^{220}\text{Rn}$  concentration during this period is found to be  $27.44 \pm 5.21 \text{ Bqm}^{-3}$  which is more than the world average value of  $10 \text{ Bqm}^{-3}$  [34, 37]. The value of EERC varied from  $0.68 \text{ Bqm}^{-3}$  to  $20.30 \text{ Bqm}^{-3}$  with an average of  $6.31 \pm 5.92$ , while EETC varied from  $0.05 \text{ Bqm}^{-3}$  to  $1.75 \text{ Bqm}^{-3}$  with an average of  $0.50 \pm 0.34$ .

**Table 3.5:** Seasonal concentration of indoor  $^{222}\text{Rn}$  and  $^{220}\text{Rn}$  in Mokokchung district, Nagaland.

|        |         | $^{222}\text{Rn}$<br>( $\text{Bqm}^{-3}$ ) | $^{220}\text{Rn}$<br>( $\text{Bqm}^{-3}$ ) | EERC<br>( $\text{Bqm}^{-3}$ ) | EETC<br>( $\text{Bqm}^{-3}$ ) |
|--------|---------|--|--|-------------------------------|-------------------------------|
| Summer | Average | $39.49 \pm 10.66$                          | $27.44 \pm 5.21$                           | $6.31 \pm 5.92$               | $0.50 \pm 0.34$               |
|        | Minimum | 5.61                                       | 9.26                                       | 0.68                          | 0.05                          |
|        | Maximum | 170.54                                     | 87.41                                      | 20.30                         | 1.75                          |
| Rainy  | Average | $54.96 \pm 13.44$                          | $35.10 \pm 6.19$                           | $5.25 \pm 3.07$               | $0.48 \pm 0.22$               |
|        | Minimum | 6.67                                       | 16.81                                      | 0.99                          | 0.003                         |
|        | Maximum | 147.06                                     | 83.48                                      | 54.86                         | 3.78                          |
| Winter | Average | $79.58 \pm 16.25$                          | $57.09 \pm 25.44$                          | $12.12 \pm 5.31$              | $1.04 \pm 0.61$               |
|        | Minimum | 3.69                                       | 16.85                                      | 1.62                          | 0.09                          |
|        | Maximum | 289.91                                     | 276.83                                     | 64.62                         | 4.51                          |

In comparison to the summer season, the average  $^{222}\text{Rn}$  concentration during the rainy season was found to be  $54.96 \pm 13.44 \text{ Bqm}^{-3}$  while the average  $^{220}\text{Rn}$  concentration was  $35.10 \pm 6.19 \text{ Bqm}^{-3}$ . The EERC varied from  $0.99 \text{ Bqm}^{-3}$  to  $54.86 \text{ Bqm}^{-3}$  with an average of  $5.25 \pm 3.07 \text{ Bqm}^{-3}$  while EETC varied from  $0.003 \text{ Bqm}^{-3}$  to  $3.78 \text{ Bqm}^{-3}$  with an average of  $0.48 \pm 0.22 \text{ Bqm}^{-3}$ . During the winter season,  $^{222}\text{Rn}$  concentration varied from  $3.69 \text{ Bqm}^{-3}$  to  $289.91 \text{ Bqm}^{-3}$  with an average of  $79.58 \pm 16.25 \text{ Bqm}^{-3}$ , while  $^{220}\text{Rn}$  concentration varied from  $16.85 \text{ Bqm}^{-3}$  to  $276.83 \text{ Bqm}^{-3}$  with an average of  $57.09 \pm 25.44 \text{ Bqm}^{-3}$ . EERC varied from  $1.62 \text{ Bqm}^{-3}$  to  $64.62 \text{ Bqm}^{-3}$  with an average of  $12.12 \pm 5.31 \text{ Bqm}^{-3}$  while EETC varied from  $0.09 \text{ Bqm}^{-3}$  to  $4.51 \text{ Bqm}^{-3}$  with an average of  $1.04 \pm 0.61 \text{ Bqm}^{-3}$ .

### 3.3.3 Variation of $^{222}\text{Rn}$ , and $^{220}\text{Rn}$ concentrations in different types of house

The variation of indoor  $^{222}\text{Rn}$  and  $^{220}\text{Rn}$  concentrations in different types of houses was also studied and the results are presented in figure 3.5. It is clear from the results that there are no apparent changes in both radon and thoron concentration in the dwellings made of different building materials.

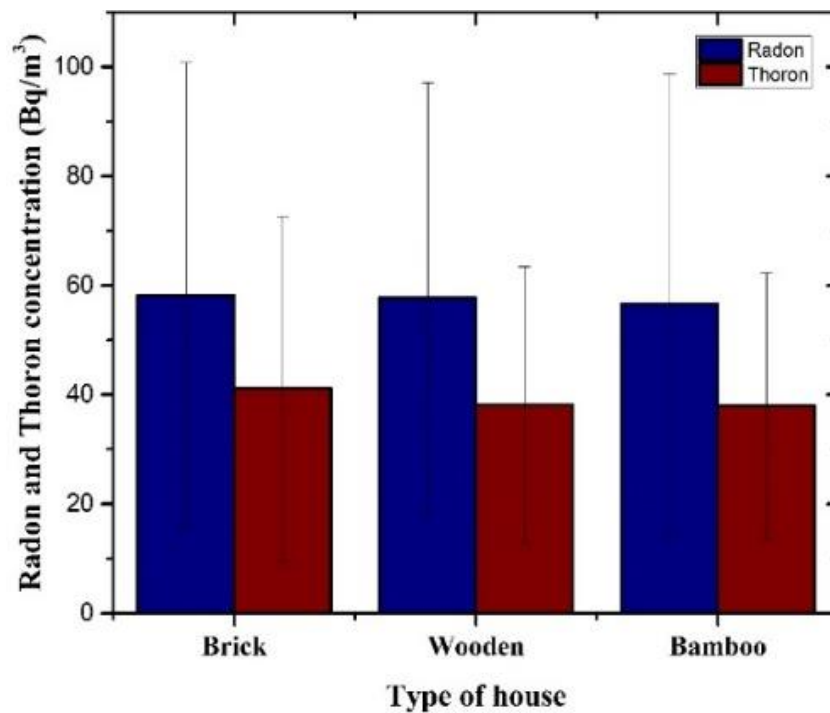


**Fig. 3.5:** Variation of indoor  $^{222}\text{Rn}$  and  $^{220}\text{Rn}$  concentration in different types of houses.

### 3.3.4 Equilibrium Factor (EF)

The E.F between  $^{222}\text{Rn}$ , and  $^{220}\text{Rn}$  along with their progenies  $^{214}\text{Po}$  and  $^{212}\text{Po}$  respectively is shown in table 3.6. The equilibrium factor (EF) between  $^{222}\text{Rn}$  and its progeny range between 0.06 to 0.29 with a mean value of 0.13 which is less than the world average value of 0.4 as reported by UNSCEAR, 2000 [2]. Similarly, the E.F for  $^{220}\text{Rn}$  and its progeny range between 0.01 to 0.02 with a mean value of 0.01 which is also less than the world average value of 0.02 as reported by UNSCEAR, 2000 [2]. The low value of the equilibrium factor may be attributed to the low level of dust and aerosol concentration in the study region. Figure 3.6 shows the box-whisker plot of radon and thoron equilibrium factors in different types of houses. It is observed that the maximum IQR (Interquartile) value for radon EF is found to be 0.28 in the brick type of house and the maximum IQR for thoron EF is found to be 0.02. Clearly, it is seen that the variability of radon EF in brick types of houses is more than the variability of thoron in bamboo types of houses.

**Table 3.6:** Annual average E.F observed in Mokokchung district, Nagaland.

| <b>Name of the Village</b> | <b>E.F<br/>(Radon)</b> | <b>E.F<br/>(Thoron)</b> |
|----------------------------|------------------------|-------------------------|
| Changki                    | 0.22                   | 0.02                    |
| Changtongya                | 0.08                   | 0.01                    |
| Chuchuyimlang              | 0.06                   | 0.01                    |
| Chuchuyimpang              | 0.10                   | 0.02                    |
| Chungtia                   | 0.14                   | 0.02                    |
| Khensa                     | 0.09                   | 0.02                    |
| Longkum                    | 0.17                   | 0.02                    |
| Merangkong                 | 0.29                   | 0.02                    |
| Mokokchung                 | 0.12                   | 0.02                    |
| Tuli                       | 0.09                   | 0.01                    |
| Ungma                      | 0.12                   | 0.01                    |
| <b>Mean</b>                | <b>0.13</b>            | <b>0.01</b>             |

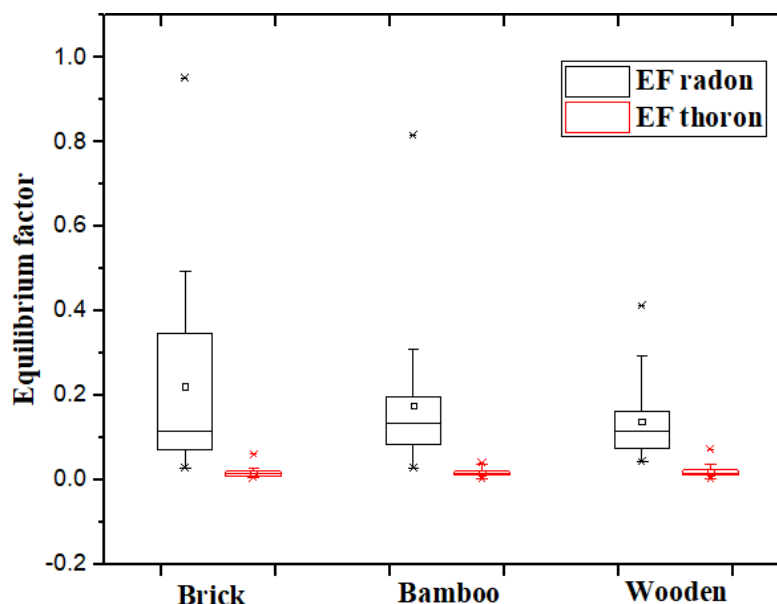


**Fig. 3.6:** Box and whisker plot of radon and thoron equilibrium factor in different house types.

### 3.3.5 Inhalation dose

Inhalation of higher doses of  $^{222}\text{Rn}$ , and  $^{220}\text{Rn}$  gases may have adverse effects on the human body when exposed over a prolonged period [1]. In the present investigation, the total inhalation doses were obtained and the results are presented in table 3.7.

**Table 3.7:** Annual average dose in Mokokchung district, Nagaland.

| Name of the Village | Total inhalation Dose |
|---------------------|-----------------------|
| Changki             | 1.14                  |
| Changtongya         | 0.39                  |
| Chuchuyimlang       | 0.35                  |
| Chuchuyimpang       | 0.73                  |
| Chungtia            | 0.99                  |
| Khensa              | 0.75                  |
| Longkum             | 0.73                  |
| Merangkong          | 1.64                  |
| Mokokchung          | 0.87                  |
| Tuli                | 0.58                  |
| Ungma               | 0.73                  |

Figure 3.7 and figure 3.8 also show the annual average inhalation doses due to indoor  $^{222}\text{Rn}$ ,  $^{220}\text{Rn}$ , and their progenies in the dwellings of the Mokokchung district. It is observed that the annual effective inhalation dose of radon ranges from  $0.26 \pm 0.15 \text{ mSv y}^{-1}$  to  $1.17 \pm 0.59 \text{ mSv y}^{-1}$  (figure 3.7). For thoron, it ranges from  $0.09 \pm 0.03 \text{ mSv y}^{-1}$  to  $0.47 \pm 0.28 \text{ mSv y}^{-1}$  which is within the reference value of  $4\text{--}14 \text{ mSv y}^{-1}$  as prescribed by ICRP, 2018 (figure 3.8) [1].

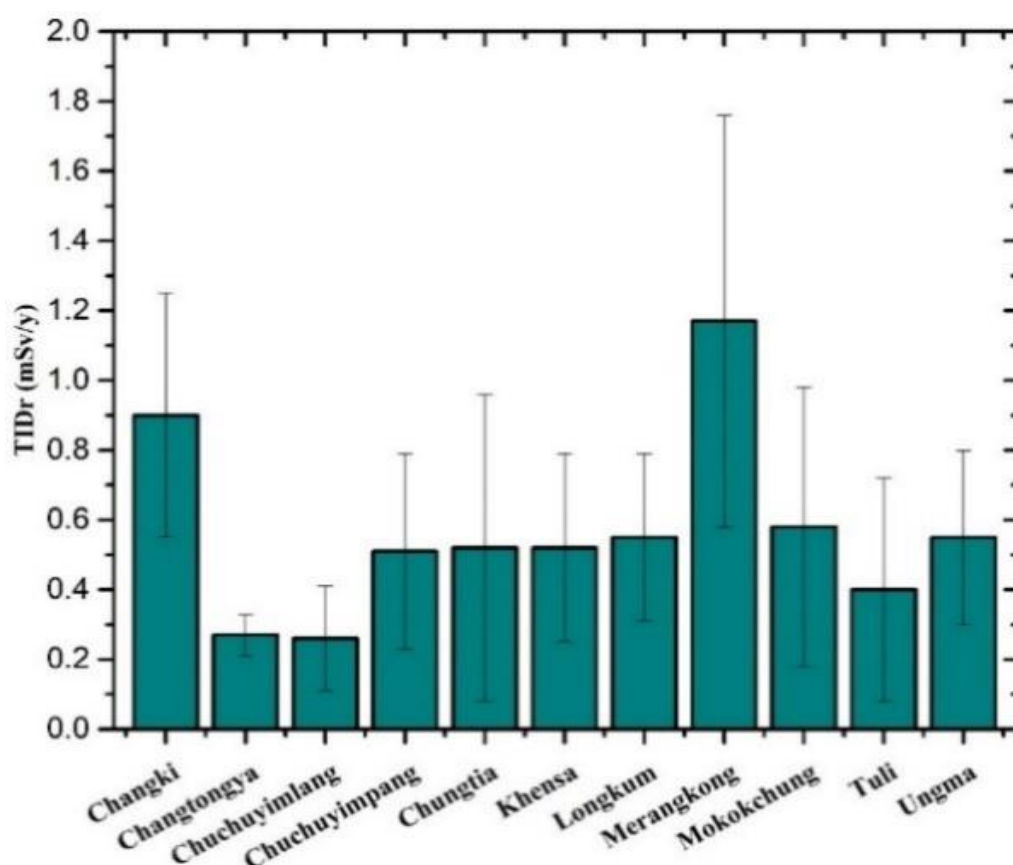


**Fig. 3.7:** Annual average inhalation dose due to  $^{222}\text{Rn}$  and its progeny.

The results obtained indicated that among the villages, Merangkong had the highest exposure to radon inhalation dose and Chuchuyimlang had the lowest (figure 3.7), whereas Chungtia and Merangkong had the highest thoron inhalation doses and Chuchuyimlang had the lowest exposure (figure 3.8). It was also observed that in all the villages, the inhalation dose was higher during the winter season. This could be due to an increase in indoor radon concentration in the dwellings due to reduced ventilation. On the other hand, results revealed the least inhalation doses during summer.



Nonetheless, all the observed dwellings have inhalation doses within the reference value of 4 (at a workplace) to 14 mSv/y (in residential buildings) as recommended by ICRP, 2018 [1]. Since all the indoor radon and thoron concentrations are well below the permissible limit as recommended by ICRP and UNSCEAR, we can say that there is no significant risk associated with the present survey areas due to indoor  $^{222}\text{Rn}$ ,  $^{220}\text{Rn}$ , and their progenies.

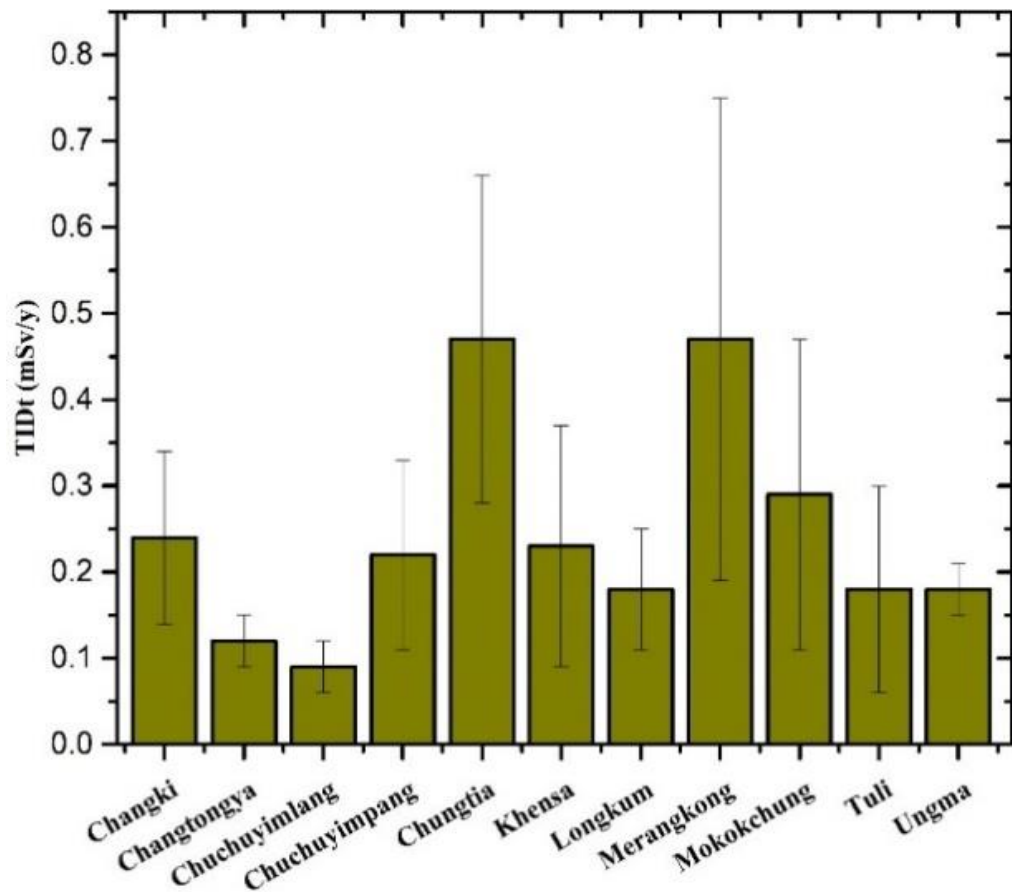


**Fig. 3.8:** Annual average inhalation dose due to  $^{220}\text{Rn}$  and its progeny.

### 3.4 Conclusion

In this present study, a wide variation of indoor  $^{222}\text{Rn}$ ,  $^{220}\text{Rn}$ , and their progenies are observed in the study area. This may be due to the geological locations, topography, and building materials used in the construction of dwellings surveyed and also to the influence of environmental factors such as temperature, pressure, humidity, and weather. From the present study, it can be concluded that:

1. The concentration of annual average indoor  $^{222}\text{Rn}$ ,  $^{220}\text{Rn}$  along with their daughter products are below the recommended value as approved by ICRP.
2. The equilibrium factor between  $^{222}\text{Rn}$  and its progeny range between 0.06 to 0.29 with a mean value of 0.13 which is less than the world average value of 0.4. Similarly, the E.F for  $^{220}\text{Rn}$  and its progeny range between 0.01 to 0.02 with a mean value of 0.016 which is also less than the world average value of 0.02. The low value of the equilibrium factor may be attributed to the low level of dust and aerosol concentration and the clean environment in the study region.
3. The total inhalation dose ranges from 0.35 mSv/y to 1.64 mSv/y and is within the recommended levels as suggested by ICRP, 2018.
4. The level of  $^{222}\text{Rn}$  and  $^{220}\text{Rn}$  concentration was higher in winter as compared to summer and rainy seasons.
5. The level of  $^{222}\text{Rn}$  concentration was higher than the level of  $^{220}\text{Rn}$  concentration in most of the dwellings in the study area.

## References

1. ICRP (2018) International Commission on Radiological Protection. Radiological protection against radon exposure. ICRP Publication ref 4836-9756-8598. ICRP, Stockholm, Sweden.
2. UNSCEAR (2000) United Nation Scientific Committee on the Effect of Atomic Radiation. Sources, Effects and Risks of Ionizing Radiation. Report to the General Assembly. United Nation, New York.
3. WHO (2009) Handbook on indoor radon: a public health perspective. World Health Organization, Geneva, Switzerland (ISBN: 978 92 4 154767 3).
4. Darby S, Hill D, Auvinen A, Barros-Dios JM, Baysson H, Bochicchio F, Deo H, Falk R, Forastiere F, Hakama M, Heid I, Kreienbrock L, Kreuzer M, Lagarde F, Mäkeläinen I, Muirhead C, Oberaigner W, Pershagen G, Ruano-Ravina A, Ruosteenoja E, Schaffrath Rosario A, Tirmarche M, Tomásek L, Whitley E, Wichmann H.E, Doll R (2005) Radon in homes and risk of lung cancer. Collaborative analysis of individual data from 13 European case-control studies. *Br Med J* 330 (7485): 223-226. <https://doi.org/10.1136/bmj.38308.477650.63>
5. Krewski D, Lubin JH, Zielinski JM, Alavanja M, Catalan VS, Field RW, Klotz JB, Létourneau EG, Lynch CF, Lyon JL, Sandler DP, Schoenberg JB, Steck DJ, Stolwijk JA, Weinberg C, Wilcox HB (2006) A combined analysis of north American case-control studies of residential radon and lung cancer. *J Toxicol Environ Health Part A* 69: 533–597. <https://doi.org/10.1080/15287390500260945>
6. Butterweck G, Schuler C, Vezzù G, Müller R, Marsh JW, Thrift S, Birchall A, (2002) Experimental determination of the absorption rate of unattached radon progeny from respiratory tract to blood. *Radiat Prot Dosim* 102: 343–348. <https://doi.org/10.1093/oxfordjournals.rpd.a006103>
7. Nazaroff WW (1992) Radon transport from soil to air. *Reviews of Geophysics* 30(2): 137. <https://doi:10.1029/92rg00055>
8. Sahoo BK, Sapra BK, Gaware JJ, Kanse SD, Mayya YS (2011) A model to predict radon exhalation from walls to indoor air based on the exhalation from building material samples. *Sci Total Environ* 409. <https://doi.org/10.1016/j.scitotenv.2011.03.031>
9. Ishimori Y, Lange K, Martin P, Mayya YS, Phaneuf M (2013) Measurement

and Calculation of Radon Releases from NORM Residues. IAEA Technical Reports Series No 474 IAEA ISBN: 978-92-0-142610-9

10. Deka PC, Sarkar S, Bhattacharjee B, Goswami TD, Sarma BK, Ramachandran TV (2003) Measurement of radon and thoron concentration by using LR-115 type-II plastic track detectors in the environ of Brahmaputra Valley, Assam, India, in. *Radiat Meas* 36: 431–434. [https://doi.org/10.1016/S1350-4487\(03\)00165-3](https://doi.org/10.1016/S1350-4487(03)00165-3)
11. Dwivedi KK, Mishra R, Tripathy SP (2005) An extensive indoor  $^{222}\text{Rn}/^{220}\text{Rn}$  monitoring in North-East India. *Radiat Meas* 40: 621–624. <https://doi.org/10.1016/j.radmeas.2005.04.026>
12. Dwivedi KK, Mishra R, Tripathy SP, Kulshreshtha A, Sinha D, Srivastava A, Deka P, Bhattacharjee B, Ramachandran TV, Nambi KSV (2001) Simultaneous determination of radon, thoron and their progeny in dwellings. *Radiat Meas* 33: 7–11. [https://doi.org/10.1016/S1350-4487\(00\)00131-1](https://doi.org/10.1016/S1350-4487(00)00131-1)
13. BEIR VI (1999) Report of the Committee on the biological effects of ionizing radiation: health effects of exposure to radon. Natl. Res. Council. Natl. Acad. Press, Washington. <https://doi.org/10.17226/5499>
14. Lubin JH, Liang Z, Hrubec Z, Pershagen G, Schoenberg JB, Blot WJ, Klotz JB, Xu ZY, Boice JD (1994) Radon exposure in residences and lung cancer among women: Combined analysis of three studies. *Cancer Causes Control* 5: 114–128. <https://doi.org/10.1007/BF01830257>
15. Smith H (1987) Lung Cancer Risk from Indoor Exposures to Radon Daughters. *Radiat Prot Dosim* 20: 195–196. <https://doi.org/10.1093/oxfordjournals.rpd.a080031>
16. Žunić ZS, Mishra R, Čeliković I, Stojanovska Z, Yarmoshenko IV, Malinovsky G, Veselinović N, Gulán L, Čurguz Z, Vaupotič J, Ujic P, Kolarž P, Milić G, Kovacs T, Sapra BK, Kavasi N, Sahoo SK (2019) Effective doses estimated from the results of direct radon and thoron progeny sensors (DRPS/DTPS), exposed in selected regions of BALKANS. *Radiat Prot Dosim* 185(3): 387-390. <https://doi.org/10.1093/rpd/ncz025>
17. Mishra R, Prajith R, Sapra BK, Mayya YS (2010) Response of direct thoron progeny sensors (DTPS) to various aerosol concentrations and ventilation rates. *Nucl Instrum Methods Phys Res B* 268(6): 671-675. <http://dx.doi.org/10.1016/j.nimb.2009.12.012>

18. Rout RP, Mishra R, Prajith R, Tripathy SP, Sapra BK and Jalaluddin S (2018) Application of UV-Visible spectroscopy for measurement of Track density in LR-115 SSNTD based DTPS/DRPS. *J Instrum* 13(6): P06007. <https://doi.org/10.1088/1748-0221/13/06/P06007>
19. Pyngrope A, Khardewsaw A, Sharma Y, Maibam D, Saxena A, Sahoo BK (2020) Study of indoor radon, thoron and their progeny in southwest Khasi hills district of Meghalaya, India. *Radiat prot dosim* 189(3): 347-353. <https://doi.org/10.1093/rpd/ncaa048>
20. Singh B, Kant K, Garg M, Singh A, Sahoo BK (2019) A study of seasonal variations of radon, thoron and their progeny levels in different types of dwellings in Faridabad district, Southern Haryana, India. *J Radioanal Nucl Chem* 320: 841–857. <https://doi.org/10.1007/s10967-019-06544-3>
21. Singla AK, Kansal S, Mehra R (2021) Dose distribution to individual tissues and organs due to exposure of alpha energies from radon and thoron to local population of Hanumangarh, Rajasthan, India. *J Radioanal Nucl Chem* 327: 1073–1085. <https://doi.org/10.1007/s10967-021-07604-3>
22. Didier TSS, Saïdou, Tokonami S, Hosoda M, Suzuki T, Kudo H, Bouba O (2019) Simultaneous measurements of indoor radon and thoron and inhalation dose assessment in Douala City, Cameroon. *Isot Environ Health Stud* 55(5): 499-510. <https://doi.org/10.1080/10256016.2019.1649258>
23. Szabó Z, Jordan G, Szabó C, Horváth A, Holm O, Kocsy G, Csige I, Szabó P, Homoki Z (2014) Radon and thoron levels, their spatial and seasonal variations in adobe dwellings – a case study at the great Hungarian plain. *Isot Environ Health Stud* 50(2): 211-225. <https://doi.org/10.1080/10256016.2014.862533>
24. Ao A, Bhowmik SK (2014) Cold subduction of the Neotethys: the metamorphic record from finely banded lawsonite and epidote blueschists and associated metabasalts of the Nagaland Ophiolite Complex, India. *J Metamorph Geol* 32: 829–860. <https://doi.org/10.1111/jmg.12096>
25. Godish T, Raton B (2001) FL. CRC Press LLC.
26. Sinha D, Sinha UB, Kibami D, Pongener C, Mishra R, Prajith R, Mayya YS (2013) Measurement of Radon and Thoron progeny concentration in some dwellings of Nagaland state- an initial report. *J Appl chemistry* 2: 825–831.
27. Singh AK, Khan AJ, Prasad R (1997) Distribution of  $^{222}\text{Rn}$  levels in Indian dwellings. *Radiat Prot Dosim* 74:189–192. <https://doi.org/10.1093/oxfordjour>

[nals.rpd.a032196](https://nals.rpd.a032196)

28. Tiakumla (2014) Dynamics of biodiversity and its impact on environment in Mokokchung district, Nagaland xv, 327p. <http://hdl.handle.net/10603/125734>
29. Sahoo BK, Sapra BK, Kanse SD, Gaware JJ, Mayya YS (2013) A new pin-hole discriminated  $^{222}\text{Rn}/^{220}\text{Rn}$  passive measurement device with single entry face. Radiat Meas 58: 52–60. <https://doi.org/10.1016/j.radmeas.2013.08.003>
30. Eappen KP, Mayya YS (2004) Calibration factors for LR-115 (type-II) based radon thoron discriminating dosimeter. Radiat Meas 38: 5–17. <https://doi.org/10.1016/j.radmeas.2003.09.003>
31. Mishra R, Mayya YS, Kushwaha HS (2009) Measurement of  $^{220}\text{Rn}/^{222}\text{Rn}$  progeny deposition velocities on surfaces and their comparison with theoretical models. J Aerosol Sci 40: 1–15. <https://doi.org/10.1016/j.jaerosci.2008.08.001>
32. Mishra R, Mayya YS (2008) Study of a deposition-based direct thoron progeny sensor (DTPS) technique for estimating equilibrium equivalent thoron concentration (EETC) in indoor environment. Radiat Meas 43: 1408–1416. <https://doi.org/10.1016/j.radmeas.2008.03.002>
33. Mayya YS, Eappen KP, Nambi KSV (1998) Methodology for mixed field inhalation dosimetry in monazite areas using a twin-cup dosimeter with three track detectors. Radiat Prot Dosim 77: 177–184. <https://doi.org/10.1093/oxfordjournals.rpd.a032308>
34. UNSCEAR (2008) Report: Sources and effects of ionizing radiation, Volume II, United Nations, New York, 2011 (e-ISBN-13: 978-92-1-054482-5).
35. International Commission on Radiological Protection (ICRP) (2014) Radiological protection against radon exposure. ICRP Publication 126. Ann ICRP 43: 3–37.
36. Kumar A, Sharma S, Mehra R, Narang S, Mishra R (2017) Assessment of indoor radon, thoron concentrations, and their relationship with seasonal variation and geology of Udhampur district, Jammu & Kashmir, India. Int J Occup Environ Health 23: 202–214. <https://doi.org/10.1080/10773525.2018.1450326>
37. United Nations Scientific Committee on the Effect of Atomic Radiation (UNSCEAR) (2006) Report A/AC.82/644, exposures of workers and the public from various sources of radiations. United Nations, New York.

## CHAPTER- 4

### A comprehensive study on indoor radon, thoron, and their progeny level in Dimapur district of Nagaland, India

---

*Indoor radon ( $^{222}\text{Rn}$ ), thoron ( $^{220}\text{Rn}$ ), and their progeny concentrations were detected in several homes in Dimapur district, Nagaland, utilizing Direct Radon and Thoron progeny sensors based on solid-state Nuclear Track Detectors (Type-2 film) and pinhole type radon-thoron discriminating dosimeters. For three separate seasons, the radon, thoron, and their progeny level were been determined in 80 different houses in the study area. The residences were chosen to have various types of housing, such as concrete, semi-wood/bamboo, and bamboo, with varying levels of ventilation that contribute to indoor  $^{222}\text{Rn}$ ,  $^{220}\text{Rn}$ , and their progeny. The inhalation dose in the survey area lies between  $0.33$  and  $3.04 \text{ mSvy}^{-1}$  and is within the reference value as suggested by ICRP, 2018.*

---

---

The text of this chapter has been published as:

**Jamir S, Sahoo BK, Mishra R, and Sinha D (2022) A comprehensive study on indoor radon, thoron and their progeny level in Dimapur district of Nagaland, India. J. Radiat. Prot. Dosim. 198 (12), 1–9. <https://doi.org/10.1093/rpd/ncac150>**

## 4.1 Introduction

Radioactive noble gas radon ( $^{222}\text{Rn}$ ) and thoron ( $^{220}\text{Rn}$ ) are formed by the continuous disintegration of  $^{238}\text{U}$  (Uranium) that are present in rocks and soils [1-4]. They enter into the indoor environment primarily through exhalation from the soil, rocks, and building materials used for the construction of the house. Soil infiltration is reckoned as the most significant cause of residential radon [5]. It is reported that  $^{222}\text{Rn}$ ,  $^{220}\text{Rn}$ , and their decay products contribute about 52% of the radiation dose received by humans from natural sources of radiation [6]. Epidemiological studies have discovered significant evidence of a relationship between indoor radon and lung cancer, even at relatively low radon levels often encountered in residential dwellings [7-9]. The radon progeny enters the respiratory system when air is inhaled, and the radon progeny deposited in the human respiratory tract contributes to the lung dosage [10, 11]. Currently, radon is the leading cause of lung cancer in nonsmokers and the second leading cause among smokers [12, 13]. As a result, radon research has gotten a lot of interest from the international community, and a lot of radon research has been done and reported by many researchers throughout the world [14-17].  $^{220}\text{Rn}$  and their progeny, on the other hand, are paid little attention due to their short half-life (~55.6 seconds). In this regard, several studies were conducted by researchers and found that at some locations thoron concentrations can be comparable to or even higher than the concentrations of radon [18-26]. These findings triggered the interest in studying indoor radon as well as thoron and their progeny in more detail. Since the decay products impart a major portion of the inhalation doses, it is necessary to assess the progeny level along with their corresponding gas concentrations.

Igneous, metamorphic, and sedimentary rocks are found in Nagaland, including shale (Disang group), sandstone (Barail group), limestone, volcanic deposits, and Pelagic. A comprehensive analysis of the radon level is necessary since it will provide an overview of the radiation present in the area [27, 28]. In the state of Nagaland, there is very limited information accessible on the details of radon research. In various sections of Nagaland, the average radon progeny concentration value ranged from  $1.85 \text{ Bqm}^{-3}$  to  $10.68 \text{ Bqm}^{-3}$ , while the  $^{220}\text{Rn}$  concentration ranged from  $0.06 \text{ Bqm}^{-3}$  to  $2.67 \text{ Bqm}^{-3}$  [29]. A geometrical mean of the potential alpha energy concentration (PAEC) measured in the Kohima district in 1997 using LR-115 film in bare mode was found to be  $88 \text{ Bqm}^{-3}$  in



another investigation [30]. Earlier the studies were mainly concentrated on measuring the  $^{222}\text{Rn}$  and  $^{220}\text{Rn}$  gas, and the progeny concentration (EERC and EETC) was determined with the use of an assumed equilibrium factor. But the development of deposition-based Direct progeny sensors (DRPS and DTPS) provided a means to directly measure the progeny concentration. This is important because it is the progeny which is the major dose givers. UNSCEAR has also given a dose-conversion-coefficient of 0.17 and 0.11 nSvBq<sup>-1</sup>h<sup>-1</sup>m<sup>3</sup> for  $^{222}\text{Rn}$  and  $^{220}\text{Rn}$  gas respectively, but 9 and 40 nSvBq<sup>-1</sup>h<sup>-1</sup>m<sup>3</sup> for EERC and EETC respectively. Recently our group used DRPS and DTPS and reported on the Mokokchung district of Nagaland [31]. The average  $^{222}\text{Rn}$  in the Mokokchung district was found to vary from  $44 \pm 6 \text{ Bqm}^{-3}$  to  $75 \pm 16 \text{ Bqm}^{-3}$  and its corresponding EERC varies with an average from  $3.2 \pm 2.1 \text{ Bqm}^{-3}$  to  $17.3 \pm 8.7 \text{ Bqm}^{-3}$ . While average  $^{220}\text{Rn}$  concentration varies from  $25 \pm 2 \text{ Bqm}^{-3}$  to  $62 \pm 49 \text{ Bqm}^{-3}$  and its corresponding EETC varies with an average from  $0.21 \pm 0.06 \text{ Bqm}^{-3}$  to  $1.49 \pm 0.86 \text{ Bqm}^{-3}$  respectively. So far no detailed studies are done about  $^{222}\text{Rn}$ ,  $^{220}\text{Rn}$ , and their progeny level variation in the present study region. Therefore, it is planned to carry out a comprehensive study on indoor  $^{222}\text{Rn}$ ,  $^{220}\text{Rn}$ , and their progeny level in the Dimapur district of Nagaland. In this study, a single-entry pinhole dosimeter and deposition-based direct radon/thoron progeny sensors (DRPS/DTPS) were employed to conduct time-integrated  $^{222}\text{Rn}$ ,  $^{220}\text{Rn}$ , and progeny assessments in 80 houses across eight sites in the Dimapur district over three seasons. The dwellings have been chosen according to the material (bamboo, semi-wood/bamboo, concrete) used for construction. Based on these settings, the concentration of radon, thoron, equilibrium equivalent concentration, and inhalation dose in the indoor environment was determined and analyzed.

## 4.2 Methodology

### 4.2.1 Study area

Dimapur is one of Nagaland's districts, and it is bordered on the south and east by Kohima district, on the west by Karbi Anglong district of Assam, and on the north by a stretch of Golaghat district of Assam (figure 4.1). It is located at a latitude of 25°54'45"N and a longitude of 93°44'30"E. It covers 927 Km<sup>2</sup> (195 meters above sea level). Summers are hot and humid (with temperatures reaching 36°C and humidity levels reaching 93%), while winters are mild and pleasant [32]. The rocks found in the

district are of tertiary to quaternary period. Also, alluvium deposits comprising pebbles, sands, boulders, and silts occupy a major portion of the region [33].

There is various type of houses found in the study area. In this regard, the houses are divided into three main groups (figure 4.2) as follows:

(i) Type A: The house is built of concrete (the floor is cemented, walls and roof is made of concrete). This group accounts for approximately 35% of the homes in the research area.

(ii) Type B: The house is built of semi-wood/bamboo (the floor is cemented, the roof is either made of wooden or bamboo, and the walls are made of half cement and half wooden/bamboo). This group accounts for approximately 35% of the homes in the research area.

(iii) Type C: The house is built of bamboo (floors are cemented, walls and roof is made of bamboo). This group accounts for approximately 30% of the homes in the research area.

The study was carried out between 25<sup>th</sup> of June, 2018, and 25<sup>th</sup> of July, 2019. The year was divided into three seasons: summer, rainy, and winter season, each of which lasted about 120 days.

#### 4.2.2 $^{222}\text{Rn}/^{220}\text{Rn}$ and progeny measurement

For this study, two methods; pin-hole twin cup dosimeter, and DTPS/DRPS were deployed for the measurement of  $^{222}\text{Rn}$ ,  $^{220}\text{Rn}$ , and progeny concentration in indoors [34-37]. The details of the methods of measurement have already been described in chapter 2.

#### 4.2.3 Deployment strategy

DTPS, DRPS, and pin-hole dosimeter were deployed to measure the indoor  $^{222}\text{Rn}$ ,  $^{220}\text{Rn}$ , and their short-lived decay products. A total of 80 households in 8 different places in the Dimapur district were selected for this study during the survey period. The detectors were retained inside the buildings by suspending 30 cm away from the adjacent wall, and three distinct types of dwellings were chosen for the study: concrete (38), bamboo (19), and semi-wood/bamboo houses (23) (figure 4.3)

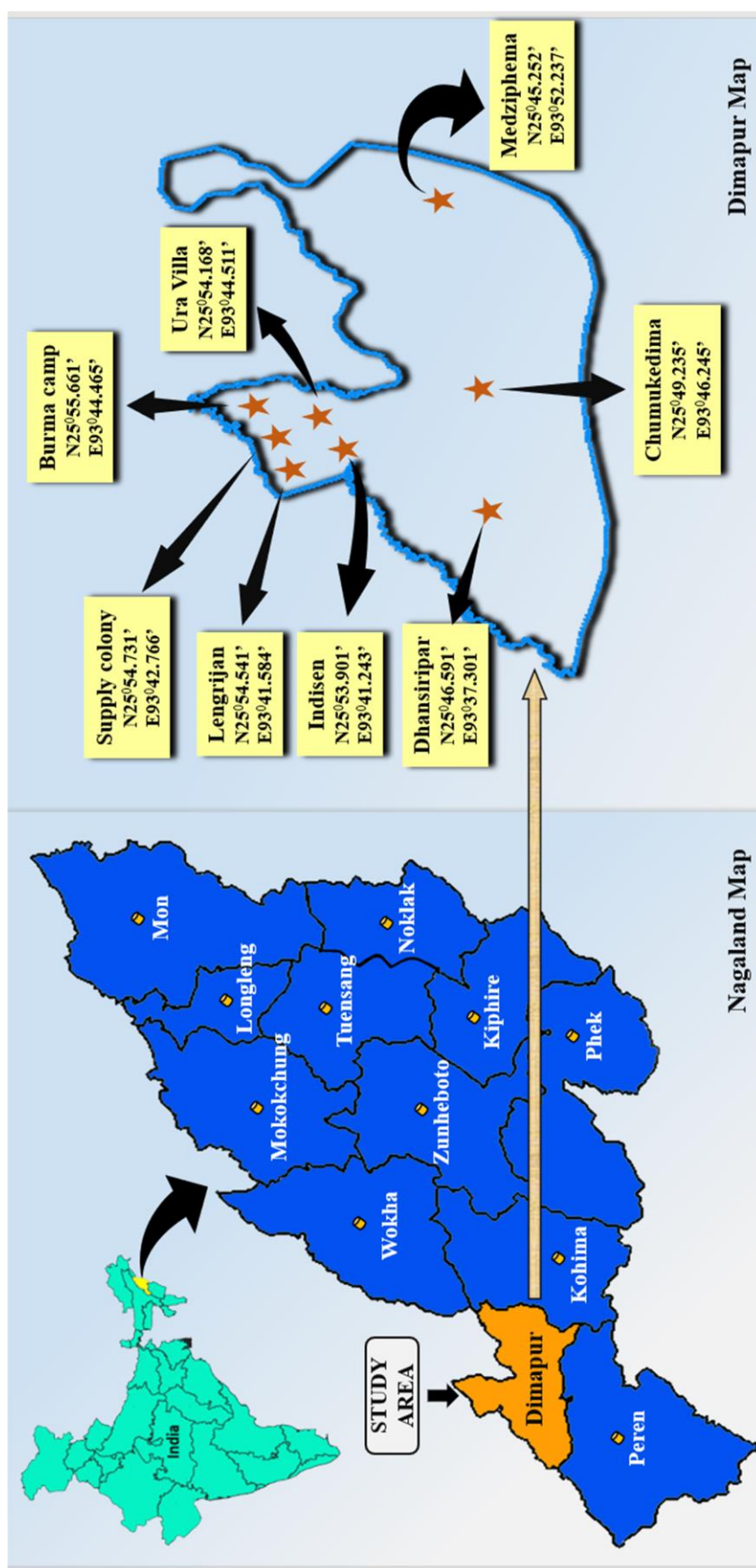


**Fig. 4.1:** Map of the area under study in Dimapur district, Nagaland, India. Dimapur is a district in Nagaland that is bordered on the south and east by Kohima district, on the west by Assam's Karbi Anglong district, and on the north by a stretch of Assam's Golaghat district.

(a)



(b)



(c)



**Fig. 4.2:** Types of houses (a) concrete (b) semi-wood/bamboo (c) bamboo





(a)



(b)



(c)

**Fig.4.3:** Deployment of DTPS/DRPS and Pin hole dosimeter in different types of houses a) concrete house b) semi-wood/bamboo house c) bamboo house.

#### 4.2.3.1 Gamma survey for site selection

The selection of sites of the dwellings was based on a preliminary gamma survey carried out to assess the gamma level falling into different zones.

**Table 4.1:** Gamma level in different houses of the study in Dimapur district, Nagaland, India.

| SI. No. of houses | Gamma level<br>(nSvhr <sup>-1</sup> ) | SI. No. of houses | Gamma level<br>(nSvhr <sup>-1</sup> ) |
|-------------------|---------------------------------------|-------------------|---------------------------------------|
| 1.                | 93                                    | 19.               | 127                                   |
| 2.                | 91                                    | 20.               | 135                                   |
| 3.                | 95                                    | 21.               | 137                                   |
| 4.                | 126                                   | 22.               | 132                                   |
| 5.                | 120                                   | 23.               | 132                                   |
| 6.                | 113                                   | 24.               | 160                                   |
| 7.                | 110                                   | 25.               | 136                                   |
| 8.                | 128                                   | 26.               | 151                                   |
| 9.                | 122                                   | 27.               | 145                                   |
| 10.               | 123                                   | 28.               | 150                                   |
| 11.               | 124                                   | 29.               | 147                                   |
| 12.               | 123                                   | 30.               | 139                                   |
| 13.               | 119                                   | 31.               | 145                                   |
| 14.               | 114                                   | 32.               | 155                                   |
| 15.               | 130                                   | 33.               | 168                                   |
| 16.               | 129                                   | 34.               | 169                                   |
| 17.               | 127                                   | 35.               | 165                                   |
| 18.               | 123                                   | 36.               | 160                                   |

|     |     |     |     |
|-----|-----|-----|-----|
| 37. | 157 | 59. | 196 |
| 38. | 151 | 60. | 198 |
| 39. | 150 | 61. | 182 |
| 40. | 158 | 62. | 199 |
| 41. | 161 | 63. | 197 |
| 42. | 152 | 64. | 185 |
| 43. | 180 | 65. | 197 |
| 44. | 189 | 66. | 201 |
| 45. | 180 | 67. | 190 |
| 46. | 183 | 68. | 193 |
| 47. | 176 | 69. | 188 |
| 48. | 190 | 70. | 200 |
| 49. | 206 | 71. | 206 |
| 50. | 222 | 72. | 210 |
| 51. | 209 | 73. | 188 |
| 52. | 199 | 74. | 189 |
| 53. | 194 | 75. | 184 |
| 54. | 190 | 76. | 180 |
| 55. | 205 | 77. | 195 |
| 56. | 210 | 78. | 214 |
| 57. | 207 | 79. | 183 |
| 58. | 194 | 80. | 189 |

Initially, before the installation of the detectors, gamma dose rate measurements were carried out in the different types of selected houses using the gamma survey meter.

Table 4.1 shows the gamma levels that were measured in some of the residences where the detectors were kept.

Based on the multivariate regression analysis, the gamma level was divided into three zones in each type of house (concrete, semi-wood/bamboo, bamboo) in the study area as shown in table 4.2 given below: The gamma levels were found to be in the range of 171-210 nSv/hr in concrete houses, 131-170 nSv/hr in semi-wood/bamboo houses, and 91-130 nSv/hr in bamboo houses.

**Table 4.2:** Zone-wise house distribution of Dimapur district, Nagaland, India where DTSP/DRPS and Pinhole twin cup dosimeters were installed.

| Total no. of dosimeters to be deployed= 80 |                                    |        |        |        |
|--|------------------------------------|--------|--------|--------|
| Fitting parameter, K= 1.00E + 00           |                                    |        |        |        |
| Zone                                       | Gamma level (nSvhr <sup>-1</sup> ) | Type A | Type B | Type C |
| 1  | 91-130                             | 9      | 7      | 6      |
| 2  | 131-170                            | 14     | 9      | 6      |
| 3  | 171-210                            | 15     | 7      | 7      |

#### 4.2.3.2 Deployment of detectors

Deployment of detectors was calculated using the formula provided, where the number of detectors to be installed was calculated by dividing the zone of gamma radiation level as well as the types of houses. Based on statistical distribution, selection of various types of houses among 80 houses were selected in the pattern as shown in table 4.3.

The village falling into different gamma zones was categorized based on the range of gamma radiation levels recorded during the preliminary survey, an index for the radioactivity content in the location. Once the gamma data is acquired, zone wise house statistic table was made by using a multivariate regression analysis for estimating the number of dosimeters to be deployed in each type of dwelling in the respective zone.



Subsequently, after the selection of dwellings according to the above protocol, dosimeters were deployed in the study region. Around six to eighteen dwellings of each village were selected for the radon and thoron assessment and the GPS coordinates of the location where the detectors were deployed were also recorded. Accordingly, deployment was done in 80 households in the study area as given in table 4.3.

**Table 4.3:** Distribution of detectors in each site of Dimapur district, Nagaland.

| Sl.no | Name of place | No. of DTPS/DRPS and Pinhole dosimeters deployed in different types of houses | Total No. of DTPS/DRPS and Pinhole dosimeters deployed in different types of houses |
|-------|---------------|---|---|
| 1     | Burma camp    | (concrete=2, semi-wood/bamboo=2, bamboo=2)                                    | 6   |
| 2     | Chumukedima   | (concrete=4, semi-wood/bamboo=2, bamboo=1)                                    | 7   |
| 3     | Indisen       | (concrete=3, semi-wood/bamboo =3, bamboo=2)                                   | 8   |
| 4     | Lengrijan     | (concrete=4, semi-wood/bamboo =5, bamboo=3)                                   | 12  |
| 5     | Ura vila      | (concrete=2, semi-wood/bamboo =2, bamboo=1)                                   | 5   |
| 6     | Supply        | (concrete=5, semi-wood/bamboo =5, bamboo=2)                                   | 12  |
| 7     | Medziphema    | (concrete=10, semi-wood/bamboo =2, bamboo=3)                                  | 15  |
| 8     | Dhansiriphar  | (concrete=8, semi-wood/bamboo =2, bamboo=5)                                   | 15  |
|       | <b>Total</b>  | <b>80</b>   | <b>80</b>   |

#### 4.2.4 Post-processing of dosimeters

Dosimeters and progeny sensors were removed from the residences after a 120-day exposure period. Exposed LR-115 was etched in a constant water bath for 90 minutes with a 2.5N NaOH solution at a constant temperature of 60°C. The etched films were

cleaned with clean water and dried overnight in a tissue roll once the etching procedure was completed. The alpha tracks of the LR-115 were pre-sparked at 900 V and tallied using a spark counter (model PSI-SCI) operating at 500 V.

#### 4.2.5 Calculation of $^{222}\text{Rn}$ , $^{220}\text{Rn}$ , and Progeny

Following are the formulas used for the calculations of different parameters of  $^{222}\text{Rn}$ ,  $^{220}\text{Rn}$ , and their Progeny concentrations. The details of the calculation have been discussed in chapter 2.

The following formula was used to calculate the concentration of  $^{222}\text{Rn}$ ,  $C_r$  ( $\text{Bqm}^{-3}$ ), and the concentration of  $^{220}\text{Rn}$ ,  $C_t$  ( $\text{Bqm}^{-3}$ ) [34]

$$C_r = \frac{T_1}{d.K_r} \quad (1)$$

$$C_t = \frac{T_2 - T_1}{d.K_t} \quad (2)$$

Where  $T_1$ , and  $T_2$  are the tracks registered in ' $^{222}\text{Rn}$ ' and ' $^{222}\text{Rn} + ^{220}\text{Rn}$ ' compartments respectively,  $d$  is the exposure time in days. The calibration factors for  $^{222}\text{Rn}$  and  $^{220}\text{Rn}$  in the dosimeter are  $K_r = 0.017 \pm 0.002 \text{ tr.cm}^{-2}\text{d}^{-1}\text{Bqm}^{-3}$  and  $K_t = 0.010 \pm 0.001 \text{ tr.cm}^{-2}\text{d}^{-1}\text{Bqm}^{-3}$ , respectively [34].

Equations (3) and (4) were used to calculate the EERC and EETC respectively [37, 38].

$$EERC = T_c(\text{Tracks.cm}^{-2}.d^{-1})/S_R(\text{Tracks.cm}^{-2}.d^{-1})/EEC(\text{Bq.m}^{-3}) \quad (3)$$

$$EETC = T_c(\text{Tracks.cm}^{-2}.d)/S_T(\text{Tracks.cm}^{-2}.d^{-1})/EEC(\text{Bq.m}^{-3}) \quad (4)$$

Where  $S_R = 0.09 \text{ trcm}^{-2}\text{d}^{-1}\text{Bqm}^{-3}$  corresponds to the sensitivity factor for Radon progeny in DRPS, while  $S_T = 0.94 \text{ trcm}^{-2}\text{d}^{-1}\text{Bqm}^{-3}$  corresponds to the sensitivity factor for Thoron progeny in DTPS [37, 38]. When assessing the tracks owing to radon progeny alone in DRPS, the contribution of thoron progeny tracks were excluded.

Equilibrium factors have been calculated by dividing the progeny to their respective parent  $^{222}\text{Rn}$  and  $^{220}\text{Rn}$  gas. In assessing human radon exposure, the equilibrium factor (E.F) between radon and its short-lived progenies is a critical parameter. Globally, indoor radon has an E.F of 0.4, while indoor thoron has an E.F of 0.02 [6]. Because it is influenced by environmental elements such as pressure, temperature, and humidity,

this projected value may change in different scenarios. It is required to know the value of the equilibrium factor in each scenario to calculate the accurate dose caused by radon and its progeny [6].

Using equations (5) and (6), the inhalation dosage due to radon and thoron was calculated [38, 39].

$$\text{TID}_r (\text{mSvy}^{-1}) = [(C_r \times 0.17) + (\text{EERC} \times 9)] \times 8760 \times 0.8 \times 10^{-6} \quad (5)$$

$$\text{TID}_t (\text{mSvy}^{-1}) = [(C_t \times 0.11) + (\text{EETC} \times 40)] \times 8760 \times 0.8 \times 10^{-6} \quad (6)$$

Where the dosage conversion factors for  $^{222}\text{Rn}$  and  $^{220}\text{Rn}$  concentrations are 0.17 and 0.11  $\text{nSvBq}^{-1}\text{h}^{-1}\text{m}^3$ , respectively, while the dose conversion factors for  $^{222}\text{Rn}$  and  $^{220}\text{Rn}$  progeny concentrations are 9, and 40  $\text{nSvBq}^{-1}\text{h}^{-1}\text{m}^3$ , respectively. The standard occupancy factor for a one-year exposure period is 0.8 [38, 39].

### 4.3 Results and discussions

#### 4.3.1 Annual average $^{222}\text{Rn}$ , $^{220}\text{Rn}$ , EERC/EETC

Table 4.4 gives the details about the annual  $^{222}\text{Rn}$ ,  $^{220}\text{Rn}$ , EERC, and EETC during the study period of each site. It was found that the  $^{222}\text{Rn}$  concentration varied from  $16 \pm 7$  to  $138 \pm 26 \text{ Bqm}^{-3}$  with an average of  $63 \pm 3 \text{ Bqm}^{-3}$  and  $^{220}\text{Rn}$  concentration varied from  $35 \pm 6$  to  $288 \pm 74 \text{ Bqm}^{-3}$  with an average of  $203 \pm 6 \text{ Bqm}^{-3}$ . EERC varied from  $3 \pm 1$  to  $37 \pm 1 \text{ Bqm}^{-3}$  with an average of  $12.1 \pm 0.7 \text{ Bqm}^{-3}$  and EETC varied from  $0.25 \pm 0.02$  to  $2.83 \pm 1.15 \text{ Bqm}^{-3}$  with an average of  $0.79 \pm 0.07 \text{ Bqm}^{-3}$ .

**Table 4.4:** Annual average radon, thoron, and their progeny concentration in Dimapur district, Nagaland.

| Colony (No. of dosimeters and DTPS/DRPS deployed) | Pinhole                                    |  | DTPS/DRPS                     |                               |
|---|--|--|-------------------------------|-------------------------------|
|   | $^{222}\text{Rn}$<br>( $\text{Bqm}^{-3}$ ) | $^{220}\text{Rn}$<br>( $\text{Bqm}^{-3}$ ) | EERC<br>( $\text{Bqm}^{-3}$ ) | EETC<br>( $\text{Bqm}^{-3}$ ) |
| Burma camp (6)                                    | $55 \pm 20$                                | $75 \pm 12$                                | $8 \pm 1$                     | $0.75 \pm 0.12$               |
|   | $58 \pm 24$                                | $100 \pm 29$                               | $11 \pm 1$                    | $0.51 \pm 0.08$               |
|   | $36 \pm 12$                                | $75 \pm 17$                                | $6 \pm 1$                     | $1.60 \pm 0.69$               |
|   | $64 \pm 12$                                | $198 \pm 47$                               | $8 \pm 1$                     | $1.06 \pm 0.33$               |

|                 |              |               |             |                 |
|-----------------|--------------|---------------|-------------|-----------------|
|                 | $31 \pm 6$   | $93 \pm 15$   | $4 \pm 1$   | $1.04 \pm 0.65$ |
|                 | $48 \pm 13$  | $72 \pm 13$   | $8 \pm 1$   | $0.97 \pm 0.28$ |
|                 | $55 \pm 20$  | $75 \pm 12$   | $8 \pm 1$   | $0.75 \pm 0.12$ |
|                 | $58 \pm 24$  | $100 \pm 29$  | $11 \pm 1$  | $0.51 \pm 0.08$ |
|                 | $36 \pm 12$  | $75 \pm 17$   | $6 \pm 1$   | $1.60 \pm 0.69$ |
|                 | $64 \pm 12$  | $198 \pm 47$  | $8 \pm 1$   | $1.06 \pm 0.33$ |
|                 | $31 \pm 6$   | $93 \pm 15$   | $4 \pm 1$   | $1.04 \pm 0.65$ |
|                 | $48 \pm 13$  | $72 \pm 13$   | $8 \pm 1$   | $0.97 \pm 0.28$ |
| Chumukedima (7) | $65 \pm 23$  | $54 \pm 27$   | $16 \pm 3$  | $1.26 \pm 0.49$ |
|                 | $41 \pm 30$  | $65 \pm 27$   | $15 \pm 6$  | $1.24 \pm 0.38$ |
|                 | $63 \pm 26$  | $133 \pm 58$  | $14 \pm 4$  | $2.43 \pm 1.17$ |
|                 | $43 \pm 27$  | $88 \pm 70$   | $23 \pm 12$ | $0.89 \pm 0.29$ |
|                 | $62 \pm 15$  | $110 \pm 14$  | $14 \pm 3$  | $1.87 \pm 0.62$ |
|                 | $41 \pm 27$  | $42 \pm 13$   | $9 \pm 3$   | $0.71 \pm 0.21$ |
|                 | $36 \pm 18$  | $68 \pm 39$   | $9 \pm 3$   | $0.82 \pm 0.12$ |
| Indisen (8)     | $111 \pm 94$ | $87 \pm 70$   | $20 \pm 10$ | $0.97 \pm 0.44$ |
|                 | $76 \pm 51$  | $145 \pm 118$ | $12 \pm 8$  | $1.87 \pm 1.36$ |
|                 | $73 \pm 59$  | $84 \pm 55$   | $37 \pm 1$  | $2.01 \pm 0.79$ |
|                 | $54 \pm 28$  | $185 \pm 86$  | $13 \pm 7$  | $0.79 \pm 0.23$ |
|                 | $61 \pm 50$  | $54 \pm 35$   | $12 \pm 4$  | $0.65 \pm 0.31$ |
|                 | $74 \pm 58$  | $118 \pm 84$  | $17 \pm 8$  | $0.52 \pm 0.28$ |
|                 | $115 \pm 95$ | $115 \pm 70$  | $15 \pm 6$  | $0.57 \pm 0.18$ |
|                 | $47 \pm 31$  | $132 \pm 78$  | $15 \pm 5$  | $1.13 \pm 0.37$ |
| Lengrijan (12)  | $52 \pm 23$  | $98 \pm 32$   | $26 \pm 7$  | $1.51 \pm 0.43$ |
|                 | $72 \pm 35$  | $180 \pm 123$ | $25 \pm 10$ | $2.83 \pm 1.15$ |
|                 | $46 \pm 14$  | $136 \pm 61$  | $22 \pm 12$ | $0.97 \pm 0.29$ |
|                 | $54 \pm 25$  | $93 \pm 33$   | $15 \pm 2$  | $1.93 \pm 1.30$ |
|                 | $62 \pm 21$  | $56 \pm 7$    | $7 \pm 1$   | $0.58 \pm 0.04$ |
|                 | $57 \pm 25$  | $88 \pm 26$   | $25 \pm 7$  | $2.27 \pm 1.23$ |
|                 | $123 \pm 42$ | $288 \pm 74$  | $23 \pm 11$ | $1.64 \pm 0.92$ |
|                 | $64 \pm 25$  | $116 \pm 31$  | $26 \pm 10$ | $1.17 \pm 0.19$ |
|                 | $114 \pm 47$ | $240 \pm 107$ | $23 \pm 8$  | $1.75 \pm 0.88$ |
|                 | $89 \pm 42$  | $98 \pm 59$   | $13 \pm 7$  | $1.36 \pm 0.66$ |
|                 | $79 \pm 31$  | $151 \pm 59$  | $22 \pm 11$ | $1.05 \pm 0.68$ |
|                 | $52 \pm 8$   | $135 \pm 80$  | $9 \pm 6$   | $0.38 \pm 0.17$ |
| Ura vila (5)    | $46 \pm 8$   | $253 \pm 50$  | $11 \pm 2$  | $0.35 \pm 0.08$ |

|                   |              |              |            |                 |
|-------------------|--------------|--------------|------------|-----------------|
|                   | $16 \pm 7$   | $59 \pm 9$   | $9 \pm 2$  | $0.45 \pm 0.12$ |
|                   | $25 \pm 6$   | $35 \pm 6$   | $3 \pm 1$  | $0.25 \pm 0.09$ |
|                   | $50 \pm 9$   | $67 \pm 11$  | $5 \pm 1$  | $1.35 \pm 0.25$ |
|                   | $23 \pm 7$   | $120 \pm 21$ | $10 \pm 2$ | $0.37 \pm 0.15$ |
| Supply (12)       | $33 \pm 22$  | $135 \pm 53$ | $7 \pm 1$  | $0.54 \pm 0.18$ |
|                   | $39 \pm 15$  | $102 \pm 58$ | $10 \pm 4$ | $0.95 \pm 0.29$ |
|                   | $46 \pm 13$  | $59 \pm 18$  | $7 \pm 3$  | $0.42 \pm 0.14$ |
|                   | $58 \pm 33$  | $107 \pm 38$ | $12 \pm 6$ | $0.42 \pm 0.11$ |
|                   | $54 \pm 38$  | $74 \pm 38$  | $11 \pm 6$ | $0.80 \pm 0.35$ |
|                   | $39 \pm 24$  | $48 \pm 14$  | $6 \pm 2$  | $1.30 \pm 0.24$ |
|                   | $52 \pm 33$  | $75 \pm 27$  | $9 \pm 4$  | $0.53 \pm 0.24$ |
|                   | $63 \pm 53$  | $49 \pm 35$  | $10 \pm 2$ | $0.60 \pm 0.12$ |
|                   | $58 \pm 45$  | $101 \pm 63$ | $9 \pm 3$  | $0.69 \pm 0.40$ |
|                   | $45 \pm 27$  | $141 \pm 67$ | $10 \pm 6$ | $0.54 \pm 0.21$ |
|                   | $44 \pm 25$  | $79 \pm 48$  | $9 \pm 4$  | $1.17 \pm 0.71$ |
|                   | $39 \pm 27$  | $38 \pm 19$  | $9 \pm 3$  | $0.88 \pm 0.59$ |
| Medziphema (15)   | $67 \pm 18$  | $87 \pm 9$   | $9 \pm 1$  | $0.39 \pm 0.07$ |
|                   | $94 \pm 27$  | $134 \pm 19$ | $13 \pm 1$ | $0.25 \pm 0.02$ |
|                   | $53 \pm 8$   | $56 \pm 8$   | $9 \pm 2$  | $0.31 \pm 0.04$ |
|                   | $64 \pm 21$  | $80 \pm 34$  | $14 \pm 5$ | $0.44 \pm 0.06$ |
|                   | $75 \pm 15$  | $80 \pm 15$  | $9 \pm 4$  | $0.41 \pm 0.06$ |
|                   | $76 \pm 27$  | $93 \pm 38$  | $6 \pm 2$  | $0.40 \pm 0.07$ |
|                   | $138 \pm 26$ | $185 \pm 39$ | $8 \pm 4$  | $0.33 \pm 0.06$ |
|                   | $81 \pm 23$  | $117 \pm 44$ | $11 \pm 1$ | $0.46 \pm 0.06$ |
|                   | $129 \pm 36$ | $171 \pm 27$ | $10 \pm 3$ | $0.43 \pm 0.07$ |
|                   | $113 \pm 40$ | $149 \pm 58$ | $15 \pm 7$ | $0.30 \pm 0.03$ |
|                   | $102 \pm 31$ | $173 \pm 65$ | $9 \pm 4$  | $0.34 \pm 0.03$ |
|                   | $76 \pm 27$  | $100 \pm 38$ | $10 \pm 4$ | $0.32 \pm 0.03$ |
|                   | $29 \pm 6$   | $172 \pm 83$ | $8 \pm 2$  | $0.29 \pm 0.03$ |
|                   | $37 \pm 8$   | $57 \pm 16$  | $8 \pm 2$  | $0.34 \pm 0.04$ |
|                   | $38 \pm 12$  | $178 \pm 69$ | $9 \pm 3$  | $0.32 \pm 0.03$ |
| Dhansiriphar (15) | $61 \pm 13$  | $99 \pm 6$   | $13 \pm 3$ | $0.36 \pm 0.03$ |
|                   | $85 \pm 20$  | $113 \pm 12$ | $17 \pm 3$ | $0.26 \pm 0.03$ |
|                   | $52 \pm 8$   | $98 \pm 4$   | $9 \pm 2$  | $0.31 \pm 0.03$ |
|                   | $63 \pm 21$  | $123 \pm 14$ | $11 \pm 2$ | $0.40 \pm 0.05$ |
|                   | $71 \pm 18$  | $95 \pm 3$   | $9 \pm 2$  | $0.39 \pm 0.05$ |

|  |              |              |            |                 |
|--|--------------|--------------|------------|-----------------|
|  | $83 \pm 18$  | $161 \pm 34$ | $6 \pm 2$  | $0.37 \pm 0.04$ |
|  | $96 \pm 32$  | $159 \pm 23$ | $7 \pm 1$  | $0.26 \pm 0.03$ |
|  | $84 \pm 20$  | $118 \pm 12$ | $18 \pm 4$ | $0.45 \pm 0.04$ |
|  | $104 \pm 48$ | $163 \pm 54$ | $11 \pm 2$ | $0.39 \pm 0.04$ |
|  | $74 \pm 14$  | $132 \pm 29$ | $6 \pm 2$  | $0.30 \pm 0.03$ |
|  | $105 \pm 23$ | $248 \pm 25$ | $7 \pm 1$  | $0.33 \pm 0.03$ |
|  | $58 \pm 11$  | $131 \pm 16$ | $9 \pm 3$  | $0.34 \pm 0.03$ |
|  | $38 \pm 8$   | $144 \pm 14$ | $9 \pm 2$  | $0.27 \pm 0.03$ |
|  | $37 \pm 8$   | $136 \pm 12$ | $9 \pm 3$  | $0.37 \pm 0.04$ |
|  | $33 \pm 7$   | $203 \pm 38$ | $10 \pm 3$ | $0.30 \pm 0.03$ |

### 4.3.2 Seasonal variations of radon, thoron, and their corresponding EEC

The study year was divided into three seasons namely summer, rainy, and winter (table 4.5). It was observed that the indoor  $^{222}\text{Rn}$ ,  $^{220}\text{Rn}$ , and its progeny were found to be higher during the winter season as compared to the summer and rainy seasons as shown in figure 4.4a and figure 4.4b. This could be due to comparatively less ventilation during the winter season, as windows and doors are kept closed for a longer period during winter.

**Table 4.5:**  $^{222}\text{Rn}$  (and its progeny) and  $^{220}\text{Rn}$  (and its progeny) parameters in different seasons in Dimapur district, Nagaland.

| Seasons |         | $^{222}\text{Rn}$<br>( $\text{Bqm}^{-3}$ ) | $^{220}\text{Rn}$<br>( $\text{Bqm}^{-3}$ ) | EERC<br>( $\text{Bqm}^{-3}$ ) | EETC<br>( $\text{Bqm}^{-3}$ ) |
|---------|---------|--|--|-------------------------------|-------------------------------|
| Summer  | Average | $35 \pm 3$                                 | $84 \pm 8$                                 | $9.7 \pm 1$                   | $0.55 \pm 0.06$               |
|         | Minimum | 4  | 6  | 1.7                           | 0.01                          |
|         | Maximum | 170  | 290  | 47.4                          | 2.82                          |
| Rainy   | Average | $48 \pm 4$                                 | $90 \pm 8$                                 | $10.5 \pm 0.9$                | $0.71 \pm 0.08$               |
|         | Minimum | 4  | 3  | 0.1                           | 0.09                          |
|         | Maximum | 131  | 324  | 46.4                          | 4.69                          |
| Winter  | Average | $106 \pm 6$                                | $173 \pm 10$                               | $16.2 \pm 1.1$                | $1.10 \pm 0.12$               |
|         | Minimum | 24   | 47   | 3.5                           | 0.29                          |
|         | Maximum | 306  | 425  | 54.9                          | 4.88                          |

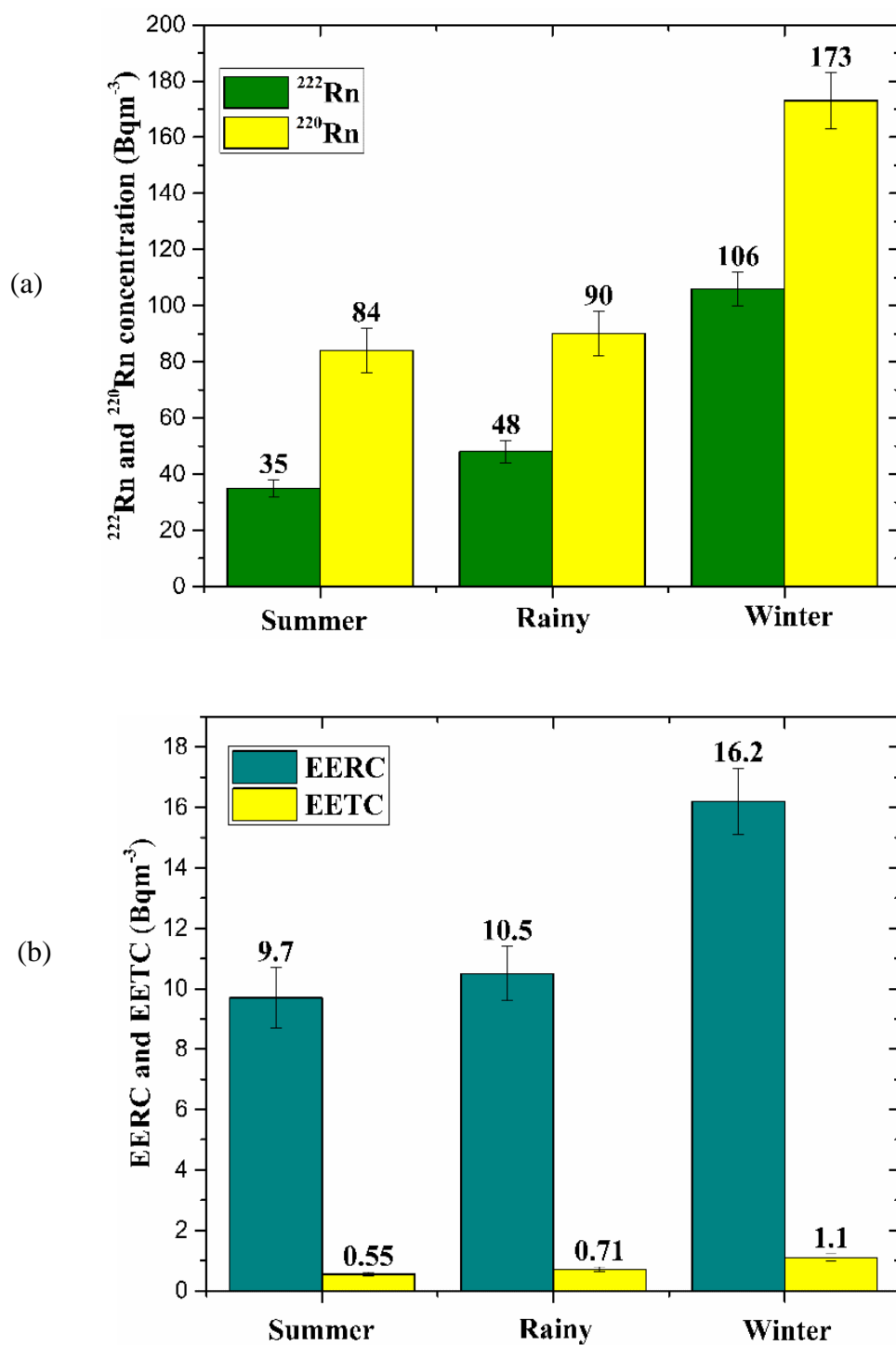


**Fig. 4.4:** (a)  $^{222}\text{Rn}$  and  $^{220}\text{Rn}$  in different seasons (b) EERC and EETC in different seasons.

Indoor  $^{222}\text{Rn}$  concentrations vary from 4 Bqm<sup>-3</sup> to 170 Bqm<sup>-3</sup> throughout the summer, with an average of  $35 \pm 3$  Bqm<sup>-3</sup>, while thoron concentrations range from 6 Bqm<sup>-3</sup> to 290 Bqm<sup>-3</sup>, with an average of  $84 \pm 8$  Bqm<sup>-3</sup>. The radon concentration is within the

ICRP's 2018 recommended range (ICRP, 2018) [40]. On the other hand, the thoron value appears to be more than the global average of  $10 \text{ Bqm}^{-3}$  [39, 41]. The  $^{222}\text{Rn}$  progeny were calculated to be between  $1.7$  and  $47.4 \text{ Bqm}^{-3}$ , with an average of  $9.7 \pm 1 \text{ Bqm}^{-3}$ . The average  $^{220}\text{Rn}$  progeny was  $0.55 \pm 0.06 \text{ Bqm}^{-3}$ , with a range of  $0.01$  to  $2.82 \text{ Bqm}^{-3}$ .

The average indoor  $^{222}\text{Rn}$  concentration was  $48 \pm 4 \text{ Bqm}^{-3}$  during the rainy season, while the  $^{220}\text{Rn}$  concentration was  $90 \pm 8 \text{ Bqm}^{-3}$ .  $^{220}\text{Rn}$  progeny ranged from  $0.09 \text{ Bqm}^{-3}$  to  $4.69 \text{ Bqm}^{-3}$ , with an average of  $0.71 \pm 0.08 \text{ Bqm}^{-3}$ .  $^{222}\text{Rn}$  progeny ranged from  $0.1 \text{ Bqm}^{-3}$  to  $46.4 \text{ Bqm}^{-3}$ , with an average of  $10.5 \pm 0.9 \text{ Bqm}^{-3}$ .

During the winter season, indoor  $^{222}\text{Rn}$  concentrations vary from  $24 \text{ Bqm}^{-3}$  to  $306 \text{ Bqm}^{-3}$ , with an average of  $106 \pm 6 \text{ Bqm}^{-3}$ , while indoor  $^{220}\text{Rn}$  concentrations range from  $47 \text{ Bqm}^{-3}$  to  $425 \text{ Bqm}^{-3}$ , with an average of  $173 \pm 10 \text{ Bqm}^{-3}$ . Similarly,  $^{222}\text{Rn}$  progeny ranged from  $3.5 \text{ Bqm}^{-3}$  to  $54.9 \text{ Bqm}^{-3}$ , with an average of  $16.2 \pm 1.1 \text{ Bqm}^{-3}$ , whereas  $^{220}\text{Rn}$  progeny had a range of  $0.29 \text{ Bqm}^{-3}$  to  $4.88 \text{ Bqm}^{-3}$ , with an average of  $1.10 \pm 0.12 \text{ Bqm}^{-3}$ .

Figure 4.5 show the Box plot of  $^{222}\text{Rn}$ ,  $^{220}\text{Rn}$ , EERC, and EETC for three different seasons. From figure 4.5a and figure 4.5b, it can be seen that during the winter season  $^{222}\text{Rn}$  and  $^{220}\text{Rn}$  shows a maximum interquartile range (IQR) of  $72.12 \text{ Bqm}^{-3}$  and  $127.67 \text{ Bqm}^{-3}$  respectively. Thus, the graph clearly depicts that the variability of thoron is more as compared to radon.

The typical variation of temperature in Dimapur in the three seasons is like Summer varies with an average from  $23^\circ\text{C}$  to  $32.2^\circ\text{C}$ , rainy with an average from  $18^\circ\text{C}$  to  $30^\circ\text{C}$ , and winter temperature with an average from  $9.3^\circ\text{C}$  to  $22.5^\circ\text{C}$ . So, in winter since the doors and windows are closed, thereby ventilation becomes less which facilitates the build-up of  $^{222}\text{Rn}$ ,  $^{220}\text{Rn}$ , and progeny. Hence, the activity concentration is more in winter. Interestingly the  $^{220}\text{Rn}$  concentration is more than the  $^{222}\text{Rn}$  concentration in all the seasons, which needs to be studied further.



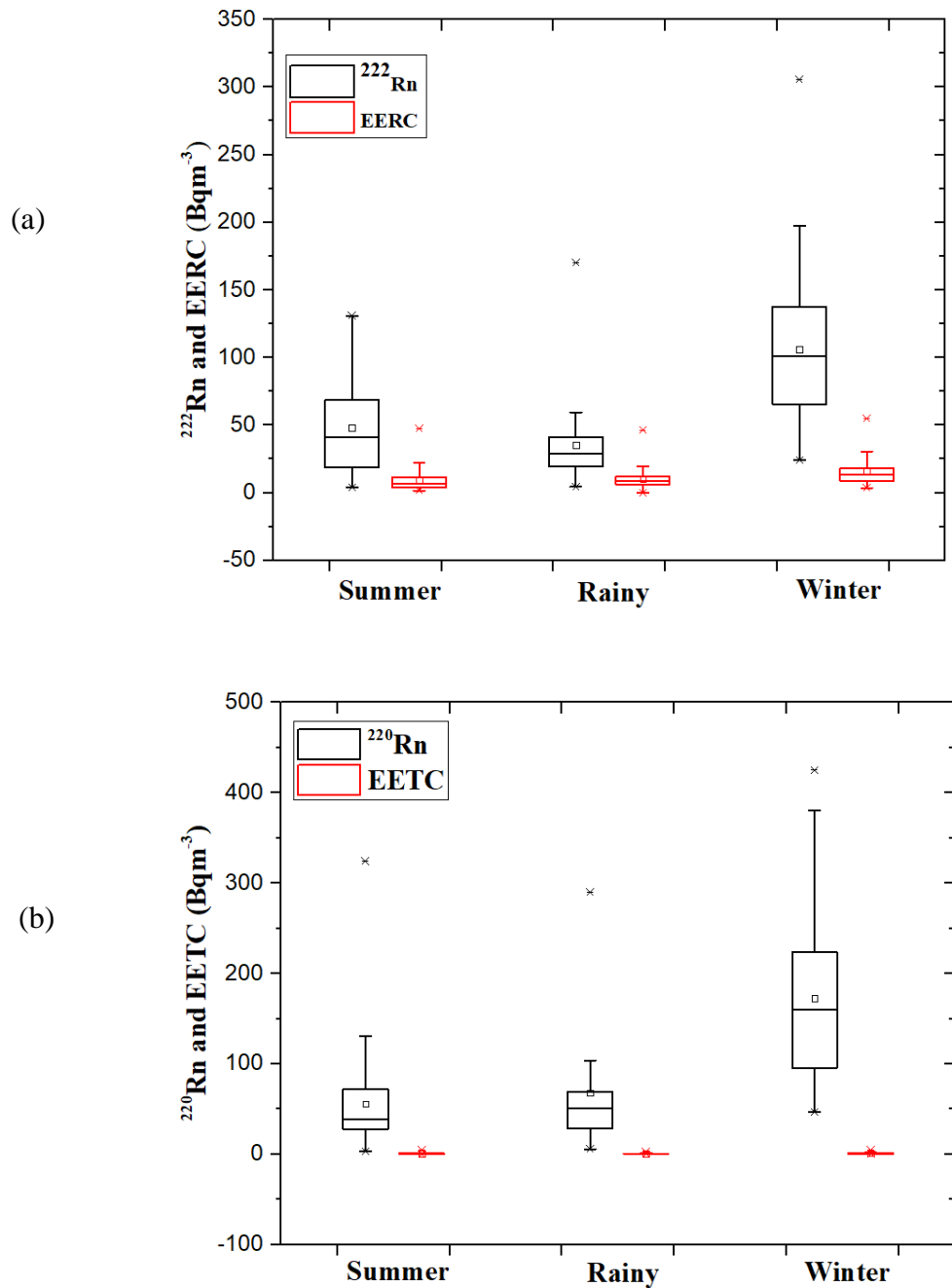


**Fig. 4.5:** (a) Box plot of  $^{222}\text{Rn}$  and EERC in different seasons (b) Box plot of  $^{220}\text{Rn}$  and EETC in different seasons.

#### 4.3.3 $^{222}\text{Rn}$ , $^{220}\text{Rn}$ , EERC, EETC in various types of houses

The variation of average indoor  $^{222}\text{Rn}$ ,  $^{220}\text{Rn}$ , and its progeny in various types of dwellings are shown in figures 4.6a and figure 4.6b. Indoor levels of  $^{222}\text{Rn}$ , and  $^{220}\text{Rn}$ , and their progeny are observed to be higher in concrete types of houses.

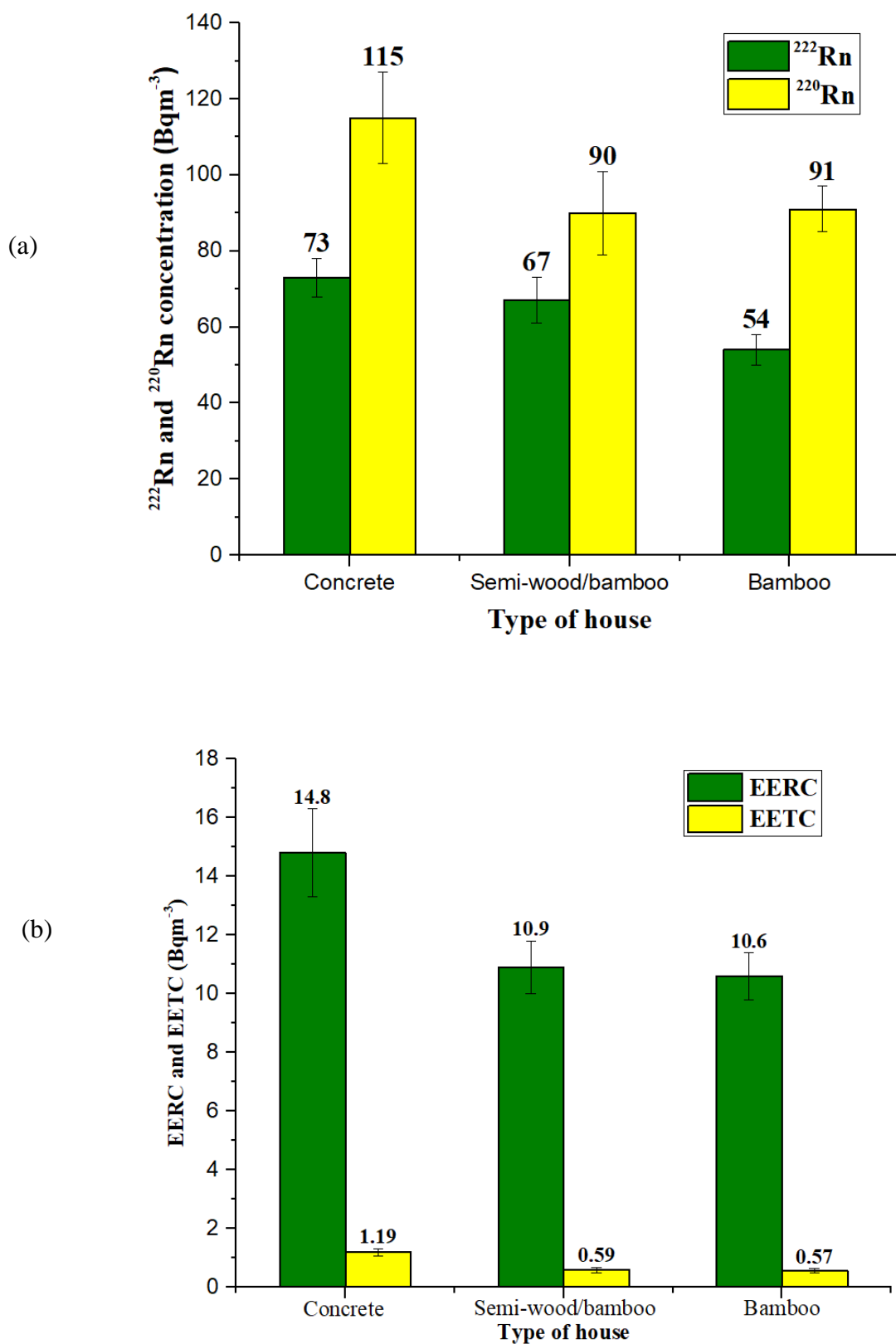


**Fig. 4.6:** (a)  $^{222}\text{Rn}$  and  $^{220}\text{Rn}$  in different types of houses (b) EERC and EETC in different types of houses.

#### 4.3.4 Equilibrium factor (E.F) in various types of houses

The equilibrium factor of radon in concrete, semi- wood/bamboo, and bamboo house types are found to vary with an average of 0.20, 0.16, and 0.20 respectively. These values are consistent with the earlier reports carried out in the Mokokchung district where the radon E.F varied from 0.06 to 0.29 [31]. The low value of the equilibrium factor may be attributed to the low level of dust and aerosol concentration in the study region.

Figure 4.7 demonstrates that among all the house types, concrete type of housing had the highest interquartile range (IQR) of radon and thoron equilibrium factor i.e., radon IQR= 0.11, and thoron IQR= 0.01. As a result, the concrete type of house has more radon and thoron E.F variability than the other types of dwellings in the study region.

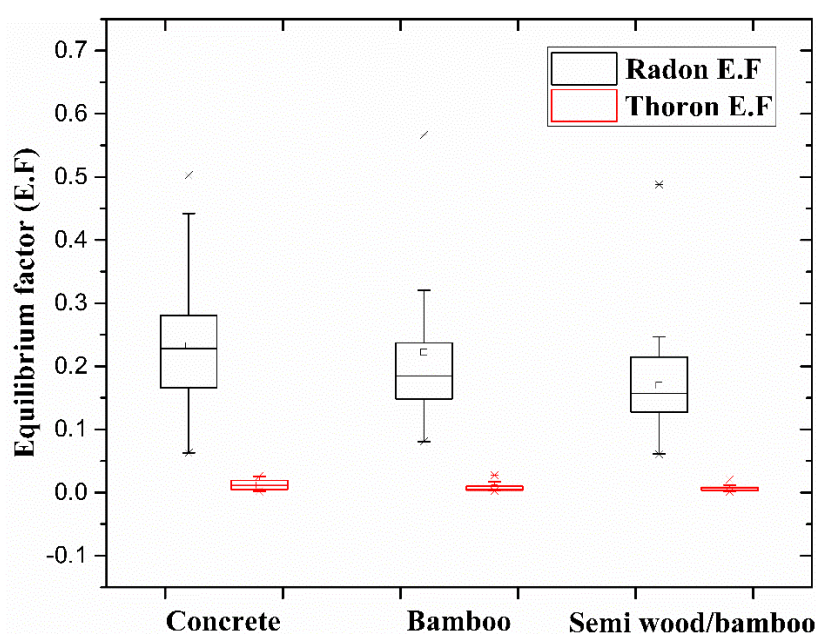


**Fig. 4.7:** Equilibrium factor in different types of houses.

#### 4.3.5 Inhalation dose

The yearly inhalation dosage attributable to  $^{222}\text{Rn}$ ,  $^{222}\text{Rn}$ , and their progeny ranges from  $0.33 \text{ mSvy}^{-1}$  to  $3.04 \text{ mSvy}^{-1}$ , with an average of  $1.15 \pm 0.06 \text{ mSvy}^{-1}$ , which is well within the UNSCEAR's recommended value (UNSCEAR, 2000) [6].

From figure 4.8, it can be seen that 1 out of 80 dwellings lies in the dose range below  $0.60 \text{ mSvy}^{-1}$ , and 7 percent are in the dose range of  $2.13 - 2.63 \text{ mSvy}^{-1}$ . The majority of the dwellings (66 %) fall between  $0.60 \text{ mSvy}^{-1}$  and  $1.10 \text{ mSvy}^{-1}$ . Only 1 out of every 80 dwellings is exposed to a dose greater than  $2.63 \text{ mSvy}^{-1}$ . Nevertheless, the obtained dose values are within the range recommended by ICRP [40].

Thus, we could say that there is no significant risk associated with the present survey area.

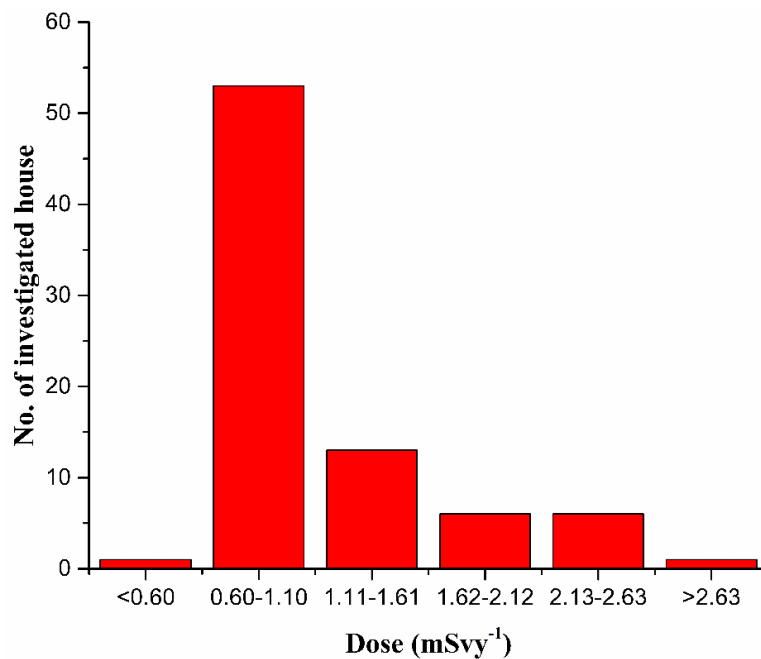


**Fig. 4.8:** Total inhalation dosage frequency distribution.

#### 4.4 Conclusion

The present study region shows a large variance of indoor  $^{222}\text{Rn}$ ,  $^{220}\text{Rn}$ , and their progenies which could be attributable to building materials, geological sites, and topography and also due to various ventilation patterns existing in different types of houses. Based on the results obtained, the following conclusions may be made:

1. The annual average indoor  $^{222}\text{Rn}$ ,  $^{220}\text{Rn}$  concentration, and progeny levels are found to be below the recommended value made by ICRP [42, 43].
2. The annual equilibrium factor of radon lies in the range from 0.06 to 0.56 and thoron lies in the range from 0.002 to 0.12.

3. The total inhalation dosage ranged from 0.33 to 3.04 mSvy<sup>-1</sup>, which is well within the ICRP's recommended limits [40].
4. <sup>222</sup>Rn and <sup>220</sup>Rn concentrations were higher in winter than in other seasons.
5. In most of the homes in the study region, the <sup>220</sup>Rn concentration was higher than the <sup>222</sup>Rn concentration.
6. Among the three types of houses, the concrete house showed higher indoor <sup>222</sup>Rn and <sup>220</sup>Rn concentrations.

## References

1. Butterweck G, Schuler C, Vezzù G, Müller R, Marsh JW, Thrift S, Birchall A (2002) Experimental determination of the absorption rate of unattached radon progeny from respiratory tract to blood. *Radiat Prot Dosim* 102: 343–348. <https://doi.org/10.1093/oxfordjournals.rpd.a006103>
2. Nazaroff WW (1992) Radon transport from soil to air. *Reviews of Geophysics* 30(2): 137. <https://doi:10.1029/92rg00055>
3. Sahoo BK, Sapra BK, Gaware JJ, Kanse SD, Mayya YS (2011) A model to predict radon exhalation from walls to indoor air based on the exhalation from building material samples. *Sci Total Environ* 409: 2635-2641. <https://doi.org/10.1016/j.scitotenv.2011.03.031>
4. Ishimori Y, Lange K, Martin P, Mayya YS, Phaneuf M (2013) Measurement and Calculation of Radon Releases from NORM Residues. IAEA Technical Reports Series No 474 IAEA ISBN: 978–92–0–142610–9.
5. Sahoo BK, Sapra BK (2015) Advances in measurement of indoor  $^{222}\text{Rn}$  and  $^{220}\text{Rn}$  gas concentrations using solid state nuclear track detectors. *Solid State Phenom* 238: 116–126. <https://doi.org/10.4028/www.scientific.net/SSP.238.116>.
6. UNSCEAR (2000) United Nation Scientific Committee on the Effect of Atomic Radiation. Sources, Effects and Risks of Ionizing Radiation. Report to the General Assembly. United Nation, New York.
7. Darby S, Hill D, Auvinen A, Barros-Dios JM, Baysson H, Bochicchio F et al (2005) Radon in homes and risk of lung cancer: collaborative analysis of individual data from 13 European case-control studies. *Br Med J* 330: 223–226. <https://doi.org/10.1136/bmj.38308.477650.63>
8. Krewski D, Lubin JH, Zielinski JM, Alavanja M, Catalan VS, Field RW, Klotz JB, Létourneau EG, Lynch CF, Lyon JL, Sandler DP, Schoenberg JB, Steck DJ, Stolwijk JA, Weinberg C, Wilcox HB (2006) A combined analysis of North American case-control studies of residential radon and lung cancer. *J Toxicol Environ Health Part A* 69: 533–597. <https://doi.org/10.1080/15287390500260945>
9. WHO (2009) Who handbook on indoor radon - a public health perspective. World Heal. Organ. 110. <https://doi.org/10.1080/00207230903556771>

10. Sevc J, Kunz E and Placek V (1976) Lung cancer in Uranium miners after long term exposure to radon daughter products. *Health phys* 30: 433-437.
11. Henshaw DL, Eatough JP, Richardson RB (1990) Radon as a causative factor in induction of myeloid leukemia and other cancers. *Lancet* 355: 1008-1012. [https://doi.org/10.1016/0140-6736\(90\)91071-H](https://doi.org/10.1016/0140-6736(90)91071-H)
12. Frutos B, Martín-consuegra F, Alonso C, Frutos F De et al (2019) Geolocation of premises subject to radon risk: Methodological proposal and case study in Madrid. *Environ Pollut* 247: 556–563. <https://doi.org/10.1016/j.envpol.2019.01.083>
13. Obenchain R, Young SS, Krstic G (2019) Low-level radon exposure and lung cancer mortality. *Regul Toxicol Pharmacol* 107: 104418. <https://doi.org/10.1016/j.yrtph.2019.104418>
14. Dudney CS, Hawthorne AR, Wallace RG, Reed RP (1990) Radon-222,  $^{222}\text{Rn}$  progeny, and  $^{220}\text{Rn}$  progeny levels in 70 houses. *Health Phys* 58: 297-311. <https://doi.org/10.1097/00004032-199003000-00008>
15. Miles J (1998) Development of maps of radon-prone areas using radon measurements in houses. *J Hazard Mater* 61: 53-58. [https://doi.org/10.1016/S0304-3894\(98\)00107-1](https://doi.org/10.1016/S0304-3894(98)00107-1)
16. Yu KN, Cheung T, Guan ZJ, Young ECM, Mui BN, Wong YY (1999) Concentrations of  $^{222}\text{Rn}$ ,  $^{220}\text{Rn}$  and their progeny in residences in Hong Kong. *J Environ Radioact* 45: 291-308. [https://doi.org/10.1016/S0265-931X\(98\)00114-3](https://doi.org/10.1016/S0265-931X(98)00114-3)
17. Zhang Z, Smith B, Steck DJ, Guo Q, Field RW (2007) Variation in yearly residential radon concentrations in the upper midwest. *Health Phys* 93(4): 288-297. <https://doi.org/10.1097/01.hp.0000266740.09253.10>
18. Yamada Y, Sun Q, Tokonami S, Akiba A, Zhuo W, Hou C, Zhang S, Ishikawa T, Furukawa M, Fukutsu K, Yonehara H (2006) Radon-thoron discriminative measurements in Gansu Province, China, and their implication for dose estimates. *J Toxicol Environ Health Part A* 69: 723–734. <https://doi.org/10.1080/15287390500261265>
19. Kovacs T (2010) Thoron measurements in Hungary. *Radiat Prot Dosim* 141(4): 328–334. <https://doi.org/10.1093/rpd/ncq232>
20. Chen J, Moir D, Pronk T, Goodwin T, Janik M, Tokonami S (2011) An update

- on thoron exposure in Canada with simultaneous  $^{222}\text{Rn}$  and  $^{220}\text{Rn}$  measurements in Fredericton and Halifax. *Radiat Prot Dosim* 147(4): 541–547. <http://dx.doi.org/10.1093/rpd/ncq567>
21. Pyngrope A, Khardewsaw A, Sharma Y, Maibam D, Saxena A, Sahoo BK (2020) Study of indoor radon, thoron and their progeny in southwest Khasi hills district of Meghalaya, India. *Radiat Prot Dosim* 189(3): 347–353. <https://doi.org/10.1093/rpd/ncaa048>
22. Singh B, Kant K, Garg M, Singh A, Sahoo BK (2019) A study of seasonal variations of radon, thoron and their progeny levels in different types of dwellings in Faridabad district, Southern Haryana, India. *J Radioanal Nucl Chem* 320: 841–857. <https://doi.org/10.1007/s10967-019-06544-3>
23. Singla AK, Kansal S, Mehra R (2021) Dose distribution to individual tissues and organs due to exposure of alpha energies from radon and thoron to local population of Hanumangarh, Rajasthan, India. *J Radioanal Nucl Chem* 327: 1073–1085. <https://doi.org/10.1007/s10967-021-07604-3>
24. Dutt S, Joshi V, Sajwan RS et al (2021). Study of indoor radon, thoron and their decay products level in residences of Udham Singh Nagar district of Uttarakhand, India. *J Radioanal Nucl Chem* 330: 1509–1515. <https://doi.org/10.1007/s10967-021-07958-8>
25. Kumar A, Sharma S, Mehra R, Narang S & Mishra R (2017). Assessment of indoor radon, thoron concentrations, and their relationship with seasonal variation and geology of Udhampur district, Jammu & Kashmir, India. *Int J Occup Environ Health* 23(3): 202–214. <https://doi.org/10.1080/10773525.2018.1450326>
26. Suman G, Reddy KVK, Reddy MS et al (2021) Radon and thoron levels in the dwellings of Buddonithanda: a village in the environs of proposed uranium mining site, Nalgonda district, Telangana state, India. *Sci Rep* 11, 6199. <https://doi.org/10.1038/s41598-021-85698-1>
27. Ao A, Bhowmik SK (2014) Cold subduction of the Neotethys: the metamorphic record from finely banded lawsonite and epidote blueschists and associated metabasalts of the Nagaland Ophiolite Complex, India. *J Metamorph Geol* 32: 829–860. <https://doi.org/10.1111/jmg.12096>
28. Godish T, Raton B (2001) CRC Press LLC, FL



29. Sinha D, Sinha UB, Kibami D, Pongener C, Mishra R, Prajith R, Mayya YS (2013) Measurement of Radon and Thoron progeny concentration in some dwellings of Nagaland state- an initial report. *J Appl chem* 2: 825–831.
30. Singh AK, Khan AJ, Prasad R (1997) Distribution of  $^{222}\text{Rn}$  levels in Indian dwellings. *Radiat Prot Dosim* 74: 189–192. <https://doi.org/10.1093/oxfordjournals.rpd.a032196>
31. Jamir S, Sahoo BK, Mishra R, Bhomick PC, Sinha D (2021) A study on indoor radon, thoron and their progeny level in Mokokchung district of Nagaland, India. *J Radioanal Nucl Chem* 331: 21–30. <https://doi.org/10.1007/s10967-021-08096-x>
32. Changkery Imlisunep (2012) Economics of urban informal sector in Nagaland A case study of Dimapur city, 184 p. <http://hdl.handle.net/10603/194735>
33. CGWB (2013) Groundwater information booklet, Technical Report Series D pp 10.
34. Sahoo BK, Sapra BK, Kanse SD, Gaware JJ, Mayya YS (2013) A new pin-hole discriminated  $^{222}\text{Rn}/^{220}\text{Rn}$  passive measurement device with single entry face. *Radiat Meas* 58: 52–60. <https://doi.org/10.1016/j.radmeas.2013.08.003>
35. Eappen KP, Mayya, YS (2004) Calibration factors for LR-115 (type-II) based radon thoron discriminating dosimeter. *Radiat Meas* 38: 5–17. <https://doi.org/10.1016/j.radmeas.2003.09.003>
36. Mishra R, Mayya YS, Kushwaha HS (2009) Measurement of  $^{220}\text{Rn}/^{222}\text{Rn}$  progeny deposition velocities on surfaces and their comparison with theoretical models. *J Aerosol Sci* 40: 1–15. <https://doi.org/10.1016/j.jaerosci.2008.08.001>
37. Mishra R, Mayya YS (2008) Study of a deposition-based direct thoron progeny sensor (DTPS) technique for estimating equilibrium equivalent thoron concentration (EETC) in indoor environment. *Radiat Meas* 43: 1408–1416. <https://doi.org/10.1016/j.radmeas.2008.03.002>
38. Mayya YS, Eappen KP, Nambi KSV (1998) Methodology for mixed field inhalation dosimetry in monazite areas using a twin-cup dosimeter with three track detectors. *Radiat Prot Dosim* 77: 177–184. <https://doi.org/10.1093/oxfordjournals.rpd.a032308>
39. UNSCEAR (2008) Report: Sources and effects of ionizing radiation, Volume II, United Nations, New York, 2011 (e-ISBN-13: 978–92–1–054482–5).

40. ICRP (2018) International Commission on Radiological Protection. Radiological protection against radon exposure. ICRP Publication ref 4836-9756-8598. ICRP, Stockholm, Sweden.
41. UNSCEAR (2006) United Nations Scientific Committee on the Effect of Atomic Radiation. Report A/AC.82/644, exposures of workers and the public from various sources of radiations. United Nations, New York.
42. ICRP (2010) International Commission on Radiological Protection Lung cancer risk from radon and progeny and statement on radon. ICRP Publication-115. Pergamon Press, Oxford.
43. ICRP (2014) International Commission on Radiological Protection Radiological protection against radon exposure. ICRP Publication 126. Ann ICRP 43:3–37.

## CHAPTER- 5

### **A case study on seasonal and annual average indoor radon, thoron, and their progeny level in Kohima district, Nagaland, India**

---

*Indoor radon and thoron survey has been carried out in 50 dwellings under Kohima district, Nagaland, India, using the latest measurement technology. The survey has been carried out for a one-year period in 3 different seasons, and the dwellings were selected according to the building materials used for construction. Indoor radon and thoron concentrations, as well as their progeny followed a predictable pattern with greater levels in the winter and lower levels in the summer. Concrete housing had greater radon and thoron concentrations than bamboo and semi-wood/bamboo homes. The equilibrium factor (E.F) and inhalation dose due to radon, thoron, and their corresponding progeny were also studied in the present study.*

---

---

The text of this chapter has been published as:

**Jamir S, Sahoo BK, Mishra R and Sinha D (2022) A case study on seasonal and annual average indoor radon, thoron, and their progeny level in Kohima district, Nagaland, India. Isot Environ Health Stud. <https://doi.org/10.1080/10256016.2022.2140147>**

## 5.1 Introduction

Indoor radon contributes about 52 % to the ionizing radiation received by the general population [1]. The radioactive noble gases radon ( $^{222}\text{Rn}$ ) and thoron ( $^{220}\text{Rn}$ ) are produced inside rocks and soils and travel to the environment through emanation or exhalation [2-4]. Exhalation from the ground (41%) and construction materials (21%) are the principal sources of radon, followed by infiltration of external air (20%), de-emanation from the water supply (2%), and natural gas use (1%) [5-7]. Epidemiological studies have provided convincing evidence of an association between lung cancer and indoor radon even at relatively low radon levels [8-12]. Due to this, in recent years, radon ( $^{222}\text{Rn}$ ) and its progeny have gained considerable attention. However, not much importance was given to thoron ( $^{220}\text{Rn}$ ) and its progeny. This was based on the assumption that because thoron has a short half-life (55.6 seconds), only a little part of it is discharged into dwelling spaces, contributing only a small fraction to total inhalation doses, and so should not be treated as a contaminant in radon readings. This may not be totally true, as studies show that  $^{220}\text{Rn}$  levels can be comparable to, if not greater than,  $^{222}\text{Rn}$  levels [13-15]. It is worth noting that gases are easily exhaled out of the respiratory tract during the breath-out process, whereas progeny, being particles, are deposited in the respiratory tracts and continue to deliver alpha dose to lung tissue, causing lung cancer in humans.

It is the progeny, rather than  $^{222}\text{Rn}/^{220}\text{Rn}$  gas, that is responsible for the majority of the inhalation dose to the respiratory tract [12, 16, 17]. Hence, priority should be given to measuring progeny concentration as accurately as possible. The typical technique is to detect  $^{222}\text{Rn}/^{220}\text{Rn}$  gas concentration and estimate progeny concentration using an assumed/default equilibrium factor because direct measurement of progeny is challenging. This method, however, may result in an unreliable/inaccurate estimation of progeny concentration as well as uncertainty in the predicted inhalation dose. As a result, along with direct measurement of  $^{222}\text{Rn}/^{220}\text{Rn}$  gases, direct measurement of progeny concentration should be used in order to provide an accurate estimate of inhalation dose to people. Thus, estimating inhalation dose is an excellent way to analyze both  $^{222}\text{Rn}$  and  $^{220}\text{Rn}$  levels, as well as the health risks connected with them. In this regard, simultaneous measurements of indoor  $^{222}\text{Rn}$ ,  $^{220}\text{Rn}$ , and their corresponding EECs (equilibrium equivalent concentrations) have been carried out by

researchers worldwide [18-21]. Thus, the current study seeks to use the most up-to-date technique to conduct a comprehensive measurement of  $^{222}\text{Rn}$ ,  $^{220}\text{Rn}$ , and their offspring concentrations in Kohima district, Nagaland (it is the first study to be done monitoring radon and thoron concentration in this district). Time-integrated  $^{222}\text{Rn}$ ,  $^{220}\text{Rn}$ , and progeny were measured with a newly constructed single-entry pinhole-based  $^{222}\text{Rn}$ - $^{220}\text{Rn}$  discriminating dosimeter in 50 dwellings across six locations in Kohima district, Nagaland, over three seasons, while deposition-based direct radon/thoron progeny sensors (DRPS/DTPS) were used to measure their corresponding EECs. The homes were chosen based on the materials used (concrete, bamboo, and semi-wood/bamboo) used for construction. To understand the related risk factor, this study was used to evaluate the variance in equilibrium equivalent concentration (EEC), equilibrium factors, and inhalation dose for  $^{222}\text{Rn}$  and  $^{220}\text{Rn}$  concentrations in the research area. To understand the associated risk, this setting was employed to determine the variation of equilibrium equivalent concentration (EEC), equilibrium factors, and inhalation dose for  $^{222}\text{Rn}$  and  $^{220}\text{Rn}$  concentrations in the study area.

## 5.2 Methodology

### 5.2.1 Study area

Nagaland is an Indian state with a diverse range of igneous, sedimentary, and metamorphic rocks, including sandstone (Barail category), shale (Disang category), volcanic deposits, limestone, and pelagic rocks [22, 23]. As indicated on the map (figure 5.1), Kohima district is one of Nagaland's twelve districts and it borders Dimapur district to the west, Phek district to the east, Manipur state and Peren district to the south, and Wokha district to the north. It is located in the southern portion of Nagaland, between  $94^{\circ}5'11''$  and  $94^{\circ}7'12''$  and  $25^{\circ}28'20''$  and  $25^{\circ}31'51''$ . It covers 1,463 square kilometers and rises to a height of 1,444 meters (4,738 feet) above sea level.

The study region's houses were chosen based on the building materials utilized in their construction (figure 5.2) as follows:

- (i) Type A: Walls/roof are made of concrete and the floor is cemented.
- (ii) Type B: Walls/roof are made of bamboo and the floor is cemented.

(iii) Type C: Walls are made of semi-wood/bamboo, the roof is made of bamboo and the floor is cemented.

The research was carried out between 17<sup>th</sup> of July, 2018, and 11<sup>th</sup> of August, 2019. The year was divided into three seasons: summer, rainy, and winter season, each of which lasted about 120 days.

### **5.2.2 $^{222}\text{Rn}/^{220}\text{Rn}$ and progeny measurement**

For this study, two methods; pin-hole twin cup dosimeter, and DTPS/DRPS were deployed for the measurement of  $^{222}\text{Rn}$ ,  $^{220}\text{Rn}$ , and progeny concentration in indoors [24-27]. The details of the methods of measurement have already been described in chapter 2.

### **5.2.3 Deployment strategy**

DTPS, DRPS, and pin-hole dosimeter were deployed to measure the indoor  $^{222}\text{Rn}$ ,  $^{220}\text{Rn}$ , and their short-lived decay products. A total of 50 households in 6 different places in the Dimapur district were selected for this study during the survey period. The detectors were retained inside the buildings by suspending 30 cm away from the adjacent wall, and three distinct types of dwellings were chosen for the study: concrete (20), bamboo (15), and semi-wood/bamboo houses (15) (figure 5.3)

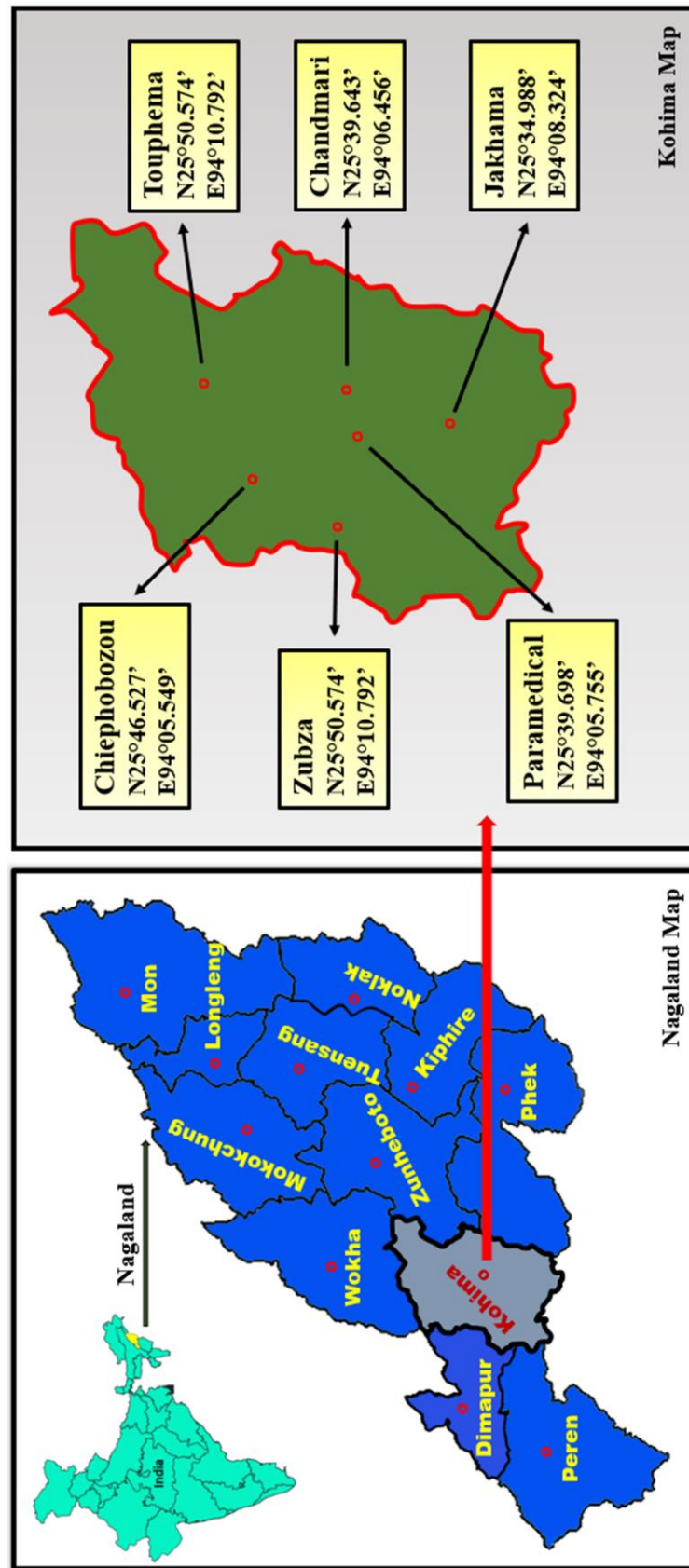


Fig. 5.1: Map of the area under study in Kohima district.



(a)



(b)



(c)



**Fig. 5.2:** Types of houses (a) concrete (b) semi-wood/bamboo (c) bamboo.





(a)



(b)



(c)

**Fig. 5.3:** Deployment of DTPS/DRPS and Pin hole dosimeter in different types of houses (a) concrete house (b) semi-wood/bamboo house (c) bamboo house.

### 5.2.3.1 Gamma survey for site selection

The selection of sites of the dwellings was based on a preliminary gamma survey carried out to assess the gamma level falling into different zones. Initially, before the installation of the detectors, gamma dose rate measurements were carried out in the different types of selected houses using the gamma survey meter. Table 5.1 shows the gamma levels that were measured in some of the residences where the detectors were kept.

**Table 5.1:** Gamma level in different houses of the study in Kohima district, Nagaland, India.

| SI. No. of house | Gamma level<br>(nSvhr <sup>-1</sup> ) | SI. No. of house | Gamma level<br>(nSvhr <sup>-1</sup> ) |
|------------------|---------------------------------------|------------------|---------------------------------------|
| 1.               | 101                                   | 16.              | 141                                   |
| 2.               | 139                                   | 17.              | 145                                   |
| 3.               | 105                                   | 18.              | 147                                   |
| 4.               | 126                                   | 19.              | 155                                   |
| 5.               | 120                                   | 20.              | 162                                   |
| 6.               | 113                                   | 21.              | 160                                   |
| 7.               | 110                                   | 22.              | 166                                   |
| 8.               | 128                                   | 23.              | 151                                   |
| 9.               | 122                                   | 24.              | 145                                   |
| 10.              | 132                                   | 25.              | 150                                   |
| 11.              | 134                                   | 26.              | 157                                   |
| 12.              | 140                                   | 27.              | 170                                   |
| 13.              | 129                                   | 28.              | 180                                   |
| 14.              | 134                                   | 29.              | 179                                   |
| 15.              | 136                                   | 30.              | 168                                   |

|     |     |     |     |
|-----|-----|-----|-----|
| 31. | 129 | 41. | 169 |
| 32. | 127 | 42. | 165 |
| 33. | 123 | 43. | 160 |
| 34. | 157 | 44. | 196 |
| 35. | 151 | 45. | 198 |
| 36. | 150 | 46. | 182 |
| 37. | 158 | 47. | 199 |
| 38. | 161 | 48. | 197 |
| 39. | 210 | 49. | 218 |
| 40. | 219 | 50. | 215 |

Based on the multivariate regression analysis, gamma level was divided into three zones in each type of houses (concrete, semi-wood/bamboo, bamboo) in the study area as shown in the table 5.2 given below: The gamma levels were found to be in the range of 181-220 nSv/hr in concrete houses, 141-180 nSv/hr in semi-wood/bamboo houses, and 101-140 nSv/hr in bamboo houses.

**Table 5.2:** Zone wise house distribution of Kohima district, Nagaland, India where DTSPS/DRPS and Pinhole twin cup dosimeters were installed.

| Total no. of dosimeters to be deployed= 50 |                                       |        |        |        |
|--|---------------------------------------|--------|--------|--------|
| Fitting parameter, K= 1.00E + 00           |                                       |        |        |        |
| Zone                                       | Gamma level<br>(nSvhr <sup>-1</sup> ) | Type A | Type B | Type C |
| 1  | 91-130                                | 5      | 5      | 5      |
| 2  | 131-170                               | 5      | 5      | 5      |
| 3  | 171-210                               | 10     | 5      | 5      |

### 5.2.3.2 Deployment of detectors

Deployment of detectors was calculated using the formula provided, where the number of detectors to be installed was calculated by dividing the zone of gamma radiation level as well as types of house. Based on statistical distribution 50 houses were selected in the following pattern as shown in table 5.3. The villages falling into different gamma zones were categorized based on the range of gamma radiation levels recorded during the preliminary survey, an index for the radioactivity content in the location.

**Table 5.3:** Distribution of detectors in each site of Dimapur district, Nagaland.

| Sl.no | Name of place | No. of DTPS/DRPS and Pinhole dosimeters deployed in different types of houses | Total No. of DTPS/DRPS and Pinhole dosimeters deployed in different types of houses |
|-------|---------------|---|---|
| 1     | Paramedical   | (concrete=8, semi-wood/bamboo=4, bamboo=4)                                    | 16  |
| 2     | Chandmari     | (concrete=4, semi-wood/bamboo=3, bamboo=3)                                    | 10  |
| 3     | Chiephobozou  | (concrete=2, semi-wood/bamboo=2, bamboo=2)                                    | 6   |
| 4     | Jakhama       | (concrete=2, semi-wood/bamboo=2, bamboo=2)                                    | 6   |
| 5     | Tuophema      | (concrete=2, semi-wood/bamboo=2, bamboo=2)                                    | 6   |
| 6     | Zubza         | (concrete=2, semi-wood/bamboo=2, bamboo=2)                                    | 6   |
|       | <b>Total</b>  | <b>50</b>   | <b>50</b>   |

Once the gamma data is acquired, zone wise house statistic table was made to use in multivariate regression analysis for estimating the number of dosimeters to be deployed

in each type of dwelling in the respective zone. Subsequently, after the selection of dwellings according to the above protocol, dosimeters were deployed in the study region. Around six to sixteen dwellings of each village were selected for the radon and thoron assessment and the G.P.S coordinates of the location where the detectors were deployed were also recorded. Accordingly, deployment was done in 50 households in the study area as given in table 5.3.

### 5.2.3.3 Post-processing of dosimeters

Dosimeters and progeny sensors were removed from the residences after a 120-day exposure period. Exposed LR-115 was etched in a constant water bath for 90 minutes with a 2.5N NaOH solution at a constant temperature of 60°C. The etched films were cleaned with clean water and dried overnight in a tissue roll once the etching procedure was completed. The alpha tracks of the LR-115 were pre-sparked at 900 V and tallied using a spark counter (model PSI-SCI) operating at 500 V.

### 5.2.4 Calculation of $^{222}\text{Rn}$ , $^{220}\text{Rn}$ , EEC, E.F, and inhalation dose

The tracks formed in the exposed LR-115 of the detectors were used to determine the  $^{222}\text{Rn}$ ,  $^{220}\text{Rn}$ , EECs, EF, and inhalation dose. The following formulas are used for the calculations of different parameters of  $^{222}\text{Rn}$ ,  $^{220}\text{Rn}$ , and their Progeny concentrations. The details of the calculation have been discussed in chapter 2.

#### 5.2.4.1 $^{222}\text{Rn}$ and $^{220}\text{Rn}$ gas measurement

The tracks formed due to the  $^{222}\text{Rn}$  and  $^{220}\text{Rn}$  gas in the Exposed LR-115 inside the twin cup pinhole dosimeters were calculated by using the following equations [24]

$$C_r = \frac{T_1}{d.K_r} \quad (1)$$

$$C_t = \frac{T_2 - T_1}{d.K_t} \quad (2)$$

Where  $T_1$ ,  $T_2$  are the tracks registered in ' $^{222}\text{Rn}$ ' and ' $^{222}\text{Rn} + ^{220}\text{Rn}$ ' compartments respectively,  $d$  is the exposure time in days. The calibration factors for  $^{222}\text{Rn}$  and  $^{220}\text{Rn}$  in the dosimeter are  $K_r = 0.017 \pm 0.002 \text{ tr.cm}^{-2}\text{d}^{-1}\text{Bqm}^{-3}$  and  $K_t = 0.010 \pm 0.001 \text{ tr.cm}^{-2}\text{d}^{-1}\text{Bqm}^{-3}$ , respectively [24].

#### 5.2.4.2 Progeny measurement

The tracks registered in the exposed LR-115 due to the radon and thoron progeny (EERC and EETC) in the DRPS/DTPS were measured by using the following equations [27, 28].

$$EERC = T_c(Tracks.cm^{-2}.d^{-1})/S_R(Tracks.cm^{-2}.d^{-1})/EEC(Bq.m^{-3}) \quad (3)$$

$$EETC = T_c(Tracks.cm^{-2}.d)/S_T(Tracks.cm^{-2}.d^{-1})/EEC(Bq.m^{-3}) \quad (4)$$

Where  $S_R = 0.09 \text{ trcm}^{-2}\text{d}^{-1}\text{Bqm}^{-3}$  corresponds to the sensitivity factor for Radon progeny in DRPS, while  $S_T = 0.94 \text{ trcm}^{-2}\text{d}^{-1}\text{Bqm}^{-3}$  corresponds to the sensitivity factor for Thoron progeny in DTPS [27, 28]. When assessing the tracks owing to radon progeny alone in DRPS, the contribution of thoron progeny tracks were excluded.

#### 5.2.4.3 Measurement of the equilibrium factor (EF) and inhalation dosage

The E.F is obtained by dividing the EETC/EERC by their respective  $^{222}\text{Rn}$  and  $^{220}\text{Rn}$  concentration [1].

The inhalation dose due to  $^{222}\text{Rn}$ ,  $^{220}\text{Rn}$ , and their corresponding progeny is calculated by using the following equations [28, 29].

$$\text{TID}_r (\text{mSva}^{-1}) = [(C_r \times 0.17) + (EERC \times 9)] \times 8760 \times 0.8 \times 10^{-6} \quad (5)$$

$$\text{TID}_t (\text{mSva}^{-1}) = [(C_t \times 0.11) + (EETC \times 40)] \times 8760 \times 0.8 \times 10^{-6} \quad (6)$$

Where the dosage conversion factors for  $^{222}\text{Rn}$  and  $^{220}\text{Rn}$  concentrations are 0.17 and 0.11  $\text{nSvBq}^{-1}\text{h}^{-1}\text{m}^3$ , respectively, while the dose conversion factors for  $^{222}\text{Rn}$  and  $^{220}\text{Rn}$  progeny concentrations are 9, and 40  $\text{nSvBq}^{-1}\text{h}^{-1}\text{m}^3$ , respectively. The standard occupancy factor for a one-year exposure period is 0.8 [28, 29].

### 5.3 Results and discussions

#### 5.3.1 Annual average $^{222}\text{Rn}$ , $^{220}\text{Rn}$ concentration values and also their EEC, E.F, and inhalation dose.

Table 5.4 shows that the annual average of indoor radon varied from  $25 \pm 10 \text{ Bqm}^{-3}$  to  $128 \pm 106 \text{ Bqm}^{-3}$  with an average of  $59.4 \pm 3 \text{ Bqm}^{-3}$  and falls within the reference value of  $300 \text{ Bqm}^{-3}$  as set by ICRP [30] while thoron varied from  $41 \pm 4 \text{ Bqm}^{-3}$  to  $196 \pm 107 \text{ Bqm}^{-3}$  with an average of  $111 \pm 5 \text{ Bqm}^{-3}$ . EERC was found to vary from  $5.2 \pm 0.6 \text{ Bqm}^{-3}$

$^3$  to  $42.9 \pm 15.8 \text{ Bqm}^{-3}$  with an average of  $13.8 \pm 0.989 \text{ Bqm}^{-3}$  while EETC varied from  $0.34 \pm 0.02 \text{ Bqm}^{-3}$  to  $2.74 \pm 2.10 \text{ Bqm}^{-3}$  with an average of  $1.04 \pm 0.067 \text{ Bqm}^{-3}$  and is under the reference value as set by ICRP [31], (2-50  $\text{Bqm}^{-3}$  for EERC and 0.04 to 2  $\text{Bqm}^{-3}$  for EETC). The total inhalation dose varied from  $0.55 \text{ mSva}^{-1}$  to  $3.21 \text{ mSva}^{-1}$  with an average of  $1.32 \pm 0.07 \text{ mSva}^{-1}$  and is within the recommended value as set by ICRP and WHO [30, 12].

**Table 5.4:** Annual average  $^{222}\text{Rn}$ ,  $^{220}\text{Rn}$ , EEC, and inhalation dose.

| Place (No. of dosimeters and DTPS/DRPS deployed) | Pinhole                                    |  | DTPS/DRPS                     |                               |
|--|--|--|-------------------------------|-------------------------------|
|  | $^{222}\text{Rn}$<br>( $\text{Bqm}^{-3}$ ) | $^{220}\text{Rn}$<br>( $\text{Bqm}^{-3}$ ) | EERC<br>( $\text{Bqm}^{-3}$ ) | EETC<br>( $\text{Bqm}^{-3}$ ) |
|  | A.M $\pm$ S.E                              | A.M $\pm$ S.E                              | A.M $\pm$ S.E                 | A.M $\pm$ S.E                 |
| Paramedical (16)                                 | $58 \pm 15$                                | $170 \pm 111$                              | $6.3 \pm 0.7$                 | $0.34 \pm 0.02$               |
|  | $64 \pm 7$                                 | $127 \pm 13$                               | $14.9 \pm 3$                  | $0.41 \pm 0.09$               |
|  | $35 \pm 4$                                 | $41 \pm 4$                                 | $5.5 \pm 1$                   | $0.45 \pm 0.10$               |
|  | $44 \pm 8$                                 | $112 \pm 13$                               | $14 \pm 5.7$                  | $0.78 \pm 0.16$               |
|  | $110 \pm 37$                               | $154 \pm 41$                               | $32 \pm 1.7$                  | $1.11 \pm 0.52$               |
|  | $50 \pm 18$                                | $156 \pm 51$                               | $9.2 \pm 1.2$                 | $0.81 \pm 0.34$               |
|  | $37 \pm 7$                                 | $110 \pm 5$                                | $6.1 \pm 2.7$                 | $0.57 \pm 0.20$               |
|  | $36 \pm 5$                                 | $73 \pm 24$                                | $8.6 \pm 1.8$                 | $1.65 \pm 0.34$               |
|  | $37 \pm 2$                                 | $87 \pm 22$                                | $8.9 \pm 0.8$                 | $1.46 \pm 0.56$               |
|  | $71 \pm 12$                                | $154 \pm 83$                               | $7.9 \pm 1.2$                 | $0.84 \pm 0.32$               |
|  | $43 \pm 17$                                | $157 \pm 98$                               | $8.9 \pm 4$                   | $0.68 \pm 0.25$               |
|  | $40 \pm 20$                                | $74 \pm 23$                                | $9.1 \pm 4.6$                 | $0.96 \pm 0.10$               |
|  | $73 \pm 57$                                | $77 \pm 39$                                | $18 \pm 8.9$                  | $1.26 \pm 0.62$               |
|  | $80 \pm 56$                                | $85 \pm 53$                                | $15.1 \pm 10.5$               | $1.07 \pm 0.63$               |
|  | $72 \pm 9$                                 | $66 \pm 14$                                | $15 \pm 2.5$                  | $0.48 \pm 0.07$               |

|                  |               |               |                 |                 |
|------------------|---------------|---------------|-----------------|-----------------|
|                  | $100 \pm 44$  | $117 \pm 61$  | $42.9 \pm 15.8$ | $1.06 \pm 0.35$ |
| Chandmari (10)   | $92 \pm 76$   | $105 \pm 33$  | $15.4 \pm 12.4$ | $0.68 \pm 0.50$ |
|                  | $65 \pm 50$   | $119 \pm 43$  | $18.8 \pm 4.3$  | $0.77 \pm 0.18$ |
|                  | $74 \pm 44$   | $98 \pm 53$   | $8.5 \pm 3.5$   | $0.92 \pm 0.47$ |
|                  | $66 \pm 50$   | $90 \pm 8$    | $9.1 \pm 5$     | $2.74 \pm 2.10$ |
|                  | $75 \pm 37$   | $160 \pm 64$  | $13.4 \pm 6$    | $0.74 \pm 0.28$ |
|                  | $84 \pm 58$   | $174 \pm 76$  | $12.7 \pm 6.8$  | $1.49 \pm 0.69$ |
|                  | $60 \pm 42$   | $142 \pm 56$  | $18.9 \pm 8.1$  | $0.73 \pm 0.21$ |
|                  | $128 \pm 106$ | $154 \pm 89$  | $20.6 \pm 10.9$ | $1.42 \pm 1.06$ |
|                  | $112 \pm 57$  | $146 \pm 64$  | $19.0 \pm 2$    | $2.29 \pm 1.56$ |
|                  | $54 \pm 15$   | $89 \pm 11$   | $21.1 \pm 9.8$  | $1.17 \pm 0.62$ |
| Chiephobozou (6) | $55 \pm 10$   | $122 \pm 29$  | $7.9 \pm 2.7$   | $1.00 \pm 0.47$ |
|                  | $117 \pm 50$  | $196 \pm 107$ | $24.9 \pm 3$    | $1.54 \pm 0.85$ |
|                  | $69 \pm 51$   | $191 \pm 145$ | $22.7 \pm 10.3$ | $0.98 \pm 0.29$ |
|                  | $62 \pm 34$   | $103 \pm 47$  | $14.9 \pm 5.2$  | $0.54 \pm 0.29$ |
|                  | $57 \pm 30$   | $70 \pm 33$   | $16.6 \pm 5.5$  | $0.77 \pm 0.23$ |
|                  | $70 \pm 37$   | $84 \pm 32$   | $11.5 \pm 3$    | $0.62 \pm 0.20$ |
| Jakhama (6)      | $25 \pm 10$   | $123 \pm 70$  | $9.8 \pm 4.2$   | $0.93 \pm 0.16$ |
|                  | $36 \pm 10$   | $76 \pm 33$   | $5.2 \pm 0.6$   | $1.45 \pm 0.20$ |
|                  | $38 \pm 4$    | $66 \pm 12$   | $13.2 \pm 4$    | $1.38 \pm 1$    |
|                  | $38 \pm 9$    | $124 \pm 22$  | $6.5 \pm 1.2$   | $0.63 \pm 0.05$ |
|                  | $55 \pm 25$   | $91 \pm 37$   | $11.1 \pm 2.7$  | $1.02 \pm 0.14$ |
|                  | $43 \pm 15$   | $98 \pm 32$   | $11.9 \pm 1.4$  | $1.41 \pm 0.27$ |
|                  | $28 \pm 6$    | $51 \pm 6$    | $7.9 \pm 0.6$   | $0.62 \pm 0.10$ |



|              |             |              |                |                 |
|--------------|-------------|--------------|----------------|-----------------|
| Touphema (6) | $40 \pm 7$  | $54 \pm 22$  | $11.5 \pm 4.9$ | $0.76 \pm 0.35$ |
|              | $35 \pm 12$ | $118 \pm 23$ | $22.5 \pm 8.8$ | $0.74 \pm 0.12$ |
|              | $51 \pm 17$ | $66 \pm 17$  | $12.7 \pm 2.2$ | $1.10 \pm 0.36$ |
|              | $57 \pm 12$ | $87 \pm 21$  | $5.5 \pm 1.7$  | $0.63 \pm 0.26$ |
|              | $28 \pm 7$  | $79 \pm 5$   | $11.3 \pm 2.7$ | $1.89 \pm 0.19$ |
| Zubza (6)    | $44 \pm 18$ | $153 \pm 32$ | $14.8 \pm 2.8$ | $0.94 \pm 0.42$ |
|              | $46 \pm 7$  | $137 \pm 20$ | $15.3 \pm 3.4$ | $1.48 \pm 0.47$ |
|              | $75 \pm 39$ | $86 \pm 32$  | $17.3 \pm 9.1$ | $1.33 \pm 0.23$ |
|              | $35 \pm 7$  | $109 \pm 11$ | $11.5 \pm 6$   | $0.97 \pm 0.47$ |
|              | $65 \pm 19$ | $121 \pm 32$ | $11.2 \pm 2.1$ | $1.52 \pm 0.17$ |
|              | $37 \pm 20$ | $85 \pm 34$  | $14.4 \pm 5.5$ | $0.88 \pm 0.43$ |

### 5.3.2 Seasonal changes in $^{222}\text{Rn}$ and $^{220}\text{Rn}$ , as well as their corresponding EECs

Indoor  $^{222}\text{Rn}$ ,  $^{220}\text{Rn}$ , and EECs measurements were taken in three seasons. Indoor  $^{222}\text{Rn}$ ,  $^{220}\text{Rn}$ , and their progeny were found to be higher during the winter season, as illustrated in table 5.5.

From table 5.5, we can see that during the summer season the indoor  $^{222}\text{Rn}$  varies from  $3 \text{ Bqm}^{-3}$  to  $83 \text{ Bqm}^{-3}$  with an average of  $36 \pm 3 \text{ Bqm}^{-3}$  and is less than the world average value of  $300 \text{ Bqm}^{-3}$  [30] while  $^{220}\text{Rn}$  varied from  $16 \text{ Bqm}^{-3}$  to  $162 \text{ Bqm}^{-3}$  with an average of  $60 \pm 7 \text{ Bqm}^{-3}$  and is above the world average value of  $10 \text{ Bqm}^{-3}$  [29, 32]. EERC and EETC vary from  $1.8 \text{ Bqm}^{-3}$  to  $34.3 \text{ Bqm}^{-3}$  and  $0.17 \text{ Bqm}^{-3}$  to  $1.92 \text{ Bqm}^{-3}$  with an average of  $9.6 \pm 1 \text{ Bqm}^{-3}$  and  $0.72 \pm 0.07 \text{ Bqm}^{-3}$  respectively. During the rainy season, the  $^{222}\text{Rn}$  and  $^{220}\text{Rn}$  concentrations varied with an average of  $43 \pm 4 \text{ Bqm}^{-3}$  and  $72 \pm 7 \text{ Bqm}^{-3}$  respectively. EERC varied with an average of  $13.8 \pm 1.7 \text{ Bqm}^{-3}$  while EETC varied with an average of  $0.92 \pm 0.09 \text{ Bqm}^{-3}$ . In the winter season, the  $^{222}\text{Rn}$  and  $^{220}\text{Rn}$  concentration was found to vary with an average of  $99 \pm 10 \text{ Bqm}^{-3}$  and  $144 \pm 16 \text{ Bqm}^{-3}$  respectively. EERC and EETC varied with an average of  $18 \pm 1.5 \text{ Bqm}^{-3}$  and  $1.47 \pm 0.18 \text{ Bqm}^{-3}$  respectively.

The temperature in the study region during summer varied between 23°C to 36°C and that in winter varied between 5°C to 30°C. The ventilation rate is maximum in summer and minimum in winter. Because inhabitants tend to keep their windows and doors closed for long periods during the winter, the higher concentration occurs during this time, allowing radon to gather within the home. The increase in a temperature inversion, which usually happens in the winter when the wind velocity is low, has an impact on the maximum concentration in the winter. In the warm and wet seasons, the radon concentration steadily falls; elements that may affect this include high temperatures and low pressure. Due to strong northwest winds and significant precipitation, radon concentrations decreases during the wet season. Other factors, such as the saturation of the soil with water during the rainy season, contribute to the decrease in radon levels.

**Table 5.5:** Indoor radon and thoron parameters in three seasons.

| Seasons |         | $^{222}\text{Rn}$<br>(Bqm <sup>-3</sup> ) | $^{220}\text{Rn}$<br>(Bqm <sup>-3</sup> ) | EERC<br>(Bqm <sup>-3</sup> ) | EETC<br>(Bqm <sup>-3</sup> ) |
|---------|---------|---|---|------------------------------|------------------------------|
| Summer  | Average | 36 ± 3                                    | 60 ± 7                                    | 9.6 ± 1                      | 0.72 ± 0.07                  |
|         | Minimum | 3   | 16  | 1.8                          | 0.17                         |
|         | Maximum | 83  | 162                                       | 34.3                         | 1.92                         |
| Rainy   | Average | 43 ± 4                                    | 72 ± 7                                    | 13.8 ± 1.7                   | 0.92 ± 0.09                  |
|         | Minimum | 10  | 22  | 2.5                          | 0.10                         |
|         | Maximum | 152                                       | 213                                       | 39.8                         | 2.43                         |
| Winter  | Average | 99 ± 10                                   | 144 ± 16                                  | 18 ± 1.5                     | 1.47 ± 0.18                  |
|         | Minimum | 21  | 44  | 1.7                          | 0.35                         |
|         | Maximum | 340                                       | 480                                       | 43.3                         | 6.92                         |

### 5.3.3 Equilibrium factor (E.F)

During summer, the radon E.F varied from 0.06 to 1.86 with an average of  $0.5 \pm 0.1$ , and thoron E.F varied from 0.01 to 0.08 with an average of  $0.01 \pm 0.002$  (table 5.6).

During the rainy season, the radon E.F varied with an average of  $0.4 \pm 0.04$  and thoron E.F with an average of  $0.01 \pm 0.002$ . During winter, the E.F. of radon and thoron varied with an average of  $0.2 \pm 0.02$  and  $0.01 \pm 0.002$  respectively.

**Table 5.6:** Radon and thoron E.F in different seasons.

| Seasons |         | E.F<br>Radon   | E.F<br>Thoron    |
|---------|---------|----------------|------------------|
| Summer  | Average | $0.5 \pm 0.1$  | $0.01 \pm 0.002$ |
|         | Minimum | 0.06           | 0.01             |
|         | Maximum | 1.86           | 0.08             |
| Rainy   | Average | $0.4 \pm 0.04$ | $0.01 \pm 0.002$ |
|         | Minimum | 0.06           | 0.01             |
|         | Maximum | 1.20           | 0.06             |
| Winter  | Average | $0.2 \pm 0.02$ | $0.01 \pm 0.002$ |
|         | Minimum | 0.06           | 0.01             |
|         | Maximum | 0.79           | 0.07             |

#### 5.3.4 Correlation of $^{222}\text{Rn}$ (and its EERC) and $^{220}\text{Rn}$ (and its EETC)

From figure 5.4a, it can be seen that a weak positive correlation coefficient of 0.4 is observed in the case of  $^{222}\text{Rn}$  and its progeny. While a very weak positive coefficient of 0.001 is observed for  $^{220}\text{Rn}$  and its progeny as shown in figure 5.4b.

#### 5.3.5 $^{222}\text{Rn}$ , $^{220}\text{Rn}$ , EERC, EETC in various types of houses

Indoor  $^{222}\text{Rn}$ ,  $^{220}\text{Rn}$ , and their respective EECs were also estimated in various types of houses in the study region, and it was observed that  $^{222}\text{Rn}$ ,  $^{220}\text{Rn}$ , and their corresponding EECs were found to be relatively higher in the concrete type of house and relatively lower in the bamboo type of house as shown in figure 5.5 and figure 5.6 respectively. This might be due to the fact that in bamboo houses, the air movement is

more, and exhalation from the building material is negligible, so in the bamboo houses minimum activity concentration was obtained.

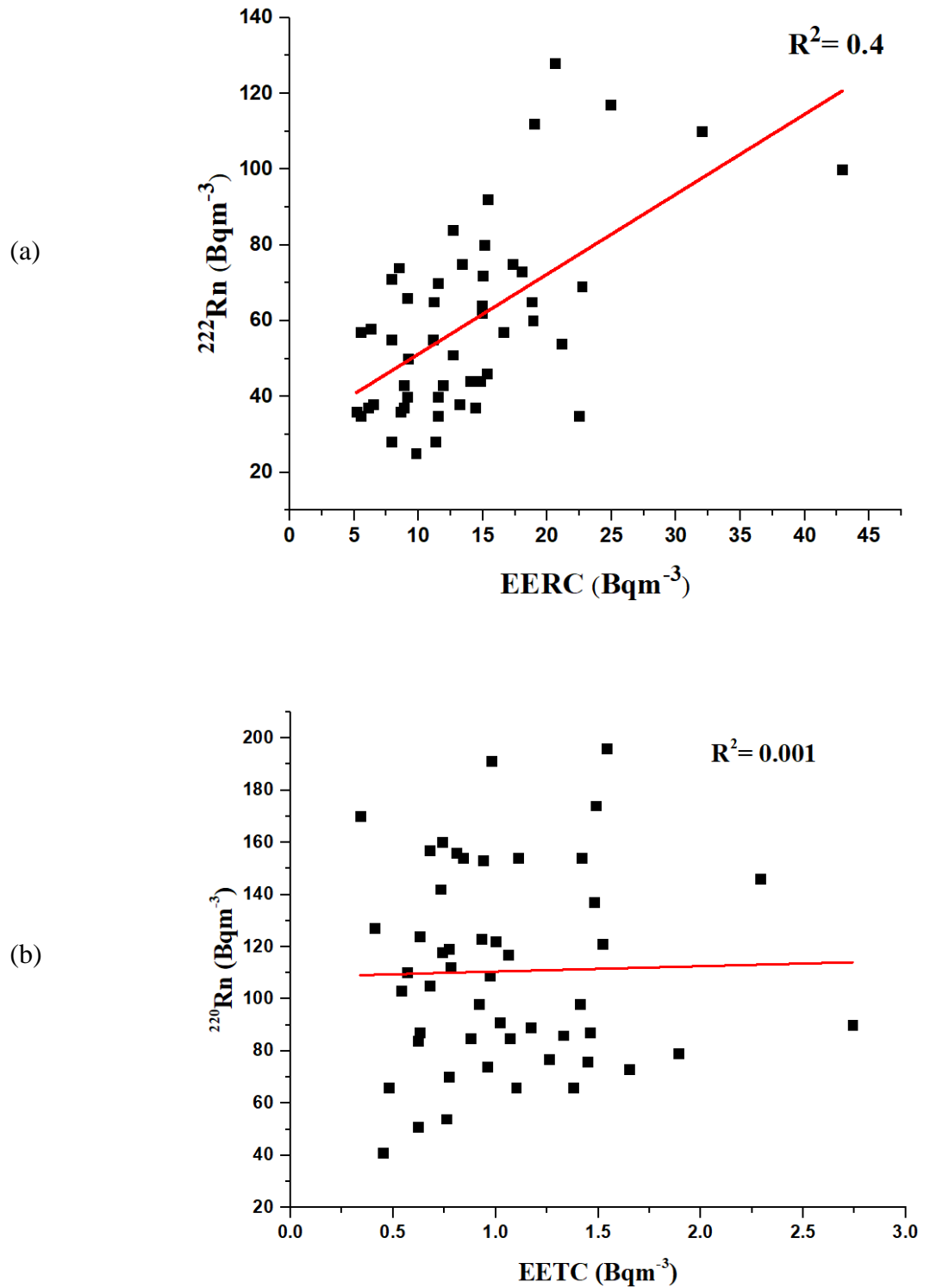


**Fig 5.4:** (a)  $^{222}\text{Rn}$  and its progeny correlation plot (b)  $^{220}\text{Rn}$  and its progeny correlation plot.

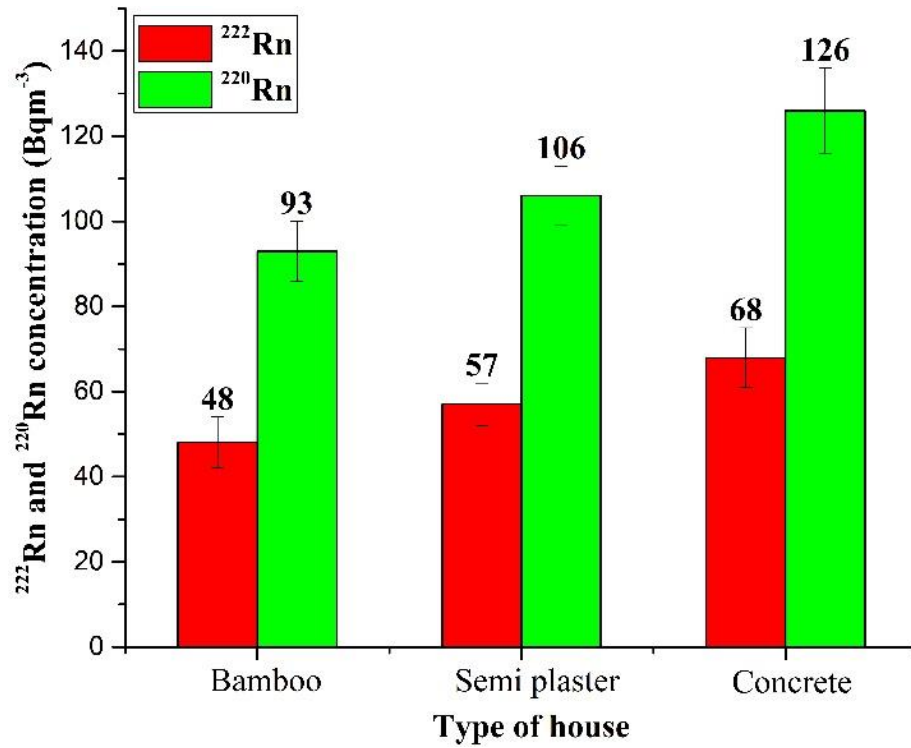


**Fig. 5.5:**  $^{222}\text{Rn}$  and  $^{220}\text{Rn}$  in different house types.

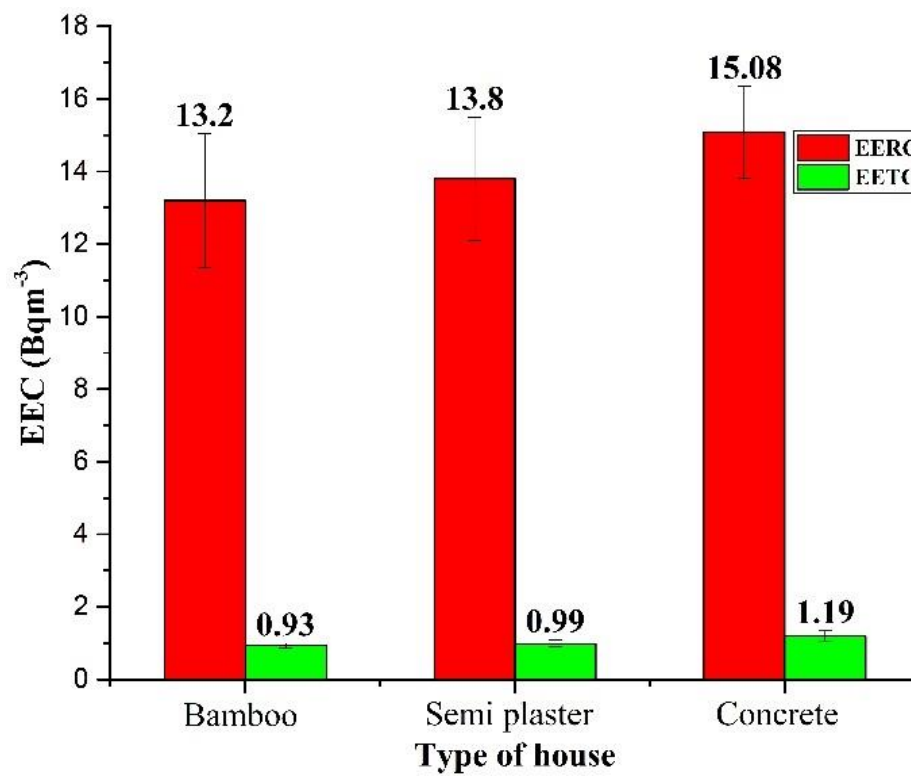


**Fig. 5.6:** EEC in different house types.

### 5.3.6 Inhalation dose

Inhalation of  $^{222}\text{Rn}$ ,  $^{220}\text{Rn}$ , and its progeny may have adverse effects on humans. As a result, in this investigation, the total inhalation dose (due to  $^{222}\text{Rn}$  /  $^{220}\text{Rn}$  and progeny) observed in the study region varied, as indicated in figure 5.7. It can be seen that 1 out of 50 houses are exposed in the dose range below  $0.60 \text{ mSv a}^{-1}$  and 22% of the house are exposed in the dose range of  $0.60 - 1.20 \text{ mSv a}^{-1}$ , 64% in the dose range of  $1.21 - 1.81 \text{ mSv a}^{-1}$ , 8% in the dose range of  $1.82 - 2.42 \text{ mSv a}^{-1}$ , 1 house lied in the dose range of  $2.43 - 3.03 \text{ mSv a}^{-1}$ . Only 1 out of 50 houses are exposed in the dose range of greater than  $3.03 \text{ mSv a}^{-1}$  which happens to be a concrete type of house.

These results are comparable to the results obtained from the previous study conducted in the Mokokchung district of Nagaland where the annual average  $^{222}\text{Rn}$  and  $^{220}\text{Rn}$  varied from  $44 \pm 6 \text{ Bqm}^{-3}$  to  $75 \pm 16 \text{ Bqm}^{-3}$  and  $25 \pm 2 \text{ Bqm}^{-3}$  to  $62 \pm 49 \text{ Bqm}^{-3}$  respectively, EERC and EETC value ranged from  $3.2 \pm 2.1 \text{ Bqm}^{-3}$  to  $17.3 \pm 8.7 \text{ Bqm}^{-3}$  and  $0.21 \pm 0.06 \text{ Bqm}^{-3}$  to  $1.49 \pm 0.86 \text{ Bqm}^{-3}$ , and inhalation dose varied from  $0.35 \text{ mSv a}^{-1}$  to  $1.64 \text{ mSv a}^{-1}$  [33]. While in another report, the inhalation dose varied from 0.33 to  $3.04 \text{ mSv a}^{-1}$  in the Dimapur district of Nagaland [34]. These findings are fairly consistent with those found in the present study area.

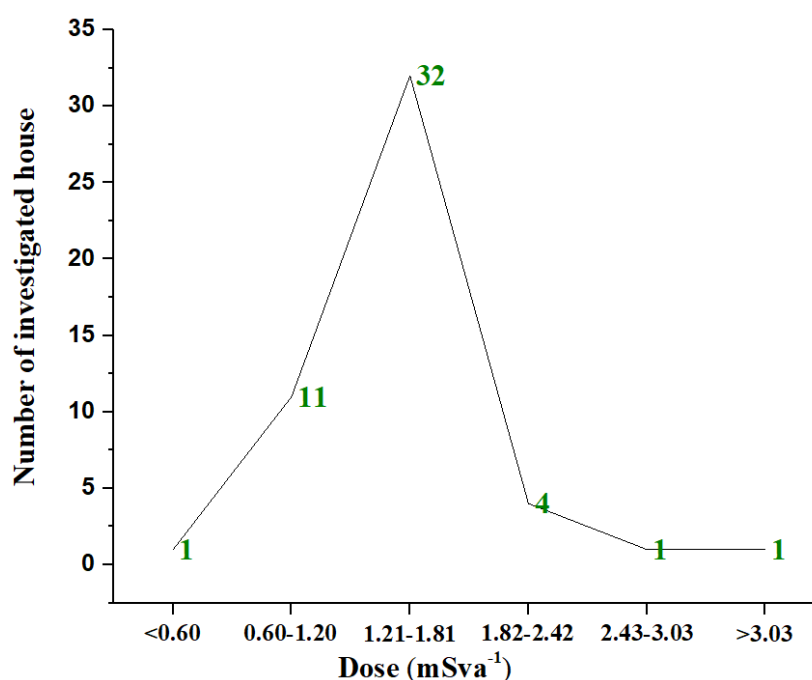


Fig. 5.7: Dose distribution frequency in 50 dwellings.

## 5.4 Conclusion

1. The  $^{222}\text{Rn}$  and  $^{220}\text{Rn}$  concentrations were well below the ICRP's recommended reference limit of  $300 \text{ Bqm}^{-3}$ .
2. The concentration of  $^{220}\text{Rn}$  in the majority of the homes in the research region was higher than the concentration of  $^{222}\text{Rn}$ .
3. In comparison to the summer and wet seasons, the levels of  $^{222}\text{Rn}$ ,  $^{220}\text{Rn}$ , and their EECs were higher in the winter.
4. In the research area, the E.F owing to  $^{222}\text{Rn}$ ,  $^{220}\text{Rn}$ , and their EECs were likewise lower than the global norm.
5. The total inhalation dosage ranged from  $0.55$  to  $3.21 \text{ mSva}^{-1}$ , which is well within the ICRP and WHO standard values.
6. Since, the concentrations of  $^{222}\text{Rn}$ ,  $^{220}\text{Rn}$ , and their EECs are less than the world average value defined by the ICRP, WHO, and UNSCEAR, it may be stated that the residents of the current research region pose no major risk.

## References

1. UNSCEAR (2000) United Nation Scientific Committee on the Effect of Atomic Radiation. Sources, Effects and Risks of Ionizing Radiation. Report to the General Assembly. United Nation, New York.
2. Nazaroff WW (1992) Radon transport from soil to air. *Reviews of Geophysics* 30(2): 137. <https://doi:10.1029/92rg00055>
3. Sahoo BK, Sapra BK, Gaware JJ, et al (2011) A model to predict radon exhalation from walls to indoor air based on the exhalation from building material samples. *Sci Total Environ* 409: 2635–2641. <https://doi.org/10.1016/j.scitotenv.2011.03.031>
4. Ishimori Y, Lange K, Martin P, et al (2013) Measurement and Calculation of Radon Releases from NORM Residues. IAEA Technical Reports Series No 474 IAEA ISBN: 978–92–0–142610–9
5. Deka PC, Sarkar S, Bhattacharjee B, et al (2003) Measurement of radon and thoron concentration by using LR-115 type-II plastic track detectors in the environ of Brahmaputra Valley, Assam, India, in. *Radiat Meas* 36: 431–434. [https://doi.org/10.1016/S1350-4487\(03\)00165-3](https://doi.org/10.1016/S1350-4487(03)00165-3)
6. Dwivedi KK, Mishra R, Tripathy SP (2005) An extensive indoor  $^{222}\text{Rn}/^{220}\text{Rn}$  monitoring in North-East India. *Radiat Meas* 40: 621–624. <https://doi.org/10.1016/j.radmeas.2005.04.026>
7. Dwivedi KK, Mishra R, Tripathy SP, et al (2001) Simultaneous determination of radon, thoron and their progeny in dwellings. *Radiat Meas* 33: 7–11. [https://doi.org/10.1016/S1350-4487\(00\)00131-1](https://doi.org/10.1016/S1350-4487(00)00131-1)
8. Darby S, Hill D, Auvinen A, et al (2005) Radon in homes and risk of lung cancer: collaborative analysis of individual data from 13 European case-control studies. *Br Med J* 330: 223–226. <https://doi.org/10.1136/bmj.38308.477650.63>
9. Krewski D, Lubin JH, Zielinski JM, et al (2006) A combined analysis of north American case-control studies of residential radon and lung cancer. *J Toxicol Environ Health Part A* 69: 533–597. <https://doi.org/10.1080/15287390500260945>.
10. Obenchain R, Young SS, Krstic G (2019) Low-level radon exposure and lung cancer mortality. *Regul Toxicol Pharmacol* 107: 104418. <https://doi.org/10.1016/j.yrtph.2019.104418>.
11. Sahoo BK, Mayya YS, Sapra, BK, et al (2010) Radon exhalation studies in an



- Indian uranium tailings pile. Radiat Meas 45: 237–241. <https://doi.org/10.1016/j.radmeas.2010.01.008>.
12. WHO (2009) Who handbook on indoor radon - a public health perspective. World Heal Organ 110. <https://doi.org/10.1080/00207230903556771>
  13. Singla AK, Kansal S, Mehra R (2021) Dose distribution to individual tissues and organs due to exposure of alpha energies from radon and thoron to local population of Hanumangarh, Rajasthan, India. J Radioanal Nucl Chem 327: 1073–1085. <https://doi.org/10.1007/s10967-021-07604-3>
  14. Singh B, Kant K, Garg M, et al (2019) A study of seasonal variations of radon, thoron and their progeny levels in different types of dwellings in Faridabad district, Southern Haryana, India. J Radioanal Nucl Chem 320: 841–857. <https://doi.org/10.1007/s10967-019-06544-3>
  15. Suman G, Vinay Kumar Reddy K, Sreenath Reddy M, et al (2021) Radon and thoron levels in the dwellings of Buddonithanda: a village in the environs of proposed uranium mining site, Nalgonda district, Telangana state, India. Sci Rep 11: 6199. <https://doi.org/10.1038/s41598-021-85698-1>
  16. ICRP (2010) Lung cancer risk from radon, progeny, and statement on radon. ICRP Publication 115. Ann. ICRP 40.
  17. UNSCEAR (2009) (United Nations Scientific Committee on the Effects of Atomic Radiation), Annex E. Sources to Effects Assessment for Radon in Homes and Workplaces. United Nations, New York, NY.
  18. Dutt S, Joshi V, Sajwan RS, et al (2021) Study of indoor radon, thoron and their decay products level in residences of Udham Singh Nagar district of Uttarakhand, India. Radioanal. Nucl Chem 330: 1509–1515. <https://doi.org/10.1007/s10967-021-079588>
  19. Pyngrope A, Khardewsaw A, Sharma Y, et al (2020) Study of indoor radon, thoron and their progeny in southwest Khasi hills district of Meghalaya, India. Radiat Prot Dosim 189(3): 347–353. <https://doi.org/10.1093/rpd/ncaa048>
  20. Salupeto-Dembo J, Szabó-Krausz Z, Völgyesi P, et al (2020) Radon and thoron radiation exposure of the Angolan population living in adobe houses. J Radioanal Nucl Chem 325: 271–282. <https://doi.org/10.1007/s10967-020-07215-4>
  21. Reddy BL, Reddy GS, Reddy KVK, et al (2021) Inhalation dose due to residential radon and thoron exposure in rural areas: a case study at Erravalli and Narasannapet

- model villages of Telangana state, India. *Radiat Environ Biophys* 60: 437–445. <https://doi.org/10.1007/s00411-021-00912-y>
22. Ao A, Bhowmik SK (2014) Cold subduction of the Neotethys: the metamorphic record from finely banded lawsonite and epidote blueschists and associated metabasalts of the Nagaland Ophiolite Complex, India. *J Metamorph Geol* 32: 829–860. <https://doi.org/10.1111/jmg.12096>
23. Godish T, Raton B (2001) FL. CRC Press LLC.
24. Sahoo BK, Sapra BK, Kanse SD, et al (2013) A new pin-hole discriminated  $^{222}\text{Rn}/^{220}\text{Rn}$  passive measurement device with single entry face. *Radiat Meas* 58: 52–60. <https://doi.org/10.1016/j.radmeas.2013.08.003>
25. Eappen KP, Mayya YS (2004) Calibration factors for LR-115 (type-II) based radon thoron discriminating dosimeter. *Radiat Meas* 38: 5–17. <https://doi.org/10.1016/j.radmeas.2003.09.003>
26. Mishra R, Mayya YS, Kushwaha HS (2009) Measurement of  $^{220}\text{Rn}/^{222}\text{Rn}$  progeny deposition velocities on surfaces and their comparison with theoretical models. *J Aerosol Sci* 40: 1–15. <https://doi.org/10.1016/j.jaerosci.2008.08.001>
27. Mishra R, Mayya YS (2008) Study of a deposition-based direct thoron progeny Sensor (DTPS) technique for estimating equilibrium equivalent thoron concentration (EETC) in indoor environment. *Radiat Meas* 43: 1408–1416. <https://doi.org/10.1016/j.radmeas.2008.03.002>
28. Mayya YS, Eappen KP, Nambi KSV (1998) Methodology for mixed field inhalation dosimetry in monazite areas using a twin-cup dosimeter with three track detectors. *Radiat Prot Dosim* 77: 177–184. <https://doi.org/10.1093/oxfordjournals.rpd.a032308>
29. UNSCEAR (2008) Report: Sources and effects of ionizing radiation, Volume II, United Nations, New York, 2011 (e-ISBN-13: 978-92-1-054482-5).
30. ICRP (2018) International Commission on Radiological Protection. Radiological Protection against radon exposure. ICRP Publication ref 4836-9756-8598. ICRP, Stockholm, Sweden.
31. ICRP (2014) International Commission on Radiological Protection against radon exposure. ICRP Publication 126. *Ann ICRP* 43: 3–37.
32. UNSCEAR (2006) United Nations Scientific Committee on the Effect of Atomic

Radiation Report A/AC.82/644, exposures of workers and the public from various sources of radiations. United Nations, New York.

33. Jamir S, Sahoo BK, Mishra R, et al (2022) A study on indoor radon, thoron and their Progeny level in Mokokchung district of Nagaland, India. J Radioanal Nucl Chem 331: 21–30. <https://doi.org/10.1007/s10967-021-08096-x>
34. Jamir S, Sahoo BK, Mishra R, et al (2022) A Comprehensive Study on Indoor Radon, Thoron and Their Progeny Level in Dimapur District of Nagaland, India. Radiat Prot Dosim 198: 853-861. <https://doi.org/10.1093/rpd/ncac150>

## CHAPTER- 6

### **Estimation of radon in groundwater and analysis of radon and thoron exhalation rates of the soil in Mokokchung, Dimapur, and Kohima districts of Nagaland, India**

---

*The present study of the analysis of radon in groundwater and its exhalation rates in soil was carried out in the Mokokchung, Dimapur, and Kohima districts of Nagaland, India. The survey was carried out by employing a portable scintillation-based smart RnDuo monitor. All the obtained values were lower than the global values established by the UNSCEAR, USEPA, and WHO. Additionally, the effective dose due to  $^{222}\text{Rn}$  in water was also lower than the WHO values (2003).*

---

---

A part of the text of this chapter has been published as:

**Jamir S, Sahoo BK, Mishra R, and Sinha D (2022) Estimation of radon in groundwater and analysis of radon and thoron exhalation rates of the soil in Mokokchung district, Nagaland, India.** Groundw. Sustain. Dev. 20, 100874. <https://doi.org/10.1016/j.gsd.2022.100874>

## 6.1 Introduction

In the wake of radon and thoron's threat to people in both natural and man-made environments every day, much public attention has focused on their speculations due to their adverse health effects [1]. This may be attributed to the alterations to the ecological processes that govern terrestrial systems including soil fertility for food production, surface water bodies (for flood prevention), and groundwater (drinking water supply) [2]. Radon in homes is primarily produced by soil. The amount of radon in soil ranges from a few  $\text{KBqm}^{-3}$  up to a few hundred of  $\text{KBqm}^{-3}$  [3].

The decay of radium and thorium in the earth's crust produces the radon and thoron gas which are then transported to indoor environments via two different mechanisms from the soil matrix and building material. In the earth's crust,  $^{222}\text{Rn}$  and  $^{220}\text{Rn}$  gas are formed by the decay of radium and thorium, respectively and they access the interior space through two different mechanisms from the soil and construction materials matrix. The first step involves an emanation from the material while the second step involves an exhalation from the matrix. Emanation is the step where  $^{222}\text{Rn}$  atoms move from the dense mineral grains to the pores covered with air while Exhalation involves the movement of air-filled pores releasing  $^{222}\text{Rn}$  gas into the atmosphere [4].

If the  $^{222}\text{Rn}$  concentrations in the soil near a house are high, then there is a probability of high radon concentrations in nearby water wells [5]. Thus, it is desired that in addition to the study of radon in the soil, equal emphasis may also be given to the study of radon in the water. Radon is present in groundwater because of the interaction it has during movement with rocks that contain primordial uranium minerals under the surface [6, 7]. When water is used for various purposes and becomes agitated, the  $^{222}\text{Rn}$  gas, which is only very slightly water soluble, finds its way into the atmosphere (both inside as well as outdoors) [8-11]. Radon accounts for approximately 50% of the natural exposure to humans in the world, and between 3 and 14% of lung cancer deaths in people are attributable to radon exposure [12], making it the second largest cause of death for people with lung cancer after smoking. During respiration, the majority of the radon gas absorbed into the lungs is breathed out, however, a certain fraction of the radon progeny gets attached to the lung tissue and has the potential to harm DNA in the lung's delicate tissues and can cause lung cancer. In this regard, UNSCEAR

recommends a reference value of 9 nSv (Bqhm<sup>-3</sup>)<sup>-1</sup>. For example, a person living (7000 hy<sup>-1</sup>) in a concentration of 40 Bqm<sup>-3</sup> receives an effective dose of 1 mSvy<sup>-1</sup> [1]. It has been reported that miners with cumulative exposures less than 30 MBqhm<sup>-3</sup> have an excessive relative risk from radon exposure of 1.8% per mega becquerel hours per cubic meter (MBqhm<sup>-3</sup>) [13].

Simultaneous measurements of radon in soil and water can provide valuable/significant indicators/predictions of the radon potential of an area [3]. There are numerous studies on radon in water and measurements of exhalation rates of <sup>222</sup>Rn/<sup>220</sup>Rn in soil have been assessed by researchers worldwide [14-34]. However, there are no reports on radon studies in soil and water in the residential area of the Mokokchung, Dimapur, and Kohima districts of Nagaland.

In view of this, the present study area was originally chosen due to its geological characteristics. The state of Nagaland in India is an area containing metamorphic, igneous, and sedimentary rocks—predominantly shale (Disang category), sandstone (Barail category), volcanic sediments, limestone, and pelagic [35]. These types of rocks and stones are known to contain naturally-occurring radioactive elements like radium, uranium, and thorium. These naturally-occurring elements can break down or decay into the radioactive gas radon. Depending on the amount of these materials present, they may also cause small increases in radiation levels.

Thus, the present study's main goal is to perform a thorough <sup>222</sup>Rn analysis in water as well as <sup>222</sup>Rn/<sup>220</sup>Rn exhalation rates in the soils of the Mokokchung, Dimapur, and Kohima districts of Nagaland. A portable radon monitor (Smart RnDuo) designed by BARC (Bhabha Atomic Research Centre), Mumbai, was the device employed for the current investigation.

## 6.2 Materials and method

The soil samples were taken from the 19 villages of Mokokchung district, Nagaland, and mass exhalation rates have been calculated for Radon and thoron using a Smart RnDuo monitor. The soil samples were taken from the neighboring residence using a hoe. The samples were dug and collected at a depth of 30cm to get pure soil samples.

About 1kg of soil samples was brought to the lab in zip-lock bags for analysis. In the process of collecting, care was taken to remove unwanted particles (stones/rocks, grass, etc.) from the soil. In general, roughly 500-600 grams of soil are confined in a tight metallic container coupled to the Smart RnDuo.

Similarly, water samples from the 19 borewells were gathered for the assessment of the  $^{222}\text{Rn}$  level in the water utilizing a container with a tubing directly linked to the faucet to prevent water from being exposed to the atmosphere. The water was gathered in 60-ml leak-proof glass bottles with little permeability that had already been cleaned. To prevent the formation of bubbles or agitation in the water, care was given when sampling into the bottle. To prevent losing any  $^{222}\text{Rn}$  owing to radioactive decay, the concentration of dissolved  $^{222}\text{Rn}$  was measured within 2-4 hours after the sample time. A scintillation detector-based Smart RnDuo radon monitor was employed to evaluate the exhalation rates of  $^{222}\text{Rn}/^{220}\text{Rn}$  from the soil. A photomultiplier tube (PMT) and related counting electronics are used to measure the alpha scintillations produced by  $^{222}\text{Rn}$  and its daughter products. This monitor is employed to assess the radon levels in soil, water, and Naturally Occurring Radioactive Materials (NORMs) [36]. The procedures for assessing the exhalation rates of  $^{222}\text{Rn}/^{220}\text{Rn}$  are described in the following sections. Radon/thoron exhalation rates can be sampled into Smart RnDuo using diffusion or flow mode of sampling.

### 6.2.1 $^{222}\text{Rn}$ mass exhalation rate measurement

Radon exhalation rate is defined as the amount of radon liberated from a material's surface area per unit of time. As a result, the diffusion mode of sampling was used to determine the rate of mass exhalation of radon. For the investigation of the soil's mass exhalation rate of  $^{222}\text{Rn}$ , about 500–600g of the dried soil sample are contained in the mass exhalation chamber, a leak-tight accumulation chamber connected to the RnDuo monitor (Model number: RnDuo, Serial number: 1615). A schematic view of the measurement is shown in figure 6.1. Smart RnDuo monitor is attached to a stainless-steel accumulation chamber close to cylindrical and leak-free. For the purpose of measuring  $^{222}\text{Rn}$ , the Smart RnDuo monitor was programmed to operate for 24 hours on a 60-minute cycle.

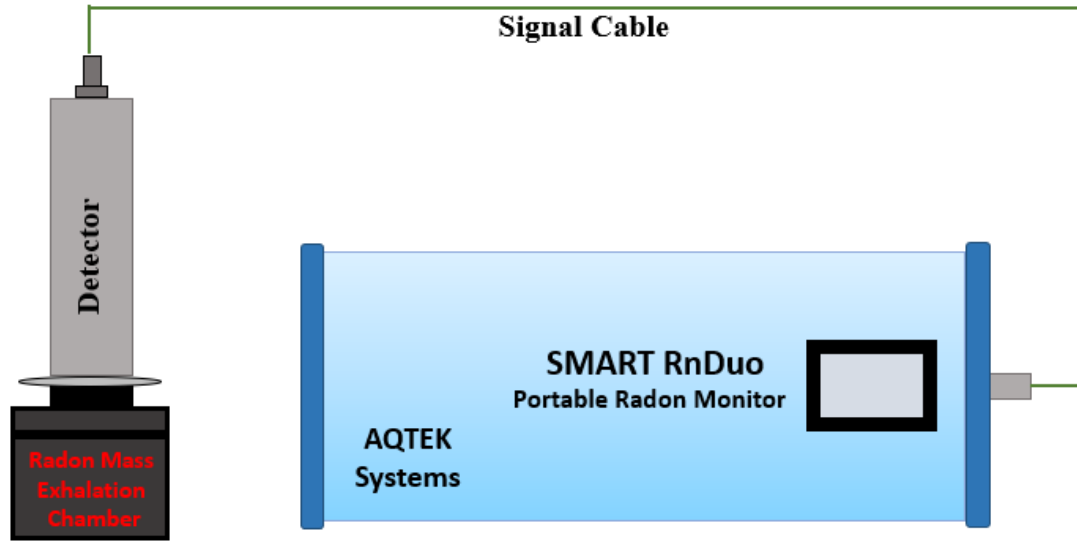


**Fig. 6.1:**  $^{222}\text{Rn}$  mass exhalation rate set-up.

The Smart RnDuo monitor was set to run for 24 hours on a 60-minute cycle for  $^{222}\text{Rn}$  measurement. The basis for the detection technique is founded on the scintillation with ZnS:Ag method for detecting alpha particles released from sampling air ( $^{222}\text{Rn}$ ) and their decay products. A pinhole plate that serves as a  $^{220}\text{Rn}$  discriminator pushes air into the scintillation chamber. The pinhole plate's diffusion time delay prevents the short-lived  $^{220}\text{Rn}$  from passing through it. The release of  $^{222}\text{Rn}$  and its daughter products' scintillations is measured with a photomultiplier tube (PMT). The monitor's microprocessor uses a smart algorithm to translate the values for each cycle into concentrations of  $^{222}\text{Rn}$ . Since there is no interference from humidity or trace gases because the detection principle is based on direct scintillation, there is no need for any extra setup in the sample path. The algorithm built into the microprocessor automatically adjusts the background readings caused by radon's residual decay products, providing a continuous reading of radon concentration. A detailed description of the Smart RnDuo and the measurement method is given elsewhere [37].

The accumulation of radon data over time can be recovered at the end of the measurements, and the least square fitting can be performed using the model eq. (1) [38].

$$C(t) = (J_m M/V)t + C_0 \quad (1)$$



Where  $J_m$  may be derived from the fitted slope after the data from the previous equation was least-square fitted.

At time  $t$ ,  $C(t)$  is the concentration of  $^{222}\text{Rn}$  ( $\text{Bqm}^{-3}$ ).

At time  $t = 0$ ,  $C_0$  represents the amount of  $^{222}\text{Rn}$  ( $\text{Bqm}^{-3}$ ) in the chamber volume.

$M$  is the dried sample's overall mass (kg).

$V$  stands for effective volume, which is made up of the detector volume, the porous sample volume, and the residual air volume in the mass exhalation chamber ( $\text{m}^3$ ).

### 6.2.2 $^{220}\text{Rn}$ surface exhalation rate measurement

The  $^{220}\text{Rn}$  was measured in flow mode, as illustrated in figure 6.2. The monitor includes an in-built micropump with a flow capacity of  $0.71 \text{ min}^{-1}$  and is connected to the scintillation cell of the monitor and used to circulate the air in the accumulation chamber. A 15-minute cycle was selected for the monitor. Upon activation of the pump, both  $^{222}\text{Rn}$  and  $^{220}\text{Rn}$  gases in the chamber pass through the progeny filter and into the scintillation cell.

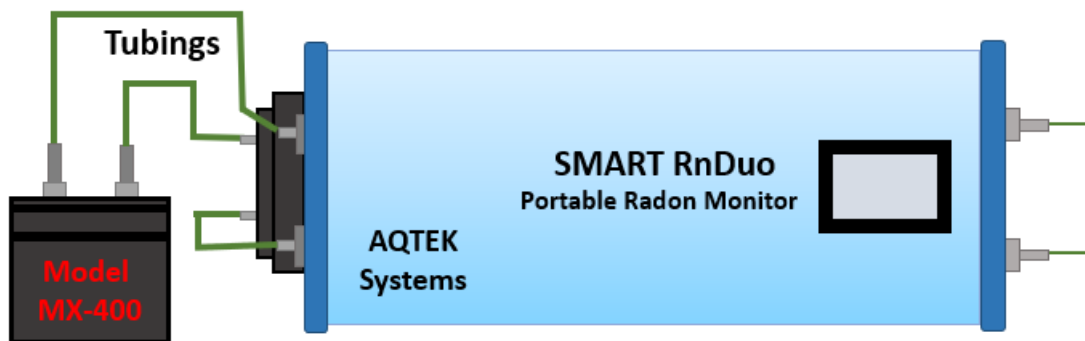


**Fig. 6.2:**  $^{220}\text{Rn}$  surface exhalation rate set up.

As a result,  $^{222}\text{Rn}/^{220}\text{Rn}$  levels are measured in the first five minutes and have a long-term background. Later, a 5-minute delay is utilized to assure that the thoron decays almost completely (half-life 55.6 s). The final 5 minutes provide radon and long-lived background measurement. The microcontroller estimates thorium concentration by subtracting counts obtained during the first 5 minutes from counts measured during the last 5 minutes and using an appropriate calibration factor. For 60 minutes, measurements were made with a 15-minute cycle interval to determine the accumulation chamber's  $^{220}\text{Rn}$  concentration equilibrium value.

$^{220}\text{Rn}$  surface exhalation rate can be determined by using the formula as [39]

$$J_s = \frac{C_{eq} V \lambda}{A} \quad (2)$$

Where  $C_{eq}$  = equilibrium concentration of  $^{220}\text{Rn}$  ( $\text{Bq m}^{-3}$ ),  $\lambda$  = decay constant for  $^{220}\text{Rn}$  ( $0.0126 \text{ s}^{-1}$ ),  $V$  = residual volume of mass exhalation chamber + the internal volume of RnDuo detector + tubing volumes ( $\text{m}^3$ ).  $A$  = surface area ( $\text{m}^2$ ) of the sample emitting  $^{220}\text{Rn}$ .

### 6.2.3 $^{222}\text{Rn}$ concentration in water

As illustrated in figure 6.3, flexible tubing was used to collect water samples into sampling glass bottles (Borosilicate glass, 60 ml in capacity). While sampling into the bottle, caution has been taken to avoid formation of bubbles/agitation in the liquid. This was carried out by gently transferring the sample by putting one end of the sampling tube inside the tap (or open end of the flowing water) and the other end put at the bottom of the sampling bottle held in a bucket or other container as shown in figure 6.3.

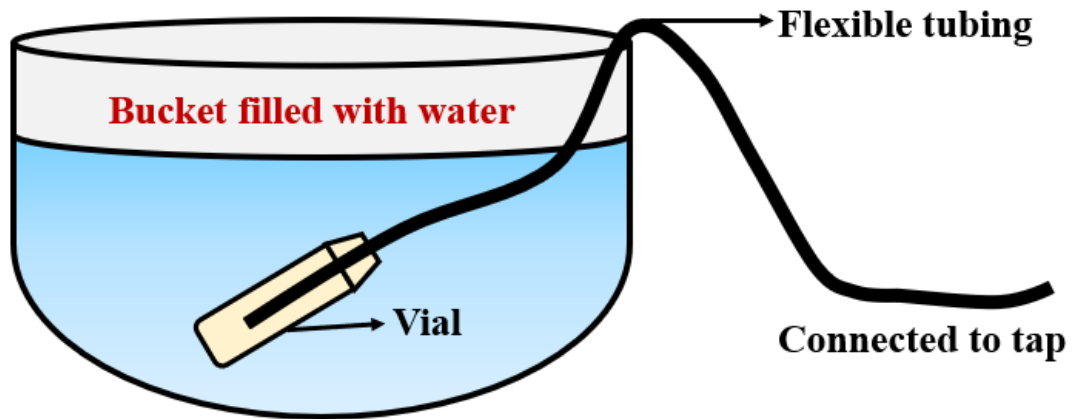


**Fig. 6.3:** Schematic diagram of water sample collection.

The bottles were filled completely and the volume in the bottle was replaced 4 to 5 times with the liquid sample without leaving any air volume and closed tightly to avoid any leakage. The time of sampling should be noted and measurement of dissolved radon should be done within 2-4 hours after the sampling. A proper decay correction should be given for the delay in measurement.

A five-minute pumping operation was used to extract freshwater from an underground source. The sampling bottle was put in a bucket of water, which allowed the water to refill itself numerous times while completely exhausting the bottle's air. To stop dissolved radon from escaping, the bottle was tightly sealed underwater. To eliminate any radon loss owing to radioactive decay, on-site measurements were made immediately following sample collection to determine the amount of dissolved radon in the sampling vial. Figure 6.4 depicts the setup used to conduct radon measurements.

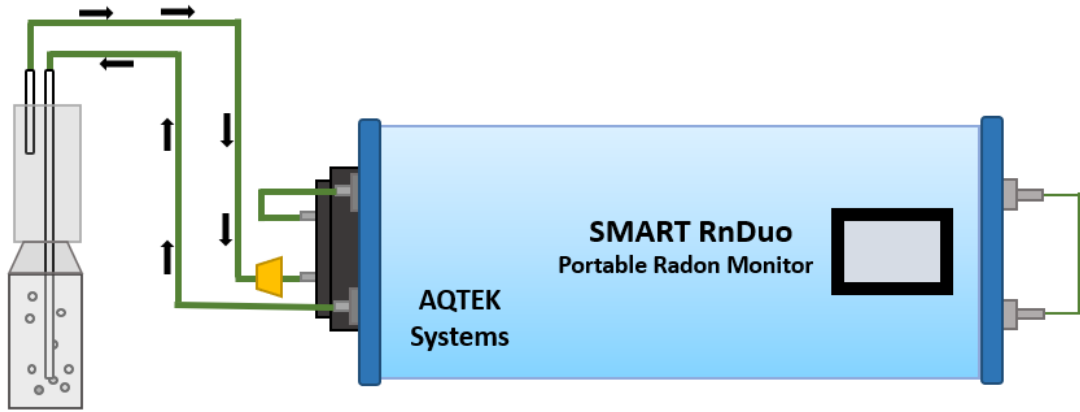


**Fig. 6.4:**  $^{222}\text{Rn}$  in the water measurement setup.

A water bubbler is connected to a SMART RnDuo in the experimental setup (AQTEK System, India). The SMART RnDuo has an inbuilt ZnS:Ag coating and a  $153\text{ cm}^3$  active volume scintillation cell [37, 38]. The instrument was routinely calibrated (once a year) against a reference radon source (Model RN-1025, Activity: 110.6 kBq) purchased from Pylon Electronics Inc., Ottawa, Canada, in order to confirm the accuracy of the calibration factor. By using a photomultiplier tube (PMT), a user-programmable counting interval was used to continuously count the alpha scintillations [39].

The following formula can be used to determine the amount of  $^{222}\text{Rn}$  in water [37]

$$C_{\text{water}} = C_{\text{air}} \left( K + \frac{V_{\text{air}}}{V_{\text{water}}} \right) \quad (3)$$

where  $C_{\text{air}}$  denotes the mean  $^{222}\text{Rn}$  concentration which is counted by the radon monitor,

$V_{\text{air}}$  = amount of air that is contained (in  $\text{m}^3$ ) by the bubbler, tubings, and detector in a closed-loop arrangement.  $K$  = partition coefficient for an air-water interface, and its value is 0.25.

$V_{\text{water}}$  is equal to 60 ml, and  $V_{\text{air}}$  is the sum of the volumes of air—153  $\text{cm}^3$  for the detector, 31.43  $\text{cm}^3$  for the tubing, and 60 ml for the bubbler—together (65 ml).

#### 6.2.4 Dose calculations due to $^{222}\text{Rn}$ in water

The following formula can be used to determine the effective ingestion dose ( $D_{\text{ing}}$ ) [1]

$$D_{\text{ing}} (\mu\text{Svy}^{-1}) = C_{\text{water}} (\text{BqL}^{-1}) \times 365 \text{ Ly}^{-1} \times A_{\text{DWI}}^{-3} \times \text{DF} \quad (4)$$

$D_{\text{ing}}$  is the annual ingested dosage ( $\mu\text{Svy}^{-1}$ ),  $C_{\text{water}}$  is the water's radon content, and  $A_{\text{DWI}}$  is the age-wise daily water intake, for newborns (0-2 years) (0.8 L), children (8-12 years) (2.5 L), and adults (above 17 years) (3 L) [25]. DF stands for dose conversion factor. Radon doses for adults are 3.5  $\text{nSvBq}^{-1}$ , for children are 5.9  $\text{nSvBq}^{-1}$ , and for newborns are 23  $\text{nSvBq}^{-1}$  [1].

The following formula can be used to determine the effective inhalation dose ( $D_{\text{inh}}$ ) [1]

$$D_{\text{inh}} (\mu\text{Svy}^{-1}) = C_{\text{water}} (\text{BqL}^{-1}) \times \frac{R_a}{w} \times F \times I \times \text{DF} \quad (5)$$

where  $C_{\text{water}}$  represents  $^{222}\text{Rn}$  content in water,  $\frac{R_a}{w}$  is the ratio of radon in the air to radon in water ( $=10^{-4}$ ), and  $F$  is the ratio at which radon and its daughter products are in equilibrium ( $F=0.4$ ). For newborns/infants, children, and adults, the conversion factors for radon inhalation are 33  $\text{nSv}/(\text{Bqh}/\text{m}^{-3})^{-1}$ , 31.4  $\text{nSv}/(\text{Bqh}/\text{m}^{-3})^{-1}$ , and 28.3  $\text{nSv}/(\text{Bqh}/\text{m}^{-3})^{-1}$ , respectively.  $I$  is the average amount of time spent indoors per person ( $=7000 \text{ hy}^{-1}$ ) [40].

### 6.3 Study Area-1

Among Nagaland's 12 districts, Mokokchung is one, bordering Assam to the north, Tuensang district to the east, Wokha and Zunheboto districts to the south. The district stretches across 1615  $\text{km}^2$  and is situated between  $25^\circ 56'\text{N}$  and  $27^\circ 40'\text{N}$  latitude and  $93^\circ 53'\text{E}$  and  $94^\circ 53'\text{E}$  longitude. Its elevation is 1325 m above sea level (figure 6.5).

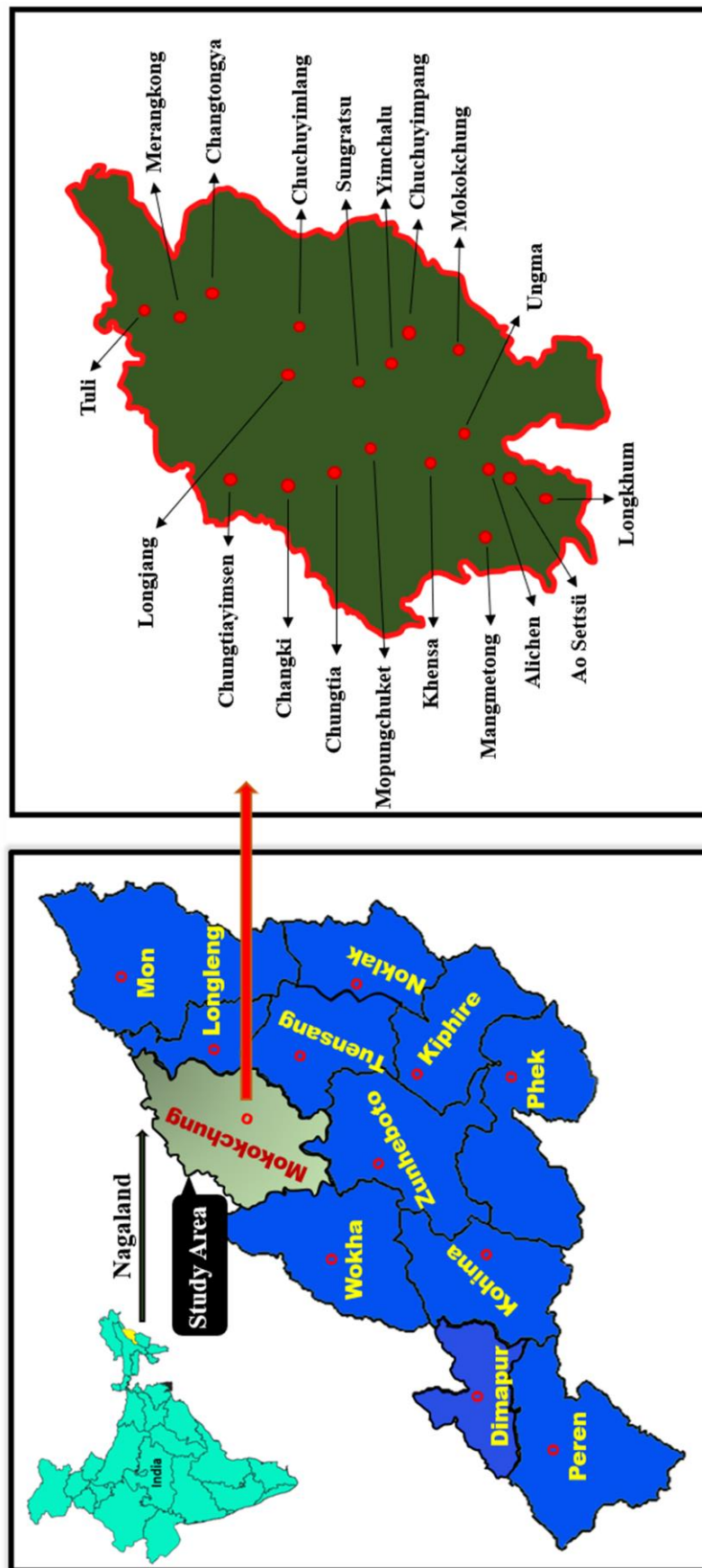


**Fig. 6.5:** Various sites of the study area in Mokokchung district, Nagaland, India.

### 6.3.1 Results and discussions of study area-1

The Gamma radiation level of the area under study is considered a baseline factor for the evaluation of exhalation rates and radionuclide content beneath the soil. The Gamma dose rate in the air was measured using a portable gamma survey meter (Model: PM-1405 manufactured by Polimaster Ltd., Republic of Belarus). Gamma dose at 1 m from the ground is not affected by airborne decay products. The main cause of the gamma dose is the daughter products of radon ( $^{214}\text{Pb}$ ,  $^{214}\text{Bi}$ , and  $^{210}\text{Pb}$ ) and thoron ( $^{212}\text{Pb}$ ,  $^{212}\text{Bi}$ , and  $^{208}\text{Tl}$ ) that are present in the soil matrix. At 1 m above the ground, the outdoor gamma level was measured. Gamma measurements range from  $0.13 \mu\text{Sv h}^{-1}$  to  $0.32 \mu\text{Sv h}^{-1}$  as shown in table 6.1.

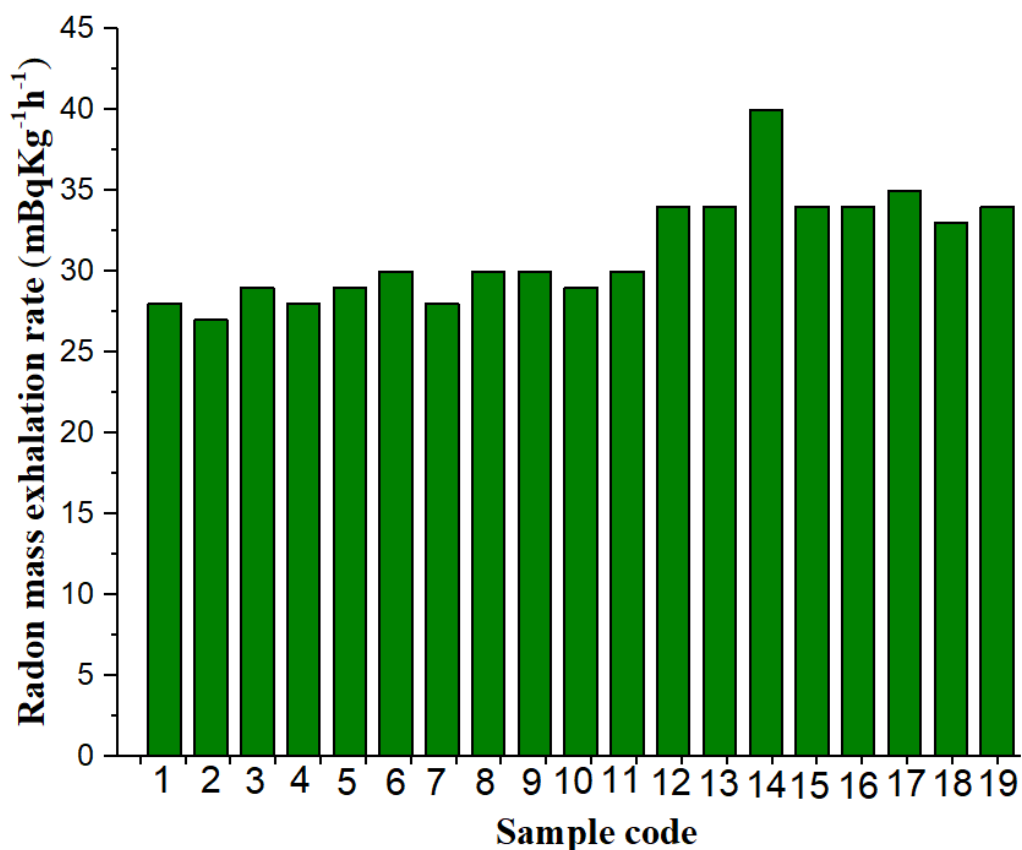
**Table 6.1:** Exhalation rates of  $^{222}\text{Rn}$ ,  $^{220}\text{Rn}$ .

| Place (Sample code) | Gamma level ( $\mu\text{Sv h}^{-1}$ ) | Mass exhalation rate of $^{222}\text{Rn}$ ( $\text{mBq Kg}^{-1}\text{h}^{-1}$ ) | Surface exhalation rate of $^{220}\text{Rn}$ ( $\text{Bqm}^{-2}\text{h}^{-1}$ ) |
|---------------------|---------------------------------------|---|---|
| Changki (1)         | 0.17                                  | 28  | 1033.4  |
| Tuli (2)            | 0.16                                  | 27  | 1246.6  |
| Ungma (3)           | 0.14                                  | 29  | 1396.6  |
| Longkhum (4)        | 0.2                                   | 28  | 2166.6  |
| Chuchuyimpang (5)   | 0.32                                  | 29  | 1089  |
| Chungtia (6)        | 0.13                                  | 30  | 836   |
| Chuchuyimlang (7)   | 0.14                                  | 28  | 910.8   |
| Merangkong (8)      | 0.32                                  | 30  | 1094.6  |
| Changtongya (9)     | 0.32                                  | 30  | 1043.6  |
| Khensa (10)         | 0.14                                  | 29  | 737.3   |
| Mokokchung (11)     | 0.18                                  | 30  | 726   |
| Alichen (12)        | 0.22                                  | 34  | 714.6   |
| Ao settsü (13)      | 0.31                                  | 34  | 850.8   |
| Mangmetong (14)     | 0.2                                   | 40  | 748.7   |
| Mopungchuket (15)   | 0.18                                  | 34  | 918.8   |
| Sungratsu (16)      | 0.21                                  | 34  | 782.7   |
| Yimchalu (17)       | 0.29                                  | 35  | 1020.9  |
| Longjang (18)       | 0.3                                   | 33  | 1054.9  |
| Chungtiayimsen (19) | 0.31                                  | 34  | 816.7   |

Smart RnDuo monitor (developed by BARC, Mumbai, India) was employed for the determination of radon and thoron exhalation rates in soil samples and radon activity concentration in water samples.

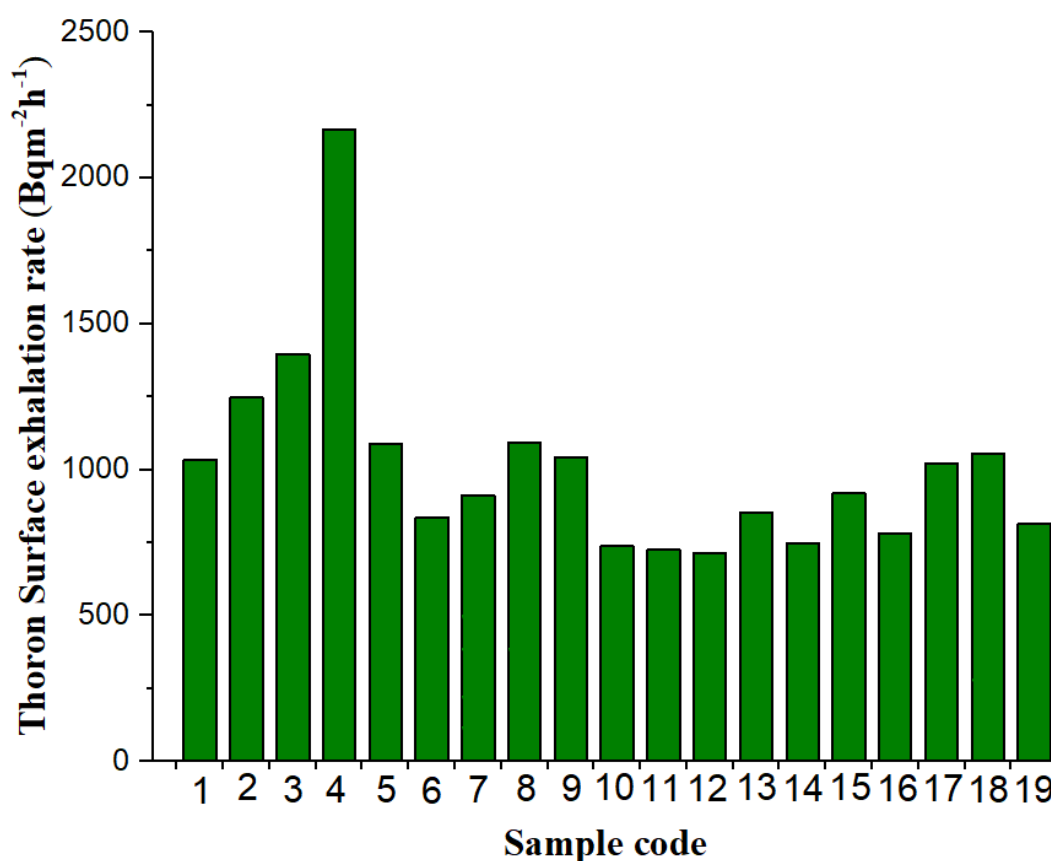
### 6.3.1.1 $^{222}\text{Rn}/^{220}\text{Rn}$ exhalation rates

Table 6.1 contains the exhalation rates of  $^{222}\text{Rn}/^{220}\text{Rn}$  that were determined from the soil samples used in this investigation. The  $^{222}\text{Rn}$  mass exhalation rates were shown to range from 27  $\text{mBqKg}^{-1}\text{h}^{-1}$  to 40  $\text{mBqKg}^{-1}\text{h}^{-1}$  with an average of  $31 \pm 0.8 \text{ mBqKg}^{-1}\text{h}^{-1}$  (table 6.1). It is observed that though the topography and geology conditions at each measurement site were not similar, the exhalation rates did not vary significantly between them. Nevertheless, the mass exhalation rate of  $^{222}\text{Rn}$  was observed highest in Mangmetong village and lowest in Tuli as shown in figure 6.6. The higher level of radon mass exhalation rate might be due to appreciably enriched radium contents in this soil and underlying bedrock.



**Fig. 6.6:** Mass exhalation rate of  $^{222}\text{Rn}$  in various villages of Mokokchung district, Nagaland, India.

In the case of thoron surface exhalation rate, sampling was carried out preferably by using flow mode. It is observed that there is a significant variation in thoron surface exhalation rate which may be attributed to different topography and geological location of soil samples. The gathered samples from various sites have different geometries and soil compositions, which could have impacted the  $^{220}\text{Rn}$  exhalation rate from the soil. The  $^{220}\text{Rn}$  surface exhalation rate ranged from  $714.6 \text{ Bqm}^{-2}\text{h}^{-1}$  to  $2166.6 \text{ Bqm}^{-2}\text{h}^{-1}$  having a mean value of  $1009.9 \pm 77.1 \text{ Bqm}^{-2}\text{h}^{-1}$ . The surface exhalation rate of  $^{220}\text{Rn}$  was observed highest in Longkhum village as shown in figure 6.7. The high level of thoron might be due to appreciably large thorium contents in the soil of this region.



**Fig. 6.7:** Surface exhalation rate of  $^{220}\text{Rn}$  in various villages of Mokokchung district, Nagaland, India.

Table 6.2 shows a comparison of the findings from the current data with those from prior data in different regions of India. There could be a number of reasons for the variation of exhalation rates reported for different regions including differences in



methodology as well as soil morphology, lithology, and geographical condition. Overall, our findings are consistent with the reported values.

**Table 6.2:** Comparing the current data on  $^{222}\text{Rn}/^{220}\text{Rn}$  exhalation rates with those obtained from other parts of the nation.

| Regions                     | $^{222}\text{Rn}$ mass exhalation rate ( $\text{mBqKg}^{-1}\text{h}^{-1}$ ) | $^{220}\text{Rn}$ surface exhalation rate ( $\text{Bqm}^{-2}\text{h}^{-1}$ ) | References    |
|-----------------------------|---|--|---------------|
|                             | <b>Average</b>  | <b>Average</b>   |               |
| Chikkaballapur, Karnataka   | $143 \pm 61$  | $10443 \pm 5669$   | [18]          |
| Faridabad, Southern Haryana | $31 \pm 12$   | $5846 \pm 1424$  | [19]          |
| Fazilka, Punjab             | 118.7   | $32.3 \times 10^3$   | [20]          |
| East Khasi Hills, Meghalaya | $11.6 \pm 0.06$   | $(24.1 \pm 0.14) \times 10^3$  | [21]          |
| Mokokchung, Nagaland        | $31 \pm 0.8$  | $1009.9 \pm 77.1$  | Present study |

### 6.3.1.2 $^{222}\text{Rn}$ in water

$^{222}\text{Rn}$  content in water was shown to be between  $1.66 \text{ BqL}^{-1}$  and  $2.22 \text{ BqL}^{-1}$  having a mean value of  $1.82 \pm 0.04 \text{ BqL}^{-1}$  as shown in table 6.3. The highest  $^{222}\text{Rn}$  concentration in the water is observed in Mokokchung village as shown in figure 6.8. This may be because radon's escape path is constrained under subterranean water because it immediately interacts with rock that continually emits  $^{222}\text{Rn}$ . The various types of underlying bedrock found in the study area's Earth's crust also influence the amount of  $^{222}\text{Rn}$  in drinking water which includes mainly sandstone, shale, limestone, etc. Additionally, it has been discovered that igneous rocks tend to have greater radiation levels than sedimentary rocks like sandstone, whereas certain shales and phosphate rocks have higher radioactive contents [41].

**Table 6.3:**  $^{222}\text{Rn}$  content and its effective dose in the water samples of Mokokchung district of Nagaland.

| Place (Sample code) | $^{222}\text{Rn}$ (BqL <sup>-1</sup> ) in water | Yearly effective dose because of inhalation ( $\mu\text{Svy}^{-1}$ ) |                       |                         | Yearly effective dose because of ingestion ( $\mu\text{Svy}^{-1}$ ) |                       |                         |
|---------------------|---|--|-----------------------|-------------------------|---|-----------------------|-------------------------|
|                     |   | Infants (0–2 years)  | Children (8–12 years) | Adults (above 17 years) | Infants (0–2 years)   | Children (8–12 years) | Adults (above 17 years) |
| Changki (1)         | 1.73  | 11.59  | 9.29                  | 6.61                    | 15.95   | 15.17                 | 13.67                   |
| Tuli (2)            | 1.90  | 12.78  | 10.24                 | 7.29                    | 17.58   | 16.72                 | 15.07                   |
| Ungma (3)           | 1.97  | 13.24  | 10.62                 | 7.56                    | 18.22   | 17.34                 | 15.62                   |
| Longkhum (4)        | 1.69  | 11.32  | 9.07                  | 6.46                    | 15.57   | 14.82                 | 13.35                   |
| Chuchuyimpang (5)   | 1.88  | 12.60  | 10.10                 | 7.19                    | 17.33   | 16.49                 | 14.86                   |
| Chungtia (6)        | 1.89  | 12.69  | 10.17                 | 7.24                    | 17.46   | 16.62                 | 14.98                   |
| Chuchuyimlang (7)   | 1.88  | 12.65  | 10.14                 | 7.22                    | 17.41   | 16.56                 | 14.93                   |
| Merangkong (8)      | 1.89  | 12.66  | 10.15                 | 7.23                    | 17.42   | 16.58                 | 14.94                   |
| Changtongya (9)     | 1.72  | 11.58  | 9.28                  | 6.61                    | 15.93   | 15.16                 | 13.66                   |
| Khensa (10)         | 1.74  | 11.67  | 9.36                  | 6.66                    | 16.06   | 15.28                 | 13.77                   |
| Mokokchung (11)     | 2.22  | 14.89  | 11.94                 | 8.50                    | 20.49   | 19.50                 | 17.57                   |
| Alichen (12)        | 1.72  | 11.55  | 9.26                  | 6.59                    | 15.89   | 15.12                 | 13.63                   |
| Aosettsu (13)       | 2.15  | 14.47  | 11.60                 | 8.26                    | 19.91   | 18.94                 | 17.07                   |
| Mangmetong (14)     | 1.94  | 13.04  | 10.45                 | 7.44                    | 17.93   | 17.06                 | 15.38                   |
| Mopungchuket (15)   | 1.48  | 9.91   | 7.95                  | 5.66                    | 13.64   | 12.98                 | 11.70                   |
| Sungratsu (16)      | 1.78  | 11.98  | 9.60                  | 6.84                    | 16.48   | 15.68                 | 14.13                   |
| Yimchalu (17)       | 1.54  | 10.34  | 8.29                  | 5.90                    | 14.22   | 13.53                 | 12.20                   |
| Longjang (18)       | 1.72  | 11.58  | 9.28                  | 6.61                    | 15.93   | 15.16                 | 13.66                   |
| Chungtiayimsen (19) | 1.66  | 11.18  | 8.96                  | 6.38                    | 15.38   | 14.63                 | 13.19                   |

The concentration of  $^{222}\text{Rn}$  in subterranean water samples may be related to increasing depth, which lengthened the time that flowing water and the aquifer had to interact. Additionally, larger depths of soil and rocks with higher porosities accelerate the flow of water and dissolve  $^{222}\text{Rn}$  dissolution, increasing the concentration of  $^{222}\text{Rn}$  in subterranean water sources.

Nevertheless, the obtained values are below the USEPA-recommended range of 11  $\text{BqL}^{-1}$  (1991) and much less than 100  $\text{BqL}^{-1}$  and 4-40  $\text{BqL}^{-1}$  as set by WHO (2004) and UNSCEAR (2008) respectively [42-44].

So, from the perspective of health, drinking water is safe for the population of this region.

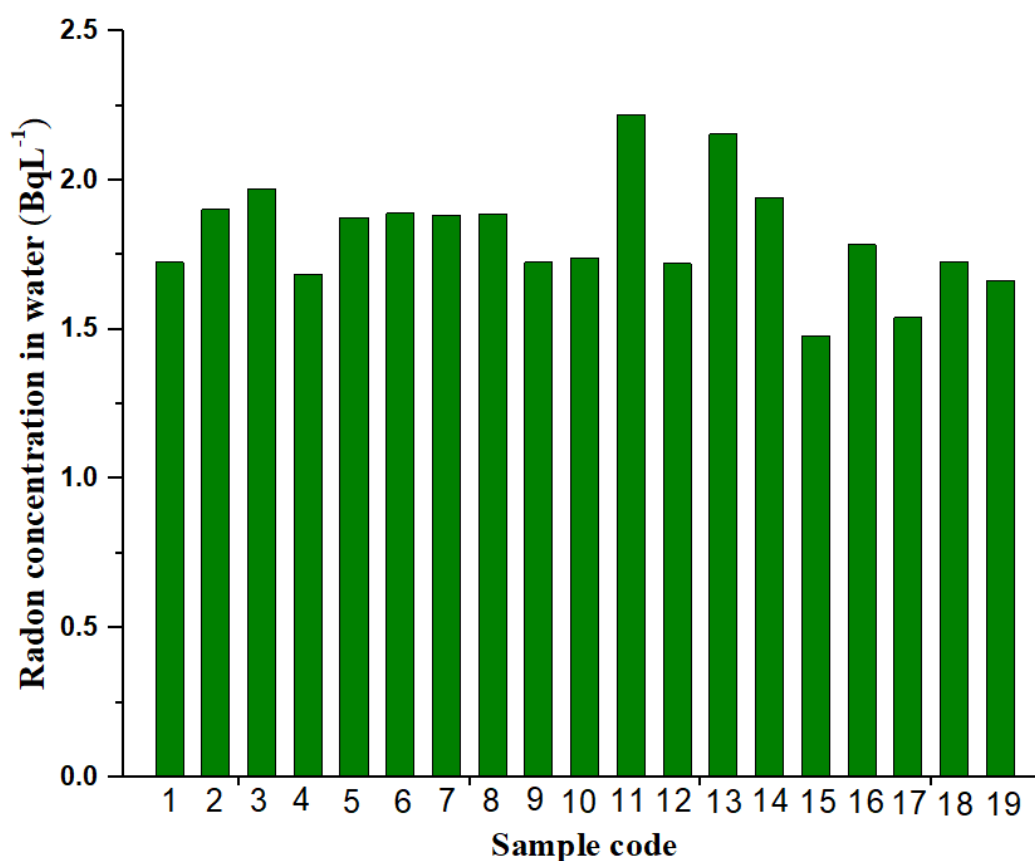


**Fig. 6.8:** Radon concentration in water in various villages of Mokokchung district, Nagaland, India.

From table 6.3, we can see that the range of the yearly ingestion dosage from drinking water is 9.91 to 14.89  $\mu\text{Svy}^{-1}$  having a mean value of  $12.20 \pm 0.28 \mu\text{Svy}^{-1}$  for infants while varying from 7.95 to 11.94  $\mu\text{Svy}^{-1}$  having a mean value of  $9.78 \pm 0.23 \mu\text{Svy}^{-1}$  for children. For adults, it is between 5.66 to 8.50  $\mu\text{Svy}^{-1}$  having a mean value of  $6.96 \pm 0.16 \mu\text{Svy}^{-1}$ .

The range of the yearly inhalation dose is from 13.64 to 20.49  $\mu\text{Svy}^{-1}$  having a mean value of  $16.78 \pm 0.39 \mu\text{Svy}^{-1}$ , in the range of 12.98 to 19.50  $\mu\text{Svy}^{-1}$  having a mean value of  $15.96 \pm 0.37 \mu\text{Svy}^{-1}$  and in the range of 11.70 to 17.57  $\mu\text{Svy}^{-1}$  having a mean value of  $14.39 \pm 0.34 \mu\text{Svy}^{-1}$  for infants, children, and adults respectively. Infants receive larger annual doses of ingestion and inhalation than it does children and adults, according to research. However, the estimated dosage for each sample is within the permissible range of 100  $\mu\text{Svy}^{-1}$  [45].

## **6.4 Study Area-2**

Dimapur is one of Nagaland's districts, and it is bordered on the south and east by the Kohima district, on the west by the Karbi Anglong district of Assam, and on the north by a stretch of the Golaghat district of Assam (figure 6.9).

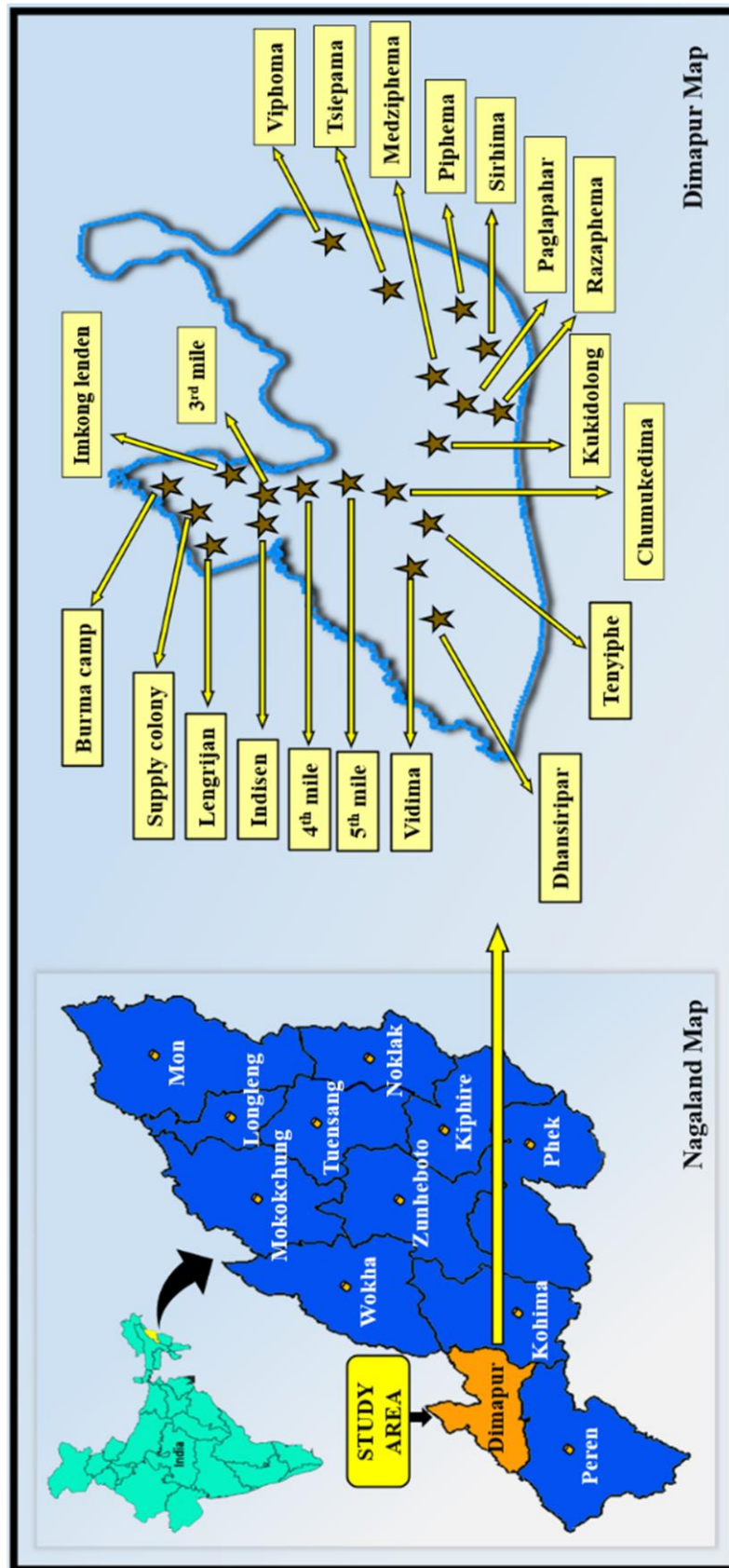


**Fig. 6.9:** Various sites of the study area in Dimapur district, Nagaland, India.

### 6.4.1 Results and discussions of study area-2

Gamma estimations were made in the research region because they serve as a basis for assessing exhalation rates and radioactive concentration in the soil. The measurements were performed one meter above the soil surface to prevent disturbance from progeny (by means of a portable gamma survey Polimaster Ltd., Republic of Belarus, manufacturer's model number: PM-1405). The gamma level in the study region varies from 0.13 to 0.32  $\mu\text{Svh}^{-1}$  (table 6.4).

**Table 6.4:** Exhalation rates of  $^{222}\text{Rn}$  and  $^{220}\text{Rn}$  obtained from Dimapur district, Nagaland.

| Location (Sample code)    | Gamma level ( $\mu\text{Svh}^{-1}$ ) | $^{222}\text{Rn}$ mass exhalation rate ( $\text{mBqKg}^{-1}\text{h}^{-1}$ ) | $^{220}\text{Rn}$ surface exhalation rate ( $\text{Bqm}^{-2}\text{h}^{-1}$ ) |
|---------------------------|--------------------------------------|---|--|
| Burma camp (1)            | 0.13                                 | 16.20   | 778.15   |
| Chumukedima (2)           | 0.14                                 | 33.17   | 1650.46  |
| Indisen (3)               | 0.14                                 | 32.00   | 746.39   |
| Lengrijan (4)             | 0.14                                 | 35.09   | 767.94   |
| Imkong Lenden (5)         | 0.16                                 | 33.25   | 623.88   |
| Supply (6)                | 0.17                                 | 31.97   | 778.15   |
| Dhansiripar (7)           | 0.18                                 | 30.14   | 744.12   |
| Medziphema (8)            | 0.18                                 | 35.89   | 1554.04  |
| 3 <sup>rd</sup> mile (9)  | 0.2                                  | 31.04   | 805.38   |
| 4 <sup>th</sup> mile (10) | 0.2                                  | 30.57   | 816.72   |
| 5 <sup>th</sup> mile (11) | 0.21                                 | 32.04   | 725.97   |
| Vidima (12)               | 0.22                                 | 32.70   | 850.75   |
| Tenyiphe (13)             | 0.29                                 | 36.78   | 884.78   |
| Kukidolong (14)           | 0.3                                  | 35.32   | 703.29   |
| Razaphema (15)            | 0.31                                 | 27.14   | 839.41   |
| Paglapahar (16)           | 0.31                                 | 28.48   | 805.38   |
| Sirhima (17)              | 0.32                                 | 33.37   | 1667.47  |
| Piphema (18)              | 0.32                                 | 33.30   | 862.09   |
| Tsiepama (19)             | 0.32                                 | 32.91   | 805.38   |
| Viphoma (20)              | 0.22                                 | 33.98   | 923.69   |

#### 6.4.1.1 $^{222}\text{Rn}/^{220}\text{Rn}$ exhalation rates

$^{222}\text{Rn}/^{220}\text{Rn}$  exhalation rates discovered from soil samples analyzed in the present experiment are shown in table 6.4. Although each measuring site's terrain and geology were different from the others, it was found that the exhalation rates were not considerably different. The  $^{222}\text{Rn}$  mass exhalation rates vary from 16.20 to 35.89  $\text{mBqKg}^{-1}\text{h}^{-1}$  (mean=  $31.77 \pm 0.97 \text{ mBqKg}^{-1}\text{h}^{-1}$ ) (table 6.4). According to figure 6.10, the Medziphema colony had the highest mass exhalation rate of  $^{222}\text{Rn}$ , and the Burma camp colony had the lowest. The increased mass exhalation rate of  $^{222}\text{Rn}$  may be caused by the soil's and the bedrock's significantly enriched radium concentration. These values are significantly below the  $57 \text{ mBqKg}^{-1}\text{h}^{-1}$  average global values [1].

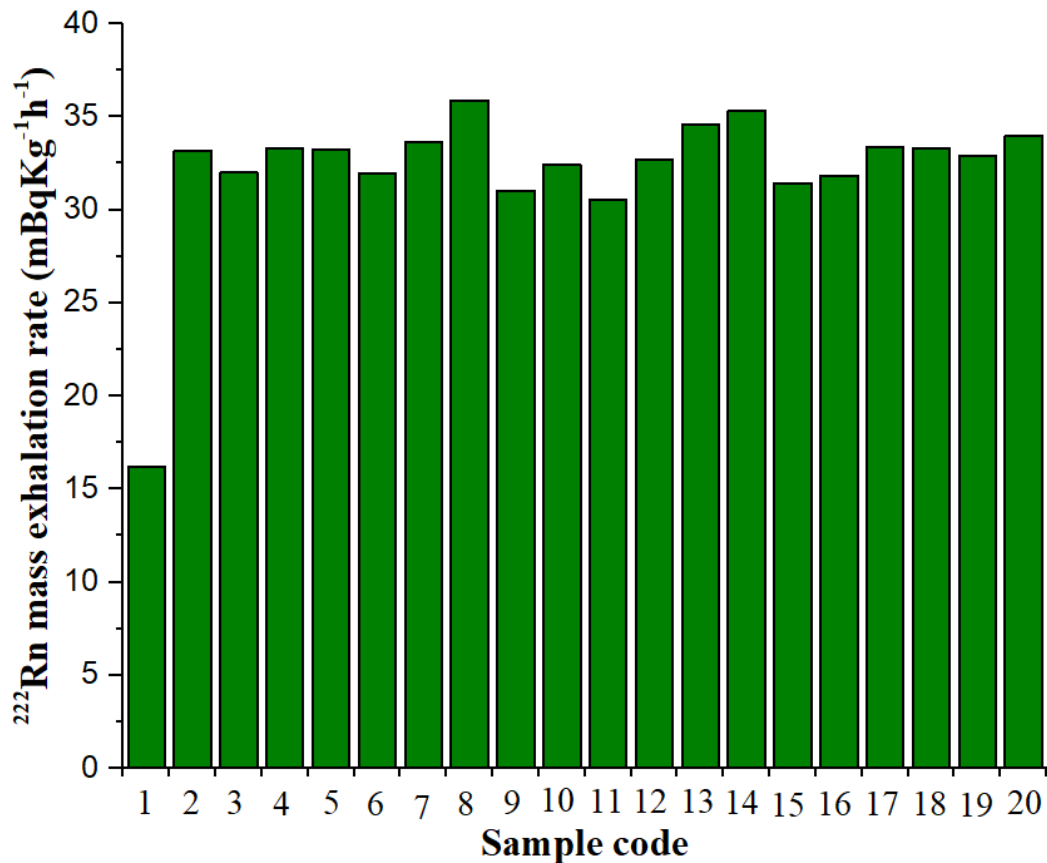


**Fig. 6.10:**  $^{222}\text{Rn}$  mass exhalation rate.

While  $^{220}\text{Rn}$  surface exhalation rate varies from 623.88 to 1667.47  $\text{Bqm}^{-2}\text{h}^{-1}$  (mean=  $916.67 \pm 69.90 \text{ Bqm}^{-2}\text{h}^{-1}$ ). The surface exhalation rate of  $^{220}\text{Rn}$  was detected maximum

in the Sirhima colony (figure 6.11). The soil texture and geometry of the samples taken from different locations may have affected the rate at which  $^{220}\text{Rn}$  was exhaled from the soil. These values, however, are also less than the  $3600 \text{ Bqm}^{-2}\text{h}^{-1}$  global average values [1].

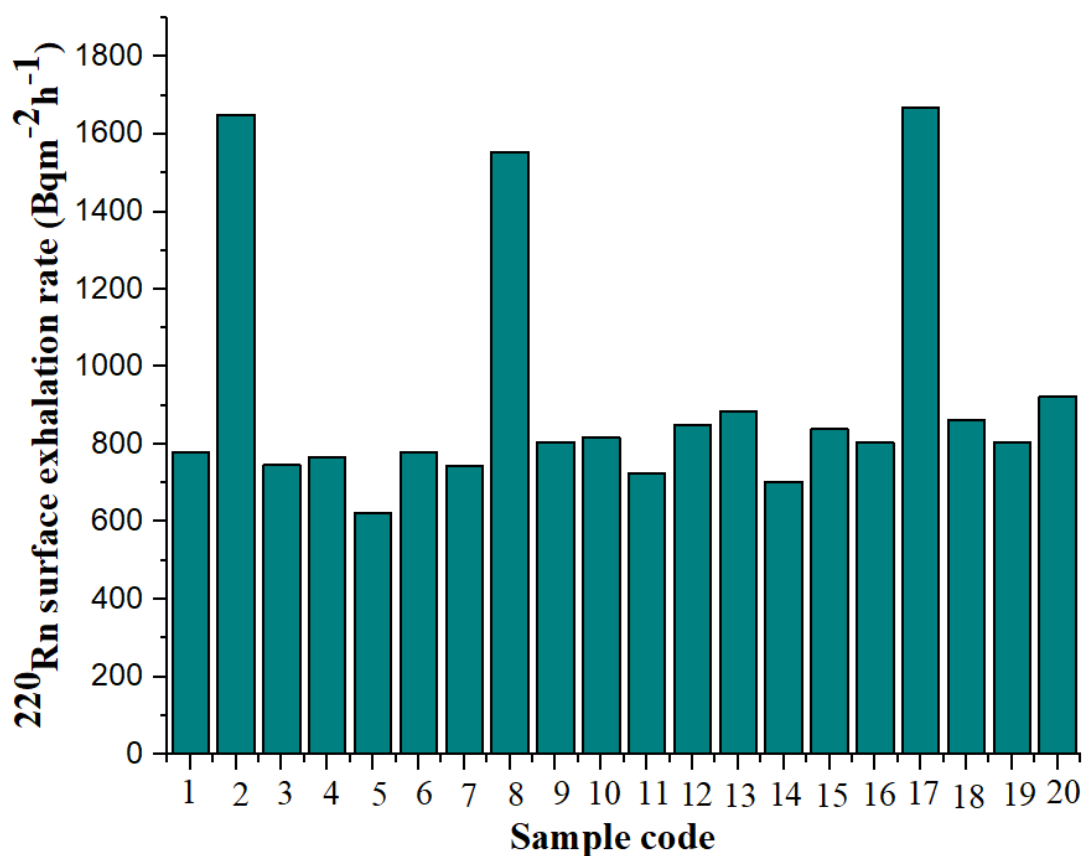


**Fig. 6.11:**  $^{220}\text{Rn}$  surface exhalation rate.

Table 6.5 compares the results of the current investigation with those discovered in other regions of the world. The findings of the current investigation revealed that the  $^{222}\text{Rn}/^{220}\text{Rn}$  exhalation rate found in the present study is in agreement with the research results reported by other researchers around the world.

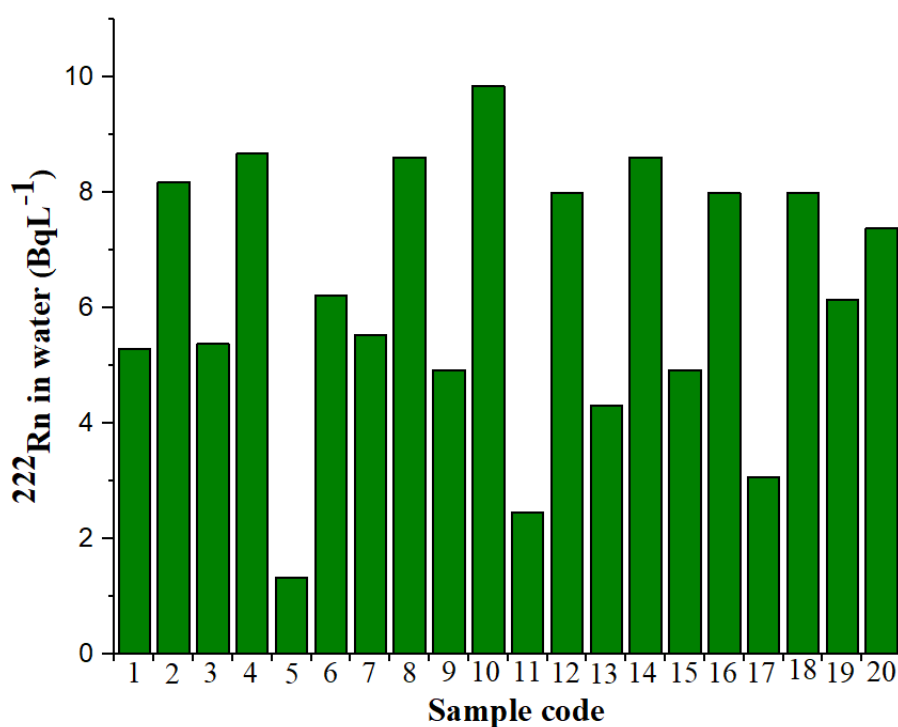


**Table 6.5:** Inter-comparison of the current data of  $^{222}\text{Rn}/^{220}\text{Rn}$  exhalation rates with worldwide values.

| Regions                  | $^{222}\text{Rn}$ mass exhalation Rate ( $\text{mBqKg}^{-1}\text{h}^{-1}$ ) | $^{220}\text{Rn}$ exhalation surface rate ( $\text{Bqm}^{-2}\text{h}^{-1}$ ) | References    |
|--------------------------|---|--|---------------|
|                          | Range (Mean)  | Range (Mean)   |               |
| Sakarya, Turkey          | 35-253 (112)  | -  | [46]          |
| Indonesia                | -   | 144-9470   | [47]          |
| Palwal, Haryana, India   | 16-48 (28)  | 1800-6331 (3850)   | [48]          |
| Liberian Peninsula       | 4.3-823   | 14-2485  | [49]          |
| Dimapur, Nagaland, India | 16.20-35.89 (31.77)   | 623.88-1667.47 (916.67)  | Present study |

#### 6.4.1.2 $^{222}\text{Rn}$ in water

The amount of  $^{222}\text{Rn}$  in water varies from 1.32 to 9.84  $\text{BqL}^{-1}$  (mean=  $6.24 \pm 0.52 \text{ BqL}^{-1}$ ) (table 6.6).  $^{222}\text{Rn}$  level was observed highest in the water samples collected from the 5<sup>th</sup>-mile colony while the lowest was observed in the Imkong Lenden colony (figure 6.12). The higher  $^{222}\text{Rn}$  concentration in the water of the 5<sup>th</sup>-mile colony is presumably a result of subsurface water restricting radon's escape path.

**Fig. 6.12:**  $^{222}\text{Rn}$  in water in different sites.

After all, it interacts instantly with bedrock that is constantly emitting  $^{222}\text{Rn}$ . The amount of  $^{222}\text{Rn}$  in drinking water is also influenced by the different forms of the bedrock present beneath the research area's Earth's crust, which primarily consists of shale, limestone, sandstone, etc. Further, it was established that volcanic rocks often possess higher radiation levels compared to sedimentary rocks such as sandstone, although specific shales and phosphate rocks possess greater radioactive concentrations [41].

**Table 6.6:**  $^{222}\text{Rn}$  and its dose detected in drinking water of Dimapur district, Nagaland.

| Location (Sample code)    | $^{222}\text{Rn}$ ( $\text{BqL}^{-1}$ ) in water | Annual effective dose due to inhalation ( $\mu\text{Svy}^{-1}$ ) |                       |                         | Annual effective dose due to ingestion ( $\mu\text{Svy}^{-1}$ ) |                       |                         |
|---------------------------|--|--|-----------------------|-------------------------|---|-----------------------|-------------------------|
|                           |  | Infants (0–2 years)  | Children (8–12 years) | Adults (above 17 years) | Infants (0–2 years)   | Children (8–12 years) | Adults (above 17 years) |
| Burma camp (1)            | 5.30   | 35.56  | 28.51                 | 20.29                   | 48.93   | 46.55                 | 41.96                   |
| Chumukedima (2)           | 8.18   | 54.93  | 44.04                 | 31.35                   | 75.58   | 71.91                 | 64.81                   |
| Indisen (3)               | 5.38   | 36.10  | 28.94                 | 20.60                   | 49.67   | 47.26                 | 42.59                   |
| Lengrijan (4)             | 8.67   | 58.24  | 46.69                 | 33.23                   | 80.12   | 76.24                 | 68.71                   |
| Imkong Lenden (5)         | 1.32   | 8.84   | 7.09                  | 5.04                    | 12.16   | 11.57                 | 10.43                   |
| Supply (6)                | 6.21   | 41.72  | 33.44                 | 23.81                   | 57.39   | 54.61                 | 49.22                   |
| Dhansiripar (7)           | 5.54   | 37.17  | 29.80                 | 21.21                   | 51.14   | 48.66                 | 43.86                   |
| Medziphema (8)            | 8.61   | 57.82  | 46.35                 | 33.00                   | 79.56   | 75.70                 | 68.23                   |
| 3 <sup>rd</sup> mile (9)  | 4.92   | 33.04  | 26.49                 | 18.86                   | 45.46   | 43.26                 | 38.99                   |
| 4 <sup>th</sup> mile (10) | 9.84   | 66.09  | 52.98                 | 37.71                   | 90.92   | 86.51                 | 77.97                   |
| 5 <sup>th</sup> mile (11) | 2.46   | 16.52  | 13.24                 | 9.43                    | 22.73   | 21.63                 | 19.49                   |
| Vidima (12)               | 8.00   | 53.69  | 43.04                 | 30.64                   | 73.87   | 70.29                 | 63.35                   |
| Tenyiphe (13)             | 4.31   | 28.91  | 23.18                 | 16.50                   | 39.78   | 37.85                 | 34.11                   |
| Kukidolong (14)           | 8.61   | 57.82  | 46.35                 | 33.00                   | 79.56   | 75.70                 | 68.23                   |
| Razaphema (15)            | 4.92   | 33.04  | 26.49                 | 18.86                   | 45.46   | 43.26                 | 38.99                   |
| Paglapahar (16)           | 8.00   | 53.69  | 43.04                 | 30.64                   | 73.87   | 70.29                 | 63.35                   |
| Sirhima (17)              | 3.08   | 20.65  | 16.56                 | 11.78                   | 28.41   | 27.04                 | 24.37                   |
| Piphema (18)              | 8.00   | 53.69  | 43.04                 | 30.64                   | 73.87   | 70.29                 | 63.35                   |
| Tsiepama (19)             | 6.14   | 41.26  | 33.08                 | 23.55                   | 56.77   | 54.02                 | 48.68                   |
| Viphoma (20)              | 7.38   | 49.56  | 39.73                 | 28.28                   | 68.19   | 64.88                 | 58.48                   |

An increase in depth may have increased the amount of time the aquifers need to interact with moving water, which could explain why there is more  $^{222}\text{Rn}$  in subterranean water samples. Additionally, deeper soil layers and more porous rocks speed up water flow and  $^{222}\text{Rn}$  dissolution, raising the intensity of  $^{222}\text{Rn}$  in underground water tables.

However, the measured values are significantly lower than the  $100 \text{ BqL}^{-1}$  (prescribed by WHO, 2004) and  $4\text{-}40 \text{ BqL}^{-1}$  (prescribed by UNSCEAR, 2008), and below the safe limit of  $11 \text{ BqL}^{-1}$  (prescribed by USEPA, 1991) [42-44]. As a result, residents of this area can safely drink the water.

The annual ingestion dosage from drinking water falls between the ranges of 35.56 to  $49.56 \mu\text{Svy}^{-1}$  (average value =  $41.92 \pm 3.49 \mu\text{Svy}^{-1}$ ) for infants, while for children vary from 28.51 to  $39.73 \mu\text{Svy}^{-1}$  (average =  $33.60 \pm 2.79 \mu\text{Svy}^{-1}$ ) and for adults lies in the range of 20.29 to  $28.28 \mu\text{Svy}^{-1}$  (average value =  $23.92 \pm 1.99 \mu\text{Svy}^{-1}$ ) (table 6.6).

The annual inhalation dosage ranges from 12.16 to  $90.92 \mu\text{Svy}^{-1}$  with an average value of  $57.67 \pm 4.80 \mu\text{Svy}^{-1}$  for infants, in the range of 11.57 to  $86.51 \mu\text{Svy}^{-1}$  with an average of  $54.88 \pm 4.56 \mu\text{Svy}^{-1}$  for children and in the range of 10.43 to  $77.97 \mu\text{Svy}^{-1}$  (mean value =  $49.46 \pm 4.11 \mu\text{Svy}^{-1}$ ) for adults. Infants receive the most yearly dose (ingestion and inhalation) as compared to adults and children, based on the current findings. The overall dose, however, remains within the permitted range of  $100 \mu\text{Svy}^{-1}$  for each sample [45].

### **6.5 Study Area-3**

As indicated on the map (figure 6.13), Kohima district is one of Nagaland's twelve districts and it borders Dimapur district to the west, Phek district to the east, Manipur state and Peren district to the south, and Wokha district to the north. It is located in the southern portion of Nagaland, between  $94^{\circ} 5'11''$  and  $94^{\circ}7'12''$  and  $25^{\circ}28'20''$  and  $25^{\circ}31'51''$ .

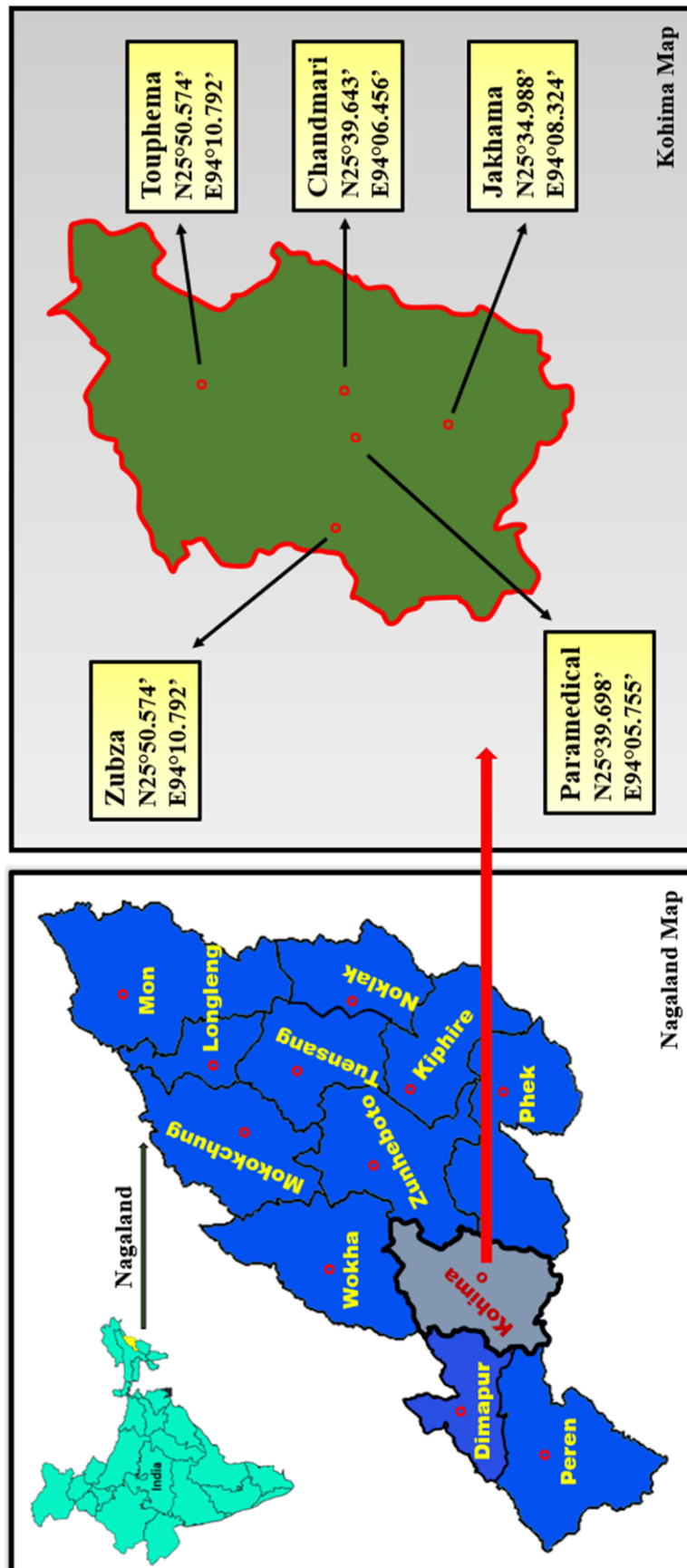


Fig. 6.13: Various sites of the study area in Kohima district, Nagaland, India.

### 6.5.1 Results and discussions of study area-3

The gamma level in the study region varies from 0.14 to 0.29  $\mu\text{Svh}^{-1}$  (table 6.7).

#### 6.5.1.1 $^{222}\text{Rn}/^{220}\text{Rn}$ exhalation rates

$^{222}\text{Rn}/^{220}\text{Rn}$  exhalation rates discovered from soil samples analyzed in the present experiment are shown in table 6.7. The  $^{222}\text{Rn}$  mass exhalation rates vary from 11 to 31.21  $\text{mBqKg}^{-1}\text{h}^{-1}$  (mean=  $19.03 \pm 3.82 \text{ mBqKg}^{-1}\text{h}^{-1}$ ) (table 6.7).

**Table 6.7:** Exhalation rates of  $^{222}\text{Rn}$ ,  $^{220}\text{Rn}$ .

| Place (Sample code) | Gamma level ( $\mu\text{Svh}^{-1}$ ) | Mass exhalation rate of $^{222}\text{Rn}$ ( $\text{mBqKg}^{-1}\text{h}^{-1}$ ) | Surface exhalation rate of $^{220}\text{Rn}$ ( $\text{Bqm}^{-2}\text{h}^{-1}$ ) |
|---------------------|--------------------------------------|--|---|
| Chandmari           | 0.15                                 | 12.19  | 1000  |
| Jakhama             | 0.21                                 | 31.21  | 1200  |
| Paramedical         | 0.14                                 | 16.62  | 1395  |
| Touphema            | 0.29                                 | 24.12  | 2100  |
| Zubza               | 0.28                                 | 11   | 1500  |

According to figure 6.14, Jakhama village had the highest mass exhalation rate of  $^{222}\text{Rn}$ , and Zubza had the lowest. The increased mass exhalation rate of  $^{222}\text{Rn}$  may be caused by the soil's and the bedrock's significantly enriched radium concentration. These values are significantly below the 57  $\text{mBqKg}^{-1}\text{h}^{-1}$  average global values [1].

While  $^{220}\text{Rn}$  surface exhalation rate varies from 1000 to 2100  $\text{Bqm}^{-2}\text{h}^{-1}$  (mean=  $1439 \pm 186 \text{ Bqm}^{-2}\text{h}^{-1}$ ). The surface exhalation rate of  $^{220}\text{Rn}$  was detected maximum in Touphema village (figure 6.15). The soil texture and geometry of the samples taken from different locations may have affected the rate at which  $^{220}\text{Rn}$  was exhaled from the soil. These values, however, are also less than the 3600  $\text{Bqm}^{-2}\text{h}^{-1}$  global average values [1].

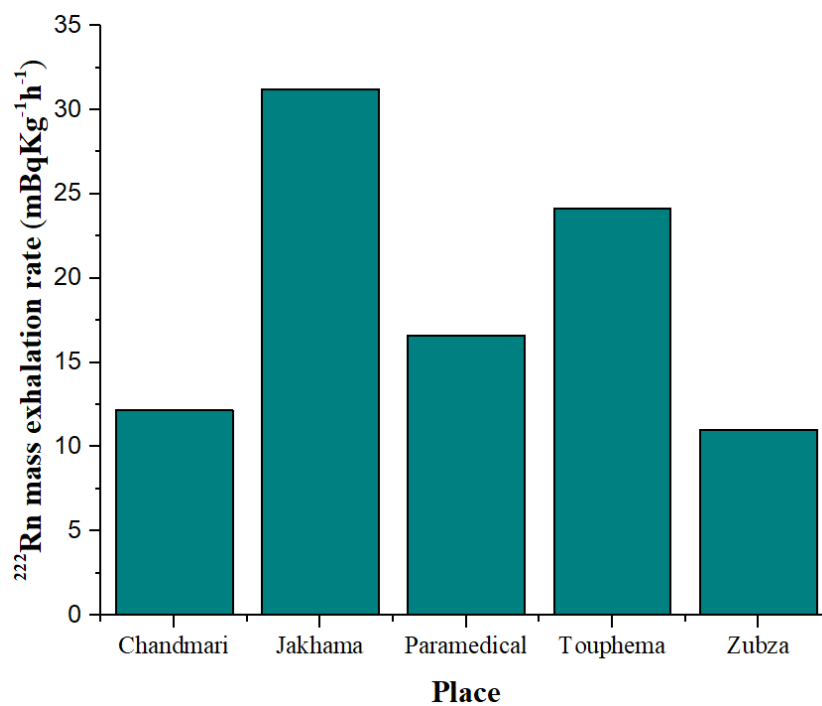


**Fig. 6.14:** Mass exhalation rate of  $^{222}\text{Rn}$  in various sites of Kohima district, Nagaland, India.

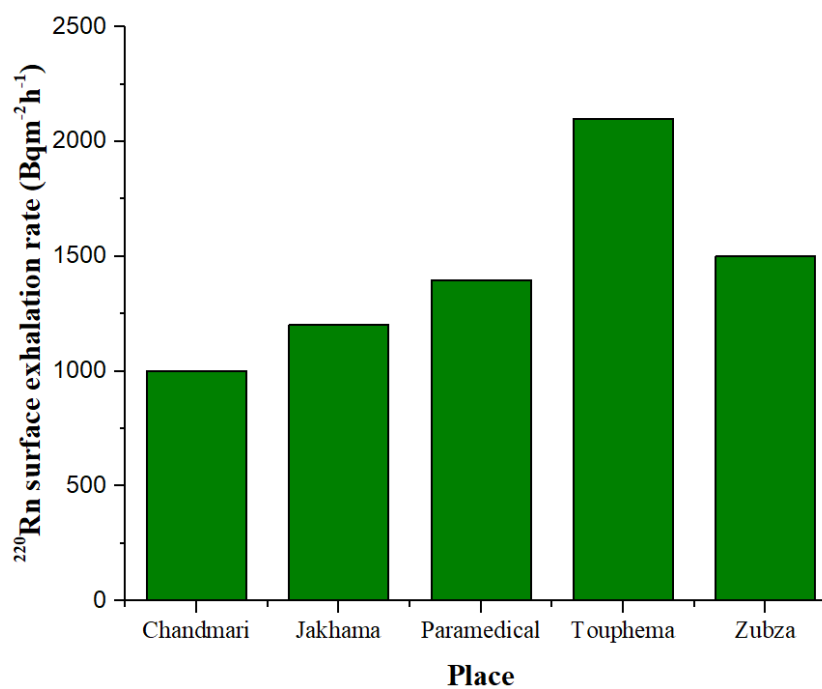


**Fig. 6.15:** Surface exhalation rate of  $^{220}\text{Rn}$  in various sites of Kohima district, Nagaland, India.

Table 6.8 shows a comparison of the findings from the current data with those from prior data in different regions of India. Overall, the present study findings were consistent with the reported values.

**Table 6.8:** Comparing the current data on  $^{222}\text{Rn}/^{220}\text{Rn}$  exhalation rates with those obtained from other parts of the nation.

| Regions                        | $^{222}\text{Rn}$ exhalation<br>( $\text{mBqKg}^{-1}\text{h}^{-1}$ ) | mass rate | $^{220}\text{Rn}$ surface<br>exhalation rate<br>( $\text{Bqm}^{-2}\text{h}^{-1}$ ) | References    |
|--------------------------------|--|-----------|--|---------------|
|                                | <b>Average</b>   |           | <b>Average</b>   |               |
| Chikkaballapur,<br>Karnataka   | $143 \pm 61$   |           | $10443 \pm 5669$   | [18]          |
| Faridabad, Southern<br>Haryana | $31 \pm 12$  |           | $5846 \pm 1424$  | [19]          |
| Fazilka, Punjab                | 118.7  |           | $32.3 \times 10^3$   | [20]          |
| East Khasi Hills,<br>Meghalaya | $11.6 \pm 0.06$  |           | $(24.1 \pm 0.14) \times 10^3$  | [21]          |
| Kohima, Nagaland               | $19.03 \pm 3.82$   |           | $1439 \pm 186$   | Present study |

#### 6.5.1.2 $^{222}\text{Rn}$ in water

The amount of  $^{222}\text{Rn}$  in water varies from 0.17 to 1.20  $\text{BqL}^{-1}$  (mean=  $0.56 \pm 0.17 \text{ BqL}^{-1}$ ) (table 6.9).  $^{222}\text{Rn}$  level was observed highest in the water samples collected from Toupheema village while the lowest was observed in Chandmari colony (figure 6.16). The higher  $^{222}\text{Rn}$  concentration in the water is presumably due to the result of subsurface water restricting radon's escape path.

After all, it interacts instantly with bedrock that is constantly emitting  $^{222}\text{Rn}$ . The amount of  $^{222}\text{Rn}$  in drinking water is also influenced by the different forms of the bedrock present beneath the research area's Earth's crust, which primarily consists of shale, limestone, sandstone, etc. Further, it was established that volcanic rocks often possess higher radiation levels compared to sedimentary rocks such as sandstone,

although specific shales and phosphate rocks possess greater radioactive concentrations [41].

**Table 6.9:**  $^{222}\text{Rn}$  content and its effective dose in the water samples of Kohima district of Nagaland.

| Place (Sample code) | $^{222}\text{Rn}$ (BqL <sup>-1</sup> ) in water | Yearly effective dose because of inhalation (μSvy <sup>-1</sup> ) |                       |                         | Yearly effective dose because of ingestion (μSvy <sup>-1</sup> ) |                       |                         |
|---------------------|---|---|-----------------------|-------------------------|--|-----------------------|-------------------------|
|                     |   | Infants (0–2 years)   | Children (8–12 years) | Adults (above 17 years) | Infants (0–2 years)  | Children (8–12 years) | Adults (above 17 years) |
| Chandmari           | 0.48  | 3.24  | 2.59                  | 1.85                    | 4.45   | 4.24                  | 1.53                    |
| Jakhama             | 0.47  | 3.15  | 2.53                  | 1.80                    | 4.34   | 4.13                  | 1.49                    |
| Paramedical         | 0.49  | 3.31  | 2.66                  | 1.89                    | 4.56   | 4.34                  | 1.56                    |
| Touphema            | 1.20  | 8.07  | 6.47                  | 4.60                    | 11.10  | 10.56                 | 3.81                    |
| Zubza               | 0.17  | 1.13  | 0.90                  | 0.64                    | 1.55   | 1.48                  | 0.53                    |

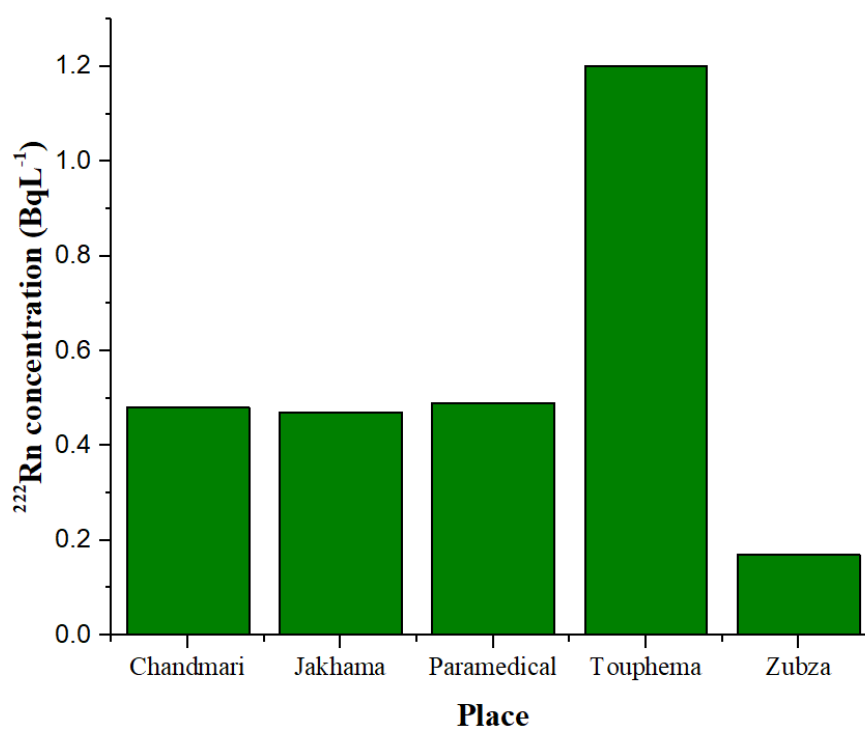


**Fig. 6.16:**  $^{222}\text{Rn}$  in water in different sites.



The annual ingestion dosage from drinking water falls between the ranges of 1.13 to 8.07  $\mu\text{Svy}^{-1}$  (average =  $3.78 \pm 1.15 \mu\text{Svy}^{-1}$ ) for infants, while for children vary from 0.90 to 6.47  $\mu\text{Svy}^{-1}$  (average =  $3.03 \pm 0.92 \mu\text{Svy}^{-1}$ ) and for adults lies in the range of 0.64 to 4.60  $\mu\text{Svy}^{-1}$  (average value =  $2.16 \pm 0.65 \mu\text{Svy}^{-1}$ ) (table 6.9).

The annual inhalation dosage ranges from 1.55 to 11.10  $\mu\text{Svy}^{-1}$  with an average value of  $5.20 \pm 1.58 \mu\text{Svy}^{-1}$  for infants, in the range of 1.48 to 10.56  $\mu\text{Svy}^{-1}$  with an average of  $4.95 \pm 1.50 \mu\text{Svy}^{-1}$  for children and in the range of 0.53 to 3.81  $\mu\text{Svy}^{-1}$  (mean value =  $1.78 \pm 0.54 \mu\text{Svy}^{-1}$ ) for adults. Infants receive the most yearly dose (ingestion and inhalation) as compared to adults and children, based on the current findings. The overall dose, however, remains within the permitted range of 100  $\mu\text{Svy}^{-1}$  for each sample [45].

## 6.6 Conclusion

1. The mass exhalation rate of  $^{222}\text{Rn}$  values in all three districts was found to vary below the range set by UNSCEAR (2000).
2. The surface exhalation rate of  $^{220}\text{Rn}$  values was found to vary below the range as set by UNSCEAR (2000) in all three districts.
3. The combined yearly effective dosage from inhalation and ingestion was found to be greater in infants as compared to children and adults. However, all of the obtained results are below the WHO recommended limit of 100  $\mu\text{Svy}^{-1}$  (World Health Organisation, 2003) in all three districts.
4. Since all the  $^{222}\text{Rn}$  and  $^{220}\text{Rn}$  values resulting from the research area are lower than the global average value, it can be said that the current research regions are not related to any substantial risk.

## References

1. UNSCEAR (2000) Sources and effects of ionizing radiation. Report to the general assembly with scientific annexes. United Nations Scientific Committee on the Effects of Atomic Radiation, New York.
2. Froehlich K (2010) Radioactivity in the Environment, Elsevier, Radarweg 29, PO Box 211, 1000 AE Amsterdam, The Netherlands Linacre House, Jordan Hill, Oxford OX2 8DP, UK.
3. Constantin Cosma, Alexandra Cucos-Dinu, Botond Papp, Robert Begy, Carlos Sainz (2013) Soil and building material as main sources of indoor radon in Băița-Ștei radon prone area (Romania). J Environ Radioact 116: 174-179. <https://doi.org/10.1016/j.jenvrad.2012.09.006>.
4. Sahoo BK, Mayya YS, Sapra BK, Gaware JJ, Banerjee KS, Kushwaha HS (2010) Radon exhalation studies in an Indian uranium tailings pile. Radiat Meas 45(2): 237-241. <https://doi.org/10.1016/j.radmeas.2010.01.008>
5. Moldovan M, Benea V, Niță DC, Papp B, Burghele BD, Bican-Brișan N, Cosma C (2014) Radon and radium concentration in water from North-West of Romania and the estimated doses. Radiat Prot Dosim 162(1-2): 96-100. <https://doi.org/10.1093/rpd/ncu230>
6. Sachs HM, Manlow R, Hernandez TL et al (1981) In the proceedings of the international symposium on indoor air quality, Mass, Amherst.
7. Hess CT, Fleischer RL, Turner LG (1978) Measurement of indoor radon-222 in Maine: summer versus winter variations and effects of draftiness of homes, Tech. Inform. Series Report No. 83 CRD 278, General Electric, New York, USA.
8. Somlai K, Tokonami S, Ishikawa T et al (2007) <sup>222</sup>Rn concentrations of water in the Balaton Highland and in the southern part of Hungary and the assessment of the resulting dose. Radiat Meas 42: 491-495.
9. Nazaroff WW, Doyle SM, Nero AV et al (1997) Potable water as a source of airborne Rn-222 in US dwellings: a review and assessment. Health Phys 52: 281-295.
10. Watson JE, Evans JP, Mabry AM (1993) Analysis of <sup>222</sup>Rn concentration in North Carolina household water supplies derived from private wells. Health Phys 65: 156-160. <https://doi.org/10.1097/00004032-199308000-00004>

11. Fitzgerald B, Hopke PK, Datye V et al (1997) Experimental assessment of the short- and long-term effects of  $^{222}\text{Rn}$  from domestic shower water on the dose burden incurred in normally occupied homes. *Environ Sci Technol* 31(6): 1822–1829. <https://doi.org/10.1021/es950936l>
12. WHO (World Health Organization) (2009) Who handbook on indoor radon. A public health perspective (available online).
13. UNSCEAR (2006) United Nations Scientific Committee on the Effect of Atomic Radiation. In: Report A/AC.82/644, exposures of workers and the public from various sources of radiations (New York: United Nations).
14. Kumar A, Sharma S, Mehra R et al (2022) Assessment of natural radioactivity levels in the Lesser Himalayas of the Jammu and Kashmir, India. *J Radioanal Nucl Chem* 331: 1907–1921. <https://doi.org/10.1007/s10967-021-08164-2>
15. Singla AK, Kansal S and Mehra R (2021) Quantification of radon contamination in drinking water of Rajasthan, India. *J Radioanal Nucl Chem* 327: 1149-1157. <https://doi.org/10.1007/s10967-021-07599-x>
16. Rani S, Kansal S, Singla AK, Mehra R (2021) Radiological risk assessment to the public due to the presence of radon in water of Barnala district, Punjab, India. *Environ Geochem Health* 43(12): 5011-5024. <https://doi.org/10.1007/s10653-021-01012-y>
17. Singh B, Kant K, Garg M, Singh A, Sahoo BK, Sapra BK (2019) A comparative study of radon levels in underground and surface water samples of Faridabad district of Southern Haryana, India. *J Radioanal Nucl Chem* 319: 907–916. <https://doi.org/10.1007/s10967-018-6384-1>
18. Poojitha CG, Sahoo BK, Ganesh KE, Pranisha TS, Sapra BK (2020) Assessment of radon and thoron exhalation from soils and dissolved radon in ground water in the vicinity of elevated granitic hill, Chikkaballapur district, Karnataka, India. *Radiat Prot Dosim* 190(2): 185-192. <https://doi.org/10.1093/rpd/ncaa099>
19. Singh B, Kant K, Garg M, Sahoo BK (2020) Quantification of radon/thoron exhalation rates of soil samples collected from district Faridabad of Southern Haryana, India. *J Radioanal Nucl Chem* 326: 831–843. <https://doi.org/10.1007/s10967-020-07365-5>
20. Narang S, Kumar D, Sharma DK et al (2018) A study of indoor radon, thoron and their exhalation rates in the environment of Fazilka district, Punjab,

- India. *Acta Geophys* 66: 1233–1241. <https://doi.org/10.1007/s11600-018-0114-5>.
21. Pyngrope A, Saxena A, Khardewsaw A et al (2022) Effect of soil's porosity and moisture content on radon and thoron exhalation rates. *J Radioanal Nucl Chem* 331: 1975–1984. <https://doi.org/10.1007/s10967-021-08168-y>
22. Almayahi BA, Tajuddin AA & Jaafar MS (2014) Calibration technique for a CR-39 detector for soil and water radon exhalation rate measurements. *J Radioanal Nucl Chem* 301: 133–140. <https://doi.org/10.1007/s10967-014-3146-6>
23. Noverques A, Juste B, Sancho M, García-Fayos B & Verdú G (2020) Study of the influence of radon in water on radon levels in air in a closed location. *Radiat Phys Chem* 171: 108761. <https://doi.org/10.1016/j.radphyschem.2020.108761>
24. Jalili-Majrareshin A, Behtash A & Rezaei-Ochbelagh D (2012) Radon concentration in hot springs of the touristic city of Sarein and methods to reduce radon in water. *Radiat Phys Chem* 81(7): 749–757. <https://doi.org/10.1016/j.radphyschem.2012.03.015>
25. Lee JM & Kim G (2006) A simple and rapid method for analyzing radon in coastal and ground waters using a radon-in-air monitor. *J Environ Radioact* 89 (3): 219–228. <https://doi.org/10.1016/j.jenvrad.2006.05.006>
26. Jobbágy V, Altzitzoglou T, Malo P, Tanner V & Hult M (2017) A brief overview on radon measurements in drinking water. *J Environ Radioact* 173: 18–24. <https://doi.org/10.1016/j.jenvrad.2016.09.019>
27. Masahiro Hosada, Michikuni Simo, Masato Sugino, Masahide Furukawa & Masahiro Fukushi (2007) Effect of Soil Moisture Content on Radon and Thoron Exhalation. *J Nucl Sci Technol* 44(4): 664–672. <http://dx.doi.org/10.1080/18811248.2007.9711855>
28. Schery SD (1990) Thoron in the Environment. *J Air Waste Manage Assoc* 40(4): 493–497. <https://doi.org/10.1080/10473289.1990.10466704>.
29. Dinh Chau N, Chruściel E & Prokólski Ł (2005) Factors controlling measurements of radon mass exhalation rate. *J Environ Radioact* 82(3): 363–369. <https://doi.org/10.1016/j.jenvrad.2005.02.006>

30. Kainan Sun, Qiuju Guo & Weihai Zhuo (2004) Feasibility for Mapping Radon Exhalation Rate from Soil in China. *J Nucl Sci Technol* 41(1): 86-90. <http://dx.doi.org/10.1080/18811248.2004.9715462>
31. Chitra N, Danalakshmi B, Supriya D, Vijayalakshmi I, Sundar SB, Sivasubramanian K, Baskaran R, Jose MT (2018) Study of Radon and Thoron exhalation from soil samples of different grain sizes. *Appl Radiat Isot* 133: 75–80. <https://doi.org/10.1016/j.apradiso.2017.12.017>
32. Thabayneh KM (2018) Determination of radon exhalation rates in soil samples using sealed can technique and CR-39 detectors. *J Environ Health Sci Engineer* 16: 121–128. <https://doi.org/10.1007/s40201-018-0298-2>
33. Saad AF, Abdallah RM & Hussein NA (2018) Physical and geometrical parameters controlling measurements of radon emanation and exhalation from soil. *Appl Radiat Isot* 137: 273–279. <https://doi.org/10.1016/j.apradiso.2018.03.022>
34. Syarbaini S & Pudjadi E (2015) Radon and Thoron Exhalation Rates from Surface Soil of Bangka - Belitung Islands, Indonesia. *IJG*: 2(1): 35-42. <https://doi:10.17014/ijog.2.1.35-42>
35. Ao A, Bhowmik SK (2014) Cold subduction of the Neotethys: the metamorphic record from finely banded lawsonite and epidote blueschists and associated metabasalts of the Nagaland Ophiolite Complex, India. *J Metamorph Geol* 32: 829–860. <https://doi.org/10.1111/jmg.12096>
36. Sapra BK, Sahoo BK, Mishra R et al (2016) Handbook on radon transport models and measurement methods. Radiological Physics and Advisory Division, Bhabha Atomic Research Centre, Mumbai, pp 51–52.
37. Sapra BK, Sahoo BK, Mishra R, Kanse SD, Rout RP, Aggarwal TK, Prajith R, Gaware JJ, Jalaluddin S and Kumbhar DS (2010) Handbook BARC, Vol. 51 (BARC Newsletter, Mumbai).
38. Sahoo BK, Nathwani D, Eappen KP, Ramachandran TV, Gaware JJ, Mayya YS (2007) Estimation of radon emanation factor in Indian building materials. *Radiat Meas* 42(8): 1422–1425. <https://doi.org/10.1016/j.radmeas.2007.04.002>
39. Sahoo BK, Agarwal TK, Gaware JJ et al (2014) Thoron interference in radon exhalation rate measured by solid state nuclear track detector based can technique. *J Radioanal Nucl Chem* 302: 1417–1420.

40. Brudecki K, LiWB, Meisenberg O, Tschiersch J, Hoeschen C, & Oech U (2014) Age dependent inhalation dose to members of the public from indoor short-lived radon progeny. *Radiat Environ Biophys* 53(3): 535–549. [https://doi.org/ 10.1007/s00411-014-0543-8](https://doi.org/10.1007/s00411-014-0543-8)
41. Bonotto DM (2014)  $^{222}\text{Rn}$ ,  $^{220}\text{Rn}$  and other dissolved gases in mineral waters of southeast Brazil. *J Environ Radioact* 132: 21–30. <https://doi.org/10.1016/j.jenvrad.2014.01.005>
42. WHO (2004) Guidelines for drinking-water quality. Recommendations.
43. USEPA (1991) Federal Register 40 parts 141 and 142; National primary Drinking Water regulations; Radionuclides; proposed Rule (U.S. Environmental Protection Agency). U.S. Government Printing Office.
44. UNSCEAR (2008) Report, Volume 1, Annex B: Exposure from Natural Radiations Sources.
45. World Health Organisation (2003) Guidelines for drinking water quality. Health criteria and other information. WHO Press, Geneva.
46. Tabar E, Yakut H, Kuş A (2018) Measurement of the radon exhalation rate and effective radium concentration in soil samples of southern Sakarya, Turkey. *Indoor Built Environ* 27(2): 278-288. [https://doi.org/ 10.1177/ 1420326X16672510](https://doi.org/10.1177/1420326X16672510)
47. Syarbaini and Pudjadi E (2015) Radon and Thoron Exhalation Rates from Surface Soil of Bangka - Belitung Islands, Indonesia. *Indo J Geo* 2(1): 35-42. <http://dx.doi.org/10.17014/ijog.2.1.35-42>
48. Bhupender S, Krishan K & Maneesha G (2021) Monitoring of natural radionuclides by alpha scintillometry and gamma spectrometry techniques in soil of district Palwal, Southern Haryana, India. *Int J Environ Anal Chem*. [https://doi.org/ 10.1080/03067319.2021.2016726](https://doi.org/10.1080/03067319.2021.2016726)
49. Frutos-Puerto S, Pinilla-Gil E, Andrade E, Reis M, Madruga MJ, Miró Rodríguez C (2020) Radon and thoron exhalation rate, emanation factor and radioactivity risks of building materials of the Iberian Peninsula. *Peer J* 8:e10331. <https://doi.org/10.7717/peerj.10331>

## ***APPENDIX-I***

---

### **PLAGIARISM REPORT**

---





# नागालैण्ड विश्वविद्यालय NAGALAND UNIVERSITY

(केंद्रीय विश्वविद्यालय) / (A Central University)

मुख्यालय : लुमामी, जिला : जुन्हेबोटो (नागालैण्ड) – 798 627

Hqrs: Lumami, Dist: Zunheboto, Nagaland – 798 627

**Department of Chemistry**

## Ph.D. Thesis Certificate on Plagiarism check

|  |  |
|--|--|
| Name of the research scholar                             | Supongtoshi Jamir  |
| Ph.D. registration number                                | PhD/CHE/00002  |
| Title of Ph.D. thesis                                    | A study of gamma, radon, thoron and their progeny levels in Mokokchung, Dimapur and Kohima districts of Nagaland, India. |
| Name & institutional address of the supervisor           | Prof. Dipak Sinha<br>Department of Chemistry<br>Nagaland University, Lumami  |
| Name of the department and school                        | Department of Chemistry, School of Sciences  |
| Date of submission                                       | 24/01/2023   |
| Date of plagiarism check                                 | 24/01/2023   |
| Percentage of similarity detected by the URKUND software | 6%   |

I hereby declare that/certify that the Ph.D. thesis submitted by me is complete in all respect as per the guidelines of Nagaland University (NU) for this purpose. I also certify that the thesis (soft copy) has been checked for plagiarism using URKUND similarity check software. It is also certified that the contents of the electronic version of the thesis are the same as the final hard copy of the thesis. Copy of the report generated by the URKUND software is also enclosed.

Place: LUMAMI

*Supongtoshi*  
(Name & signature of the Scholar)

Date: 3/2/23



*Dipak Sinha*  
3/2/23  
Name & signature of the Supervisor



## Document Information

|                   |   |
|-------------------|---|
| Analyzed document | Supongtoshi Jamir Ph.D. Thesis.pdf (D156810291) |
| Submitted         | 1/24/2023 2:12:00 PM                            |
| Submitted by      | Dipak Sinha                                     |
| Submitter email   | dipaksinha@gmail.com                            |
| Similarity        | 6%  |
| Analysis address  | dipaksinha.naga@analysis.arkund.com             |

## Sources included in the report

|          |  |   |
|----------|--|---|
| <b>J</b> | <b>9_chapter_1.pdf</b><br>URL: ede554d8-52ec-488f-8dbe-9311652796b8<br>Fetched: 8/20/2022 10:39:35 AM                                    |  9   |
| <b>W</b> | URL: https://www.vdh.virginia.gov/radiological-health/indoor-radon-program/history/<br>Fetched: 8/11/2020 8:50:45 PM                     |  1   |
| <b>J</b> | <b>07_chapter_1.pdf</b><br>URL: 5d6215b9-b7fb-40f1-aa1e-9ccde4c9723e<br>Fetched: 8/21/2022 2:56:38 PM                                    |  1   |
| <b>W</b> | URL: https://www.researchgate.net/publication/8155455_Radon_and_thoron_monitoring_in_the_enviromen...<br>Fetched: 10/22/2020 11:06:28 AM |  1   |
| <b>W</b> | URL: https://www.frontiersin.org/articles/10.3389/fpubh.2020.00017/full<br>Fetched: 7/23/2020 1:03:08 PM                                 |  1 |

## Entire Document

## ***APPENDIX-II***

---

### **WORKSHOP AND SEMINARS ATTENDED**

---

### **Workshop and Seminars attended**

- Poster presentation at National seminar on Chemistry in interdisciplinary research, organized by the Department of Chemistry, Nagaland University, March 16<sup>th</sup> -17<sup>th</sup> 2017.
- Oral presentation at National seminar on Chemistry in interdisciplinary research, organized by the Department of Chemistry, Nagaland University, November 9<sup>th</sup> -10<sup>th</sup> 2018.
- Attended one day workshop on the importance of IPR in academic Institutions 29<sup>th</sup> May 2019.
- Oral presentation at National e-Seminar on “Chemistry in emerging trends of interdisciplinary research” (NeSCETIR- 2020), organized by Department of Chemistry, Nagaland University, November 18<sup>th</sup>-20<sup>th</sup> 2020.
- Oral presentation at International seminar on Recent Advances in Science and Technology (ISRAST), organized by NEAST, Mizoram University, November 16<sup>th</sup> – 18<sup>th</sup>, 2020.

## ***APPENDIX-III***

---

### **LISTS OF PUBLICATIONS**

---

## Lists of Publications

### Papers published:

- **Jamir S**, Sahoo BK, Mishra R, Bhomick PC and Sinha D (2021) A study on indoor radon, thoron and their progeny level in Mokokchung district of Nagaland, India. Radioanal Nucl Chem 331: 21–30. <https://doi.org/10.1007/s10967-021-08096-x>. (Publisher: Springer).
- **Jamir S**, Sahoo BK, Mishra R, and Sinha D (2022) A comprehensive study on indoor radon, thoron and their progeny level in Dimapur district of Nagaland, India. J. Radiat Prot Dosim 198(12): 1–9. <https://doi.org/10.1093/rpd/ncac150> (Publisher: Oxford University Press).
- **Jamir S**, Sahoo BK, Mishra R and Sinha D (2022) A case study on seasonal and annual average indoor radon, thoron, and their progeny level in Kohima district, Nagaland, India. Isot Environ Health Stud. <https://doi.org/10.1080/10256016.2022.2140147> (Publisher: Taylor and Francis).
- **Jamir S**, Sahoo BK, Mishra R, and Sinha D (2022) Estimation of radon in groundwater and analysis of radon and thoron exhalation rates of the soil in Mokokchung district, Nagaland, India. Groundw Sustain Dev 20: 100874. <https://doi.org/10.1016/j.gsd.2022.100874> (Publisher: Elsevier).
- Bhomick PC, **Jamir S**, Sinha UP, Sahoo BK, Sinha D (2019) Biomass-derived activated carbon for removal of  $^{222}\text{Rn}$  from air. Sustain Chem Pharm 14: 100193. <https://doi.org/10.1016/j.scp.2019.100193> (Publisher: Elsevier).

**Papers communicated:**

- Radon analysis in the soil and water in different residential areas of Dimapur district, Nagaland, India.
- Estimation of  $^{222}\text{Rn}$  in groundwater and analysis of radon and thoron exhalation rates of the soil in Kohima district, Nagaland, India.